UNIVERSIDADE DE LISBOA

FACULDADE DE MEDICINA VETERINÁRIA

RETINAL ERYTHROPOIETIN DISTRIBUTION AND NEUROPROTECTIVE EFFECT IN A NANOPARTICULATE DRUG DELIVERY SYSTEM AFTER SUBCONJUNCTIVAL AND TOPICAL ADMINISTRATION IN AN ANIMAL GLAUCOMA MODEL

BEATRIZ ROSA FERNANDES DUARTE DA SILVA

Orientadora: Professora Doutora Esmeralda Sofia da Costa Delgado

Co-Orientadoras: Professora Doutora Berta Maria Fernandes Ferreira São Braz

Professora Doutora Lídia Maria Diogo Gonçalves

Tese especialmente elaborada para obtenção do grau de
Doutor em Ciências Veterinárias na especialidade de Clínica

2023

UNIVERSIDADE DE LISBOA

FACULDADE DE MEDICINA VETERINÁRIA

RETINAL ERYTHROPOIETIN DISTRIBUTION AND NEUROPROTECTIVE EFFECT IN A NANOPARTICULATE DRUG DELIVERY SYSTEM AFTER SUBCONJUNCTIVAL AND TOPICAL ADMINISTRATION IN AN ANIMAL GLAUCOMA MODEL

BEATRIZ ROSA FERNANDES DUARTE DA SILVA

Orientadora: Professora Doutora Esmeralda Sofia da Costa Delgado

Co-Orientadoras: Professora Doutora Berta Maria Fernandes Ferreira São Braz

Professora Doutora Lídia Maria Diogo Gonçalves

Tese especialmente elaborada para obtenção do grau de
Doutor em Ciências Veterinárias na especialidade de Clínica

Júri

Presidente: Professor Doutor Luís Filipe Lopes da Costa
Vogais:
- Professora Doutora Felisbina Luísa Pereira Guedes Queiroga
- Professora Doutora Catarina Falcão Trigoso Vieira Branco Lavrador
- Professor Doutor Carlos Alberto Matinho Marques Neves
- Professor Doutora Ana Francisca de Campos Simão Bettencourt
- Professora Doutora Esmeralda Sofia da Costa Delgado

2023

DECLARAÇÃO RELATIVA ÀS CONDIÇÕES DE REPRODUÇÃO DA TESE

Nome: Beatriz Rosa Fernandes Duarte da Silva

Título da Tese ou Dissertação: Retinal erythropoietin distribution and neuroprotective effect in a nanoparticulate drug delivery system after subconjunctival and topical administration in an animal glaucoma model

Ano de conclusão (indicar o da data da realização das provas públicas): 2023

Designação do curso de Mestrado ou de Doutoramento: Doutoramento em Ciências Veterinárias

Área científica em que melhor se enquadra:

☒ Clínica ☐ Produção Animal e Segurança Alimentar

☐ Morfologia e Função ☐ Sanidade Animal

Declaro sobre compromisso de honra que a tese ou dissertação agora entregue corresponde à que foi aprovada pelo júri constituído pela Faculdade de Medicina Veterinária da ULISBOA.

Declaro que concedo à Faculdade de Medicina Veterinária e aos seus agentes uma licença não-exclusiva para arquivar e tornar acessível, nomeadamente através do seu repositório institucional, nas condições abaixo indicadas, a minha tese ou dissertação, no todo ou em parte, em suporte digital.

Declaro que autorizo a Faculdade de Medicina Veterinária a arquivar mais de uma cópia da tese ou dissertação e a, sem alterar o seu conteúdo, converter o documento entregue, para qualquer formato de ficheiro, meio ou suporte, para efeitos de preservação e acesso.

Retenho todos os direitos de autor relativos à tese ou dissertação, e o direito de a usar em trabalhos futuros (como artigos ou livros).

Concordo que a minha tese ou dissertação seja colocada no repositório da Faculdade de Medicina Veterinária com o seguinte estatuto:

1. ☒ Disponibilização imediata do conjunto do trabalho para acesso mundial;
2. ☐ Disponibilização do conjunto do trabalho para acesso exclusivo na Faculdade de Medicina Veterinária durante o período de ☐ 6 meses, ☐ 12 meses, sendo que após o tempo assinalado autorizo o acesso mundial*;

DE ACORDO COM A LEGISLAÇÃO EM VIGOR, NÃO É PERMITIDA A REPRODUÇÃO DE QUALQUER PARTE DESTA TESE/TRABALHO.

Faculdade de Medicina Veterinária da Universidade de Lisboa, 2 de Março de 2023

Assinatura: Beatriz Rosa Fernandes Duarte da Silva

Acknowledgements

O meu primeiro agradecimento vai para as minhas queridas orientadoras, Profª Doutora Esmeralda Delgado, Profª Doutora Berta São Braz e Profª Doutora Lídia Gonçalves, por me terem presenteado e inspirado com a vossa sabedoria, dedicação incondicional e sede de conhecimento, mas também pela vossa preciosa amizade, companheirismo e preocupação, que lembrarei sempre com muito carinho.

Um obrigada muito especial para todo o staff da Faculdade de Medicina Veterinária e da Faculdade de Farmácia da Universidade de Lisboa: corpo docente e discente, assistentes e chefes de laboratório, investigadores, estagiários, médicos, enfermeiros, auxiliares, enfim, todos os que, direta ou indiretamente, contribuíram para a realização deste projeto. Às vezes, basta estar a pessoa certa, no sítio certo, à hora certa, para tornar o dia de um estudante de doutoramento bastante mais fácil. Muito obrigada, Prof. Doutor António Almeida e Profª Doutora Joana Marto, pela valiosa disponibilidade e ajuda no mundo das nanopartículas. Muito obrigada, Inês Dias e Andreia Grilo, pelo apoio e preciosa ajuda nos trabalhos, e pela companhia no cafezinho a meio do dia. Muito obrigada, Sandra Carvalho, pela disponibilidade em todo o processamento histopatológico, sempre acompanhada de uma boa conversa.

Obrigada aos meus colegas de doutoramento pelo ambiente ímpar que vivi enquanto enfrentávamos juntos as unidades curriculares. Um abraço especial para cada um de vós.
Muito obrigada aos meus amigos e à minha família, por serem o pilar da minha vida. Sem o vosso apoio incondicional, em todos os momentos, este percurso teria sido muito mais áspero. E um agradecimento especial vai para o João Dinis, o meu pequeno de 4 anos que me acompanhou desde o início deste doutoramento. Cuidar de ti e ver-te crescer foram a minha força motriz. Obrigada por seres o filho mais que perfeito.

Financial support

This project was funded by:
Fundação para a Ciência e a Tecnologia (FCT): PhD fellowship SFRH/BD/130476/2017.
Research Institute for Medicines (iMed), Faculty of Pharmacy, University of Lisbon: UID/DTP/04138/2013; UID/DTP/04138/2019; UIDB/04138/2020.
Centre for Interdisciplinary Research in Animal Health (CIISA), Faculty of Veterinary Medicine, University of Lisbon: UID/CVT/276/2013; UIDB/00276/2020.
Associate Laboratory for Animal and Veterinary Sciences (AL4AnimalS): LA/P/0059/2020.
European Society of Veterinary Ophthalmology (ESVO): Research Grant of 2019.

Resumo

DISTRIBUIÇÃO E EFEITO NEUROPROTETOR DA ERITROPOIETINA NA RETINA APÓS ADMINISTRAÇÃO TÓPICA E SUBCONJUNTIVAL DE UM SISTEMA DE NANOPARTÍCULAS NUM MODELO ANIMAL DE GLAUCOMA

O glaucoma é uma doença ocular neurodegenerativa com impacto substancial na saúde pública, causando degeneração das células ganglionares da retina (CGR) e cegueira irreversível. Várias estratégias neuroprotetoras têm sido estudadas no glaucoma e a epoetina beta (EPOβ), uma forma recombinante da eritropoietina, demonstrou efeitos antiapoptóticos nas CGR. Desta forma, surgiu o interesse em criar uma formulação com EPOβ para administração tópica ocular, com vista a neuroproteção da retina em casos de glaucoma, com o mínimo de efeitos secundários e com a vantagem de promover a adesão dos pacientes ao tratamento. Para tal foram desenvolvidas nanopartículas de quitosano e ácido hialurónico (CS/HA) às quais foi adicionada epoetina beta (EPOβ). Inicialmente, foram realizados estudos *in vitro* e *ex vivo* da estabilidade físico-química, citotoxicidade, perfis de libertação e permeação e mucoadesividade das nanopartículas CS/HA-EPOβ. Estas permitiram a permeação de EPOβ em membranas oculares nos ensaios *ex vivo*, sem citotoxicidade *in vitro*. Seguidamente, ratos Wistar Hannover saudáveis foram usados para administração subconjuntival e tópica das nanopartículas CS/HA-EPOβ, para avaliar o impacto local e sistémico da formulação, a tolerância biológica e segurança, o efeito na eletrofisiologia da retina e a distribuição da EPOβ nos tecidos oculares. Observou-se uma permeação sustentada de EPOβ até à retina em ambas as vias de administração, sem efeitos adversos. Finalmente, estudámos a via ocular tópica utilizando um modelo experimental de glaucoma em ratos. Avaliámos as alterações morfológicas e fisiológicas da retina em resposta à nanoformulação, através de eletrorretinografia e avaliação histológica por imunofluorescência e coloração de hematoxilina-eosina, e avaliação de apoptose (caspase-3 clivada). A administração tópica ocular de nanopartículas de CS/HA-EPOβ em ratos glaucomatosos permitiu a permeação da EPOβ, inclusive por via transcorneal, até à retina. No grupo de animais tratados ocorreram, mais cedo e de forma mais considerável, melhorias na atividade elétrica e na espessura da retina, e na redução da apoptose. Em suma, a EPOβ chegou à retina, onde foi possível constatar a sua ação neuroprotetora, demonstrando assim a viabilidade da administração tópica de agentes neuroprotetores em nanoformulações, visando o segmento posterior do olho. Os resultados foram promissores e oferecem um contributo significativo para o desenvolvimento de novas formas terapêuticas para preservar a acuidade visual de pacientes com glaucoma ou outras doenças oculares neurodegenerativas.

Palavras-chave: nanopartículas; quitosano; ácido hialurónico; epoetina beta; glaucoma.

Abstract

RETINAL ERYTHROPOIETIN DISTRIBUTION AND NEUROPROTECTIVE EFFECT IN A NANOPARTICULATE DRUG DELIVERY SYSTEM AFTER SUBCONJUNCTIVAL AND TOPICAL ADMINISTRATION IN AN ANIMAL GLAUCOMA MODEL

Glaucoma is a neurodegenerative ocular disease with substantial impact in public health, as it causes retinal ganglion cells (RGC) degeneration and irreversible blindness. Neuroprotective strategies have been a focus of research in glaucoma, and the use of erythropoietin and its recombinant forms, like epoetin beta (EPOβ), have shown anti-apoptotic effects on RGC. We aimed to create a nanoformulation carrying EPOβ, adequate for topical ocular administration, that could provide neuroprotection to the retina in cases of glaucoma, with absent or residual secondary effects and the advantage of promoting patients' compliance to the treatment. Therefore, chitosan and hyaluronic acid (CS/HA) nanoparticles for topical ocular deliver of epoetin beta (EPOβ) were developed, aiming to deliver EPOβ to the retina in a sustained profile. Firstly, *in vitro* and *ex vivo* studies of the physicochemical stability, cytotoxicity, release and permeation profiles and mucoadhesive strength of the CS/HA-EPOβ nanoparticles were performed. These nanoparticles allowed EPOβ permeation through ocular membranes in *ex vivo* assays, with no *in vitro* cytotoxicity. Afterwards, healthy Wistar Hannover rats were used for subconjunctival and topical administrations of CS/HA-EPOβ nanoparticles, to assess the formulation's local and systemic influence, its biological tolerance and safety, its effect in retinal electrophysiology, and EPOβ's distribution in ocular tissues. A sustained EPOβ delivery to the retina was observed using both routes of administration, with no side-effects. Finally, we explored the topical ocular delivery of CS/HA-EPOβ nanoparticles using a rat glaucoma model. We assessed retinal morphological and physiological changes in response to the nanoformulation applied through topical ocular route, using electroretinography and histological evaluation, which comprised immunofluorescence, hematoxylin and eosin staining and apoptosis assessment (cleaved caspase-3). Topical ocular administration of CS/HA-EPOβ nanoparticles in glaucomatous rats allowed EPOβ permeation, including by transcorneal pathway, reaching the inner retina. Improvements in retinal electrical activity and thickness, and in apoptosis reduction occurred earlier and more significantly in the treatment group. In conclusion, EPOβ reached the retina, where its neuroprotective action was observed, thus demonstrating the feasibility of topical administration of neuroprotective agents in nanoformulations, targeting the posterior ocular segment. Results were promising and contribute to the development of new therapeutic strategies to preserve the visual acuity of patients with glaucoma or other neurodegenerative ocular diseases.

Key-words: nanoparticles; chitosan; hyaluronic acid; epoetin beta; glaucoma.

Resumo alargado

DISTRIBUIÇÃO E EFEITO NEUROPROTETOR DA ERITROPOIETINA NA RETINA APÓS ADMINISTRAÇÃO TÓPICA E SUBCONJUNTIVAL DE UM SISTEMA DE NANOPARTÍCULAS NUM MODELO ANIMAL DE GLAUCOMA

O glaucoma é uma doença neurodegenerativa caracterizada por uma degeneração lenta e progressiva das células ganglionares da retina (CGRs) e dos seus axónios. Desta forma, o interesse na neuroprotecção como parte do tratamento de glaucoma tem crescido nos últimos anos. A eritropoetina (EPO) é um fator de crescimento hematopoiético com importantes propriedades neuroprotetoras e neurorregenerativas, devido à sua capacidade de diminuir apoptose, inflamação, oxidação e excitotoxicidade e aumentar a proliferação de células progenitoras, sendo considerada uma valiosa estratégia para prevenir a apoptose das CGRs. A epoetina beta (EPOβ), uma variante recombinante da EPO, demonstrou efeitos neuroprotetores a nível da retina em ratos glaucomatosos, quando administrada por via subconjuntival. Dando continuidade a esta linha de investigação, a nossa equipa desenvolveu nanopartículas de quitosano e ácido hialurónico (CS/HA) para encapsular EPOβ, com vista a administração ocular (subconjuntival e tópica), pretendendo desenvolver uma terapêutica coadjuvante para retinopatia secundária a glaucoma. A inovação do projeto prende-se não só com a via de administração tópica, mas também com a inclusão da EPOβ em nanopartículas, permitindo assim aumentar o seu tempo de permanência na superfície ocular e a sua biodisponibilidade intra-ocular.

As nanopartículas CS/HA-EPOβ foram avaliadas em termos de estabilidade fisicoquímica, citotoxicidade, perfil de libertação, mucoadesividade e permeação *ex vivo* em olhos de porco. Concluímos que foi possível encapsular EPOβ em nanopartículas de CS e HA, com tamanho, potencial zeta, índice de polidispersão e propriedades mucoadesivas adequadas. O peso molecular dos ácido hialurónicos estudados, a sua interação com diferentes solventes e o rácio CS:HA interferiram nas características das nanopartículas, mas a reologia foi o factor determinante para a escolha do HA com as melhores propriedades mucoadesivas (HA6), com vista a aumentar o tempo de residência da nanoformulação na zona pré-corneal. Em relação ao estudo da permeação de EPOβ em olhos de porco (*ex vivo*), obtivemos resultados muito superiores aos de um estudo com EPOβ em solução aquosa (Resende et al. 2017), nomeadamente até 60% mais de permeação na conjuntiva, até 85,3% mais na esclera e até 2,5x mais na córnea. Diferenças semelhantes foram observadas para os fluxos de EPOβ, embora menos notáveis. Por conseguinte, considerámos que as nanopartículas de CS/HA poderiam desempenhar um papel significativo na permeação ocular de EPOβ, reforçando a viabilidade de testar este nano-sistema *in vivo*.

Seguidamente, a formulação foi avaliada *in vivo* em termos de tolerância, segurança, impacto local e sistémico, influência na eletrofisiologia da retina e distribuição da EPOβ no meio intra-ocular. Foram utilizados ratos "Wistar Hannover" saudáveis para testar a formulação CS/HA-EPOβ administrada por via subconjuntival (n=21) e por via tópica (n=18). Primeiramente, os animais foram divididos em grupos de 3 animais e submetidos a um exame oftalmológico completo, incluindo a medição da pressão intraocular (PIO) com TonoLab®, exame do segmento anterior por biomicroscopia de lâmpada de fenda e exame do segmento posterior com oftalmoscopia direta (PanOptic®). Foi efetuada colheita de sangue para medição do microhematócrito e eletrorretinografia (ERG) para avaliar a actividade elétrica da retina. No olho direito (OD), foi administrada a formulação de nanopartículas com 1000 UI de EPOβ por via subconjuntival ou tópica, e no olho esquerdo (OS) foram administradas nanopartículas sem EPOβ. Periodicamente, procedeu-se à avaliação da PIO e da integridade das estruturas oculares em ambos os olhos, bem como à avaliação da dor através da "Rat Grimace Scale". Nova colheita de sangue e ERG, seguidas de eutanásia e enucleação bilateral, foram efetuadas às 12 horas (grupo A; n=3), 1 dia (grupo B; n=3), 3 dias (grupo C; n=3), 7 dias (grupo D; n=3), 14 dias (grupo E; n=3) e 21 dias (grupo F; n=3) após a administração da nanoformulação. Ademais, no ensaio subconjuntival, incluiu-se um grupo que foi avaliado e submetido a eutanásia 28 dias após a administração (grupo G; n=3). Após enucleação, os globos oculares foram marcados com corante para tecidos, conservados em formol 10% em PBS e processados para inclusão em bloco de parafina. Realizaram-se cortes histológicos para avaliação da estrutura tecidular com coloração hematoxilina-eosina e para deteção da EPOβ através de imunofluorescência. Não foram observados efeitos adversos a nível ocular, nem alterações no microhematócrito (40-51%) após a administração da nanoformulação, pelas vias subconjuntival e tópica. A PIO manteve-se no intervalo fisiológico (11 e 22 mmHg) em ambas as vias e não foram observadas alterações significativas entre OD e OS, e entre os períodos antes e após administração da formulação ($p > 0.05$). Em todos os grupos, das vias subconjuntival e tópica, os resultados das ERGs foram semelhantes no OD e OS, não havendo também diferenças estatisticamente significativas entre antes e após administração da formulação ($p > 0.05$). Embora o nosso protocolo de ERG possa diferir dos de outros estudos, tanto a etapa fotópica como a etapa escotópica das ERGs apresentaram ondas a e b comparáveis, em termos de forma e amplitude, às descritas na literatura para ratos albinos. Por conseguinte, as nanopartículas CS/HA, com ou sem EPOβ encapsulada, não influenciaram negativamente a actividade eléctrica da retina. Através de imunofluorescência foi possível detetar EPOβ em diversos tecidos oculares do OD e nenhuma EPOβ foi detetada no OS, após administração pelas duas vias estudadas. O grupo A subconjuntival e tópico apresentaram EPOβ no endotélio corneal, corpo ciliar, cápsula posterior do cristalino, vítreo, esclera e retina (OD). Foi também detetada EPOβ no estroma

corneal (OD) mas apenas no grupo A tópico. Do grupo B ao F (subconjuntival e tópico) foi detetada gradualmente menos EPOβ, sendo escassa nos grupos F e estando completamente ausente no grupo G. Desta forma, optou-se por não se incluir um grupo G no ensaio tópico. Concluímos assim, que as nanopartículas de CS/HA são um sistema inovador para administração ocular de EPOβ, consideradas biologicamente seguras, e permitiram a chegada de EPOβ à retina através da via subconjuntival e tópica, sendo esta última preferível devido ao seu caráter não invasivo.

A última fase do estudo *in vivo* focou-se na administração tópica de nanopartículas CS/HA-EPOβ em ratos com glaucoma induzido, cujos efeitos na retina foram avaliados através de ERG (*in vivo*) e histopatologia da retina (*most-portem*), por coloração hematoxilina-eosina, imunofluorescência e expressão da caspases-3. Estabeleceram-se 3 grupos de tratamento (T; n=12) e 3 grupos controlo (C; n=12), em que todos os animais foram submetidos a exame oftalmológico completo, seguido de microcirurgia para indução de glaucoma no OD, a qual consistiu na cauterização de três veias episclerais sob anestesia geral. Não se efetuou o procedimento no olho contralateral (OS) e a PIO foi medida em ambos os olhos, antes e após o procedimento. Foram administradas no OD as nanopartículas de CS/HA, contendo 1000 UI de EPOβ nos grupos de tratamento, e sem EPOβ nos grupos controlo. Os grupos correspondem aos "timepoints" de eutanásia, sendo eles os 7 dias (grupo T7/C7), 14 dias (grupo T14/C14) e 21 dias (grupo T21/C21) após indução do glaucoma e administração da nanoformulação. Periodicamente, foram efetuados exames oftalmológicos e avaliado o grau de dor de acordo com a "Rat Grimace Scale". No dia 3 após a microcirurgia, todos os animais foram submetidos a ERG para avaliar o sucesso da indução de glaucoma, caracterizado pela diminuição acentuada da resposta da retina do OD, em comparação com o OS. Os animais continuaram no estudo e foram eutanasiados aos 7, 14 ou aos 21 dias após a indução de glaucoma, seguido de enucleação bilateral. Após a inclusão dos olhos em parafina, foram realizados cortes histológicos para coloração com hematoxilina-eosina (avaliação estrutural), para imunofluorescência (deteção de EPOβ) e para imunohistoquímica (avaliação da caspase-3). Relativamente aos resultados, a PIO máxima medida no OD ocorreu logo após a indução do glaucoma (T = 62,6 ± 8,3 mmHg; C = 63,6 ± 7,9 mmHg), com um aumento de 3,6 vezes o limite fisiológico de PIO (p < 0,05). Os animais tratados apresentaram uma tendência para recuperação mais rápida e mais expressiva da atividade elétrica retiniana, confirmada através de ERG. De igual forma, a coloração hematoxilina-eosina revelou que os animais tratados demonstraram uma recuperação mais acentuada da espessura da retina (T = 145,6 ± 22 µm; C = 120,2 ± 10,6 µm; p < 0,05). Estes resultados denotam um potencial efeito neuroprotector da EPOβ nos animais tratados. Foi detectada EPOβ por imunofluorescência em diversos tecidos oculares, incluindo nas camadas mais internas da retina, em todos os ratos tratados. A presença de EPOβ no estroma corneal aos

14 dias e no corpo ciliar aos 21 dias, denota uma permeação transcorneal e sustentada de EPOβ. Por sua vez, foram identificadas células positivas para a caspase-3 clivada na retina neuro-sensorial do grupo C7 (n=4). Não foi detectada apoptose em nenhum animal tratado (com EPOβ), apenas nos animais do grupo controlo aos 7 dias (sem EPOβ), o que nos remete para um possível efeito neuroprotector da EPOβ no grupo de tratamento.

Em conclusão, desenvolvemos nanopartículas mucoadesivas de CS/HA-EPOβ, que não induziram efeitos secundários em ratos saudáveis e com glaucoma, aquando administração subconjuntival e tópica ocular, possibilitando a chegada de EPOβ a todas as camadas da retina. Provámos a permeação transcorneal de EPOβ e um potencial efeito neuroprotetor/ antiapoptótico da EPOβ na retina de ratos com glaucoma. Estes resultados promissores poderão contribuir para a investigação científica no âmbito da "Ocular Drug Delivery" visando o segmento ocular posterior, através da administração ocular tópica.

Table of contents

Acknowledgements iii
Financial support iv
Resumo v
Abstract vi
Resumo alargado vii
Table of contents xi
List of illustrations xii
List of tables xv
Acronyms and Abbreviations xvi
Outcomes of this Thesis xix
CHAPTER 1: Introduction, conceptualization and objectives 1
CHAPTER 2: Colloidal nanosystems with mucoadhesive properties designed for ocular topical delivery 15
CHAPTER 3: New nanoparticles for topical ocular delivery of erythropoietin 72
CHAPTER 4: Chitosan and hyaluronic acid nanoparticles as vehicles of epoetin beta for subconjunctival ocular delivery 97
CHAPTER 5: Topical ocular delivery of epoetin beta in nanoparticles: *in vivo* study using Wistar Hannover rats 121
CHAPTER 6: Topical administration of a nanoformulation of chitosan-hyaluronic acid-epoetin beta in a rat model of glaucoma 144
CHAPTER 7: General discussion, study limitations and future perspectives 176
References 182

List of illustrations

Figure 1: Ocular structures of the human eye 2
Figure 2: Representation of the retinal layers and main retinal cells in a human eye 2
Figure 3: Representation of the intrinsic and extrinsic pathways of the apoptotic process 6
Figure 4: Ophthalmological disorders under research using erythropoietin as part of the therapeutic approach.....10
Figure 5: Main absorption pathways after topical ocular drug administration. 22
Figure 6: Schematic representation of hydrophilic and hydrophobic drugs in a single bilayered liposome.....28
Figure 7: Illustration of a niosome with a hydrophilic and a hydrophobic drug in its structure 32
Figure 8: Structure of an oil-in-water nanoemulsion delivery system 36
Figure 9: Schematic illustration of a normal (A) and a reverse (B) nanomicelle 39
Figure 10: Schematic representation of a nanosuspension.....42
Figure 11: Illustration of a solid lipid nanoparticle. 46
Figure 12: Schematic representation of a particle of nanostructured lipid carriers. 49
Figure 13: Schematic examples of a nanocapsule and a nanosphere loaded with drugs.....53
Figure 14: Illustration of the structure of a nanocrystal particle 63
Figure 15: Schematic representation of a dendrimer's structure showing four generations of branches (G1, G2, G3 and G4) 66
Figure 16: The effect of different hyaluronic acids and CS:HA ratios (1:2, 1:1) on nanoparticles characteristics 82
Figure 17: The effect of 0.9% NaCl on the characteristics of nanoparticles with a 1:1 CS:HA mass ratio.....83
Figure 18: Cell viability of HaCaT (a,b) and ARPE-19 (c,d) 85
Figure 19: *In vitro* release profiles of EPOβ in STF of nanoformulations HA1, HA4 and HA6 86
Figure 20: *Ex vivo* permeation of EPOβ in nanoformulation HA6.....88
Figure 21: Immunohistochemistry for cell nucleus marker of the conjunctiva, sclera and cornea (DAPI, blue) and EPO antibody (red).....90
Figure 22: Sequence of procedures performed in each animal (n = 21).....101
Figure 23: Pictures the ERG set 102
Figure 24: Photo of the subconjunctival administration of the C/HA-EPOβ in the OD of a rat 104
Figure 25: Representation of a rat ocular globe painted with tissue dyes.....105

Figure 26: Mean IOP (mmHg) variation during the study after the subconjunctival administration of the nanoparticles 107
Figure 27: Scotopic luminesce response - mean amplitudes of the a-wave and the b-wave (μV) recorded from the OD and OS 108
Figure 28: Example of the scotopic luminesce response 109
Figure 29: Photopic luminesce response – mean amplitudes of the a-wave and the b-wave (μV) recorded from the OD and OS 111
Figure 30: Example of a photopic flicker exam 112
Figure 31: Scotopic Adaptation – mean amplitudes of the a-wave and the b-wave (μV) recorded from the OD and OS 113
Figure 32: Example of a Scotopic Adaptation exam 113
Figure 33: Immunofluorescence image showing a cross-section of the retina after CS/HA-EPOβ administration 115
Figure 34: Immunofluorescence image of the HepG2 cells 116
Figure 35: Photomicrographs of the treated eye cross-sections after CS/HA-EPOβ administration stained with hematoxylin and eosin 116
Figure 36: Representation of the ERG setup 127
Figure 37: Representation of a rat ocular globe painted with tissue dyes 128
Figure 38: Variation of the mean IOP (mmHg) through time after topical administration of CS/HA-EPOβ nanoparticles 130
Figure 39: Hematocrit (Htc) of all groups obtained from microhematocrit measurement 131
Figure 40: Example of ERG waveforms recorded in this study 131
Figure 41: Mean amplitudes of the a-wave (a) and b-wave (b) recorded from the OD and OS in the scotopic luminesce response 132
Figure 42: Photopic adaptation – a (a) and b (b) waves recorded from the OD and the OS in the five phases of light adaptation 133
Figure 43: Representation of the a and b waves mean amplitudes recorded from the OD and OS during the photopic luminesce response 134
Figure 44: Scotopic Adaptation – a and b waves mean amplitudes (μV) recorded from the OD and the OS. 135
Figure 45: Immunofluorescence images showing cross sections of the retina after CS/HA-EPOβ topical administration 137
Figure 46: Immunofluorescence image showing a cross section of the retina of a control eye (OS) from group E after CS/HA topical administration 138
Figure 47: Cross sections of the OD from group E after CS/HA-EPOβ topical administration 139
Figure 48: Representation of the ERG setup. 150

Figure 49: Representation of a rat ocular globe: yellow arrows indicate the cauterized episcleral veins.....151
Figure 50: Photos of a rat ocular globe during the microsurgical procedure.....152
Figure 52: Representation of a rat ocular globe painted with tissue dyes.....153
Figure 53: Pictures of a rat 1 hour (a) and 3 days (b) after the cauterization of the episcleral veins of the OD 156
Figure 54: Mean IOP from the OD (orange) and from the OS (blue) since the day of glaucoma induction (t = 0) until 21 days later.....158
Figure 55: Example of ERG waveforms recorded from the OD at the beginning of the study (black) and at day 3 after the glaucoma induction (orange) 161
Figure 56: ERG waveforms of the OD (orange) and the OS (black) recorded at day 3 and day 21 after the glaucoma induction.....165
Figure 57: Photomicrographs of retinal sections from the OD, 21 days after glaucoma induction, from control (C21) and treatment (T21) groups, and from a non-glaucomatous eye (OS) 166
Figure 58: Immunofluorescence photomicrographs showing cross sections of the OD (treated eye) and OS.....168
Figure 59: Photomicrographs of retinal sections submitted to immunohistochemistry for apoptosis detection (cleaved caspase-3).....169

List of tables

Table 1: Examples of the studied therapeutic agents and strategies as neuroprotective in glaucoma or in similar neurodegenerative models. 9
Table 2: Mucoadhesive liposomal formulations with possible ophthalmological applications. 31
Table 3: Mucoadhesive niosomal formulations with possible ophthalmological applications. 35
Table 4: Mucoadhesive nanoemulsions with possible ophthalmological applications 38
Table 5: Mucoadhesive nanosuspensions with possible ophthalmological applications 45
Table 6: Mucoadhesive nanostructured lipid carriers with possible ophthalmological applications. 51
Table 7: Mucoadhesive polymeric nanoparticles formulations with possible ophthalmological applications 59
Table 8: Mucoadhesive dendrimers with possible ophthalmological applications 69
Table 9: Nanoparticles encapsulation efficiency and drug loading of EPOβ using different hyaluronic acids at 1:1 CS:HA mass ratio 84
Table 10: Rheology measurements of the different formulations tested. 87
Table 11: Zeta potential of nanoparticles upon dilution 1:1 with water or mucin dispersion ..87
Table 12: *Ex vivo* permeation parameters of nanoencapsulated EPOβ 89
Table 13: Each group's hematocrit (Htc) was obtained from the microhematocrit measurement before and after the CS/HA-EPOβ nanoparticles administration 107
Table 14: Photopic adaptation – mean amplitudes of the a-wave and the b-wave (μV) recorded from the OD and OS 110
Table 15: Photopic flicker – mean amplitudes of the a-wave and b-wave (μV; mean ± SD) recorded from the OD and OS 134
Table 16: IOP measurements (mmHg) for both eyes, before and after (T=0) glaucoma induction, in treatment (n=12) and control groups (n=12).. 157
Table 17: ERG results from the OD – a-waves and b-waves recorded during the five ERG components 160
Table 18: ERG results of the OD after glaucoma induction – b-wave mean amplitudes recorded in a single step of each ERG part 162
Table 19: ERG (b-wave) comparison between timepoints T3 and T7, T14 and T21 after glaucoma induction in the OD, both in treated and control groups. 163
Table 20: Retinal thickness measurements (μm) of the OD from treatment and control groups at day 7, 14 and 21 166

Acronyms and Abbreviations

APBA-ChS – 3-aminomethylphenyl)boronic acid and chondroitin sulfate
AKT – protein kinase B
APAF – apoptosis protease activating factor
ARPE – adult retinal pigment epithelium-19
ATP – adenosine triphosphate
BAB – blood-aqueous barrier
BAD – Bcl-2 associated agonist of cell death
BAX – Bcl-2-asssociated x protein
Bcl-2 – B-cell lymphoma 2
Bcl-xL – B-cell lymphoma extra-large
BDNF – brain derived neurotrophic factor
BRB – blood-retina barrier
CB1 – cannabinoid receptor 1
CB2 – cannabinoid receptor 2
CNTF – ciliary neurotrophic factor
CS – chitosan
DAB – 3,3′-Diaminobenzidine
DAPI – 4′,6-diamidino-2-phenylindole
dATP – deoxyadenosine triphosphate
DCC – deleted in colorectal cancer
DISC – death-inducing signaling complex
%DL – drug loading capacity
DMSO – dimethyl sulfoxide
DNA – deoxyribonucleic acid
DPPC – dipalmithoyl-phosphatidylcholine
ERG – electroretinography
%EE – encapsulation efficiency
EPOβ – epoetin beta
EPO – erythropoietin
EPOR – erythropoietin receptor
ERK – extracellular signal-regulated kinase
FADD – Fas-associated death domain
FGF2 – fibroblast growth factor 2
GCL – ganglion cell layer
GPR143 – G-protein coupled receptor 143

HACC – hydroxypropyltrimethyl ammonium chloride chitosan

HA – hyaluronic acid

HCE – human corneal epithelial cells

HCE-T – human corneal epithelial cell-transformed

HDNP – hydrogel poly(lactic-co-glycolic acid) nanoparticle platform

HE – hematoxylin and eosin

HepG2 – hepatoma G2

HIF – hypoxia-inducible factor

Htc – hematocrit

IF – immunofluorescence

IL – interleukin

ILM – inner limiting membrane

INL – inner nuclear layer

IOP – intraocular pressure

IPM – interphotoreceptor matrix

IU – international units

JAK – Janus kinase

L-DOPA – Levodopa

MAPK – mitogen-activated protein kinase

MET - active metabolite of cloricromene

MIC – minimal inhibitory concentration

MMP – mitochondrial membrane permeabilization

MW – molecular weight

NaCl – sodium chloride

$NaHCO_3$ – sodium bicarbonate

NFL – nerve fiber layer

NF-κB – Nuclear factor kappa-light-chain-enhancer of activated B cells

NMDA – N-Methyl-D-Aspartate

NLC – nanostructured lipid carriers

NP – nanoparticle

OD – *oculus dexter*

OLM – outer limiting membrane

ONL – outer nuclear layer

OPL – outer plexiform layer

OS – *oculus sinister*

PA – photopic adaptation

PAMAM – polyamidoamine

PBS – phosphate buffered saline

PEG – polyethylene glycol

PF – photopic flicker

PDI – polydispersity index

PD – pharmacodynamics

PI – propidium iodide

PI3K – phosphatidylinositol 3-kinase

PK – pharmacokinetics

PLR – photopic luminescence response

RGC – retinal ganglion cells

rhEPO – recombinant human erythropoietin

RPE – retinal pigment epithelium

ROS – reactive oxygen species

SA – scotopic adaptation

SD – standard deviation

SLN – solid lipid nanoparticles

SLR – scotopic luminescence response

STAT – signal transducers and activators of transcription

STF – simulated tear fluid

TFF – trefoil factors

TMC – trimethylchitosan

TNF – tumor necrosis factor

TRAIL – TNF-related apoptosis-inducing ligand

TRAMP – TNF receptor–related apoptosis-mediating protein

TrkB – tropomyosin receptor kinase B

TUDCA – tauroursodeoxycholic acid

VEGF – vascular endothelial growth factor

ZP – zeta potential

Outcomes of this Thesis

- **Oral presentations**

B. Silva, J. Marto, B. São Braz, E. Delgado, L.M.D. Gonçalves (2018). “Nanoparticles of hyaluronic acid and chitosan for ocular delivery of erythropoietin”. European Society of Veterinary Ophthalmology (ESVO) Meeting 2018, October 11-14, Prague, Czech Republic. Abstract book page 79. Abstract published in Vet. Ophthalmology, February 12, 2019, pages E1-E8, https://doi.org/10.1111/vop.12630.

B. Silva, J. Marto, B. São Braz, E. Delgado, L.M.D. Gonçalves (2018). “Development of a hyaluronic acid and chitosan nanoparticulated system for topical ocular delivery of erythropoietin”. CIISA Congress 2018, November 16-17. Faculty of Veterinary Medicine, Universidade de Lisboa, Lisbon, Portugal. Abstract book page 57.

B. Silva, J. Marto, B. São Braz, E. Delgado, L.M.D. Gonçalves (2019). “A Novel Approach to Ocular Delivery of Erythropoietin”, in Nanostructured Systems for Overcoming Biological Barriers. Postgraduate Students Meeting & 4rd i3DU Meeting, July 15. iMed.ULisboa, Faculty of Pharmacy, Universidade de Lisboa, Lisbon, Portugal.

B. Silva, B. São Braz, L.M. Gonçalves and E. Delgado (2021). “In vivo evaluation of a nanoparticulate system for EPOβ ocular delivery by subconjunctival route: safety, electrophysiology and immunohistochemistry”. European Society of Veterinary Ophthalmology (ESVO) Virtual Meeting 2021 (won Best Presentation Award).

B. Silva, L. Gonçalves, B. São Braz, and E. Delgado (2022). “Effects of chitosan-hyaluronic acid-epoetin beta nanoparticles in glaucomatous rats after topical ocular administration”. European Society of Veterinary Ophthalmology (ESVO) Conference 2022, September 29-October 2, Berlin, Germany.

- **Poster presentations**

B. Silva, J. Marto, B. São Braz, E. Delgado, L.M.D. Gonçalves (2018). “Development of a hyaluronic acid and chitosan nanoparticulated system for topical ocular delivery of erythropoietin”. CIISA Congress 2018, November 16-17. Faculty of Veterinary Medicine, Universidade de Lisboa, Lisbon, Portugal. Abstract book page 57.

B. Silva, B. São Braz, L. Gonçalves and E. Delgado (2021). “In vivo evaluation of a nanoparticulate system for EPOβ ocular delivery by subconjunctival route: safety, electrophysiology and immunohistochemistry”, in Advanced Technologies for Drug Delivery. iMed.ULisboa Virtual Meeting 2021, June 16, 23 and 30 and July 7. Faculty of Pharmacy, Universidade de Lisboa, Lisbon, Portugal.

B. Silva, L. M. Gonçalves, B. São Braz and E. Delgado (2022). “Delivery of epoetin beta by chitosan-hyaluronic acid nanoparticles through subconjunctival and topical ocular administrations in rats”. L4Animals Congress – Laboratório Associado para Ciência Animal e Veterinária, May 6-7. Faculty of Veterinary Medicine, Universidade de Lisboa, Lisbon, Portugal.

B. Silva, L. M. Gonçalves, B. São Braz and E. Delgado (2022). “Topical ocular delivery of epoetin beta in nanoparticles in Wistar Hannover rats”. Encontro Ciência 22 – Encontro com a Ciência e a Tecnologia em Portugal, May 16-18. Lisbon Congress Centre, Lisbon, Portugal.

B. Silva, L. M. Gonçalves, B. São Braz and E. Delgado (2022). “Chitosan and hyaluronic acid nanoparticles as topical ocular delivery system for epoetin beta: in vivo study in Wistar Hannover rats” in Advanced Technologies for Drug Delivery. 13th iMed.ULisboa Meeting 2022, July 4 e 5, Faculty of Pharmacy, Universidade de Lisboa, Lisbon, Portugal.

- **Papers *in extenso***

B. Silva, J. Marto, B. São Braz, E. Delgado, A.J. Almeida, L. Gonçalves. “New nanoparticles for topical ocular delivery of erythropoietin”. Int J Pharm. 2020 Feb 25; 576:119020. doi: 10.1016/j.ijpharm.2020.119020. Epub 2020 Jan 11. PMID: 31935477.

B. Silva, B. São Braz, E. Delgado, L. Gonçalves. “Colloidal nanosystems with mucoadhesive properties designed for ocular topical delivery”. Int J Pharm. 2021 Sep 5; 606:120873. doi: 10.1016/j.ijpharm.2021.120873. Epub 2021 Jul 9. PMID: 34246741.

B. Silva, L. Gonçalves, B. São Braz, E. Delgado. “Chitosan and Hyaluronic Acid Nanoparticles as Vehicles of Epoetin Beta for Subconjunctival Ocular Delivery”. Mar. Drugs 2022, 20, 151. https://doi.org/10.3390/md20020151.

B. Silva, L. Gonçalves, B. São Braz, E. Delgado. "Topical ocular delivery of nanoparticles with epoetin beta in Wistar Hannover rats”. Sci Rep 13, 1559 (2023). https://doi.org/10.1038/s41598-023-28845-0.

B. Silva, L. Gonçalves, B. São Braz, E. Delgado. “Topical Administration of a Nanoformulation of Chitosan-Hyaluronic Acid-Epoetin Beta in a Rat Model of Glaucoma”. Pharmaceuticals 2023, 16, 164. https://doi.org/10.3390/ph16020164.

CHAPTER 1

Introduction, conceptualization and objectives

1.1. Introduction

1.1.1. Glaucoma: a neurodegenerative disorder

Despite the fact that glaucoma overall incidence in dogs is less than 1%, this disease is one of the leading causes of irreversible blindness in canine patients, and also a source of chronic pain (Ofri and Narfström 2007) that often leads to enucleation. Secondary glaucoma is generally more frequent than primary and congenital glaucoma, and its incidence can range from 0.8% (Gelatt and MacKay 2004) to 3.6% (Strom et al. 2011), depending on the characteristics of the canine population studied. In cats, glaucoma is less frequent, especially primary glaucoma which is considered rare, and the general prevalence varies from 0.3% to 0.9% (McLellan and Miller 2011). Regarding human patients, according to the last World Health Organization report, 7.7 million people in the world suffer from glaucoma, which is the second worldwide most common cause of blindness, after cataracts (World Health Organization 2014). However, in terms of public health, glaucoma represents a more concerning disorder than cataracts, as its consequent blindness is irreversible (Kingman 2004).

Glaucoma is characterized as a group of diseases that cause optic neuropathy and progressive retinal degeneration, particularly dramatic in the retinal ganglion cells (RGC) (Ghate and Edelhauser 2008; Vidal-Sanz et al. 2012). The retina is the tissue that surrounds the inner surface of the vitreous cavity (Willoughby et al. 2010), as illustrated in figure 1, and it is the light-processing center of the eye, where light is converted into electrical signals that are translated into images by the brain (J. Zhu et al. 2012). It is divided in 10 layers (Figure 2) which are, from outer to inner, the retinal pigment epithelium (RPE), the interphotoreceptor matrix (IPM), the outer limiting membrane (OLM), the outer nuclear layer (ONL), the outer plexiform layer (OPL), the inner nuclear layer (INL), the inner plexiform layer (IPL), the ganglion cell layer (GCL), the nerve fiber layer (NFL) and finally the inner limiting membrane (ILM) (J. Zhu et al. 2012). Basically, the neural retina consists of photoreceptors (cones and rods), bipolar cells, horizontal cells, amacrine cells and ganglion cells that receive and transform light, and Müller glia cells that sustain the whole neural retina (Willoughby et al. 2010), as shown in figure 2.

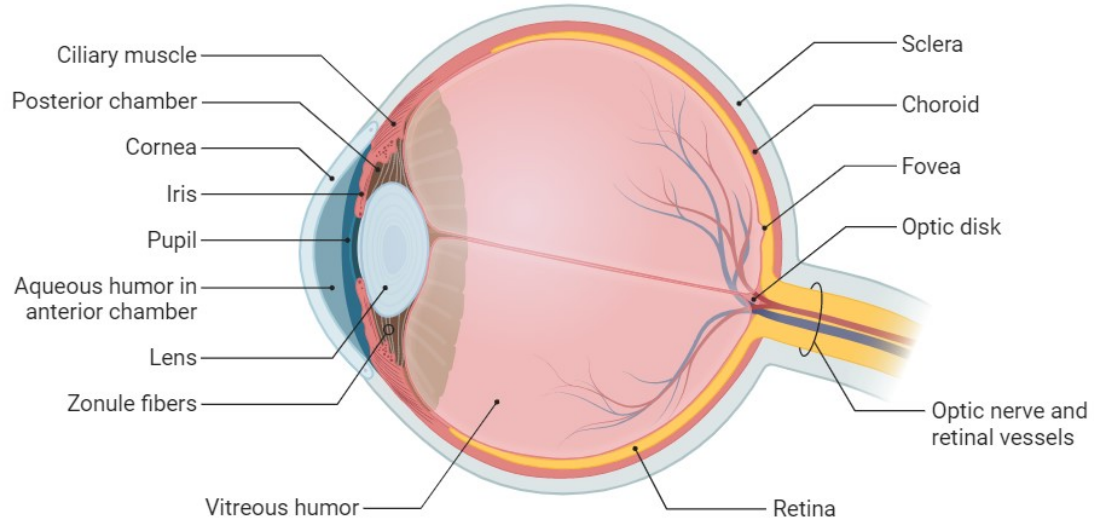

Figure 1: Ocular structures of the human eye (Adapted from "Anatomy of the Human Eye", BioRender.com).

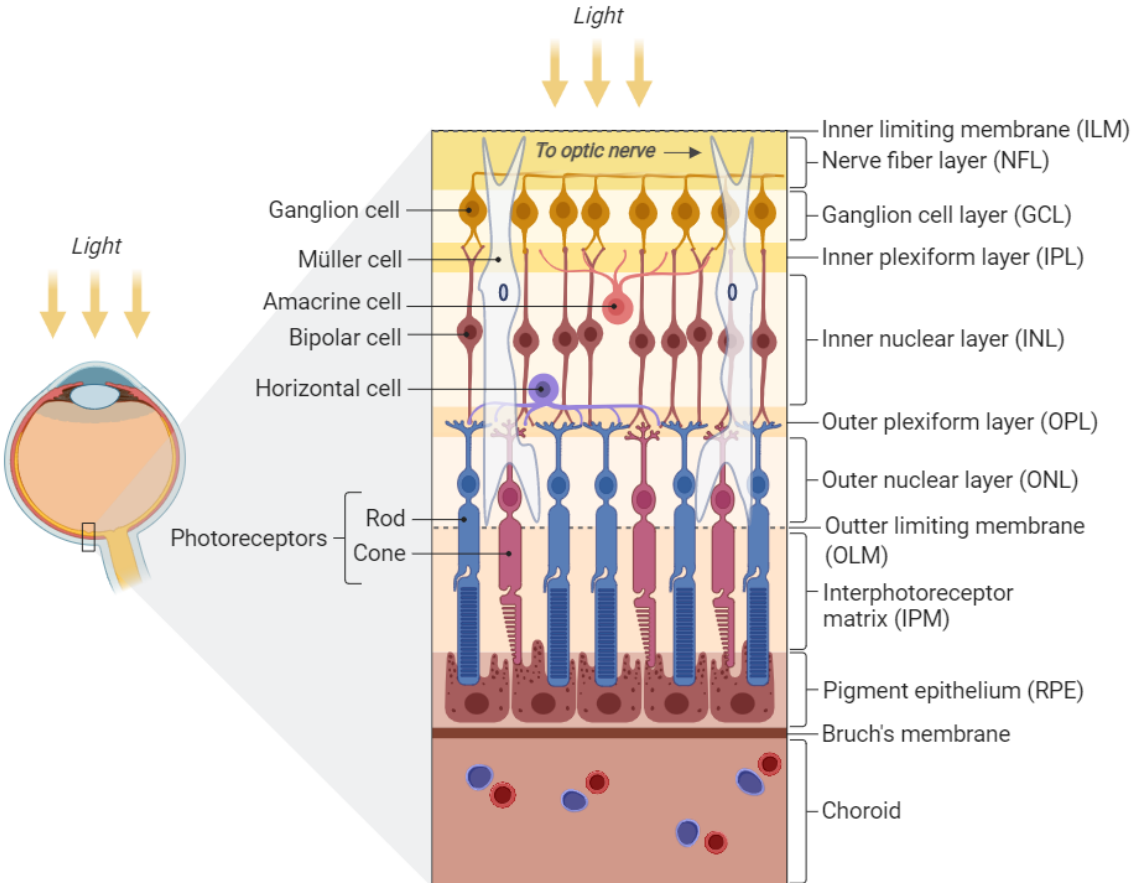

Figure 2: Representation of the retinal layers and main retinal cells in a human eye (Adapted from "Structure of the Retina", BioRender.com).

The mechanism of degeneration and death of RGC in glaucoma is complex and not fully understood, but the most significant risk factors are increased intraocular pressure (IOP), age, corneal thickness and ethnicity (Quigley 2011). Glaucoma can be classified as congenital, juvenile, primary (open-angle and closed-angle) and secondary (open-angle and closed-angle) (Goel et al. 2010) and it is know that not all glaucoma forms imply elevated IOP, but IOP has a prominent role in this disease since it is the only manageable risk factor (Ghate and Edelhauser 2008). In veterinary patients, there is no report of normal-tension glaucoma so far. IOP is physiologically maintained through a balance between the inflow and the outflow of the aqueous humor, which is produced in the ciliary body and drained by conventional (trabecular meshwork) and unconventional (uveoscleral) pathways (Goel et al. 2010). The IOP in awake individuals can vary considerably but it is, in average, 15-16 mmHg in humans (Anand 2015), 18.0 ± 2.6 mmHg in dogs (Guresh et al. 2021), 20.7 ± 0.5 mmHg in cats (Rusanen et al. 2010) and 18.4 ± 0.1 mmHg in rats (Wang et al. 2005), and it can normally vary during the day and with age.

If elevated IOP is settled, a sequence of events occur that can lead to retinal degeneration. Since the ocular globe has a semirigid structure that hinders its adaptation to extreme IOP fluctuations, high IOP potentially alters retinal perfusion and axonal transport (Almasieh et al. 2012; Vidal-Sanz et al. 2012), that could lead to deficiency of neurotrophic factors or other vital molecules in the retina, contributing to RGC loss (Almasieh et al. 2012). Neurotrophins are a group of small secreted peptides that protect the central neurons from degeneration, in which the brain derived neurotrophic factor (BDNF) is the most important to RGC survival (Almasieh et al. 2012). BDNF is retrogradely transported (from axon to cell body) by RGC axons to the retina (Herzog and Von Bartheld 1998; Ma et al. 1998), and impairments in the retrograde axonal transport are described in rat and mouse models of glaucoma (Kim et al. 2004; Salinas-Navarro et al. 2009) and in human high pressure secondary glaucomas (Knox et al. 2007). A study correlates the elevation in IOP with optic nerve head and retinal accumulation of dynein, a motor protein that mediates retrograde axonal transport in RGC, compromising axonal function and RGC viability (Martin et al. 2006). In addition, a recent study indicates that, in naturally glaucomatous mice, axonal transport failed before the RGC axons and the pre-synaptic terminals, denoting that the disease's progression is distal-to-proximal and implying that therapeutic strategies for glaucoma should firstly consider the RGC axonal transport (Crish et al. 2010).

Excitotoxicity might also contribute to neuronal death in glaucoma, and it can be associated or not with an increased IOP and/or ischemic conditions. Basically, excitotoxicity is described as the exposure of the central nervous system to glutamate in high concentrations or for long periods of time (D. Lukasiewicz 2005). In the retina, glutamate receptors are located mostly in the IPL with glutamatergic synapses connecting bipolar cells to RGC and amacrine

cells, and secondly in the OPL where photoreceptors, bipolar cells, and horizontal cells interact synaptically (D. Lukasiewicz 2005). The precise role of glutamate in the pathophysiology of glaucoma requires additional and more consistent research, but it is believed that the excess of glutamate binds to cell surface ionotropic glutamate receptors, primarily NMDA (N-Methyl-D-Aspartate) receptors, triggering massive calcium influx and activating the signaling of neuronal pro-apoptotic cascades (Almasieh et al. 2012). On the other hand, small and consistent variations in extracellular glutamate concentration could also influence glaucoma's progression, meaning that even normal amounts of glutamate in the retina could potentially be neurotoxic if the balance production-clearing is not achieved (Almasieh et al. 2012).

Another mechanism of neuronal damage in glaucoma is the oxidative stress as a consequence of the unbalance between production and elimination (by antioxidants) of reactive oxygen species (ROS), which are continuously produced by mitochondrial activity, neurotransmitters enzymatic degradation, neuroinflammatory mediators, and redox reactions (Halliwell 2006). Neurodegenerative diseases usually lead to increased levels of ROS whose origin can be mitochondrial dysfunction, abnormal protein folding, and defective ubiquitination and proteasome degradation systems (Andersen 2004). ROS can induce neuronal death through many mechanisms, including protein and DNA alteration, but it is unknown if oxidative stress is the trigger of cell death or just a component of neurodegeneration (Andersen 2004).

Neuroinflammation is an immune reaction occurring in the central nervous system in response to several insults, including glaucoma. The neuroinflammatory response involves the multiplication of microglia and astrocytes, and the release of a pro- and anti-inflammatory cytokines, neurotransmitters, chemokines and reactive oxygen/ nitrogen species, in order to stop the injury and retard the damage (Vivekanantham et al. 2015). Neuroinflammation is important to promote phagocytosis of debris, release of trophic factors, mobilization of neural precursors and axonal regeneration/ remyelination (Schwartz and London 2009), and under physiological conditions a down-regulation occurs, creating a negative feedback that stops inflammation (Griffiths et al. 2007). In case of prolonged inflammation with impairment of the blood-retinal barrier, such as in glaucoma, regulatory mechanisms might fail inducing, among other responses, a pro-apoptotic cascade of reactions in RGC, compromising their survival (Vohra et al. 2013). An extensive and recent review article on neuroinflammation in glaucoma addresses the RGC death as a consequence of multifactorial origin. Curiously, astrocytes, microglia and Müller cells activation in response to retinal insults appears to have both neuroprotective and detrimental effects on RGC, depending on the severity and duration of the insult (Russo et al. 2016). A wide variety of mechanisms comprising reactivity of astrocytes, microglia and Müller cells leads to the expression of pro-inflammatory/ inflammatory molecules, such as metalloproteases, tumor necrosis factor alpha (TNF-α), interleukins (IL), ROS and prostaglandins, which can be up-regulated in glaucoma (Russo et al. 2016).

Apoptosis is another complex mechanism of cell death in glaucoma and apoptosis of the RGC has already been confirmed in hypertensive eyes of rats using real-time imaging (Cordeiro et al. 2004). Two pathways are involved in the apoptotic process (Figure 3) – intrinsic and extrinsic – and both routes culminate in cell atrophy, chromatin condensation and nuclear/ DNA fragmentation (Kroemer et al. 2007). The intrinsic pathway of apoptosis consists in an intracellular sequence of events involving mitochondrial permeabilization, which regulates the release of cytochrome C (Kroemer et al. 2007). The presence of cytochrome C outside the mitochondria, along with ATP/dATP, enables the activation of apoptosis protease activating factor 1 (APAF-1) which activates caspase-9 ("initiator caspase", like caspase-8 and caspase-10) creating a multiprotein complex called "apoptosome". Following this event, caspase-9 catalyzes the proteolytic activation of caspases-3, -6, and -7 ("executioner caspases") which contribute to cell deterioration (Cain et al. 2002). Being so, cleaved caspase-3 is a typical apoptotic marker commonly used in RGC apoptosis (Tan et al. 2020). On the other hand, the extrinsic pathway initiates with the ligand-induced activation of death receptors, which are a subset of the TNF receptor family, including TNFR1, Fas/CD95, TRAIL (TNF-related apoptosis-inducing ligand) receptors -1 and -2, and probably the death receptor 3 (TRAMP, translocating chain-association membrane protein). This ligation of death receptors leads to the recruitment and oligomerization of the adapter molecule FADD (Fas-associating death domain-containing protein), creating the death-inducing signaling complex (DISC), which then activates caspases-8 and -10 (Debatin and Krammer 2004). Alternatively, in the absence of ligands, the extrinsic route can be activated by the dependency receptors, which apparently trigger a rapid caspase activation, creating a state of cellular dependence from their ligands. The prototype dependency receptors are the netrin-1 receptors DCC (deleted in colorectal cancer) and UNC5H-1, -2 and -3 (Mehlen and Bredesen 2004).

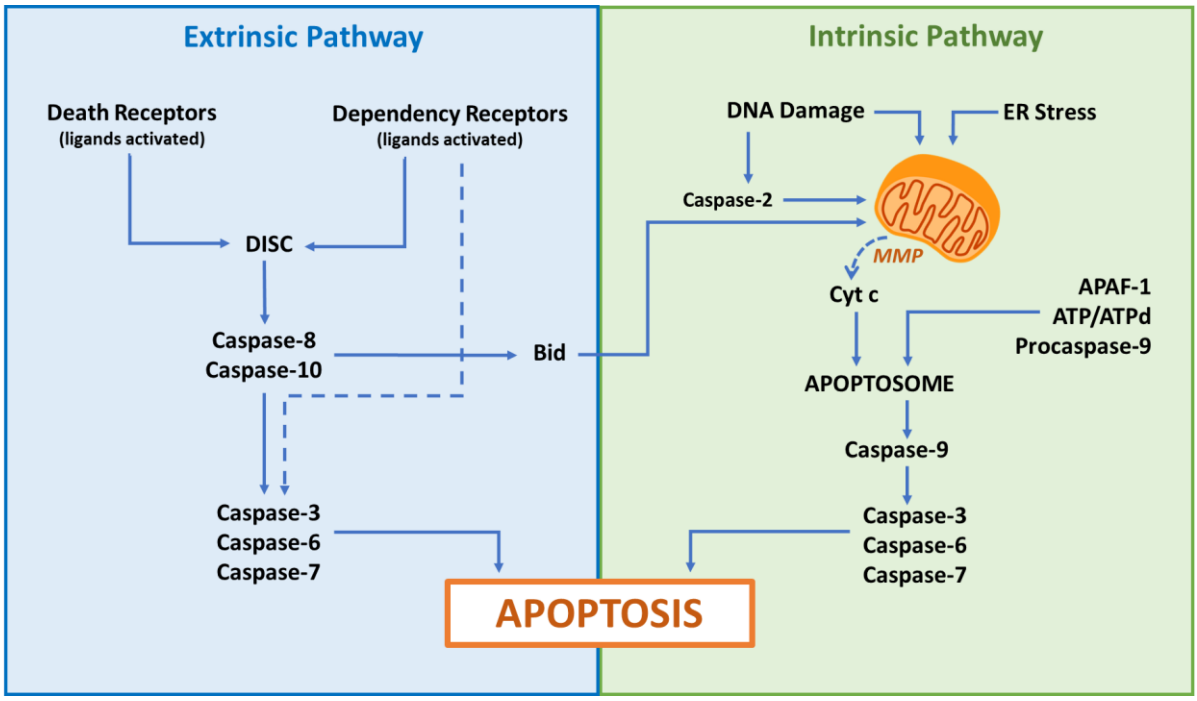

Figure 3: Representation of the intrinsic and extrinsic pathways of the apoptotic process (Adapted from Kroemer at al., 2007). DISC, death-inducing signaling complex; Bid, pro-apoptotic protein of the Bcl-2 family; ER, endoplasmic reticulum; MMP, mitochondrial membrane permeabilization; Cyt c, cytochrome c; APAF-1, apoptosis protease activating factor 1.

1.1.2. The potential of neuroprotection in glaucoma

The neurodegeneration process associated to glaucoma is not completely understood and occurs in several fronts, yet current glaucoma treatment does not address this issue. It is stablished that reducing the IOP by ocular medications prevents the onset and delays disease's progression (Heijl et al. 2002; Kass et al. 2002). Thus, medical, surgical or parasurgical treatments to lower IOP are presently the only feasible therapeutical option available (Nucci et al. 2016). Nevertheless, some patients experience disease progression, despite a controlled IOP within normal range of values (Leske et al. 2003), which supports that RGC death is not absolutely related to IOP values and other therapeutic approaches should be considered.

Studies have showed that taurine-conjugated derivative tauroursodeoxycholic acid (TUDCA) prevents apoptosis by stabilizing the mitochondrial membrane (Botla et al. 1995; Rodrigues et al. 1998), suppressing the pro-apoptotic P53 protein (Park et al. 2008), reducing endoplasmic reticulum (ER) stress by improving protein folding capacity (Omura et al. 2013), decreasing ROS (Mantopoulos et al. 2011; Oveson et al. 2011); and has anti-inflammatory effects by diminishing glial cell activation (Noailles et al. 2014; Romero-Ramírez et al. 2017).

In rodent models of photoreceptors degeneration, TUDCA preserved retinal function and promoted cell survival (Phillips et al. 2008; Oveson et al. 2011). So far, studies on RGC degeneration have not involved glaucoma (Daruich et al. 2022), but in other disease models TUDCA showed 20% more RGC survival and substantial improvements in the electroretinography (ERG) (Gómez-Vicente et al. 2015), and also reduced several ER stress markers (Chao De La Barca et al. 2016), presenting a strong potential to improve RGC survival and function in glaucoma.

Researchers studied progesterone as a neuroprotective agent and discovered that it increases anti-apoptotic proteins (Bcl-2, Bcl-xL) and reduces pro-apoptotic proteins (BAX, BAD, caspase-3) in brain trauma (Djebaili et al. 2005; Yao et al. 2005), increases BDNF levels (González et al. 2004), reduces excitotoxicity (Puia and Belelli 2001) and also decreases inflammatory cytokines, such as TNF-α and IL-6 (Ishrat et al. 2010; Allen et al. 2016). Moreover, progesterone promotes myelination (Chan et al. 1998; Ghoumari et al. 2003), and decreases the activity of microglia (Drew and Chavis 2000) and macrophages (Miller and Hunt 1998). In a model of elevated IOP and ischemia reperfusion, the preservation of the inner retinal neurons using progesterone was observed (Lu et al. 2008). In another ocular model, of ischemia, retinal function was substantially preserved, and the number of RGC was 1.3-fold higher with progesterone treatment (Allen et al. 2015). Furthermore, due to the progesterone's ability to reduce IOP (Posthumus 1952), this hormone appears to have great potential in glaucoma therapy. However, human research is contradictory and studies using oral administration often fail to differentiate between natural and synthetic hormones, requiring a better experimental design in the future (Pardue and Allen 2018).

Despite the absence of studies reporting glaucoma models to test dopamine as a neuroprotective treatment, in a light-damage model of retinal degeneration in mice, dopamine agonists diminish photoreceptors functional loss and cell death (Shibagaki et al. 2015), which was also observed in ischemic and traumatic optic neuropathies (Lyttle et al. 2016; Reza Razeghinejad et al. 2016). In type I diabetes, treatments that increase retinal dopamine decrease visual and retinal impairments, while dopamine deficiency leads to premature visual dysfunction (Aung et al. 2014). The dopaminergic system may also be involved in the regulation of IOP, with D1 receptor agonists increasing IOP, and D2 and D3 agonists decreasing IOP (Pescosolido et al. 2013). Moreover, levodopa, also known as L-DOPA, may stimulate G protein coupled receptors, like GPR143, in the RPE, which may have beneficial effects in age-related macular degeneration (Lopez et al. 2008; McKay and Schwartz 2016). It is believed that L-DOPA and dopamine agonists may re-establish dopamine levels lost during a degenerative disease, thereby restoring visual and neuronal function, but studies are needed to clarify if dopamine also has a direct neuroprotective effect.

Several neurotrophic factors are present in the eye and have revealed protective or rescue effects after mechanical trauma, environmental toxicity, or hereditary disease. Neurotrophic factors, like BDNF, ciliary neurotrophic factor (CNTF), fibroblast growth factor (FGF)-2, and IL-1α have been administered directly into the eye (Faktorovich et al. 1990; LaVail et al. 1992), through viral vectors (Cayouette and Gravel 1997; Lau et al. 2000) or encapsulate cell technology (Tao et al. 2002) as a treatment for degenerative retinal diseases. BDNF does not cross the blood brain barrier and as its level is decreased in the glaucomatous retina (Kimura et al. 2016), possible therapies have targeted activation of the BDNF receptor TrkB, with positive results in promoting RGC survival in acute and chronic glaucoma models (Bai et al. 2010; Hu et al. 2010). RGC survival was also achieved by activation of BDNF TrkB signaling through genetic means in animal models (Kimura et al. 2016). Additionally, repeated neuronal activation by visual stimulation can promote BDNF release and synaptic strength (Mui et al. 2018). Future studies are required to assess the viability of these approaches to enhance neuronal function and structure.

Cannabinoids have been extensively investigated in glaucoma as lowering IOP medication, but their effect is short-timed and affected by tolerance development (Passani et al. 2020). Nevertheless, some cannabinoids present excellent neuroprotective properties without systemic or psychotropic effects (Passani et al. 2020). Since cannabinoid receptors 1 and 2 are expressed in human retina/ RPE and ciliary body, exogenous cannabinoids administration might modulate retinal signal transduction, photo-transduction and IOP (Chen et al. 2005; Nucci et al. 2008; Dasilva et al. 2012; Cairns et al. 2016). Cannabinoids present significant neuroprotective effects on both central and peripheric nervous system, by reducing glutamate release, endothelin-1 and oxidative stress by the inhibition of nitric oxide release (Marsicano et al. 2003; Lax et al. 2014; Krishnan and Chatterjee 2015). Scientific evidence on this topic remains limited, especially in long-term treatment, but further studies assessing cannabinoids neuroprotective, vasorelaxant, and antioxidant properties in glaucoma would be of interest (Passani et al. 2020).

Table 1 presents other examples of neuroprotective agents studied in glaucoma models or in comparable neurodegenerative models.

Despite the promising scenario towards neuroprotection in glaucoma, these neuroprotective strategies still need years of dedicated research to evaluate drugs' pharmacokinetics and pharmacodynamics, optimize dosing and routes of administration, study clinical efficacy and possible long-term side effects, etc., before being available as therapeutic agents.

Table 1: Examples of the studied therapeutic agents and strategies as neuroprotective in glaucoma or in similar neurodegenerative models.

Action	Antagonized mechanism	Reference
Asiatic acid	Apoptosis	(W. Huang et al. 2018)
BDNF	Neurotrophic deprivation	(Ko et al. 2000) (Klöcker et al. 2000)
Brimonidine	Excitotoxicity	(Wheeler et al. 2003) (Vidal et al. 2010) (In Jung et al. 2015)
Coenzyme Q10	Excitotoxicity Oxidative stress	(Nucci et al. 2007) (Rossella Russo et al. 2008) (Lee et al. 2014)
Enriched environment	Oxidative stress Excitotoxicity Neuroinflammation	(Fleitas et al. 2022)
Erythropoietin*	Apoptosis Excitotoxicity	(L. Zhong et al. 2007) (Kawakami et al. 2001)
Gene therapy	Neurotrophic deprivation Oxidative stress Excitotoxicity Apoptosis	(Rhee and Shih 2021)
Glutamate receptors	Excitotoxicity	(Sucher et al. 1997) (Adachi et al. 1998) (Nucci et al. 2005)
Memantine	Excitotoxicity	(Hare and Wheeler 2009) (Ju et al. 2009)
Taurine	Excitotoxicity	(Froger et al. 2012)
Valproic acid	Neurotrophic deprivation	(Kimura et al. 2015)
17β-estradiol	Excitotoxicity	(R. Russo et al. 2008)

*Assessed in detail in the next section

1.1.3. Glaucoma and Erythropoietin

Erythropoietin as a neuroprotective agent in the retina

Erythropoietin (EPO) is a 30.4 kDa glycoprotein hormone, mainly produced in the fetal liver and adult kidney, whose core function is regulating erythropoiesis by promoting the progress of erythrocyte precursors into mature red blood cells, through apoptosis blocking in the blast cell lineage (Handelman and Levin 2008). The action of EPO is not restricted to the erythroid tissues and the presence of EPO and its receptors (EPOR) in eye, brain, spinal cord, heart, skin, smooth muscle cells and vascular endothelium, proposes autocrine and/or paracrine functions, which are vital for homeostasis (Caprara et al. 2014). In the human eye,

EPO and EPOR are present in the synaptic terminals and inner segments of the choroid, RPE, photoreceptors, INL and GCL (Rex et al. 2004). These findings justify the research that suggest EPO as a therapeutical option in several ocular disorders, as shown in figure 4.

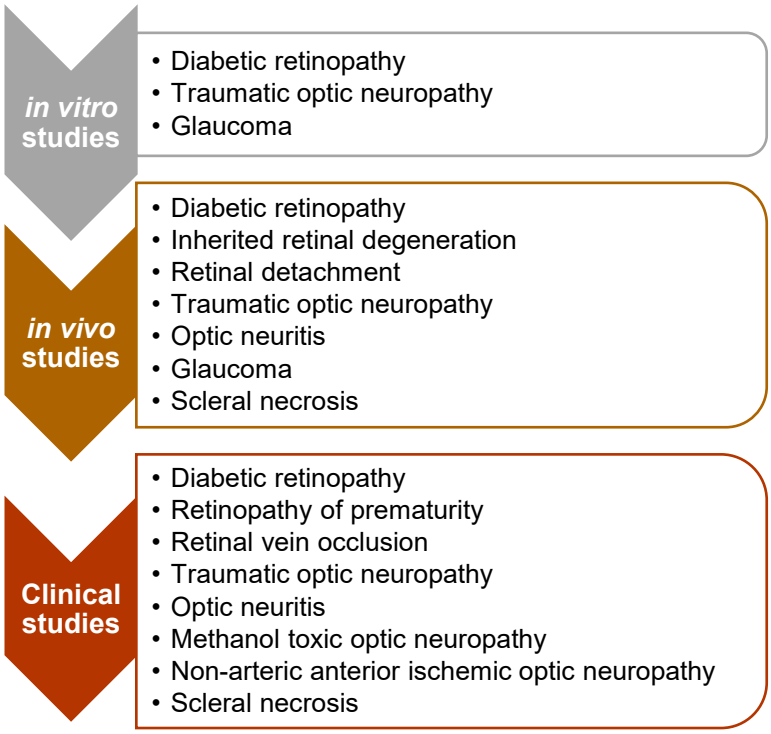

Figure 4: Ophthalmological disorders under research using erythropoietin as part of the therapeutic approach (Adapted from Feizi et al. 2021).

Recent review articles on ophthalmological applications of EPO report several neuroprotective actions through anti-apoptotic, anti-inflammatory and antioxidant effects, for example, by decreasing glutamate and ROS, preserving glia cells, recruiting stem cells, enhancing blood flow into damaged tissues, among other actions (Tsai et al. 2007; Shirley Ding et al. 2016; Feizi et al. 2021). During oxidant injury, EPO is able to prevent caspase-3-like activities and the release of inflammatory cytokines. It also promotes RPE cells integrity, protecting cells through direct modulation of ROS levels, MMP, AKT1 phosphorylation, and cysteine protease activity (Wang et al. 2009). Antioxidant effects of EPO may develop through regulating heme oxygenase-1 and glutathione peroxidase, and diminishing iron-dependent oxidative damage by depleting body iron (Katavetin et al. 2007). EPO protects the brain from ischemia by activating the ERK-1/-2 and AKT pathways, and a parallel mechanism is foreseen in the retinal transduction signaling (Luo et al. 2015). EPO also stimulates endothelial cell mitosis by STAT3 (signal transducers and activators of transcription-3) signaling route,

regulates the recruitment of endothelial progenitor cells to the injured site, inhibits the apoptosis of endothelial cells and re-establishes their intercellular tight junction proteins, by Janus kinase-2 (JAK2) and phosphatidylinositol-3-kinase/AKT (PI3-K/AKT) pathways mediation (Kretz et al. 2005; Chen et al. 2008).

The anti-inflammatory action of EPO includes the down-regulation of pro-inflammatory cytokines, such as IL-1 β, IL-6 and TNF-α through JAK/ STAT transduction pathway (Liu et al. 2006); and the reversion of TNF-α induced damage by NF-κB activation (Digicaylioglu and Lipton 2001), including in the RGCs (Fuchs et al. 2005). At the same time, an increase in the production of anti-inflammatory IL-10 can be observed (Liu et al. 2006).

Antiapoptotic effects of EPO comprise the down-regulation of caspase-3, up-regulation of B-cell lymphoma extra-large (Bcl-XL), inhibition of cytochrome C mitochondrial release and management of intracellular calcium levels (Sullivan et al. 2012; Xie et al. 2012). Since the homodimeric EPOR is triggered by EPO, JAK2 activates some pathways and produces attachment sites for molecules like PI3-K/AKT, STAT, NF-κB and mitogen-activated protein kinase (MAPK) (Sullivan et al. 2012; Xie et al. 2012), which decreases the apoptotic rate. Activation of the Wingless signaling pathway that prevents apoptosis occurs after EPO binding to the EPOR and interleukin beta-common receptor heterodimer complex (De Iongh et al. 2006; Guan et al. 2013), which can be found in the ocular stem cells, photoreceptors, INL, and RGC (Colella et al. 2011). EPO is able to reduce the reactivity of Müller cells and upregulate the expression of CNTF and BDNF by the ERK-1/-2 and AKT routes, promoting RGC and photoreceptors survival (Hu et al. 2011). Moreover, studies demonstrated that EPO promotes regeneration of RGC axons after optic nerve transections (Böcker-Meffert et al. 2002; King et al. 2007; Y. Zhong et al. 2007).

Besides its protective action, EPO can be challenging due to an uncertain pathological effect on ocular angiogenesis and microvascular permeability. The production of EPO in response to hypoxia is mostly controlled by hypoxia-inducible factor (HIF)-1α, which is a transcription factor activated by low oxygen levels (Jelkmann 2007). Similarly, angiogenesis is caused by HIF-1α activation under hypoxic conditions, which promotes vascular endothelial growth factor (VEGF) transcript expression (Maes et al. 2012). Thus, EPO can modulate angiogenesis by inducing the secretion of VEGF (Shirley Ding et al. 2016). However, EPO also seemed to down-regulate HIF-1α and VEGF protein expressions and prevent neovascularization in early diabetic retinopathy (Zhang et al. 2010), meaning that the pathological angiogenic role of EPO is not fully understood yet.

Research assessing erythropoietin in glaucoma

Scientific research in glaucoma is interested in the neuroprotection as a mean to prevent RGC loss and the consequent visual impairment. EPO has proven to be effective in improving *in vitro* RGC survival by increasing resistance to inflammation, ischemia, oxidative damage and degeneration (Yamasaki et al. 2005). The same results occurred in a rat model of acute ocular hypertension using systemic (Fu et al. 2008) and intravitreal (Tsai et al. 2005) administrations of EPO. In a rodent retinal ischemia model induced by increasing IOP, recombinant human EPO (rhEPO) was administered by systemic route before or immediately after the injury. Results showed enhanced functional recovery, assessed by electroretinography, and reduced retinal histopathological damage (Anna K. Junk et al. 2002). The subconjunctival administration of EPOβ in a rat glaucoma model caused a substantial improvement in the photopic electroretinographic response and a less marked retinal atrophy, assessed by histopathology (Resende et al. 2018), demonstrating a neuro-protective effect. Retrobulbar administration of EPO in a model of acute ocular hypertension in rats substantially promoted RGC survival and somewhat preserved their ultrastructural characteristics (Zhong et al. 2008). In a chronic ocular hypertension rat model, using an intraperitoneal injection of EPO, results showed positive effects in the b-wave amplitudes in the electroretinogram (Gui et al. 2015). In a mouse model of pigmentary glaucoma, intraperitoneal administration of rhEPO reduced the RGC loss as efficiently as memantine (L. Zhong et al. 2007).

Regarding studies in humans, evidence has been found of a relation between EPO and glaucoma pathogenesis. The concentration of EPO in the aqueous humor of eyes with primary acute angle-closure glaucoma is considerably higher than in eyes with primary open-angle and chronic angle-closure glaucoma (Wang et al. 2010). Actually, in several types of glaucoma, namely primary open-angle glaucoma, primary acute angle-closure glaucoma, chronic angle-closure glaucoma, neovascular glaucoma, and pseudo-exfoliative glaucoma, the amount of intraocular EPO is increased (Cumurcu et al. 2007; Wang et al. 2010; M. Zhou et al. 2013). A study found that plasma concentrations of EPO and soluble CD44 (sCD44), a cytotoxic protein to RGC and trabecular meshwork cells, were comparable between a group with primary open-angle glaucoma and a group with cataracts. On the other hand, the aqueous humor levels of EPO and sCD44 were substantially increased in eyes with primary open-angle glaucoma compared to those with cataract. The study also reported that the amount of EPO or sCD44 was strongly related with the visual loss severity, in mild and moderate stages of primary open-angle glaucoma (Mokbel et al. 2010).

Despite the large number of experimental studies, no human clinical trial addressing the neuroprotective potential effects of EPO in glaucoma has been found in the literature.

1.2. Conceptualization and objectives

Glaucoma is a chronic neurodegenerative disease with major impact in public health and in veterinary medicine. Considering that the current glaucoma therapy solely involves IOP reduction, and no neuroprotective agent is available in clinical practice to prevent RGC degeneration, scientific investigation on the subject is of the utmost interest. Former studies have confirmed the neuroprotective effects of EPO in several tissues, including the retina. EPO and its recombinant versions, like epoetin beta (EPOβ), have been extensively used in clinical practice for managing erythropoiesis, but their use aiming ocular neuroprotection have not reached the phase of clinical studies. Still, several *in vitro* and *in vivo* studies have been approaching the neuroprotective action of EPO in glaucoma, which has demonstrated anti-apoptotic effects on RGC, with consequent preservation of visual function. Overall results are very promising but the route of administration of EPO is still an issue, since many studies use intravenous or intravitreal administrations, that lead to systemic or local secondary effects, respectively. Moreover, other risks associated to chronic EPO administration need to be addressed. Bearing this in mind, it would be interesting to consider a non-invasive route of administration of EPO, that could enable neuroprotection in the retina, with absent or residual secondary effects even in long-term treatments, being easy to manage and promoting patients' compliance to the treatment.

Recently, our team studied the effect of EPOβ in glaucomatous rats after subconjunctival administration, with promising results concerning retinal recovery (Resende et al. 2018). In addition, we proved that in an *ex vivo* model of pig eye that permeation of EPOβ after its topical administration is possible, since it trespassed the porcine ocular membranes conjunctiva, sclera and cornea (Resende et al. 2017), opening the possibility of exploring the topical ocular administration of EPOβ as a means of reaching the retina. However, considering the general low intraocular bioavailability of drugs after their topical instillation, it would be necessary to improve the precorneal residence time of EPOβ. Therefore, we considered developing a mucoadhesive nanoformulation able to preserve EPOβ's pharmacological activity, while increasing the contact time and promoting its diffusion across the ocular barriers. Therefore, we started this project by an extensive literature research on colloidal nanosystems with mucoadhesive properties for ocular topical administration (Chapter 2), to select the most adequate delivery system for EPOβ. The next chapter (Chapter 3) was dedicated to the development and optimization of mucoadhesive nanoparticles of chitosan and hyaluronic acid, designed to carry EPOβ into the ocular globe. Characterization of the nanoparticles and their *in vitro* and *ex vivo* properties was extensively performed in this chapter. The following chapters included the *in vivo* study of the nanoformulation in healthy Wistar Hannover rats by using both

the subconjunctival (Chapter 4) and the topical (Chapter 5) ocular routes of administration. These physiological studies aimed to evaluate the biological tolerance and safety, and the nanocarriers efficacy in delivering EPOβ to the retina without causing undesired ocular or systemic side effects. Finally, our research ends in Chapter 6, which is characterized by the study of the nanoformulation's effect in a rat model of experimental glaucoma, after topical ocular administration.

In resume, our goal was to develop an eye drop system that could efficiently deliver EPOβ to the retina, assembling advantages of easy administration and safety with low-cost production, to create an adjuvant therapeutical option for neuroprotection in retinal degenerative diseases. By developing this system with chitosan-hyaluronic acid-EPOβ nanoparticles, we aimed to efficiently deliver EPOβ into the retina of both healthy and glaucomatous animals, with no adverse side-effects, and promoting neuroprotective effects on the RGC and/or other retinal cells.

CHAPTER 2

Colloidal nanosystems with mucoadhesive properties designed for ocular topical delivery

Silva B, São Braz B, Delgado E, Gonçalves L. Colloidal nanosystems with mucoadhesive properties designed for ocular topical delivery. Int J Pharm. 2021; 606:120873. doi:10.1016/j.ijpharm.2021.120873

2.1. Abstract

Over the last years, the scientific interest about topical ocular delivery targeting the posterior segment of the eye has been increasing. This is probably due to the fact that this is a non-invasive administration route, well tolerated by patients and with fewer local and systemic side effects. However, it is a challenging task due to the external ocular barriers, tear film clearance, blood flow in the conjunctiva and choriocapillaris and due to the blood-retinal barriers, amongst other features. An enhanced intraocular bioavailability of drugs can be achieved by either improving corneal permeability or by improving precorneal retention time. Regarding this last option, increasing residence time in the precorneal area can be achieved

using mucoadhesive polymers such as xyloglucan, poly(acrylate), hyaluronic acid, chitosan, and carbomers. On the other hand, colloidal particles can interact with the ocular mucosa and enhance corneal and conjunctival permeability. These nanosystems are able to deliver a wide range of drugs, including macromolecules, providing stability and improving ocular bioavailability. New pharmaceutical approaches based on nanotechnology associated to bioadhesive compounds have emerged as strategies for a more efficient treatment of ocular diseases. Bearing this in mind, this review provides an overview of the current mucoadhesive colloidal nanosystems developed for ocular topical administration, focusing on their advantages and limitations.

2.2. Graphical Abstract

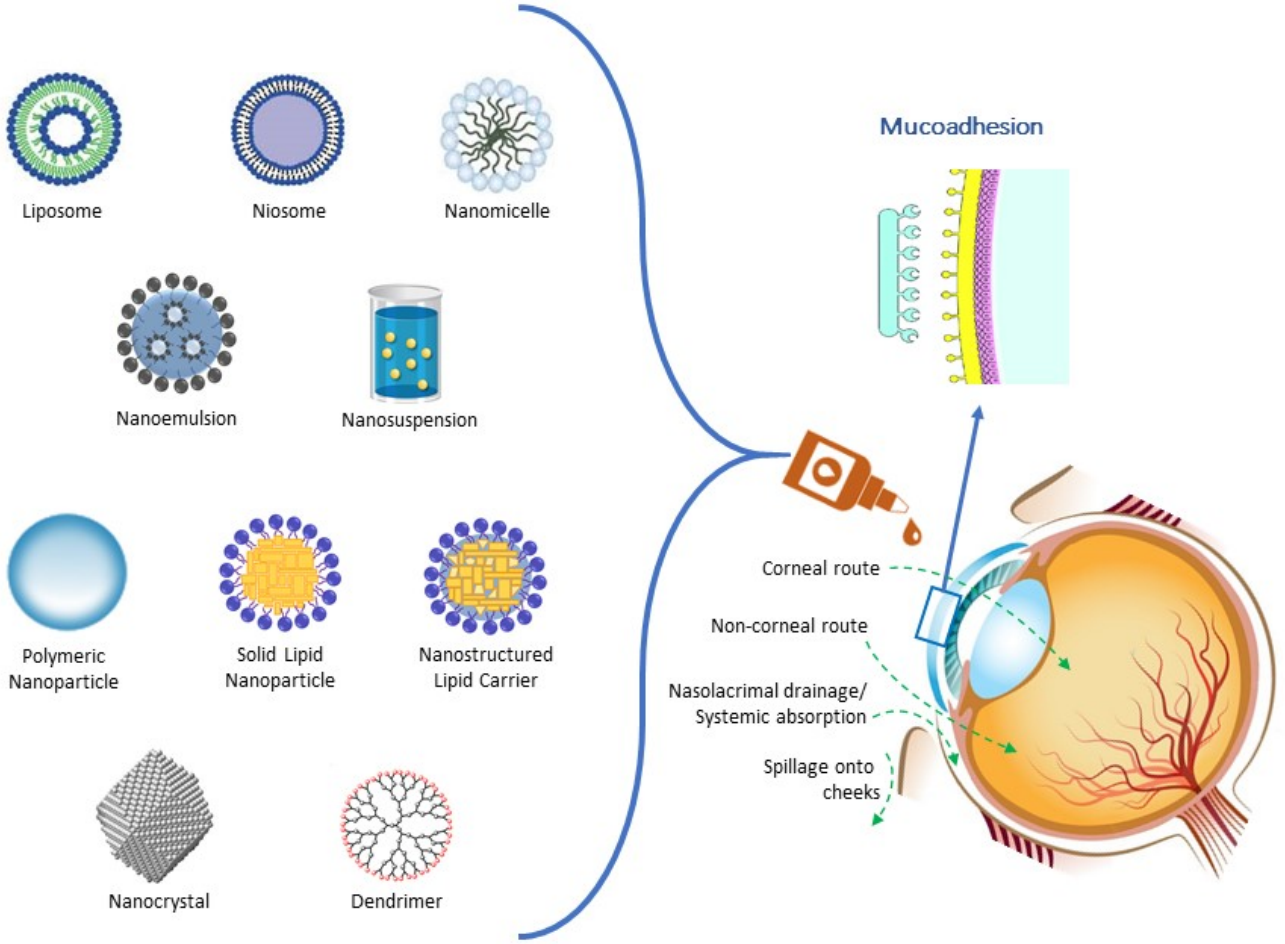

2.3. Introduction

Drug delivery remains a challenging task in Ophthalmology due to the exceptional anatomy, physiology and biochemistry of the visual system that creates a protective structure against foreign substances. Topical administration remains the preferred route for the majority of ophthalmic formulations due to the ease of management, high patient compliance and low rate of secondary effects, amongst other characteristics (De Campos et al. 2004). However, conventional eye drops require frequent instillation of highly concentrated solutions to achieve the therapeutic effects due to the ocular defense mechanisms, including a significant diluting effect caused by tears (Achouri et al. 2013). On the other hand, the frequent administration of highly concentrated solutions may induce local and systemic side effects and also local cellular damage, compromising treatment efficacy (Ludwig 2005). An efficient ocular drug absorption requires good corneal penetration as well as prolonged precorneal residence time, in order to achieve and maintain an adequate drug concentration without increasing the amount of the active pharmaceutical ingredient (Paolicelli et al. 2009).

Colloidal bioadhesive nanosystems are state-of-the-art technology developed to overcome these ocular drug delivery challenges, protecting the drug from the biological environment and enhance its permeation and transport across biological barriers (Ameeduzzafar et al. 2016). In this review, information was gathered on colloidal nanosystems with mucoadhesive properties designed for topical ocular delivery, starting with a general ocular anatomic and pharmacokinetic overview, and then approaching the mucoadhesive colloidal strategies, including their composition, the drug delivered and the main outcomes of the experiments.

2.3.1. Ocular anatomy and physiology

Ocular globe

The eyeball or ocular globe is divided in two major anatomic regions: the anterior segment (adnexa, cornea, anterior chamber and posterior chamber) and the posterior segment (sclera, vitreous chamber, retina and optic nerve) (Attar et al. 2013). Nevertheless, it can be divided into three tunics according to their histological and physiological characteristics: fibrous tunic (outer), vascular tunic (intermediate) and nervous tunic (inner), consisting this last one of the retina and the optic disc.

The fibrous tunic of the eyeball comprises the cornea and the sclera. The cornea is a transparent five layered tissue of well-organized cells with multiple gap and tight junctions.

From outside in, the layers are: epithelium, Bowman's layer, stroma, Descemet's membrane and endothelium (Ludwig 2005; Ghate and Edelhauser 2008). The epithelium is lipophilic, allowing drugs to penetrate the cornea through an intracellular route (mostly lipophilic drugs) or paracellular route (hydrophilic and/or low molecular weight drugs). The stroma is hydrophilic, being the thickest layer (450-500 μm), rich in glycosaminoglycans and collagen fibrils (Prausnitz 1998; Ghate and Edelhauser 2008). On the contrary, the endothelium is a thin monolayer cell tissue, which is crucial in maintaining the transparency of the cornea through a fluid pump (Bonanno 2012). Corneal permeation of cationic hydrophilic compounds is greater than the anionic forms, because the corneal epithelium is negatively charged above its isoelectric point (Ameeduzzafar et al. 2016). Corneal epithelium acts as a barrier for large molecules, while the stroma and endothelium can play an important role in delaying permeation of small lipophilic molecules that readily cross the epithelium. For macromolecules, the stroma seems a greater barrier than the endothelium (Prausnitz 1998). Due to its non-vascularized nature, the cornea is nourished mostly through the endothelium by the aqueous humor, but also through the epithelium by the lacrimal fluid (Ludwig 2005). The sclera is a white tissue consisting of three layers (episclera, stroma, and lamina fusca) and provides structural integrity for the ocular globe (Ameeduzzafar et al. 2016). While the episclera is vastly vascularized, the stroma contains an organized network of collagen fibrils, being fairly permeable to some macromolecules (Radhakrishnan et al. 2017; Resende et al. 2017). Its high degree of hydration facilitates the passage of hydrophilic molecules, depending on their radius and molecular weight (MW), but hinders the permeability of lipophilic forms (Ambati et al. 2000).

The uvea is the vascular tunic of the ocular globe, being divided into anterior (iris and ciliary body) and posterior uvea (choroid). The iris is extremely vascularized and divides the anterior segment of the eye forming an anterior and a posterior chambers (Attar et al. 2013). The lens is a transparent biconvex solid structure located in the posterior chamber, that helps to refract light in order to be focused in the retina. It maintains its transparency through a high enzymatic activity and active transport systems such as ions and water pumps (Attar et al. 2013). The ciliary processes of the ciliary body continuously secrete aqueous humor (2-3 μL/min) that flows from the posterior to the anterior chamber (through the pupil) and also to the vitreous chamber, with a turnover time of 1.5 to 2 hours (Nayak and Misra 2018). Aqueous humor is drained at the iridocorneal angle through the trabecular meshwork to the Schlemm's canal, and through the uveoscleral route to the systemic circulation, with the contribution of the iris venous blood flow (Attar et al. 2013; Nayak and Misra 2018).

The choroid is composed of a large mesh of fenestrated capillaries supported by the Bruch's membrane, which cover the retinal metabolic demands. The Bruch's-choroid complex is a significant drug barrier, particularly to positively charged lipophilic drugs (D. Huang et al.

2018). The vitreous chamber (between the lens and the retina) contains the vitreous, a semisolid structure consisting of water (99%), collagen and hyaluronic acid that helps to maintain the position and shape of the retina. Due to its high viscosity, it can delay the distribution and elimination of some larger drug molecules (Nayak and Misra 2018).

The nervous tunic or the retina processes and transforms the light into neural signals to be further processed by the brain. It is a complex network of synaptic layers divided into ten layers, with six different types of neurons. The outermost part of the neural retina consists of two types of photoreceptors: cones – responsible for color vision and object discrimination (photopic vision); and rods – more effective in capturing low light (scotopic vision) (J. Zhu et al. 2012). The optic nerve is part of the central nervous system and consists of the axons of the retinal ganglion cells (RGC), connecting the retina to the brain's visual processing center (J. Zhu et al. 2012).

Conjunctiva

All the tissues around the ocular globe are considered ocular adnexa, including orbital fat and connective tissues, extraocular muscles, eyelids and conjunctiva. Conjunctiva plays an important role in the mucoadhesion process, which is essentially characterized by attractive forces between a compound and mucus or mucous membranes (Smart 2005). Conjunctiva is a thin membrane that covers the inside of the eyelids (palpebral conjunctiva) and the sclera until the corneoscleral limbus (bulbar conjunctiva), and consists of a stroma and a columnar epithelium with microvilli and goblet cells. The union between the bulbar and palpebral conjunctiva forms the conjunctival sac (superior and inferior), which is a suitable reservoir for drugs instilled to the eye (Morrison and Khutoryanskiy 2014a). The goblet cells are responsible for synthesizing secretory mucins and trefoil factors (TFF)-peptides. The TFF-peptides contribute to the rheological properties of the tear film by forming non-covalent interactions with mucins which creates an entangled network (Ludwig 2005). The epithelial cells are connected by tight junctions at the apical side, hindering the paracellular diffusion of hydrophilic drugs. On the other hand, the diffusion of lipophilic molecules is considerably higher because they penetrate through a transcellular pathway (Hosoya et al. 2005). Nevertheless, the tight junctions of the conjunctival epithelium are wider than the ones we find in the cornea, thus the permeability of hydrophilic drugs is higher in the conjunctiva than in the cornea (Zambito and Di 2011).

Nasolacrimal drainage system

The nasolacrimal drainage system is composed of a secretory, a distributive and a collection part (Ludwig 2005). The lacrimal gland produces and secretes tear fluid, the maximum volume held in the human conjunctival sac being 20-30 μL (normally 7 to 9 μL). During blinking, the eyelids spread tears across the ocular surface, protecting the conjunctiva and cornea and helping to maintain a lacrimal turnover rate of nearly 0.5 to 2.2 μL/min (Ghate and Edelhauser 2008). At the medial part of the superior and inferior eyelids there are lacrimal puncta to where the tears are discharged, going through the canaliculi, the lacrimal sac and finally the nasolacrimal duct into the nasal cavity (Ludwig 2005).

The precorneal tear film has a thickness of approximately 3 to 10 μm (Ameeduzzafar et al. 2016) and covers the exposed part of the eye, being divided into three layers. The superficial lipid layer is secreted by Meibomian and Zeiss glands in the eyelids and helps to preserve a normal osmolarity (310-350 mOsm/ kg) by preventing evaporation of the aqueous part of the tear (Ludwig 2005). This layer contains bacteriostatic substances and has the mechanical function of entrapping and flushing out foreign compounds. The aqueous part is the middle layer that contains inorganic salts, glucose, urea, retinol, proteins, immunoglobulins, lysozyme and lactoferrin, being responsible for the osmotic balance and the control of infections (Ameeduzzafar et al. 2016). Finally, the inner mucus layer is secreted by the conjunctival goblet cells, and it is in intimate contact with the corneal and the conjunctival epithelia. Its composition includes mucins, proteins, lipids, electrolytes, enzymes, mucopolysaccharides and water (Ludwig 2005; Ameeduzzafar et al. 2016). The turnover of the mucus layer is approximately 15 to 20 hours, whereas the tear turnover rate is around 2 to 3 minutes. In physiological conditions, the mucus is negatively charged due to the residues of sialic acid (pKa 2.6), so it has the ability to bind positively charged molecules. On the other hand, mucus can act as a barrier to macromolecules depending on the degree of network entanglement (Ludwig 2005; Zambito and Di 2011).

2.3.2. Ocular pharmacokinetics after topical administration

Topical administration is a non-invasive, convenient, and efficient route for ocular drug delivery, widely used in the treatment of diseases of the anterior segment of the eye. Nevertheless, considering its ease of management and general low incidence of adverse effects, topical drug delivery targeting the posterior segment of the eye became an area of intense research activity. This is a challenging task due to the natural defensive mechanisms of the eye and the several layers to overcome, which reduce the drug's intraocular bioavailability (i.e., drug access to the target cells). A reflex blinking and an increase in tear secretion is observed after the instillation of a drug, due to the abrupt increase of volume in the conjunctival sac and the drug irritant features (Ghate and Edelhauser 2008). Therefore, most of the drug is immediately washed away to the nasolacrimal duct, being absorbed by the nasal mucosa and becoming systemically available (Attar et al. 2013). It is estimated that only 1% to 7% of the instilled drug reaches the aqueous humor (Ghate and Edelhauser 2008). In addition, the human conjunctival sac can held up to 30 µL of fluid, but commercial eyedrops usually deliver between 25 and 70 µL per drop (40 µL in average) (Karki et al. 2011). Considering also the lacrimal turnover, the formulation remains in the conjunctival sac for only 3 to 5 minutes (Ghate and Edelhauser 2008). After topical instillation, drugs can reach the intraocular medium by the corneal and/or the non-corneal (conjunctival-scleral) pathways (Hosoya et al. 2005). Lipophilic formulations permeate preferably by the corneal pathway while hydrophilic formulations usually use the conjunctival-scleral pathway (Hosoya et al. 2005). Once the drug reaches the blood stream by the conjunctival-scleral pathway (conjunctival blood capillaries), its access to the anterior chamber is limited by the blood-aqueous barrier (BAB), which is composed of ciliary epithelium, iridial epithelium and endothelium of iridial blood vessels (Herrero-Vanrell and Cardillo 2010; Nayak and Misra 2018). On the other hand, although drug levels in aqueous humor might be low, the delivery to the posterior segment is improved (del Amo et al. 2017). Hence, formulations designated for anterior chamber should follow the corneal pathway, while those intended for posterior segment should take the non-corneal pathway because this provides a higher surface area and the shortest route when compared to the corneal pathway (Nayak and Misra 2018). However, there is another barrier to take into consideration regarding drug delivery to the posterior segment: the blood-retinal barrier (BRB). BRB consists of the endothelium of retinal capillaries (inner BRB) and the retinal pigment epithelium (outer BRB), limiting the diffusion of drugs to the retina. Some studies proved that the retinal capillary walls are permeable to small molecules with MW of few hundred Daltons and avoid permeation of molecules with a diameter larger than 2 nm (del Amo et al. 2017). Retinal pigment epithelium (RPE) is a monolayer of cells connected by tight junctions, located between the photoreceptors and the choroid, being a stronger barrier for hydrophilic and larger

molecules than the sclera. However, the RPE and sclera behave similarly considering small lipophilic molecules (Herrero-Vanrell and Cardillo 2010). Retinal vascular leakage from BRB function loss, and consequent macular oedema, is the main cause of visual impairment and blindness in diseases like diabetic retinopathy, age-related macular degeneration, retinal vein occlusion and uveitis (Ameeduzzafar et al. 2016). Ocular membranes transporters should also be considered in drug delivery, since they play an important role in the active transport of drugs across the cornea, conjunctiva and retina. Efflux transporters drive molecules out of the cell membrane, lowering drugs bioavailability, while influx transporters facilitate the permeation of essential nutrients and xenobiotics. Considering nanotechnology, the formulation can increase drugs bioavailability by helping influx transporters while also inhibiting efflux transporters (Ameeduzzafar et al. 2016).

To summarize, the main barriers to drug diffusion through the corneal route are nasolacrimal drainage, tear turnover, corneal epithelium, trabecular and uveoscleral outflow, and iridial blood flow. On the other hand, the mucus turnover, the conjunctiva, the sclera, the choriocapillaris and the RPE are the major barriers to the non-corneal route targeting the posterior segment (Nayak and Misra 2018). Figure 5 summarily illustrates the main absorption pathways after topical ocular drug administration.

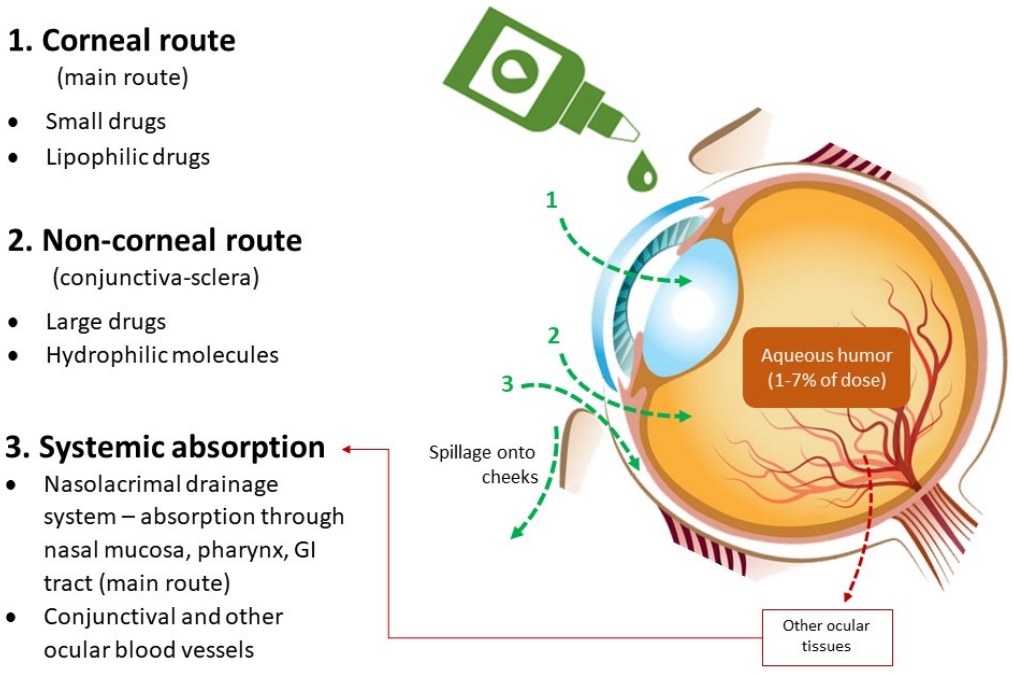

Figure 5: Main absorption pathways after topical ocular drug administration.

2.3.3. Strategies to improve topical ocular drug delivery

Over the past years, several macromolecules that could assist the treatment of diverse eye diseases have been identified. Yet, their potential remains limited due to their instability and failure to interact with the ocular surface and trespass the corneal and conjunctival epithelia. For these therapies to be effective, the design of appropriate drug delivery systems is required to overcome the ocular barriers which limit drug bioavailability (Paolicelli et al. 2009; Diebold and Calonge 2010).

Improvement of corneal permeability

One of the strategies to improve drug bioavailability after topical administration is improving corneal permeability. For instance, prodrugs are a type of drug whose molecules are pharmacologically inactivated, being activated within the ophthalmic tissues by enzymatic transformation (Vyas et al. 2011; Ye et al. 2013). On the other hand, penetration enhancers, surfactants and calcium chelating agents act by modifying membrane components and/or by disrupting epithelial tight junctions (Morrison and Khutoryanskiy 2014b; Moiseev et al. 2019). Also, ion pairs alter physicochemical properties of the ionized drug to facilitate their permeability (Y. Li et al. 2017; Ren et al. 2018) and iontophoresis enhances drugs permeation due to electrorepulsion and electroosmosis effects, using a low-intensity electrical current (Tratta et al. 2014; D. Huang et al. 2018).

Improvement of precorneal retention time

For many decades, solutions, suspensions, and ointments have been the principal vehicles of ophthalmic formulations because they are affordable, convenient and safe, but they all have considerable downsides. Aqueous formulations face various loss processes after topical application through blinking, tear drainage and turnover, and non-productive absorption, which leads to low bioavailability of the drug (Sasaki et al. 1996). Still, suspensions reveal a general enhanced contact time when compared to solutions (Patel 2013). Based on recent pharmacokinetic considerations, it has been suggested that the reduction of the drop volume could increase bioavailability (Chang 2010), yet the methods of improving the precorneal retention time seem to be more effective.

Ointments are a well-known mean to increase the ocular residence time of drugs, sustaining its release, but they are not well accepted by patients due to the interference with vision, discomfort and occasional ocular irritation (Sasaki et al. 1996; Patel 2013). High-viscosity formulations are especially appealing due to shear-thinning behavior that mimics the

tear film, but excessive viscosity could result in rapid drug elimination due to an increased reflex tearing and blinking (Sasaki et al. 1996; Chang 2010). Polymer's type, concentration, molecular mass, and amount of shear-thinning determine the formulation viscosity, yet the useful viscosity range of ophthalmic solutions is limited (Sasaki et al. 1996; Chang 2010).

To better resist the tear drainage and reduce systemic drug absorption, solid polymeric devices have been proposed and developed as valid sustained drug release systems. Several materials have been used, creating degradable (dissolution or erosion) and non-degradable ocular delivery systems. These solid strategies are usually not very well accepted by patients due to discomfort and interference with vision (Sasaki et al. 1996), and biodegradable implants have the disadvantage of interfering in the drug release profile (Chang 2010). On the other hand, *in situ* hydrogels are more promising in ocular drug delivery as they have unique gelation properties and can be administered as eye drops, simultaneously providing enhanced retention time and sustained drug release (Yavuz and Kompella 2017). They consist of polymeric solutions that start gelation upon contact with the ocular tissues, forming a viscoelastic gel in response to environmental stimuli, such as temperature, pH, ions and UV irradiation (Patel 2013; Yavuz and Kompella 2017). Research towards thermosensitive gels suggests feasibility to increase overall ocular bioavailability, even of macromolecules, for anterior and posterior segment. Thermogelling polymers like chitosan, poloxamers, polyethylene glycol, polylactide and polyglycolide, among others, have been successfully used in ocular delivery (Patel 2013).

Nanogels are also innovative mucoadhesive formulations composed of a crosslinked polymer network that swells in the presence of a solvent, usually water (Brannigan and Khutoryanskiy 2017). Further improvements in physical and chemical structures of these nanogels have been done to enhance adhesion capability. Brannigan and Khutoryanskiy (2017) synthetized crosslinked poly((2-dimethylamino)ethyl methacrylate) nanogels with posterior quaternization with acryloyl chloride, leading to mucoadhesion by electrostatic interactions and covalent bonds. *In vitro* and *ex vivo* results exhibit superior mucoadhesive properties of the quaternized nanogels compared to the native nanogels, without having a negative effect on the release profiles (Brannigan and Khutoryanskiy 2017). Tonglairoum et al. (2016) produced a nanogel using a poly(N-vinylpyrrolidone) nanogel 'scaffold' and a monomer with a pendant furan-protected maleimide, which was then deprotected to exhibit the active maleimide functional groups on their surface. Results showed that the mucoadhesive properties of the protected nanogels were significantly lower when compared to the "unprotected" ones, denoting that the free maleimide groups lead to a statistically significant higher retention capability of the nanogels (Tonglairoum et al. 2016).

Colloidal delivery nanosystems such as liposomes, niosomes, nanostructured lipid carriers, and polymeric nanoparticles have also been proposed as new approaches to improve

drug's ocular absorption (Urtti 2006; Budai et al. 2007). These are versatile systems able to carry a wide variety of drugs and enhance their intraocular bioavailability, therefore reducing drug's administration frequency and potential side effects, ultimately improving patient's compliance. They can be combined with thermogelling polymers and other natural or synthetic viscosifying agents, such as mucoadhesive polymers, that increase drug's adhesion to the ocular surface and stabilize tear film (Ludwig 2005; Ameeduzzafar et al. 2016). The next section will assess colloidal nanosystems with mucoadhesive properties designed for topical ocular delivery, which is the main purpose of this review.

2.4. Mucoadhesive colloidal systems for topical ocular delivery

The term mucoadhesion describes the phenomenon in which synthetic or biological macromolecules and hydrocolloids are capable to adhere to mucosal tissues. The force of mucoadhesion is the interfacial force that holds the adhesive material to the mucosa (Hassan and Gallo 1990), which comprises several types of bonding mechanisms, such as electrostatic or hydrogen interactions (Smart 2005). The polymer chains must be mobile and flexible to penetrate into the mucus in a sufficient depth to create a strong entangled network with mucin. The polymer-mucin interaction is made by hydrogen bonding, electrostatic or hydrophobic interactions which depend on the tear film structure and the polymer's physicochemical properties, as well as the pH value and ionic strength of the applied vehicle. For instance, low density polymer chains lead to an increased chain segment mobility, along with increased interdiffusion and physical entanglement. If coiling of the polymer chains occurs, due to pH value or osmolality of the medium, the shielding of active groups required for the bioadhesion process may happen. Therefore, a critical chain length is required for a successful mucoadhesion and prolonged precorneal residence time, because this last one can vary from few hours to one day. Some authors refer that the polymer should have a MW higher than 100 kDa (Ludwig 2005; Zambito and Di 2011).

Mucoadhesive polymers offer a mean to improve sustained delivery and potentially increase drug efficacy with reduced toxicity and minimal undesirable side effects (Rodríguez et al. 2017). Ionic cellulose-based polymers like sodium carboxymethylcellulose are often added to increase the viscosity of solutions or to form gels, exhibiting strong adhesion to epithelial tissues (Chang 2010). Water-soluble polymers that are unable to cross ocular barriers are among the most common mucoadhesive polymers used in ophthalmic formulations (Yavuz and Kompella 2017). Polysaccharides represent a group of these mucoadhesive polymers, including chitosan, polygalacturonic acid, xyloglucan, xanthan gum, gellan gum, pullulan, guar gum, scleroglucan and carrageenan (Ludwig 2005), which can also

be modified to promote their mucoadhesive properties. For example, Agibayeva et al. (2020) modified gellan gum with methacrylic anhydride and reported a significant improvement of the *in vitro* mucosa retention but a lower *in vivo* performance, probably due to the more hydrophobic nature of the methacrylated formulation (Agibayeva et al. 2020). Xyloglucan seems to promote wound healing and is very well tolerated by conjunctival cells, being able to reduce drug-related toxicity. Xanthan gum interacts moderately with mucin revealing a discrete viscoelastic synergistic effect, being a more suitable viscosifying agent than polyvinyl alcohol, hydroxyethylcellulose or hydroxypropyl methylcellulose (Ludwig 2005; Sosnik et al. 2014).

Chitosan is one of the most studied mucoadhesive natural polymers in nanoparticulate ocular delivery and can be conjugated with a wide range of natural or synthetic forms. Chitosan mucoadhesive performance is significantly higher at neutral or slightly alkaline pH as in the tear film (Ludwig 2005). It is a biodegradable, biocompatible and non-toxic cationic polymer, with antimicrobial and wound-healing properties, also having pseudoplastic and viscoelastic behaviors (Paolicelli et al. 2009; Bernkop-Schnürch and Dünnhaupt 2012). Its mucoadhesion effects are due to secondary chemical bonds, such as hydrogen bonds, or ionic interactions between the amino groups (positively charged) and the sialic acid residues of mucins (negatively charged) (Bernkop-Schnürch and Dünnhaupt 2012). Chitosan is widely and successfully used in ocular delivery, offering controlled release and improved corneal uptake of hydrophilic drugs like peptides or proteins, since it can also open tight junctions (Bernkop-Schnürch and Dünnhaupt 2012). New chitosan systems are currently being studied, like the self-assembling amphiphilic chitosan forms, which do not require crosslinking or ionic gelation chemicals to produce nanoparticles. These amphiphiles can bear both hydrophobic and hydrophilic groups that enable self-assembling at both acidic and neutral pH, which is greatly useful in drug delivery (Uchegbu et al. 2014). A recent review article approached drug delivery using chitosan amphiphiles, including ocular applications, and stated that they increased the precorneal residence time and intraocular penetration of drugs (Uchegbu et al. 2014).

Several cellulose derivatives have been included in artificial tears for their viscosifying and moistening properties, but methylcellulose stands out due to its wound healing properties. On the other hand, some cellulose-ethers cause irritation and excessive tearing because of their surface-active properties, lowering drugs bioavailability. Less surface active compounds are better tolerated but reveal poor mucoadhesive properties, except the sodium carboxymethylcellulose whose mucoadhesion is similar to that of polyacrylic acid (Ludwig 2005). The mucoadhesive properties of polyacrylate, also known as carbomer, are mostly due to hydrogen bonding, with the utmost adhesive force occurring at acidic pH. Polyacrylate presents good biocompatibility and can enhance drugs mucosal penetration by a strong interaction with mucus, which is determined by the presence of unionized carboxyl groups. There have been some combinations of polyacrylate with polyethylene glycol for ocular

purposes, in order to improve polyethylene glycol's mucoadhesion, which is a controversial matter due to its lack of functional groups that can interact with the mucin (Sosnik et al. 2014).

Hyaluronic acid is also a well-recognized mucoadhesive polymer, being non-toxic, non-immunogenic and biodegradable. Features such as high water binding capacity, pseudoplasticity and optical transparency, make hyaluronic acid ideal for ophthalmological purposes (Kirchhof et al. 2015; Guter and Breunig 2017). Hyaluronic acid is a nonsulfated anionic glycosaminoglycan consisting of repeated disaccharide units, being the main structural component of the extracellular matrix (Widjaja et al. 2014; Guter and Breunig 2017). Among other roles, hyaluronic acid is implicated in protein transportation and water homoeostasis, promoting wound healing and matrix/cell surface interactions. It is a natural component of tears and high MW hyaluronic acid seems to protect the corneal epithelium against UVB radiation (Widjaja et al. 2014; Guter and Breunig 2017). In the cornea, hyaluronic acid is normally located in CD44 receptors which are mainly located in corneal epithelium and endothelium (Guter and Breunig 2017). In vitreous, hyaluronic acid maintains hydration, stabilizes the collagen fibrils and prevents its aggregation by filling the spaces between them (Widjaja et al. 2014).

Thiomers are thiolated polymers that are considered an enhancement of mucoadhesive polymers because they are capable of mimicking the natural mechanism of mucins by forming covalent bonds (disulfide bonds) with cysteine-rich subdomains of mucus glycoproteins, resulting in increased viscosity and mucoadhesion (Bernkop-Schnürch 2005; Ludwig 2005). Cationic thiomers are mainly based on chitosan while anionic thiomers exhibit carboxylic acid groups (Makhlof et al. 2008). Ludwig (2005) reported that mucoadhesive properties of a chitosan thioglycolic acid conjugate and a polyacrylic acid-cysteine conjugate were, respectively, 10 and 100 times higher than the native polymers (Ludwig 2005). Lacrimera® is composed of chitosan with N-acetylcystein thiol groups and it is known for its significantly higher pre-ocular retention time, which is extremely useful in the treatment of dry eye disease. A recent retrospective study where patients applied Lacrimera® once a day for up to 3 months, revealed an increased tear retention and tear film stability, and also suggested that patients might benefit from a more prolonged treatment than the usually recommended. However, the authors admitted that placebo effect, concomitant medication or other biased situations could possibly interfere with the results (Nepp et al. 2020).

Combination of mucoadhesive polymers with colloidal drug delivery systems has been studied, as both are designed to increase precorneal residence time and improve drug delivery. Colloidal particles can interact with the ocular mucosa and enhance corneal and conjunctival permeabilities. These delivery systems are able to transport a wide range of drugs, including macromolecules, providing stability and improving ocular bioavailability (Yavuz and

Kompella 2017). Several examples of the most studied ophthalmic colloidal drug delivery nanosystems with mucoadhesive improvements are presented in the next section.

2.4.1. Liposomes

Liposomes were discovered in the mid-1960s and were the first nanoscale drug delivery systems to be approved for practical clinical application, being a widely recognized and studied colloidal delivery system for pharmaceuticals (Abed and Couvreur 2014; Zylberberg and Matosevic 2016). They are stable, non-toxic, non-immunogenic and biodegradable compounds due to their phospholipidic composition, also present in biological membranes, being metabolized *in vivo*. In addition, they are easy to prepare and have the ability to improve bioavailability of ophthalmic drugs after topical administration (Kaur and Kanwar 2002; Achouri et al. 2013; Ameeduzzafar et al. 2016). Liposomes are spherical vehicles with a size ranging from 20 nm to several micrometers, composed of one or more concentric lipid bilayers with the ability to carry hydrophilic or hydrophobic drugs, and occasionally both together (Figure 2). The lipid regions solubilize hydrophobic drugs, while the aqueous interior is used to encapsulate and protect hydrophilic drugs (Boyd 2008).

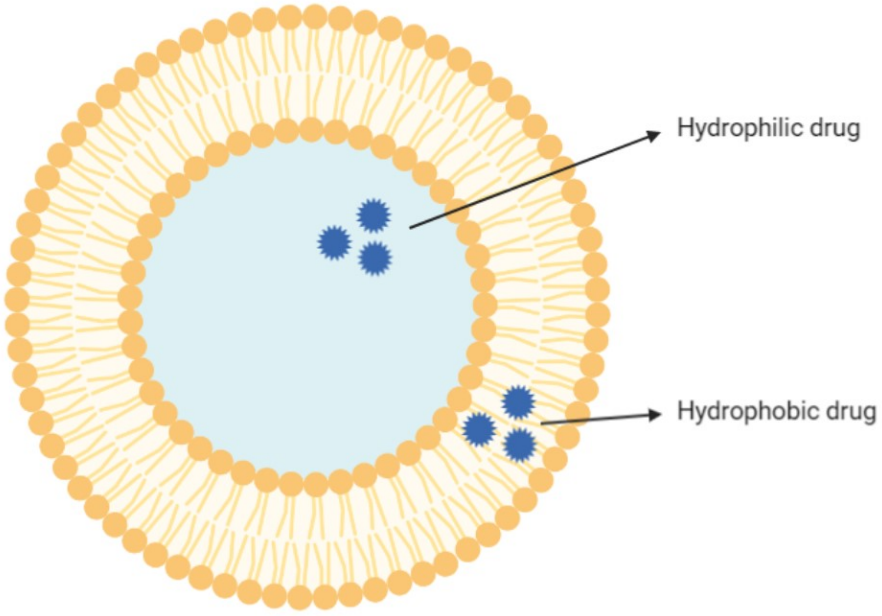

Figure 6: Schematic representation of hydrophilic and hydrophobic drugs in a single bilayered liposome (created with BioRender.com).

Depending on the lipids nature and the preparation method, it is possible to change the particle size, surface charge and sensitivity to pH or temperature (Abed and Couvreur 2014). Positively charged liposomes revealed a longer precorneal retention time when compared with neutral and negative liposomes, most probably due to electrostatic interactions with the negatively charged corneal epithelium. These liposomes can adhere to the ocular surface, enhancing the contact time and, consequently, increasing drug's absorption (Ludwig 2005). By providing an extended and controlled drug release, liposomes can reduce the frequency of administration and allow a better patient compliance (Rawas-Qalaji and Williams 2012). Nevertheless, it has been proposed that these results could be improved by the combination of liposomes with mucoadhesive polymers or gels. Different mucoadhesive polymers were studied in association with liposomes, such as polyacrylic acid, hyaluronic acid, chitosan and poloxamers (Ludwig 2005). In 1987, Fitzgerald et al. prepared mucoadhesive liposomes for ophthalmic delivery from dipalmithoyl-phosphatidylcholine (DPPC), cholesterol, egg lecithin and either stearylamine or dicetyl phosphate. The study concluded that the polymers enhanced the precorneal retention of the vesicles (Fitzgerald et al. 1987) and potentially inspired others to explore these mucoadhesive liposomal systems for ocular use. Few years later, Durrani et al. (1992) used Carbopol® 1342 as mucoadhesive for liposomes carrying pilocarpine and observed improvement in the drug's ocular bioavailability, due to an increased precorneal residence time, a sustained and prolonged release and an extended drug action (Durrani et al. 1992). Budai et al. (2007) performed *in vitro* studies using ciprofloxacin in liposomes prepared from lecithin or DPPC, with a viscosity enhancer: polymethacrylic acid or polyvinyl alcohol. Although this does not correspond to an actual mucoadhesive, it is relevant to mention that the release rates of ciprofloxacin depended on the lipid used in the liposomes along with the concentration and type of polymer. DPPC liposomes prolonged the antibiotic release to a higher extent than lecithin liposomes, because lecithin lead to a higher fluidity and permeability than DPPC (Budai et al. 2007). In fact, scarce studies use lecithin liposomes, unlike DPPC and other phosphatidylcholines, probably due to the same reason. In 2010, Mehanna et al. created liposomes coated with chitosan for ophthalmic delivery of ciprofloxacin. The encapsulation efficiency (%EE) of coated liposomes was lower than the uncoated ones, probably due to repulsion between the cationic drug and the positively charged chitosan matrix. However, the chitosan coating improved the ocular permeation of ciprofloxacin, showing a prolonged release over 24 hours. In addition, chitosan revealed its natural antimicrobial activity, enhancing the antibacterial action of ciprofloxacin liposomes both *in vitro* and *in vivo* studies, when compared to the free drug (Mehanna et al. 2010). In another study using timolol maleate liposomes, the chitosan coating improved the %EE from 70.19 ± 1.48% to 75.83 ± 1.61%. When comparing *in vitro* release profiles, timolol eye drops presented about 70% of release in 3 hours, while the liposomal formulation showed a reduced initial burst release

(29.05% ± 1.33) and almost complete release after 12 hours. Chitosan-coated liposomes presented a better sustained timolol release and prolonged timolol's precorneal retention time, improving transcorneal permeation. This novel formulation could be a suitable strategy to treat glaucoma with reduced daily administrations (Tan, Yu, Pan, et al. 2017). Other studies using chitosan as coating of liposomes are summarized in Table 1 but, generally, if an anionic drug is used, chitosan presents a superior behavior, revealing its potential to limit drug's dissolution and diffusion from the liposomes, enabling a high %EE, enhancing transcorneal penetration and increasing antimicrobial activity, aiding the therapeutic effect of some drugs.

Quinteros at al. (2014) created a hybrid formulation of liposomes and bioadhesive polymers, namely sodium hyaluronate, carboxymethylcellulose, poloxamer 188 and poloxamer 407, to improve the hypotensive effect of the 5-MCA-NAT, a melatonin analogue. All bioadhesive polymers significantly improved *in vivo* treatment efficacy, promoted the stability of the tear film and presented an excellent *in vivo* tolerance (Quinteros et al. 2014). Moustafa et al. prepared liposomes with both hyaluronic acid (Moustafa et al. 2017) and Carbopol® 940 (Moustafa et al. 2018) to increase the corneal penetration of fluconazole. The *ex vivo* permeation showed that both Carbopol-liposomes and hyaluronic-liposomes increased the corneal uptake of fluconazole 3 to 4 times (approximately) when compared to conventional liposomes and fluconazole suspension. Regarding *in vivo* studies, the fluconazole suspension maintained the drug level above the minimal inhibitory concentration (MIC) for only 6 hours, whereas Carbopol-liposomes maintained the concentration for 18 hours and the Hyaluronic-liposomes for 24 hours. Although hyaluronic acid showed superior results, both polymeric systems proved to be safe and useful carriers for fluconazole, increasing its corneal penetration and also enhancing its bioactivity and therapeutic outcomes (Moustafa et al. 2017; Moustafa et al. 2018). Hyaluronic acid is not often used as coating for liposomes although it is very suitable for poor water-soluble drugs. It may not have significant overall mucoadhesive differences among other similar polymers but has the great advantage of being of natural origin presented ubiquitously in the body, inclusively in tears, cornea and vitreous, which is ideal for ophthalmological purposes.

Cationic liposomes system is also a potential approach to improve ocular bioavailability of poor water-soluble drugs and patient compliance, according to Gai et al. (2018) study. The team decided to create an ibuprofen delivery system with the ability to trespass ocular defenses and prolong ibuprofen's therapeutic effect. Ibuprofen cationic liposomes were prepared by ethanol injection method, being then characterized (size; zeta potential; morphology) and optimized. The liposomes achieved a very good %EE (72.9 ± 3.4%) and maintained storage stability at 4 °C for 30 days. *In vitro* transcorneal permeation study in excised rabbit corneas indicated that cationic liposomes could promote ibuprofen cumulative release and elevate its release rate (1.64 times higher than eye drops). Gamma scintigraphy

studies certified the precorneal retention competence of ibuprofen cationic liposomes, confirmed by pharmacokinetic studies which indicated that this system could sustain a higher precorneal drug concentration and achieve a sustained-release effect (Gai et al. 2018). Other studies regarding ophthalmic mucoadhesive liposomes are summarily described in table 2.

Table 2: Mucoadhesive liposomal formulations with possible ophthalmological applications. Description of the studied drug, the particles main composition, and the most important results.

Drug	Materials	Essential outcomes	References
Coenzyme Q10	Soy phosphatidylcholine; cholesterol; α-tocopherol; trimethyl chitosan (coating)	%EE 98%; highly prolonged precorneal retention time; suitable viscosity; effective treatment	(Zhang and Wang 2009)
Diclofenac	Soy phosphatidylcholine; cholesterol; phosphatidylserine; chitosan (coating)	Improved precorneal retention time; enhanced transcorneal penetration; non-toxic	(Li et al., 2009)
Ciprofloxacin	L-α-phosphatidylcholine; cholesterol; stearylamine; dicetylphosphate; chitosan (coating)	Extended release; increased precorneal residence time; effective treatment; safe	(Abdelbary 2011)
Ibuprofen	Lipoid® S100; stearylamine; cholesterol; silk fibroin (coating)	Sustained corneal permeation; higher drug corneal uptake; safe	(Dong et al. 2015)
Doxorubicin	Phosphatidylcholine; stearylamine; cholesterol; hyaluronic acid (coating)	%EE ≈ 82%; higher corneal uptake; prolonged corneal permeation; cell nucleus targeting; higher drug concentration at the target	(Lin et al. 2016)
Flurbiprofen	Egg phosphatidylcholine; cholesterol/ solutol HS-15; chitosan (coating)	%EE ≈ 92%; great liposomes flexibility; prolonged precorneal retention; improved ocular penetration; non-toxic	(Chen et al. 2016)
Artificial tear	Phosphatidylcholine; cholesterol; sodium hyaluronate; trehalose; borate; vitamin E	Stable formula; increased mucoadhesion; ocular tissues hydration; tear film stability; safe	(Vicario-de-la-Torre et al. 2018)
Triamcinolone acetonide	Soybean phosphatidylcholine; cholesterol; dicetylphosphate; chitosan (coating)	Good cellular uptake; *in vivo* increased corneal permeation; effective treatment; non-toxic	(Cheng et al. 2019)

*no pharmacologically active substance

2.4.2. Niosomes

Niosomes have also been described in the literature as drug delivery systems for ophthalmic application, being present in the pharmaceutical field since the 1980's (Herrero-Vanrell et al. 2013). Niosomes are bilayered, nanosized vesicles formed by self-assembly of amphiphilic non-ionic surfactants (Figure 7), being biodegradable, biocompatible, and non-immunogenic (Bachu et al. 2018). In addition, they may contain cholesterol or its derivatives, which provides rigidity, and charged molecules, which provide stability (Bhardwaj et al. 2020). The bilayers protect the drug from the internal and external factors of the body, making these nanocarriers ideal for unstable or sensitive drugs (Ameeduzzafar et al. 2016). Like liposomes, niosomes can entrap both hydrophobic and hydrophilic drugs with an extensive range of solubilities and they provide targeted, controlled and sustained drug release in order to enhance therapeutic effects (Ameeduzzafar et al. 2016; Bachu et al. 2018). Hydrophilic drugs can be enclosed in the aqueous part (central) or they can be adsorbed on the bilayer surface, whereas hydrophobic drugs enter the vesicle by partitioning into it (Bhardwaj et al. 2020). Niosomes are chemically stable with 10 to 1000 nm in size and are able to overcome some drawbacks associated with liposomes such as chemical instability, cost, oxidative degradation of phospholipids and great variability in purity of natural phospholipids (Kaur and Kanwar 2002; Bachu et al. 2018). Being an aqueous vehicle, it leads to a better patient compliance when compared with oily formulations (Ameeduzzafar et al. 2016). Yet, niosomes have also some limitations related to physical instability: hydrolysis of encapsulated drugs, aggregation or drug leakage from the entrapment site (Emad Eldeeb et al. 2019).

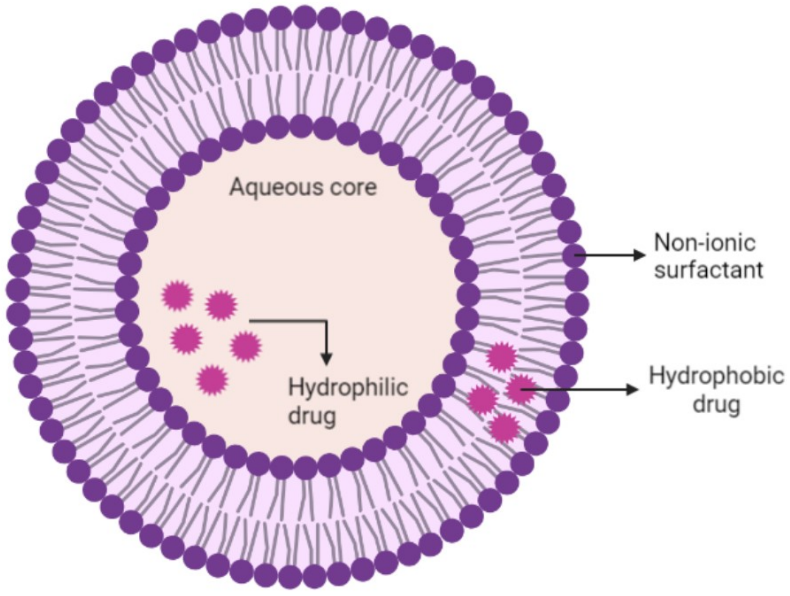

Figure 7: Illustration of a niosome with a hydrophilic and a hydrophobic drug in its structure (created with BioRender.com).

It has been reported that, depending on their composition, niosomes can widen tight junctions and modify corneal permeability to enhance ocular drug bioavailability (Reimondez-Troitiño et al. 2015). Nevertheless, improvement of niosomal drug delivery performance can be achieved through association with mucoadhesive compounds. Aggarwal and Kaur (2005) developed niosomes carrying timolol maleate for topical administration. Niosomes were prepared using Span® 60 and cholesterol, being then coated with chitosan, Carbopol® 934P or Carbopol® 974P. An extended release during a period of 10 hours was observed in the coated niosomes, contrasting with the 1.5 hours release of timolol solution. Moreover, the mucoadhesive system led to fewer systemic timolol absorption, as the IOP of the contralateral eye (control) was less affected, when compared to the solution. No significant difference was observed in the results between niosomes coated with Carbopol® 934P and 974P, but chitosan-coated niosomes presented the longest and most efficient therapeutic effect (up to 8 hours) (Aggarwal and Kaur 2005). A chitosan coating was also performed by Zubairu et al. (2014), whose team synthesized bioadhesive niosomes to carry gatifloxacin. Niosomes were prepared by solvent injection method using Span® 60 and cholesterol, and the chitosan coating was performed after niosomes optimization. There was an evident superior performance of chitosan-coated niosomes when compared to the uncoated ones and the commercial solution, as they presented the highest gatifloxacin transcorneal permeation (≈ 82% in 24 hours), the longest precorneal retention time (176 ± 5.5 min) and a superior retention capacity in corneal tissues (at least 12 hours). Moreover, chitosan coated-niosomes exhibited higher antimicrobial efficacy than the commercial solution at every concentration and no toxicity (Zubairu et al. 2014). Verma et al. (2019) developed and characterized natamycin loaded niosomes also coated with chitosan. The chitosan-niosomal formulation exhibited higher viscosity and retention in ocular tissues, along with a prolonged drug release of 12 hours, with no burst release. Chitosan coated niosomes revealed better mucoadhesive ability then the uncoated ones, proved by the decrease in Zeta potential which reveals the electrostatic interaction between the sialic groups of mucin (negative) and the formulation surface (positive). The mucoadhesive system presented the highest *ex vivo* permeation rate and achieved also the maximum concentration in deeper ocular tissues, which can also be justified by chitosan's permeation enhancement properties (Verma et al. 2019). Once more, all studies pointed out that chitosan-coating ultimately enhanced drugs therapeutic effects and could replace conventional eye drops, but more mucoadhesive polymers are appropriate for coating niosomes and reveal promising results.

Although hyaluronic acid is rarely used as niosomes coating agent, it might be valuable to improve the ocular bioavailability of hydrophobic drugs, as concluded by Zeng et al. (2016). The team developed a hybrid system combining niosomes with hyaluronic acid for ocular

deliver of tacrolimus. Niosomes were created by reconstitution of pro-niosomes followed by dropwise addition of hyaluronic acid solution. The study revealed that, when compared with non-coated niosomes, the hyaluronic acid coating increased the interaction of niosomes with mucin and enhanced the formulation viscoelasticity. *In vivo* studies revealed that tacrolimus bioavailability was improved by hyaluronic acid-coated niosomes, firstly due to the sustained release from the precorneal area; and secondly because the relative bioavailability of hyaluronic acid-coated niosomes was 2.3 and 1.2 times superior to that seen in suspension and non-coated niosomes, respectively. Furthermore, the hyaluronic acid-coated niosomes enhanced tacrolimus corneal permeability, reinforcing the idea of synergistic effect of niosomes and hyaluronic acid on corneal permeability, which was confirmed by confocal laser scanning microscopy (Zeng et al. 2016).

Regarding other polymers, Abdelbary et al. (2017) formulated a lomefloxacin niosomal system with thermo-sensitive in situ gel composed of poloxamer 188, poloxamer 407 and hydroxypropyl methylcellulose grade K15M. Niosomal formulation presented a very significant delay in lomefloxacin release and a prolonged residence time, also enabling a transcorneal lomefloxacin permeation of around 166% higher than that seen in solution. The mucoadhesive niosomes increased 2 to 5 folds lomefloxacin concentration in the ocular tissues and fluids of rabbits; and 35 folds the lomefloxacin antibacterial activity when compared to the free drug (Abdelbary et al. 2017). Recently, El-Nabarawi et al. (2019) designed niosomes loaded with natamycin dispersed in a ketorolac gel based on carboxymethylcellulose or hydroxypropyl methylcellulose-E4. Niosomes exhibited an %EE up to 96,43% and the carboxymethylcellulose formulation at 4% presented the most extended drug release and an increase in drug's permeability and bioavailability, improving its therapeutic effects in the treatment of Candida keratitis in rabbits (El-Nabarawi et al. 2019). These hybrid mucoadhesive niosomes seemed to be promising drug delivery systems to improve the treatment of ocular bacterial and fungal infections, but wider comparative studies are essential to determine the more appropriate polymer or combination of them. Additional information about mucoadhesive niosomal systems intended for ocular use are presented in table 3.

Table 3: Mucoadhesive niosomal formulations with possible ophthalmological applications. Description of the studied drug, the particles main composition, and the most important results.

Drug	Materials	Essential outcomes	References
Acetazolamide	Span® 60; cholesterol; Carbopol® 934P (coating)	Longer duration of action (6 h); high drug concentration in aqueous humor; therapeutic efficacy	(Aggarwal et al. 2007)
Timolol	Span® 60; cholesterol; chitosan (coating)	Prolonged and controlled release; higher intraocular drug concentration; effective treatment; reduced side effects	(Kaur et al. 2010)
Fluconazole	Span® 60 or Span® 80; cholesterol; poloxamer 407/ chitosan (coating)	Poloxamer showed better results; stable formulation; sustained release; enhanced drug permeation; superior antifungal activity	(Fetih 2016)
Fluconazole	Span® 60; cholesterol; poloxamer 407; hydroxypropyl methylcellulose; cyclodextrin; chitosan (coating)	High %EE; sustained drug release; enhanced corneal permeation; ocular toleration; effective treatment	(Elmotasem and Awad 2020)

2.4.3. Nanoemulsions

In the early 90s, nanoemulsions were proposed as promising candidates for delivering therapeutics to the eye (Reimondez-Troitiño et al. 2015). Being thermodynamically stable, oil-in-water (O/W) nanoemulsions are composed of a dispersed oil stabilized in an aqueous phase by surfactants (Figure 8), being of particular interest in nano-ophthalmology considering the lipophilic nature of the cornea (Hamdi et al. 2015; Lalu et al. 2017). They can also interact with the lipid layer of the tear film, remaining in the conjunctival sac for a prolonged period of time (Reimondez-Troitiño et al. 2015). Nanoemulsions structure allows the solubilization of hydrophobic drugs in the oil phase acting as a reservoir which can protect the drug from the aqueous environment (Akhter et al. 2016). Surfactants play an essential role in nanoemulsion interaction with the ocular surface and co-surfactants can be added to further increase the solubility and stability of the system (Reimondez-Troitiño et al. 2015; Lalu et al. 2017). For instance, polyoxyethylated non-ionic surfactants may open the tight junctions and inhibit the activity of the glycoprotein P on the corneal epithelia, leading to an increased drug transportation. Moreover, cationic surfactants can prolong the drug residence time though electrostatic interactions with the corneal epithelia (Reimondez-Troitiño et al. 2015). Nevertheless, some downsides should be taken into account. When compared to liposomes, nanoemulsions use a greater amount of surfactants and co-surfactants which can decrease ocular tolerance (Lalu et al. 2017). In addition, if the droplet size is above 100 nm the visual

field would potentially become hazed as the formulation tends to be milky white (Hamdi et al. 2015).

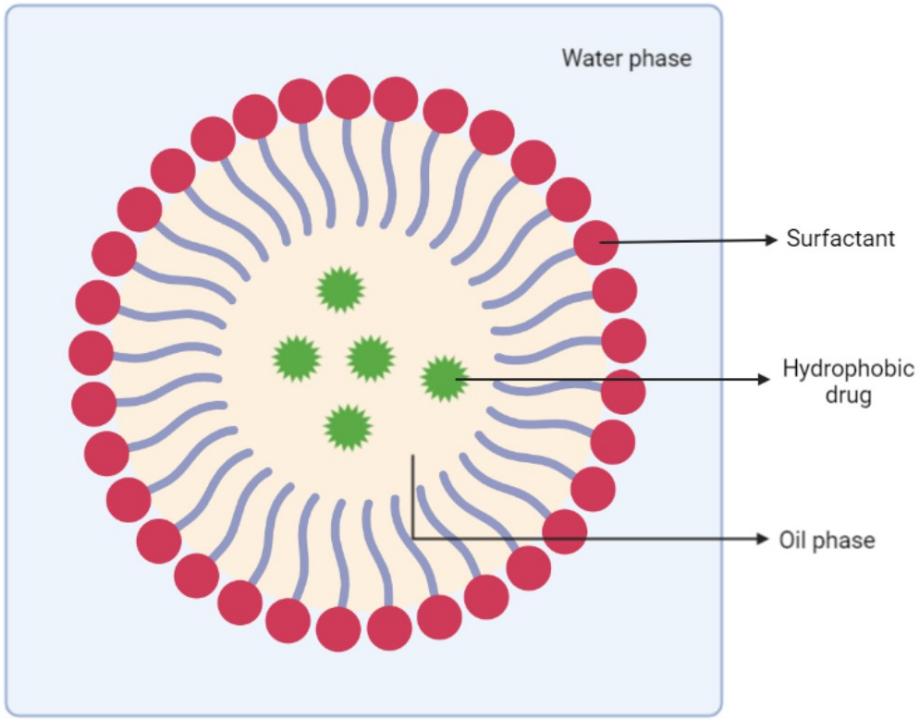

Figure 8: Structure of an oil-in-water nanoemulsion delivery system (created with BioRender.com).

Concerning mucoadhesive nanoemulsions, Gallarate et al. (2013) developed an O/W nanoemulsion for ophthalmic administration of timolol and evaluate the individual influence of mucoadhesive polymers, namely: chitosan, hydroxyethylcellulose, polivinylalcohol and polyethylenglycol. Emulsion components were first screened and the best lipidic, emulsifying and antimicrobial agents were selected. Stability assays indicated that drug loading (%DL) did not cause system destabilization, as the mean particle sizes still remained lower than 100 nm. All emulsions presented lower flow rates than the aqueous solution, also having well-tolerable osmolarity, confirming a certain protective effect against corneal irritation. Yet emulsions with chitosan presented higher diffusion rate and 3-fold decrease in flow rate, denoting its superior bioadhesive characteristics, since the viscosity was similar to the other polymers used (Gallarate et al. 2013). A very recent study developed, and optimized chitosan coated nanoemulsions carrying ibuprofen for the treatment of mild-to-moderate dry eye disease. Nanoemulsions with 5 % (w/w) Miglyol® 812 and increasing amounts of lecithin (0.1-1.0 %, w/w) were synthetized using microfluidizer, and the chitosan coating was performed using increasing amounts of low or medium Mw chitosan, via two different methods. Chitosan was

able to slow down ibuprofen release and granted a significantly stronger mucoadhesive character to the nanoemulsion. The nanoemulsion with 0.05 % (w/w) of chitosan presented better parameters when compared with the 0.3% formulation, having adequate physicochemical properties for ophthalmic administration, appropriate stability, and the possibility to be readily sterilized. Additional *in vivo* studies are required but the chitosan nanoemulsion showed excellent biocompatibility when tested on 3D human corneal epithelium (HCE-T) and *ex vivo* models (Jurišić Dukovski et al. 2020). Despite the results showing that chitosan coating was determinant for the superior performance of the formulations tested, it does not play the same highlighted role as a mucoadhesive agent in nanoemulsions, as does with liposomes and niosomes. Gellan gum alone or combined with other polymers are often used in nanoemulsions to promote mucoadhesion. Tayel et al. (2013) created ion-sensitive in situ nanoemulsion gels of terbinafine hydrochloride to help in the management of fungal keratitis. Twelve systems consisting of oils, surfactants and co-surfactant were prepared by water titration method. Then, a gellan gum 0.2% (w/w) solution with simulated tear fluid (25:7) produced a gel in which the drug-loaded nanoemulsion was incorporated. The selected nanoemulsion gel showed good mucoadhesive features and a controlled and sustained release of terbinafine, revealed by the aqueous humor concentration-time profile, resulting in a higher ocular bioavailability of the drug (Tayel et al. 2013). Likewise, Morsi et al. (2017) produced a 0.3% gellan gum gel in which added other mucoadhesive polymers individually, namely: xanthan gum, hydroxypropyl methylcellulose and Carbopol® 940. The system was based on a peanut oil nanoemulsion in situ gel intended to deliver acetazolamide to the eye. Water titration method was used to prepare six systems consisting of peanut oil, surfactants, and co-surfactant. All gellan gum formulations presented adequate pH values (4.7 - 5.8) and exhibited a shear thinning pseudoplastic behavior in both non-physiologic (before gelation) and physiologic (after gelation) conditions. The ranking of viscosity was xanthan > carbopol > hydroxypropyl methylcellulose but the mucoadhesive strength rank at 0.2% was carbopol > xanthan > hydroxypropyl methylcellulose, being this mucoadhesive polymers concentration (0.2%) chosen for further investigations. Regarding therapeutic efficacy, all nanoformulations had better and more prolonged effects than commercial eye drops, but the gellan/ xanthan system showed the highest therapeutic activity, with no systemic absorption (Morsi et al. 2017). Gellan and xanthan gums have the ability to increase corneal hydration and therefore prolong the precorneal drug residence time, improving transcorneal drugs penetration, which theoretically could lower the frequency of drugs administration and improving patient's compliance.

Another perspective was suggested by X. Li et al. (2016), whose team formulated a cationic nanoemulsion containing dexamethasone acetate (lipophilic) and polymyxin B sulfate (hydrophilic) to treat ocular infections. The lipid phase contained Eutanol G-Lipoid® S 100 and

dexamethasone and the water phase was prepared by dissolving polymyxin B, cetylpyridinium chloride and glycerol. The cationic nanoemulsion revealed good adhesion ability onto the mucin trough electrostatic interactions, thus potentially increasing drugs bioavailability. The osmolality, pH and viscosity values were in the tolerance range and no cytotoxicity was observed. In general, all physicochemical characteristics of the cationic nanoemulsion were compatible with ocular administration, including the particle size (< 200 nm), with the benefit of having a predicted long-term stability of two years. This amphiphilic cationic nanoemulsion presented the ability of delivering simultaneously hydrophilic and lipophilic forms, being considered a valuable delivery nanosystem for other ophthalmic drugs (X. Li et al. 2016). Table 4 resumes additional studies about nanoemulsion ocular systems with mucoadhesive properties, including their composition and main outcomes.

Table 4: Mucoadhesive nanoemulsions with possible ophthalmological applications. Description of the studied drugs, particles main composition, and most important results.

Drug	Materials	Essential outcomes	References
Antisense oligonucleotides	Glycerol; poloxamer 188; Lipoid® E 80; α-tocopherol; trimethylammonium salts	Adequate physicochemical characteristics; enhanced intracellular uptake; higher therapeutic efficacy	(Hagigit et al. 2012)
Ketotifen fumarate	Eudragit® RL 100; polyvinyl alcohol	Suitable physicochemical characteristics; burst followed by sustained release; higher transcorneal penetration	(Soltani et al. 2016)
Cyclosporine A	Several oils; chitosan/ Carbopol®/ gellan gum/ sodium alginate; polyethylene glycol 200/ 400; Transcutol® P	Chitosan presented the best results: superior mucoadhesive properties and ocular retention; improved drug bio-distribution; safe	(Akhter et al. 2016)
Rifampicin	Oleic acid; polysorbate 80/ poloxamer 188; chitosan; polymyxin B	Physical stability; mucoadhesive properties; effective treatment; possibility to deliver hydrophilic antibiotics	(Bazán Henostroza et al. 2020)

2.4.4. Nanomicelles

Nanomicelles are made of amphiphilic surfactant molecules which may be anionic, cationic or zwitterionic. They range from 5 to 200 nm in size, and they can present spherical, cylindrical, or star-shaped form. Normal micelles consist of a hydrophobic core and a hydrophilic outer part while reverse micelles are formed when the opposite alignment occurs (Bachu et al., 2018). Therefore, a normal nanomicelle core is able to solubilize and protect hydrophobic drugs while the hydrophilic shell allows the preparation of a clear aqueous formulation. On the other hand, reverse nanomicelles are employed to encapsulate and deliver

hydrophilic drugs (Figure 9) (Kamaleddin 2017; Bachu et al. 2018). Nanomicelles synthesis procedure is usually simpler when compared to other nanosystems, and thus they could be considered safer than more complex nanocarriers (Kamaleddin 2017). Besides, they present very appealing features such as reduced toxicity, high water solubility, monodispersity and the ability to prevent drugs degeneration while enhancing its permeation and, thus, increasing its bioavailability (Bachu et al. 2018). Stable nanomicelles have been formulated to deliver therapeutic agents to the anterior and posterior segment of the eye (Kamaleddin 2017).

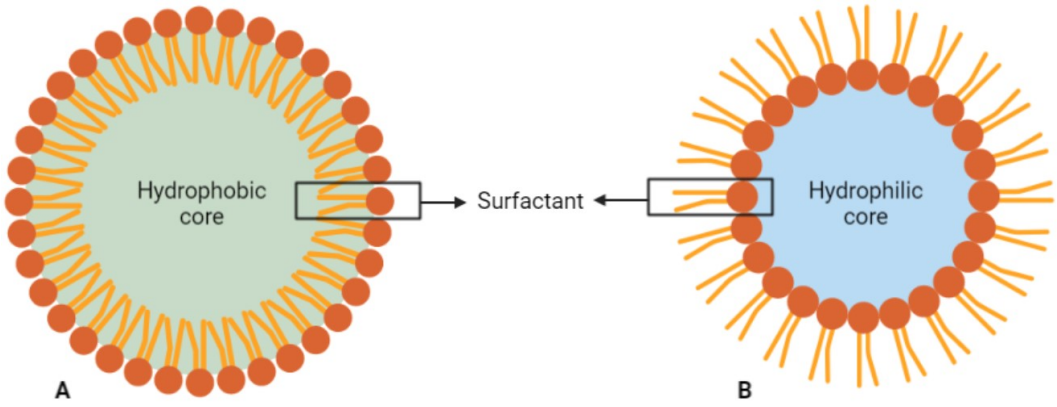

Figure 9: Schematic illustration of a normal (A) and a reverse (B) nanomicelle (created with BioRender.com).

A wide range of mucoadhesive polymers associated with nanomicelle systems were found in the literature. Pepić et al. (2010) created nanomicelles composed of the Pluronic® F127 and chitosan, using dexamethasone as a hydrophobic model drug. Dexamethasone-loaded nanomicelles were prepared by the direct dissolution method. The addition of chitosan to Pluronic® F127 nanomicelles had a significant effect on the drug release rate, producing a sustained release, and the 0.015 % (w/v) chitosan system presented higher drug release when compared to those with less chitosan amounts (0.005 and 0.01 % w/v). Similarly, a higher percentage of chitosan revealed a proportional positive influence on the absorption of dexamethasone across Caco-2 monolayers, which supported the selection of 0.015 % (w/v) chitosan concentration for the *in vivo* assays. Compared to the solution, Pluronic® F127/chitosan nanomicelles allowed an increased dexamethasone absorption and bioavailability, even using a 4-fold lower dose than the standard. This could be attributed to a synergistic transcorneal permeability enhancement triggered by both Pluronic® F127 and chitosan. Moreover, the micelle system prolonged the pharmacological effect and no ocular adverse side effects were observed (Pepić et al. 2010). Xu et al. (2020) also published a study on topical ocular drug delivery of dexamethasone with chitosan nanomicelles but using a more

complex system. They compared octoxynol-40 and hydrogenated castor oil-40 nanomicelles with chitosan oligosaccharide-stearic acid-valylvaline nanomicelles, having the goal of improving bioavailability in the posterior segment of the eye. They proved that nanomicelles entered the posterior segment mainly through the conjunctival route. Considering *in vitro* and *in vivo* studies, both nanomicelle systems were an incontestable upgrade of the traditional eyedrops regarding sustained release, precorneal retention time, permeability, and bioavailability. However, nanomicelles exhibited superior mucoadhesive properties (Xu et al. 2020), which is interesting because chitosan is well known for its superior mucoadhesive characteristics. Indeed, Prosperi-Porta et al. (2016) results suggested greater mucoadhesive properties of poly(L-lactide)-b-poly(methacrylic acid-co-phenylboronic acid) micelles when compared to chitosan micelles, demonstrating the ability to improve cyclosporine A ocular delivery. Also, an extremely prolonged drug release was observed, reaching 74-80% after 14 days. No significant cytotoxicity was observed, being further confirmed by *in vivo* ocular irritation tests in a rat model. The method used to synthesize the mucoadhesive micelles (reversible addition-fragmentation chain transfer polymerization method) was considered promising to improve the bioavailability of topically applied drugs (Prosperi-Porta et al. 2016).

Other mucoadhesive polymers were successfully added to nanomicelles systems for ocular drug delivery, presenting very good results. For instance, Sayed et al. (2018) developed and optimized a β-cyclodextrin and polyethylene oxide micellar dispersion to promote transcorneal permeation of itraconazole. The micelles were prepared by solvent-free melt dispersion method. The β-cyclodextrin/polyethylene micellar dispersion presented a rapid yet enhanced *in vitro* drug release when compared to the suspension. Both mucoadhesion and stability studies revealed better results for the micelles. *Ex vivo* permeation was performed with excised rabbits' corneas and, comparing with the drug suspension, the β-cyclodextrin/polyethylene micelles led to a significantly higher amount of cumulative permeated itraconazole, which was in agreement with the *in vivo* permeation results. The β-cyclodextrin/polyethylene micellar dispersion also revealed superior reduction in clinical symptoms of the induced fungal keratitis in rabbits, being considered biocompatible, safe and feasible for ocular application (Sayed et al. 2018).

Yingfang et al. (2016) studied the ocular delivery of pimecrolimus in nanomicelles and in a thermosensitive nano-hydrogel, using polyethylene glycol and poly (ε-caprolactone) as co-polymers. Both formulations presented sustained release with no burst effect, but the nano-hydrogel presented slower release rate than the nanomicelles. On the other hand, nanomicelles showed superior anti-inflammatory, tear production and corneal "preservation" results, along with an encapsulation efficiency of 97.9 ± 1.26% and particle sizes between 10 and 100 nm (Yingfang et al. 2016). A similar drug (tacrolimus) was incorporated into nanomicelles of amino-terminated poly(ethylene glycol)-block-poly(D,L)-lactic acid and

hydroxypropyl methylcellulose by Liu et al. (2019). The group prepared the nanosystem by a solvent-evaporation-induced self-assembly technique under ultrasonication. Nanomicelles exhibit a significantly lower surface tension and a higher cumulative percentage of permeated drug than those of the commercial suspension, probably because of the mucoadhesive nature of hydroxypropyl methylcellulose and the other polymers. The drug release profile presented a burst followed by a controlled and prolonged release pattern that lasted for 200 hours, possibly due to the encapsulation of tacrolimus in the hydrophobic core and the shell micellar barrier. High levels of tacrolimus were found in the cornea and aqueous humor after topical administration and a significantly higher degree of cellular uptake was observed, which indicates that the tacrolimus bioavailability has been greatly improved by the micellar nanocarrier. The low expression of CD25 and VEGF, and the small amount of IL-2 and IL-17 indicated that the nanomicelles possess better anti-immune rejection in rats than the commercial suspension (Liu et al. 2019). Both studies offer valuable therapeutic choices for immuno-related ocular diseases but the last one is more complete and offers more guarantee of an effective treatment.

Recently, Terreni et al. (2020) used hyaluronic acid as mucoadhesive polymer in a nanomicelles system for ocular delivery of cyclosporine A. A higher amount of cyclosporine A was released from the nanomicelles, and the sustained release was maintained for up to 30 hours. Results of the *in vitro* permeation tests were consistent with the cell viability ones, which demonstrated the protective effect of hyaluronic acid. *Ex vivo* corneal permeation suggests a probable interaction between the nanomicelles, and the ocular apical cells promoted by hyaluronic acid, which also determined a great improvement of cyclosporine A bioavailability in tear fluid, denoting its mucoadhesive characteristics that contributed to an extended residence time in the precorneal area. While the commercial cyclosporine A form was an opaque-white nanoemulsion, the developed nanoformulation was a transparent nano-colloidal dispersion, resulting in an improved chemical-physical stability and patient's acceptance. Considering all the results, the hyaluronic acid nanomicelles seemed to be a promising new system for the topical ocular delivery of cyclosporine A intended for dry eye syndrome treatment (Terreni et al. 2020).

These studies are not truly comparable among each other, and it is impossible to suggest a more suitable mucoadhesive polymer, as several different ones were explored with very satisfactory results. Broader comparative studies regarding mucoadhesive nanomicellar systems for ocular use are required.

2.4.5. Nanosuspensions

Nanosuspensions are colloidal systems composed of pure, hydrophobic or semi-hydrophobic drugs, suspended in a dispersion medium and stabilized by surfactants or polymers (Figure 10) (Ameeduzzafar et al. 2016). Typically, they consist of an inert colloidal carrier, like a polymeric resin, which is non-irritant to cornea, iris, or conjunctiva. Nanosuspensions can be employed as ocular delivery vehicles that prolong drugs' release, enhancing its bioavailability, and also improve drugs' solubility (Sahoo et al. 2008; Bachu et al. 2018), especially when therapeutic agents form crystals with high energy content, being insoluble in either lipophilic or hydrophilic media (Sahoo et al., 2008). Regarding ophthalmic use, nanosuspensions are seen as a valid alternative to conventional delivery systems, increasing the precorneal residence time, solubility and ocular bioavailability of drugs such as dexamethasone, prednisolone, and hydrocortisone (Bachu et al. 2018).

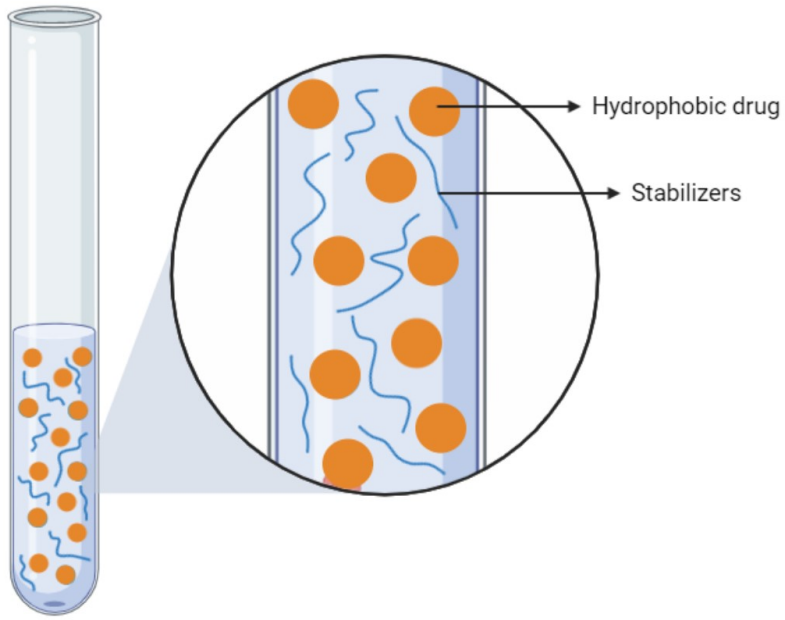

Figure 10: Schematic representation of a nanosuspension (created with BioRender.com).

Eudragit® polymers are the most mucoadhesive agents used in ocular nanosuspensions. In 2002, four articles from the same research team studying Eudragit® polymers as carriers for ophthalmic controlled drug delivery were published. Nanoparticles were prepared by an adaptation of the quasi-emulsion solvent diffusion method. Nanosuspensions of Eudragit® RS 100 and RL 100 without active principle were stable and presented suitable physicochemical characteristics, including stability up to 2 years

(refrigerated and at room temperature), with a potential for mucoadhesion and a non-irritant nature (Pignatello et al., 2002a). Two of the publications were concerning the study of ibuprofen's behavior when delivered in Eudragit® RS 100 nanosuspensions. The size of the particles was in the nano-range and no irritant effect was observed. Both studies underlined a gradual and prolonged release and an increased precorneal retention of ibuprofen. An overall increase in the intraocular drug concentration and a consequent bioavailability enhancement was detected, resulting in a more effective and prolonged therapeutic effect (Bucolo et al., 2002; Pignatello et al., 2002). Likewise, ocular delivery of flurbiprofen in a Eudragit RS100® and RL100® nanosuspension was studied. Results showed a good stability of the formulation and a controlled release profile of flurbiprofen. *In vivo* assays indicated a higher level of flurbiprofen in the aqueous humor along with an enhanced therapeutic efficacy, revealed by a higher inhibition of the miotic response to the induced trauma. Moreover, no toxicity on ocular tissues was observed (Pignatello et al., 2002b). Das and Suresh (2011) proposed an Eudragit® RS 100 polymeric nanosuspension for delivering amphotericin B to the ocular surface. A solvent displacement method was used to entrap amphotericin B in the suspension. The mean particle size varied from 150 to 290 nm and the zeta potential from +19 to +28 mV, which could provide a prolonged corneal contact time through mucoadhesion. Amphotericin B showed a slower dissolution profile from the nanosuspension when compared to a pure drug suspension. The nanoformulation exhibited an excellent tolerance when topically applied onto the rabbit's corneas. Microbiological assays showed good antifungal activity on *Fusarium solani*, comparable to those in the control. Moreover, a good stability was found upon storage after 6 months, making this polymeric nanosuspension a valid option regarding the treatment of ocular fungal infections (Das and Suresh 2011).

Although Eudragit® alone or combined with other mucoadhesive polymers present very good results in ocular drug delivery (see table 4), nanosuspensions with other polymers were also explored through the years. A chitosan-polyacrylic acid nanosuspension was developed by Lin et al. (2007) using template polymerization of acrylic acid in a chitosan solution, to be used as ophthalmic pilocarpine carrier. Optimized nanoparticles presented an %EE of 71%, very small mean diameters (92.0 ± 7.5 nm) and a stable zeta potential (+25.5 ± 2.6 mV), being these characteristics appealing for ocular delivery. About 40% of pilocarpine was released from the nanosuspension within the first 15 minutes, while almost 95% of the drug was released from the commercial formula in 5 minutes. The subsequent release from the nanosuspension was slow and sustained during the rest of the assay (6 hours). The pharmacological response in rabbits (miosis) treated with the pilocarpine nanosuspension was maintained for up to 315 minutes, which is twice the time of that in commercial eye drops (Lin et al. 2007). Maged at al. (2016) also used chitosan as mucoadhesive polymer in a nanoparticulate suspension of econazole. The formulation was created by a nano-spray drying technique, using two types of

cyclodextrins (methyl-β-cyclodextrin and hydroxylpropyl-β-cyclodextrin) as carriers, Tween® 20 and poloxamer 407 as stabilizers (surfactants), and chitosan. Hydroxylpropyl-β-cyclodextrin and Tween® 20 were selected as they revealed more potential to stabilize particle's size than methyl-β-cyclodextrin, presenting a remarkable stability during one year of storage at room temperature. The most promising release results were given by the formulation containing 10 % Tween® 80 with hydroxylpropyl-β-cyclodextrin, showing higher percentage drug released (81.3 % in 24 hours). Chitosan was then conjugated with the optimized formulation and significantly improved the system performance. Chitosan not only enhanced the nanosuspension viscosity, but also allowed an increased drug release and an improved mucoadhesion, which was corroborated by *in vivo* assays that revealed enhanced econazole bioavailability, denoting a superior mucin interaction and thus an increased residence time. In addition, the nanosystem revealed stability and no signs of ocular irritation or inflammation (Maged et al. 2016). Once more, chitosan was considered a promising mucoadhesive agent, being commonly added to nanosuspensions for ophthalmic drug delivery.

A moxifloxacin-loaded poly(dl-lactide-co-glycolide) nanosuspension was created by Mudgil and Pawar (2013), prepared by a modified nanoprecipitation technique. The %EE of the nanosystem was high (over 80 %) and the zeta potential was in the stability range. The *in vitro* release study suggested that the optimized nanosuspension provided a higher drug release profile as compared to the other formulations. The nanoformulation showed higher permeation across fresh goat corneas (≈ 48% in 4 hours) than the marketed solution. Corneal hydration was calculated to evaluate the corneal damage and all formulations had values between 78 to 80%, indicating low ocular damage. Moreover, the antimicrobial study indicated that the nanosuspension was more effective against Staphylococcus aureus than against Pseudomonas aeruginosa and presented a prolonged efficacy when compared to the commercial solution. In conclusion, poly(dl-lactide-co-glycolide)-loaded nanosuspension could be used as a promising ocular moxifloxacin carrier but further *in vivo* studies are required (Mudgil and Pawar 2013).

Recently, Güven and Yenilmez (2019) created an ophthalmic nanosuspension with Kollidon® SR (80 % w/w polyvinyl acetate and polyvinylpyrrolidone 20 %, w/w) to carry olopatadine hydrochloride, an anti-histaminic used in allergic conjunctivitis. A spray drying method was used to synthetize the nanosuspension without using crosslinkers. The nanosuspension exhibited particle sizes ranging from 75 to 145 nm, spherical shape, and satisfactory zeta potential, indicating an adequate physical stability of the formulation. Reasonable %DL and %EE values were achieved. A sustained release of olopatadine hydrochloride from the nanosuspension was observed, having reached nearly 90 % at 48 hours, in contrast with the pure drug, which achieved the same percentage in 3 hours. Moreover, the *in vivo* retention time was higher when compared to olopatadine hydrochloride

alone (Güven and Yenilmez 2019). Bearing in mind the good results and the fact that polyvinyl acetate and polyvinylpyrrolidone are both biodegradable polymers, this nanosuspension appears to be a promising drug delivery system to treat ocular allergies, enabling a lower frequency of administration and better patient compliance. Other studies concerning ophthalmic mucoadhesive nanosuspensions are summarily described in table 5, although more wide-ranging comparative studies should be performed.

Table 5: Mucoadhesive nanosuspensions with possible ophthalmological applications. Description of the studied drug, particles main composition, and most important results.

Drug	Materials	Essential outcomes	References
Cloricromene	Eudragit® RS and RL 100; Tween® 80	Adequate physicochemical characteristics; no burst release; improved corneal adhesion; storage stability	(Pignatello et al. 2006)
Methylprednisolone acetate	Eudragit® RS 100; polyvinyl alcohol	Particles in the nano-range; controlled drug release; effective and enhanced treatment	(Adibkia, Omidi, et al. 2007)
Piroxicam	Eudragit® RS 100; polyvinyl alcohol	Particles in nano-range; controlled drug release; therapeutic efficacy	(Adibkia, Shadbad, et al. 2007)
Diclofenac	Eudragit® S100; poloxamer 188	High %EE; sustained drug release; increased anti-inflammatory activity	(Ahuja et al. 2011)
Mycophenolate mofetil	Chitosan; soy lecithin; Pluronic® F68	Enhanced precorneal retention; increased bioavailability; good therapeutic results; excellent tolerance	(Wu et al. 2011)
Pilocarpine	Eudragit® RL 100	High %EE; burst followed by sustained and controlled drug release; prolonged therapeutic effect (24 h)	(Khan et al. 2013)
Itraconazole	Chitosan; lysine; poloxamer 188	Adequate physicochemical characteristics; higher corneal permeation	(Ahuja et al. 2015)

2.4.6. Solid Lipid Nanoparticles (SLN)

The first generation of lipid nanoparticles was introduced in the 90s as solid lipid nanoparticles (SLN) (Iqbal et al. 2012; Wang et al. 2015). SLN can be defined as a solid lipid matrix (Figure 11) with an average diameter between 50 and 1000 nm accommodating hydrophilic or lipophilic drugs (Goyal et al. 2016; Bachu et al. 2018). Triglycerides, fatty acids, steroids and waxes are examples of lipids used to prepare SLN, whose process do not require organic solvents, being the surfactants typically required to stabilize the lipid dispersion (Goyal

et al. 2016). Although SLN have a low %DL of around 25 % and the release of hydrophilic drugs present a burst during the initial period, they are considered a good alternative for ocular drug delivery presenting also the possibility of being formulated into eye drops (Bachu et al. 2018). SLN present low toxicity and physicochemical stability, along with biocompatibility, biodegradability, and relatively low-cost production (Wang et al. 2015; Goyal et al. 2016). They prevent or reduce the degradation of lipophilic drugs because the mobility of the reactive agents is delayed in the solid state when compared to the liquid state. This system also offers controlled drug release, prolonged ocular retention, increased corneal permeation, and drug targeting, which improves ocular bioavailability of both hydrophilic and lipophilic drugs (Bachu et al. 2018).

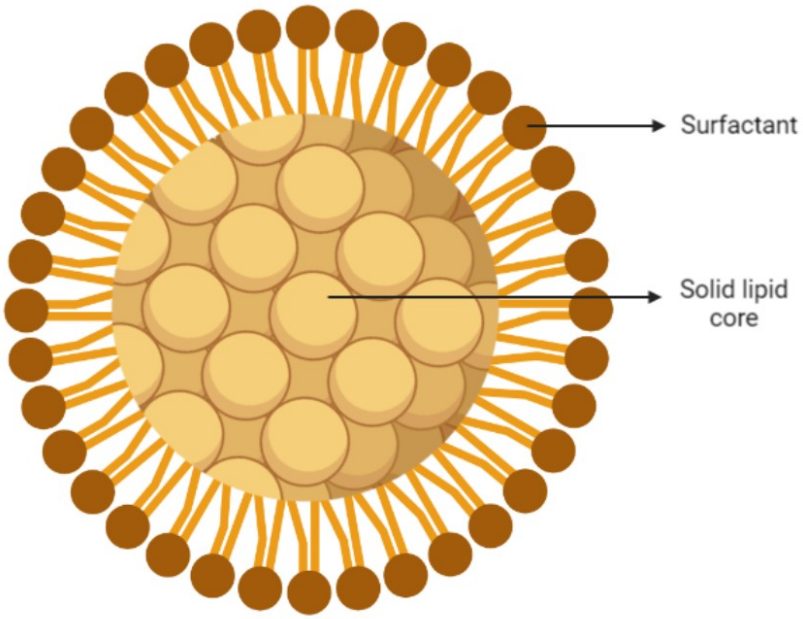

Figure 11: Illustration of a solid lipid nanoparticle (created with BioRender.com).

SLN can be conjugated with mucoadhesive polymers as well, but few published works were found in our review search. Balguri et al. (2016) formulated indomethacin-loaded SLN and nanostructured lipid carriers (NLC) with and without hydroxypropyl-β-cyclodextrin and chitosan. The addition of chitosan increased the transcorneal flux of indomethacin by 2 to 3.5-folds, depending on the formulation studied, confirming the penetration-enhancing properties of chitosan. Trans-sclera-choroid-RPE permeability studies demonstrated that the hydroxypropyl-β-cyclodextrin-SLN exhibited a higher permeability than the SLN formulation alone, which could be due to the complexation effect of cyclodextrin with the free drug. In general, indomethacin-loaded lipidic nanoparticles displayed higher drug levels in ocular

tissues than the aqueous solutions, but NLC formulations were the most effective. The chitosan-coated SLN was considered a feasible system for the delivery of indomethacin to the posterior ocular segment (Balguri et al. 2016). Another chitosan-coated SLN formulation was studied by Sandri et al. (2017). The system was prepared by a previously optimized high shear homogenization and ultrasound method. Chitosan-SLN presented an average particle size of 200 nm and a positive surface charge, enabling an improvement of the mucoadhesion which was corroborated by mucoadhesive assays. Chitosan enabled an enhancement of the formulation's bioadhesive features while keeping its nano-size and surface-charge required for an efficient ophthalmic carrier (Sandri et al. 2017). Like other colloidal systems intended for ocular use, SLN benefited from chitosan's mucoadhesive improvement and penetration-enhancing characteristics.

A mucoadhesive SLN dispersion was studied by Chetoni et al. (2016) for ocular delivery of tobramycin, using the rabbit as an animal model. The system was prepared using O/W microemulsions of stearic acid as internal phase, Epikuron 200 as surfactant, sodium taurocholate as cosurfactant, and deionized water as continuous phase. The mucin binding efficiency was nearly 87 %, a substantial result confirmed by a manifest decrease of the zeta potential. The drug released from the aqueous solution exhibited a rapid diffusion, while from the SLN showed a controlled release rate with no burst effect. After topical instillation of the commercial solution, no tobramycin was identified in vitreous humor and retina, while a high concentration of the drug was detected in both ocular tissues using the tobramycin-loaded SLN (comparable to the results after the intravenous administration). Additionally, morphological, and physicochemical characteristics of the nanoparticles were suitable for ophthalmic use. This SLN system might represent a new tobramycin delivery strategy to the posterior segment of the eye (Chetoni et al. 2016).

Gellan gum was used as the basis of an *in situ* gel containing triamcinolone acetonide-SLN created by Tatke et al. (2019). The formulation was synthetized by homogenization coupled with ultra-probe sonication technique, using Pluronic® F-68 as surfactant. Triamcinolone acetonide-SLN transcorneal flux and permeability was significantly higher than the control. On the other hand, a slightly lower flux and permeability was observed in triamcinolone acetonide-SLN in situ gel (with gellan gum) when compared to that of triamcinolone acetonide-SLN, denoting the controlled drug release from a more viscous formulation. Both SLN systems (with and without gellan gum) presented greater value of half-life than the control, probably due to enhanced entrapment in the mucin and slower drug release. Yet, the presence of gellan gum improved the drug's mean residence time and half-life, considerably enhancing its concentrations in all ocular tissues. Therefore, SLN combined with *in situ* gelling agents might be an interesting ocular drug delivery system for topical administration (Tatke et al. 2019).

Lately, Ahmad et al. (2019) formulated SLN loaded with etoposide (chemotherapy drug) for ocular application, using melt-emulsification and ultrasonication techniques. A lipid mixture of 4% w/v of Gelucire® 44/14 and Compritol® ATO 888 in the ratio of 3:1 was chosen, producing a formulation with particle sizes around 240 nm and %EE around 81 %. *In vitro* release of etoposide from the nanoformulation was biphasic, with a rapid release in the beginning and a controlled and sustained release at the end of the assay. Etoposide-loaded SLN were labelled with Tc-99m (radioactive compound) and injected into the vitreous chamber of rats. Gamma scintigraphy showed accumulation of the drug in the vitreous after 24 hours, maintaining a sustained release for at least 7 days. Retinal histological examination demonstrated that eyes treated with etoposide-SLN showed lesser toxic effects than those treated with etoposide solution, meaning that this nanosystem delivered the drug to the site of action more efficiently and with fewer side effects (Ahmad et al. 2019).

Scarce studies of mucoadhesive SLN were found in the literature. The low interest in the field is probably due to other colloidal nanosystems with better characteristics, like a higher drug loading capacity and the ability to produce a more sustained drug release. NLC were created to bridge the limitations associated with SLN, as following described.

2.4.7. Nanostructured Lipid Carriers (NLC)

Nanostructured lipid carriers are a second-generation lipid nanoparticles which also exhibit controlled release, drug targeting and increased bioavailability, along with excellent bio-tolerability and very limited toxicity (Li et al. 2009; Iqbal et al. 2012). They are composed of approximately 30% of liquid lipids but the final product is solid, with no crystalline structure (Figure 12) (Bachu et al. 2018). As SLN they have the ability to immobilize drugs and prevent the particles from coalescing (Li et al. 2009). The liquid oil droplets in the solid matrix allow an additional space between the fatty acid chains, leading to a higher amount of accommodated drug, i.e., a higher %DL when compared to SLN. Also, the formation of lipid crystals prevented drug expulsion during the storage period (Bachu et al. 2018).

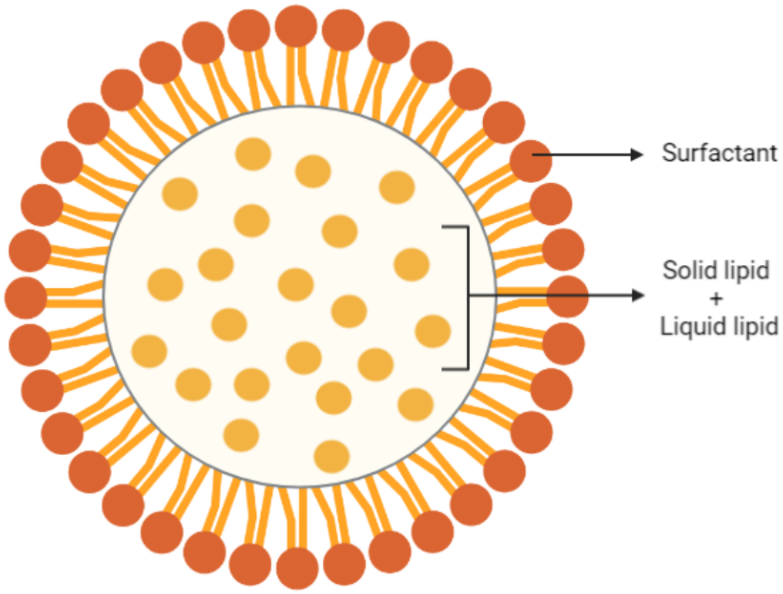

Figure 12: Schematic representation of a particle of nanostructured lipid carriers (created with BioRender.com).

On contrary of SLN, a variety of studies concerning association between NLC and mucoadhesive agents were found. The addition of **chitosan** to NLC as a mucoadhesive agent was performed by Luo et al. (2011). The group formulated flurbiprofen-loaded NLC by melt-emulsification and ultrasonication techniques, and then coated them with chitosan oligosaccharides. Compared with the solution, NLC showed a slightly higher corneal permeation of flurbiprofen, but the chitosan-NLC presented a 2.4-fold increase. Additionally, when the chitosan oligosaccharides amount in the formulations was raised from 0.3 % to 0.5 %, the drug permeation increased accordingly. Results suggest that chitosan oligosaccharides may provide a superior mucoadhesion as chitosan-NLC exhibited a substantially prolonged retention time and slower clearance than the other formulations. Histopathology of rabbit eyeballs and lids confirmed a good corneal biocompatibility and ocular tolerance of the nanoformulations (Luo et al. 2011). Tan et al. (2017) also used chitosan but in the form of hydroxypropyl trimethyl ammonium chloride chitosan (HACC)-based hydrogels. Dexamethasone was used as model drug and the thermosensitive hydrogel was prepared by simply mixing HACC and β-glycerophosphate. The NLC formulation exhibited an average low particle size, stability of the polydisperse system and good homogeneity. At the same time point (4 hours), the release rate of dexamethasone from NLC-HACC/ β-glycerophosphate gel was 39.01 % while from NLC it was 60.42 %. On the other hand, the cumulative drug release at 48 hours for NLC was 93.10% whereas for hydrogel was 84.74 %. These results clearly indicate a delayed and sustained release of dexamethasone from the NLC-HACC/ β-glycerophosphate gel over a long period of time, achieving 88.65 % of released drug at 72 hours (Tan, Yu, Li, et al. 2017). Considering also the outcomes of other studies (see table 5),

chitosan's exceptional mucoadhesive and penetration-enhancing features, along with biocompatibility and biodegradability, make it a valuable polymer to be incorporated in the NLC systems for ophthalmic applications.

However, other polymers were studied as found in the literature, like polyethylene glycol. Shen et al. (2009) investigated the mucoadhesive effect of polyethylene glycol-NLC for ocular delivery of cyclosporine A. Cysteine-polyethylene glycol stearate conjugates were synthetized and then NLC, cysteine-NLC and polyethylene glycol-NLC containing cyclosporine A were prepared by melt-emulsification method. The addition of polyethylene glycol to the NLC system resulted in a slightly increase of the particles size but remained in the nano-range, and no significant change was seen in the ZP. Surface properties of mucin particles were significantly altered by cysteine-polyethylene glycol stearate conjugates when compared to unmodified polyethylene glycol stearate, suggesting that the thiolated form had a superior affinity for mucin. The decreased viscosity of cysteine-NLC-mucin mixtures in the presence of free cysteine provided evidence of the disulphide bonds formation between thiolated NLC and the mucus layer. Moreover, free thiol groups modified on cysteine-NLC directly influenced the mucoadhesion of thiolated nanocarriers, when compared to polyethylene glycol stearate and NLC, resulting in a prolonged precorneal retention time (Shen et al. 2009). Another study from the same team evaluated the ocular distribution of cyclosporine A using a similar thiolated NLC-polyethylene glycol system. The formulation presented a comparable behavior, with a burst drug release followed by a sustained release pattern. The mucoadhesion was superior for the NLC-polyethylene glycol formulation and, therefore, an extended precorneal residence time was observed, with a correspondent increase of bioavailability (Shen et al. 2010). The NLC formulations selected from both studies should be considered promising ophthalmic carriers for cyclosporine A, as they are safe and improve drug's performance. Lakhani et al. (2019) also developed polyethylene glycol NLC for ocular delivery. Lipids and polyethylene glycol of various MW were screened and NLC were synthetized with and without polyethylene glycol. Amphotericin B-PEG-NLC was prepared using a solvent-free processing and high-pressure homogenizer. The optimized amphotericin B-PEG-NLC presented robust physicochemical values and was stable for at least 30 days. The nanoformulation was not cytotoxic to ARPE-19 cells and presented higher antifungal activity, comparable to, or better than, commercially available amphotericin B formulations. However, after topical administration, amphotericin B concentration in the tested ocular tissues was not statistically different between amphotericin B-PEG-NLC and commercial formulation, indicating that further tests are required to assess the amphotericin B precorneal retention of both formulations. Still, this polyethylene glycol NLC had potential for ocular use and could possibly yield superior *in vivo* characteristics after further optimization (Lakhani et al. 2019).

Recently, Tan et al. (2019) used chondroitin sulfate as mucoadhesive agent in a dexamethasone-NLC delivery system intended to treat dry eye disease. A polymer (APBA-ChS) was created by amide bond formation between (3-aminomethylphenyl)boronic acid and chondroitin sulfate. APBA-ChS was located at the surface of dexamethasone-NLC targeting sialic residues of mucins. Dexamethasone-APBA-ChS-NLC presented small diameter, suitable zeta potential (from +31±2 mV to +22±2 mV), low polydispersity index and high %EE. The dexamethasone release was sustained from both the uncoated NLC and the APBA-ChS-NLC, yet this last one presented a particularly extended release. Results from the mucoadhesion study revealed a higher mucin absorption of APBA-ChS-NLC, leading to prolonged precorneal retention time, which was confirmed *ex vivo* and *in vivo* by fluorescence imaging technology. When compared with dexamethasone eye drops, APBA-ChS-NLC showed a 2.3-fold increase in the *in vitro* permeation, which was also higher than that of non-coated NLC. The *in vivo* permeation was also increased, resulting in improved drug's bioavailability, validated by pharmacokinetic parameters of dexamethasone in tear fluid and aqueous humor. In the rabbit dry eye model, dexamethasone-APBA-ChS-NLC allowed a better clinical improvement when compared to other formulations, and maintained adequate corneal hydration levels, causing no ocular irritation (Tan et al. 2019). Results suggest that this innovative mucoadhesive polymer based on chondroitin sulphate is a promising tool to improve drug's bioavailability after topical ocular administration.

Mucoadhesive nanostructured lipid carriers appear to be excellent ophthalmic delivery systems for a wide variety of drugs. Several mucoadhesive polymers were studied in the last few years, where chitosan has a prominent place among them, followed by polyethylene glycol. Nevertheless, more information about mucoadhesive nanostructured lipid carriers intended for ocular use is presented in table 6.

Table 6: Mucoadhesive nanostructured lipid carriers with possible ophthalmological applications. Description of the studied drug, the particles main composition, and the most important results.

Drug	Materials	Essential outcomes	References
Flurbiprofen	Stearic acid; castor oil; Tween® 80	Adequate physicochemical features; storage stability; non-irritant	(Gonzalez-Mira et al. 2010)
Flurbiprofen	Compritol® 888 ATO/ stearic acid; Miglyol® 812; castor oil; Tween® 80	High %EE; long-term physical stability; sustained release; enhanced transcorneal permeation; well tolerated	(Gonzalez-Mira et al. 2012)
Flurbiprofen	Partially deacetylated water-soluble chitosan (coating); Compritol® 888 ATO; Gelucire® 44/14; Miglyol® 812; Tween® 80; Solutol® HS 15	%EE >90%; suitable physicochemical characteristics; improved precorneal resident time and permeability	(Tian et al. 2012)

Table 6 (continued)

Mangiferin	Glyceryl monostearate; Gelucire® 44/14; Miglyol® 812; Tween® 80	Burst followed by sustained release; enhanced precorneal retention and transcorneal permeation (up to 4.31-fold); increased bioavailability	(Liu et al. 2012)
Ofloxacin	Compritol® HD5 ATO; oleic acid; Tween® 80; chitosan oligosaccharide lactate	Extended precorneal residence time; controlled release; superior therapeutic effect; non-irritant	(Üstündağ-Okur et al. 2014)
Curcumin	Glyceryl monostearate; Miglyol® 812N; Solutol® HS 15; chitosan-N-acetyl-L-cysteine/ chitosan oligosaccharides/ carboxymethyl chitosan (coating)	Prolonged and sustained release (>72 h); higher precorneal retention; increased corneal permeation; safe	(J. Li et al. 2016)
Ibuprofen	Several solid and liquid lipids; Pluronic® F-127; chitosan	High %EE; controlled and sustained release; improved mucoadhesive properties; increased precorneal retention; non-cytotoxic	(Almeida et al. 2016)
Ibuprofen	Several solid and liquid lipids; Pluronic® F-127	Adequate physicochemical features; good stability; prolonged release; increased precorneal retention; safe	(Almeida et al. 2017)
Coumarin-6	Glyceryl monostearate; Miglyol® 812N; Solutol® HS 15; chitosan – NAC / chitosan oligosaccharides/ carboxymethyl chitosan (coating)	Suitable physicochemical characteristics; increased precorneal residence time and corneal permeation; enhanced bioavailability	(J. Li et al. 2017)
Baicalin	Compritol® 888 ATO; Miglyol® 812N; Cremophor® EL; soy lecithin; carboxymethyl chitosan; genipin; poloxamer F127	Burst followed by sustained release; increased transcorneal permeation (3.18-fold); improved precorneal retention, non-irritant	(Yu et al. 2019)
Etoposide/ Coumarin-6	Several solid and liquid lipids; glyceryl stearyl citrate; chitosan oligosaccharides (coating)	Sustained release; enhanced mucoadhesion and ocular retention; increased bioavailability; non-toxic/irritant	(Pai and Vavia 2020)
Riboflavin	Compritol® ATO 888; Gelucire® 44/14; Miglyol® 812; Cremophor® EL; Transcutol® P; Stearylamine	Controlled release; adhesive properties; increased corneal permeability; non-toxic	(Aytekin et al. 2020)

2.4.8. Polymeric nanoparticles

Nanoparticles are, by far, the most studied colloidal drug delivery system in ophthalmology. They are defined as solid and submicron-sized drug carriers with a size ranging from 1 to 1000 nm (Herrero-Vanrell et al. 2013). Considering ocular delivery, drug-loaded nanoparticles should have a size between 50 and 400 nm as they can cross physiological barriers either by passive or ligand mediated targeting mechanisms (Bachu et al. 2018). Depending on their structure and preparation method, polymeric nanoparticles can be subdivided into nanospheres and nanocapsules (Figure 13), which present different drug release profiles. Nanospheres are small solid spheres constituted by a dense polymeric network. They present a matrix type structure with a large surface area in which the drug can be either adsorbed on the surface or incorporated within the particle. On the other hand, nanocapsules consist of a small liquid core (oily droplet) surrounded by a polymeric membrane. The active substance is normally dissolved into the central cavity but it can also be adsorbed on the capsule surface (Herrero-Vanrell et al. 2013; Ameeduzzafar et al. 2016).

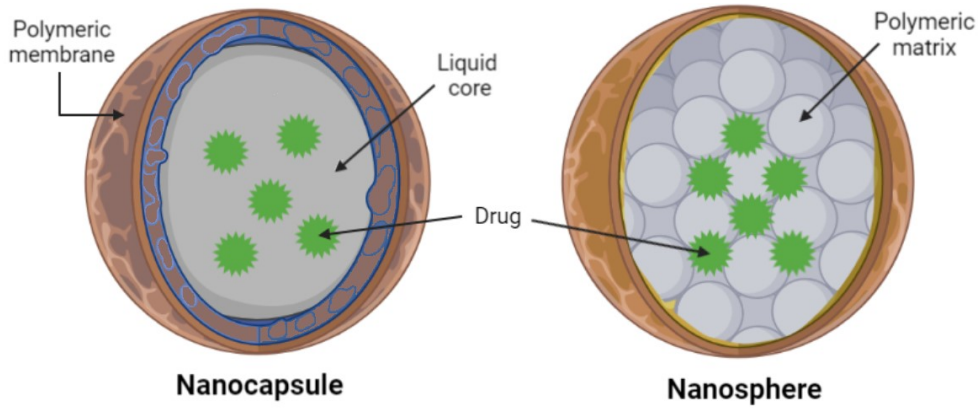

Figure 13: Schematic examples of a nanocapsule and a nanosphere loaded with drugs (created with BioRender.com).

Lipids, proteins, natural or synthetic polymers, such as albumin, sodium alginate, chitosan, polylactide-co-glycolide, polylactic acid, and polycaprolactone are examples of compounds used to develop nanoparticles for ophthalmic drug delivery. Several advantages are associated with the use of nanoparticles, which have been used in ophthalmology for both anterior and posterior segment treatment. They offer less discomfort and irritation due to the small size particles, being a very user friendly formulation, especially in chronic therapeutics (Bachu et al. 2018). Also, the small size makes them suitable to treat retinal disorders as they

can be taken up by the RPE cells (Herrero-Vanrell et al. 2013). Nanoparticles enable drug's sustained release, slow elimination rate, prevent premature degradation or non-specific uptake, significantly enhancing ocular drug absorption when compared to eye drops. This avoids frequent administration and increases patient compliance to the treatment. Moreover, nanoparticles improve intracellular penetration and provide target-specific delivery (Bachu et al. 2018). Regarding the singularity of ocular surface environment, bioadhesive nanoparticles designed for topical administration are a special focus of investigation. They generally do not induce ocular distress and ensure an intimate contact between the drug and the ocular mucins, thus increasing the precorneal retention time and improving corneal penetration (Herrero-Vanrell et al. 2013; Ameeduzzafar et al. 2016). One of the first mucoadhesive nanoparticles developed for ocular use were prepared with a polycyanoacrylate derivate (Wood et al. 1985). Despite the moderate results, this preliminary study opened the window for research in this field.

The potential value of chitosan in ophthalmology considerably expanded, due to its mucoadhesive properties, along with its versatility and biocompatibility. Calvo et al. (1997) performed a study comparing indomethacin-loaded poly-ε-caprolactone nanocapsules coated with chitosan or poly-L-lysine. These nanoparticles were prepared by a modified interfacial deposition technique followed by the coating. All formulations achieved an encapsulation efficiency higher than 90 % and similar release profiles, but the *in vivo* study was definitely favorable to chitosan-coated nanocapsules, as they significantly increased the indomethacin corneal and aqueous humor concentrations due to an enhanced corneal penetration (Calvo et al. 1997). De Campos et al. (2001) explored chitosan nanoparticles as vehicles of cyclosporin A for ocular delivery. Nanoparticles were synthetized by ionic gelation method upon the addition of sodium tripolyphosphate. The *in vivo* study revealed that drug's concentration in the conjunctiva and cornea was above the minimum effective dosage until 24 hours post-instillation, as opposed to chitosan solution. Corneal cyclosporin A levels were significantly higher than those in conjunctiva, but chitosan didn't seem to enhance cyclosporin A corneal penetration, which remained on the precorneal area. The study concluded that chitosan nanoparticles led to a selective and prolonged cyclosporin A delivery, minimizing its systemic absorption and intraocular damage (De Campos et al. 2001). The same research group investigated the interaction between the ocular mucosa and chitosan nanoparticles using chitosan-fluorescein covalent biding. *In vivo* studies demonstrated that concentration of chitosan nanoparticles in cornea and conjunctiva were significantly higher when compared with the chitosan solution, being fairly constant for up to 24 hours. Confocal laser scanning microscopy revealed that chitosan nanoparticles had a greater affinity for conjunctiva, most probably due to mucin interaction. In addition, the nanoformulation showed a high cell survival

rate and vitality, being considered a promising vehicle for drug delivery to the eye (De Campos et al. 2004).

Further studies aimed to optimize chitosan nanoparticles regarding their drug delivery purposes, widening the possible future ophthalmic applications (Verheul et al. 2010). Yoncheva et al. (2011) developed pilocarpine loaded poly(lactic-co-glycolic acid) nanoparticles prepared by solvent evaporation method and coated with mucoadhesive polymers, namely chitosan, alginate and poloxamers 407 and 188. *In vitro* drug release showed that all the polymer-coated nanoparticles had a lower burst release effect (22-35 % of release pilocarpine) than the non-coated nanoparticles (63 % of release pilocarpine), followed by a continuous and slower release. Nevertheless, chitosan-coated poly(lactic-co-glycolic acid) nanoparticles showed the best results, as the turbidity and zeta potential measurements revealed interaction with the ocular mucins up to 6 hours (Yoncheva et al. 2011). Mahmoud et al. (2011) had some similar results, but the team used econazole nitrate as a model drug. They developed chitosan nanoparticles by modified ionotropic gelation, using sulfobutylether-β-cyclodextrin as polyanionic crosslinker. Nanoparticles led to a sustained drug release pattern and promoted a greater and prolonged antifungal effect in rabbits, when compared to the solution (Mahmoud et al. 2011).

In fact, numerous studies indicate that chitosan has the ability to enhance pharmacological action of drugs. Zaki and Hafez (2012) studied chitosan nanoparticles loaded with ceftriaxone and only 23% of the drug was released within the first hour followed by a sustained release that lasted for 96 hours. Ceftriaxone loaded nanoparticles were rapidly and efficiently internalized into Caco-2 (model of enterocytes) and J774.2 (macrophages) cells with no significant cytotoxic effects and allowed a 99 % decrease in bacterial count in both cell lines. Moreover, plain chitosan nanoparticles demonstrated a lower but important antibacterial effect (Zaki and Hafez 2012). Likewise, Silva et al. (2013) developed daptomycin-loaded chitosan nanoparticles with good mucoadhesive properties, suitable sizes around 200 nm, high encapsulation efficiency (over 90 %) and continuous daptomycin release up to 4 hours, also preserving daptomycin antimicrobial efficiency after encapsulation (Silva et al. 2013). A similar conclusion was achieved from Costa et al. (2015) study with daptomycin-loaded alginate nanoparticles coated with chitosan. The nanoparticles did not interfere in daptomycin efficiency and prolonged the permeation across human corneal epithelial cell (HCE) and human retinal pigment epithelial cell (ARPE-19) lines which were used as *in vitro* models of corneal and retinal epithelia, respectively (Costa et al. 2015).

As mentioned before, ocular applications of chitosan amphiphiles have been a recent focus of investigation. Badr et al. (2021) developed Molecular Envelope Technology (MET) nanoparticles to overcome some undesirable effects of tacrolimus suspension. These particles are glycol chitosan based amphiphiles which contain 0.1 % w/v of tacrolimus and present good

stability and suitable physicochemical properties. They found out that, after a single topical dose of MET-tacrolimus, the concentration of tacrolimus in the rabbits' conjunctiva and cornea was considerably higher than the therapeutical levels described in the literature. Thus, this novel formulation could be of value in the treatment of allergic conjunctivitis (Badr et al. 2021). Chitosan is a valuable polymer that can be used by itself and in combination with other polymers, such as hyaluronic acid, which became quite common to enhance mucoadhesion of nanoparticles. For example, Wadhwa et al. (2010) assembled chitosan with hyaluronic acid for effective management of glaucoma with timolol and dorzolamide. They compared chitosan nanoparticles with chitosan-hyaluronic acid nanoparticles, both prepared by a modified ionotropic gelation technique. Both formulations could effectively control the drug release, showing an initial burst followed by a sustained release. Yet, chitosan-hyaluronic acid nanoparticles significantly increased mucoadhesion and allowed a higher drug permeation, possibly due to the secondary binding properties of hyaluronic acid. Moreover, the addition of hyaluronic acid prolonged the drug effect up to 4 hours, increased its magnitude and reduced systemic absorption (Wadhwa et al. 2010). Comparable *in vitro* results were achieved by Kalam (2016a) using the same method to create chitosan nanoparticles coated with hyaluronic acid for topical delivery of dexamethasone. Likewise, this nanoparticulate system had the potential to produce a sustained release, an increased absorption and an enhanced bioavailability of any lipophilic or hydrophilic drug, while protecting the active principal from enzymatic degradation. The formulation revealed good long-term stability as well (Kalam 2016a). Silva et al. (2017) also developed similar chitosan-hyaluronic acid nanoparticles carrying ceftazidime, presenting a sustained and extended drug release, preserving its antibacterial activity and showing no toxic *in vitro* effects (Silva et al. 2017). Chitosan and hyaluronic acid are natural and safe mucoadhesive polysaccharides with a possible synergic action, specially concerning mucoadhesion and ocular permeation, which might enhance drugs intraocular bioavailability.

Besides its association with chitosan, hyaluronic acid is vastly combined with other polymers with the same purpose of increasing mucoadhesion of formulations. Using a nanoprecipitation method, Yenice et al. (2008) created poly-ε-caprolactone/ benzalkonium chloride nanospheres coated with hyaluronic acid in order to deliver cyclosporine A to the eye. Corneal concentrations of cyclosporine A following topical instillation were 6 to 8 times superior for nanospheres than for castor oil solution (control). The hyaluronic acid coating resulted in a significant increase in the cyclosporine A corneal uptake above therapeutic levels, for at least 24 hours. However, similarly to the study of De Campos et al. (2001), cyclosporine A concentration in the aqueous humor was often undetectable. Coated nanocapsules were well tolerated *in vivo* and confocal microscopy confirmed the presence of high cyclosporine A corneal levels, which probably happened due to the penetration enhancement properties of

benzalkonium chloride and mucoadhesion of hyaluronic acid, showing potential for local treatment of immune-mediated corneal diseases (Yenice et al. 2008). Liu et al. (2016) also encapsulated cyclosporine A, but used phenylboronic acid-modified nanoparticles instead. According to the authors, phenylboronic acid has a higher affinity towards ocular mucins than chitosan, because phenylboronic acid interacts with mucins by covalent bonding instead of electrostatic interaction. Phenylboronic acid coating was able to increase ocular drug retention, improve tear production, eliminate inflammation and lead to a complete recovery of mice with induced dry eye disease (Liu et al. 2016).

Researchers keep exploring innovative nanoparticles made of synthetic and/or natural polymers and even try using different combinations. Nevertheless, the mucoadhesive form should be carefully chosen bearing in mind the therapeutic target. Redín et al. (2019) studied polyethylene glycol-coated and non-coated human serum albumin nanoparticles carrying bevacizumab to treat corneal neovascularization in rats. Nanoparticulate formulations were administered once a day. They concluded that non-coated nanoparticles exhibited higher capacity to inhibit the formation of new vessels (61 %) than polyethylene glycol-coated nanoparticles (38 %) and free drugs (11 %), probably because of polyethylene glycol lower hydrophobicity, which is a desirable characteristic to promote interaction with the lipophilic corneal epithelium (Luis de Redín et al. 2019). Nevertheless, we must consider that the mucoadhesive property of polyethylene glycol was not analyzed in this study.

Tamarind seed polysaccharide obtained from the seeds of *Tamarindus indica*, is a water-soluble polysaccharide used as thickening, stabilizing and gelling agent in the food industry. Due to its disadvantages like unpleasant odor, dull color and fast degradability it is usually modified by chemical treatment with for instance acetyl, hydroxyalkyl and carboxymethyl groups (Kaur et al. 2012). A research group conducted two studies to investigate the mucoadhesive effect of this polymer in nanoparticles for ocular delivery of tropicamide. Kaur et al. (2012) developed tropicamide-loaded carboxymethyl tamarind kernel powder (CMTKP) nanoparticles using ionotropic gelation technique. *Ex vivo* corneal permeation of tropicamide in optimized CMTKP nanoparticles was comparable to that detected in aqueous solution but the bioadhesion assay revealed that the nanosuspension adsorbed 87.67% of mucin, which indicates an excellent mucoadhesive potential. Besides, the nanoformulation presented great ocular tolerance (Kaur et al. 2012). Similarly, Dilbaghi et al. (2013) studied tamarind seed xyloglucan nanoparticles with the same purpose. Results revealed a significantly higher tropicamide permeation for tamarind seed xyloglucan nanosuspension in comparison with the commercial solution. Mucoadhesion was very promising since approximately 87 % of the mucin was adsorbed onto the tamarind seed xyloglucan nanoparticles. Moreover, the integrity of corneal epithelium and endothelium was not affected by the nanoformulation toxicity (Dilbaghi et al. 2013). On the other hand, Mittal and Kaur (2019) created nanoparticles of

carboxymethyl and amine derivatives of galactomannan gum, which was extracted from *Leucaena leucocephala* seeds, to deliver dorzolamide to the eye. Nanoparticles presented good particles size (< 200 nm) and encapsulation efficiency (≈ 80 %). Nanoparticles *in vitro* release revealed a less accentuated burst followed by a sustained release, which is actually a favorable release profile for glaucoma management. *Ex vivo* transcorneal permeation of dorzolamide was higher for nanoparticles (87.88 %) than for marketed formulation (65.54 %) within a 12 hours period, probably due to the nanoparticles mucoadhesion features which increased precorneal retention time. In addition, the nanoformulation showed a maximum IOP reduction 4 hours after the topical instillation, maintaining this effect until 12 hours post-administration compared to 3 hours for the marketed solution (Mittal and Kaur 2019). These conclusions are similar to those found by Wadhwa et al. (2010), despite the different nature of the nanoparticles.

Still regarding glaucoma, there is a new molecule called R-801, which is being used for primary open angle glaucoma treatment since it increases aqueous humor outflow through targeting the trabecular meshwork. Ibrahim and Jablonski (2019) developed a novel formulation by incorporating R-801 in a bioadhesive nanoparticulate delivery system. Nanoparticles were synthetized by a new double emulsification solvent diffusion method, using sodium alginate, Eudragit® RL 100 and soy lecithin, and chitosan and Carbopol® 940 as vehicle gels. Carbopol® 940 gel was selected because it showed the most promising *in vitro* results. The optimized nanoformulation revealed a good viscosity and a remarkable sustained R-801 release for more than 72 hours, which was confirmed by *in vivo* evaluation. Cytotoxicity study proved the safety of the formulation, also confirmed by *in vivo* tests. Drug efficacy of the nanoformulation was demonstrated using two animal models (BXD86 mice and DB rabbits). The pharmacological effect of R-801 in nanoparticles was maintained in a long-term basis with daily use, leading to constant lower IOP values without fluctuations. The group considered this novel nanoformulation a promising, safe, efficient and long acting topical glaucoma medication (Ibrahim and Jablonski 2019).

Chitosan is the predominant mucoadhesive polymer used in nanoparticles but its combination with other mucoadhesive polymers, especially hyaluronic acid, seems to potentiate this feature. Plant-based mucoadhesive polymers also offer good results and could be another interesting mean to enhance the mucoadhesion of formulations. Table 7 shows additional studies about nanoparticulate systems with mucoadhesive properties, including their composition and main outcomes.

Table 7: Mucoadhesive polymeric nanoparticles formulations with possible ophthalmological applications. Description of the studied drug, the particles main composition, and the most important results. *No pharmacologically active substance

Drug	Materials	Essential outcomes	References
Timolol maleate	Isobutyl cyanoacrylate; dextran T40 or T70; Pluronic® F68/ Tween® 20	Suitable size and MW range; influence of pH, surfactant and stabilizers on physicochemical characteristics	(Das et al. 1995)
Brimonidine	Polyacrylic acid; Span® 80; Tween® 80	Particles in the nano-range; slower and sustained release; effective cell permeability; non-toxic	(De et al. 2003)
Cloricromene (AD6 and MET)	Eudragit® RL 100; Tween® 80; benzalkonium chloride	Good stability; sustained release; increased drug intraocular permeation; safe	(Bucolo et al. 2004)
Gatifloxacin	Chitosan; sodium alginate; Pluronic® F127	%EE 61-82%; suitable particle size; stability; gradual and sustained release (24 h)	(Motwani et al. 2008)
pDNA models (pEGFP, pSEAP and pβgal)	Sodium hyaluronate; chitosan; sodium tripolyphosphate	Particles in the nano-range; increased precorneal retention time and intraocular permeation; safe	(de la Fuente et al. 2008)
Gatifloxacin/ Prednisolone	Eudragit® RL 100; Eudragit® RS 100; hyaluronic acid (coating)	High %EE; no burst release; prolonged release; increased intraocular permeation	(Ibrahim et al. 2010)
Sparfloxacin	Poly(lactic-co-glycolic acid); polyvinyl alcohol	%EE 86.6%; stable; slow and sustained release (24 h); prolonged microbial efficacy; non-irritant; well tolerated	(Gupta et al. 2010)
Ganciclovir	Chitosan; Tween® 20	Particles in the nano-range; increased ocular bioavailability; non-irritant	(Akhter et al. 2011)
Cyclosporine A	Poly(lactic-co-glycolic acid); Carbopol® or Eudragit® RL 100; polyvinyl alcohol	High %EE; suitable particle size; sustained release (24 h); higher concentration in tear film; increased cellular uptake	(Aksungur et al. 2011)
pDNA model (pSEAP)	Hyaluronic acid; chitosan	Suitable physicochemical characteristics; increased cellular uptake; significant transfection efficiency; non cytotoxic	(Contreras-Ruiz et al. 2011)
5-Fluorouracil	Chitosan; sodium tripolyphosphate	Particles in the nano-range; burst release followed by sustained release; increased intraocular bioavailability; non-irritant	(Nagarwal et al. 2011)

Table 7 (continued)

*	Poly(lactic-co-glycolic acid); chitosan; polyvinyl alcohol	Suitable physicochemical characteristics; improved retention time; better ocular interaction; non-irritant	(Jain et al. 2011)
Natamycin	Lecithin; chitosan	%EE 73.57%; slow and sustained release; higher precorneal retention time; increased therapeutic efficacy; safe	(Bhatta et al. 2012)
*	Chitosan (also thiolated); sodium alginate	Suitable physicochemical characteristics; improved mucoadhesion; increased cellular uptake; non-cytotoxic	(X. Zhu et al. 2012)
Betaxolol	Chitosan; Span® 80	Particles in the nano-range; burst followed by extended release (12 h); prolonged therapeutic effect; non irritant	(Jain et al. 2013)
Dorzolamide	Chitosan; TPP/ 6-O-carboxymethyl (OCM); calcium chloride	OCM NPs with better results; sustained release (8 h); higher mucin binding; prolonged therapeutic effect; non-irritant	(Shinde et al. 2013)
Acetazolamide	Eudragit® RL 100; polyvinyl alcohol	Good stability; sustained and prolonged release; higher efficacy and prolonged therapeutic effect	(Verma et al. 2013)
Triamcinolone acetonide	Poly β-amino ester; polyvinyl alcohol	Burst followed by sustained release; increased precorneal time and permeation; improved therapeutic effect	(Sabzevari et al. 2013)
*	Chitosan; dextran sulfate	%EE > 80%; suitable particle size; stable; good mucoadhesive properties	(Chaiyasan et al. 2013)
Levofloxacin	Chitosan; poly(lactic-co-glycolic acid); polyvinyl alcohol	Suitable physicochemical characteristics; prolonged precorneal residence time and bioavailability	(Gupta et al. 2013)
Aceclofenac	Eudragit® RL 100; Tween® 80	High %EE; burst followed by slow and sustained release; increased corneal permeation; higher therapeutic efficacy	(Katara and Majumdar 2013)
Pilocarpine	Eudragit® RS 100 or Gelucire® 44/14; octadecylamine; Tween® 80; benzalkonium chloride	Suitable physicochemical characteristics; drug loss during the stability test	(Lütfi and Müzeyyen 2013)
Amphotericin B	Polylactic acid; chitosan	Prolonged contact time; sustained release; enhanced corneal penetration; non-irritant; effective therapeutic	(W. Zhou et al. 2013)
Riboflavin	Polyacrylic acid; methylcellulose	Slow release; good mucoadhesion; prolonged precorneal retention time; non-irritant	(Khutoryanskaya et al. 2014)

Table 7 (continued)

Moxifloxacin	Chitosan; dextran sulfate	Good %EE; prolonged release profile; high corneal retention and permeation; improved therapeutic effect; safe	(Kaskoos 2014)
Amphotericin B	Lecithin; chitosan	Prolonged release; good mucoadhesion; enhanced precorneal retention time; effective treatment; safe	(Chhonker et al. 2015)
Diclofenac	Cross-linked sodium hyaluronate (CLNaHA)/ linear sodium hyaluronate (NaHA)/ Zinc hyaluronate (ZnHA)	Lower biocompatibility for ZnHA; good mucoadhesion properties; burst followed by sustained and prolonged release	(Horvát et al. 2015)
Pranoprofen	Polylactic-co-glycolic acid; polyvinyl alcohol; arachidonic acid sodium	Suitable mucoadhesive properties; sustained release; improved therapeutic effect	(Abrego et al. 2015)
Lutein	Chitosan; dextran sulfate; polyethylene glycol 400; EDC (1-ethyl-3-(3- dimethylaminopropyl)-carbodiimide hydrochloride)	Stability; good mucoadhesion; enhanced ocular surface retention time; sustained release	(Chaiyasan et al. 2015)
Loteprednol	Polybutylene adipate; N-succinyl chitosan	Appropriate size, %DL and %EE; burst followed by sustained and controlled release; good mucoadhesion; low cytotoxicity	(Nasr and Khoee 2015)
Melatonin	Lecithin; chitosan; Pluronic® F127	Good mucoadhesive properties; prolonged release; enhanced corneal permeation; non-cytotoxic	(Hafner et al. 2015)
Dexamethasone and met-enkephalin	Quaternary ammonium–chitosan conjugates (thiolated and non thiolated)	Particles in the nano-range; good mucoadhesive properties; prolonged ocular residence time	(Fabiano et al. 2015)
Brimonidine	Chitosan/ sodium alginate; lecithin; poloxamer 188/polyvinyl alcohol; hydroxypropyl methylcellulose	Suitable pH and viscosity; sustained release (no burst effect); non-toxic; more efficient and prolonged therapeutic effect	(Ibrahim et al. 2015)
Rosmarinic acid	Chitosan; sodium tripolyphosphate	Particle size 200-300 nm; ZP +20-+30mV; non cytotoxic; good mucoadhesion but no relevant *in vitro* permeability difference	(da Silva et al. 2016)
Econazole	Methyl-β-cyclodextrin or hydroxylpropyl-β-cyclodextrin; poloxamer 407 or Tween® 20; chitosan	CS greater mucin interaction; increased drug release; enhanced drug bioavailability; safe	(Maged et al., 2016)
Ketorolac	Eudragit® RL 100; polyvinyl alcohol; Pluronic® F127; hydroxypropyl methylcellulose	High %EE; sustained release; optimum mucoadhesive properties; high permeation and bioavailability; safe	(Morsi et al. 2016)

Table 7 (continued)

Norfloxacin	Chitosan; sodium tripolyphosphate; Carbopol® 934P	Sustained release; prolonged precorneal residence time; effective treatment; safe	(Upadhayay et al. 2016)
Acetazolamide	Ethylcellulose/ Eudragit® RS 100; Span® 60; Tween® 80	High %EE; mucoadhesive properties; increased corneal permeation; more efficient and prolonged therapeutic efficacy	(Quinteros et al. 2016)
Dexamethasone	Chitosan; sodium tripolyphosphate; hyaluronic acid (coating)	Prolonged precorneal retention; effective transcorneal permeation; high ocular bioavailability; non-irritant	(Kalam 2016b)
Resveratrol and Quercetin	polyethylene glycol; chitosan; sodium tripolyphosphate	Increased transcorneal permeation; enhanced and prolonged *in vivo* effect; non-toxic	(Natesan et al. 2017)
*	Poly(lactic-co-glycolic acid); chitosan/glycol chitosan/polysorbate 80; polyvinyl alcohol	Good mucoadhesion; improved drug delivery to the retina	(Tahara et al. 2017)
*	Chitosan; dextran sulfate	Suitable physicochemical characteristics; mucoadhesive properties; penetrate only corneal epithelium (no stroma)	(Chaiyasan et al. 2017)
Acetazolamide	Chitosan; sodium tripolyphosphate	High %EE; excellent mucoadhesive properties; enhanced corneal permeation; prolonged therapeutic effect	(Manchanda and Sahoo 2017)
Epigallocatechin gallate (EGCG)	Type A gelatin; hyaluronic acid	Particles in the nano-range; extended retention time; good therapeutic results; non-toxic/non-irritant	(H.Y. Huang et al. 2018)
Cyclosporine A	Span® 80; TPGS; CTAB; hyaluronic acid (coating)	Adequate physicochemical properties; higher cellular uptake (HA); effective treatment; safe	(Alvarez-Trabado et al. 2018)
5-Fluorouracil	Quaternary ammonium-chitosan conjugates; sodium tripolyphosphate; hyaluronic acid	Mucoadhesive features; prolonged ocular residence time; increased bioavailability	(Fabiano et al. 2019)
Acetazolamide	Chitosan; Span® 60; Tween® 80/20; SDC; sodium tripolyphosphate	Good mucoadhesion; prolonged release; extended therapeutic effect (24 h); non-irritant	(Abdel-Rashid et al. 2019)
Lutein	Poly(lactic-co-glycolic acid); Tween® 80; Poloxamer 407; PEO 1105	Suitable physicochemical properties; burst (48 h) followed by sustained release (5 days); mucoadhesive features; effective treatment	(Bodoki et al. 2019)
Dexamethasone	Glycol chitosan; N-(3-dimethylaminopropyl)-N'-ethylcarbodiimide hydrochloride (EDC); N-hydroxysuccinimide (NHS)	Particles in the nano range; great mucoadhesive properties; long precorneal retention; sustained release (48 h)	(Yu et al. 2020)

2.4.9. Nanocrystals

In nanocrystals (Figure 14), the drug itself forms the majority of the nanostructure, being surrounded by excipients that stabilize it and may influence the interaction with ocular barriers (Reimondez-Troitiño et al. 2015). Besides an enhanced drug solubility and dissolution rate, nanocrystals may have a high adhesion and internalization capacity influenced by the surfactants nature (Reimondez-Troitiño et al. 2015) and the particle size, which normally ranges from 10 to 1000 nm (Sharma et al. 2016). Particle size reduction leads to an increased surface area which adds mucoadhesive properties to the nanocrystals and helps the interaction with biological membranes, improving the bioavailability of poorly soluble drugs (Sharma et al. 2016). Depending on the preparation method, drug nanocrystals can be in crystalline or amorphous form, being this last the most soluble, and if the system is unstable the amorphous form is converted into crystalline. The simplicity of nanocrystals formulation and its wide applicability make it a universal approach to overcome solubility problems (Sharma et al. 2016). However, only tree studies were found in our search approaching mucoadhesive nanocrystals for topical ocular administration. Despite the scarce information, nanocrystals might be an interesting delivery system to be explored in the near future, based on their characteristics and promising results presented below.

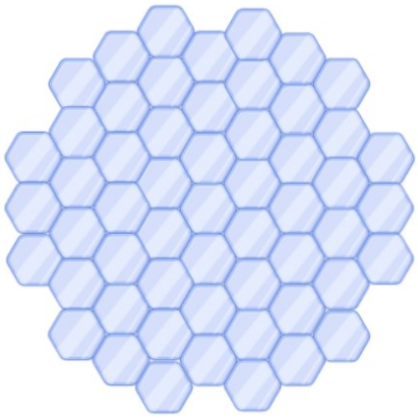

Figure 14: Illustration of the structure of a nanocrystal particle (created with BioRender.com).

Tuomela et al. (2014) created brinzolamide nanocrystals to reduce IOP in a rat model of induced ocular hypertension. They tested poloxamer F68/ F127, polysorbate 80, and hydroxypropyl methylcellulose as stabilizers at pH 4.5 and 7.4. Nanocrystals were prepared by a top-down wet milling technique using a planetary ball mill. Hydroxypropyl methylcellulose was the most effective polymer to prevent aggregation of the nanocrystal suspension.

Nanoformulations significantly decreased IOP values in the *in vivo* assay and were considered safe. When the free drug was at its highest concentration (pH 4.5), IOP reduction was enhanced. Scarce conclusions regarding mucoadhesive features could be retrieved from this study but hydroxypropyl methylcellulose is known for prolonging the contact with the ocular mucosa, having also lubricant properties and accelerating wound healing. The *in vitro* assay revealed that nanocrystals presented immediate dissolution, which is a major benefit when considering poorly soluble drugs. Additionally, as nanocrystal suspensions contain no matrix material, they present a regulatory advantage, and require a smaller amount of stabilizer when compared to polymeric nanoparticles (Tuomela et al. 2014).

Romero et al. (2016) developed cationic nanocrystals for ocular delivery of dexamethasone acetate and polymyxin B. The system was produced by a self-developed miniaturized wet bead milling method. As polymyxin B is an amphiphilic cationic molecule, the group tried to use it as the only stabilizer, but the stabilization was insufficient, so benzalkonium chloride and cetylpyridinium chloride, also cationic molecules, were added. Although both presented good results, the cetylpyridinium chloride allowed a better long-term stability. Small particle sizes were achieved, around 250 nm, which enhanced the possibility of mucoadhesion and increased the saturation solubility, thus increasing concentration gradient to the eye. Mucoadhesive results indicated that the positively charged nanocrystals became negatively charged due to electrostatic interaction with mucin molecules, which could lead to an increased retention time. Moreover, all the formulations revealed no cytotoxicity, reinforcing their potential use as an ophthalmic delivery system (Romero et al. 2016).

The behavior of cellulose nanocrystals carrying pilocarpine hydrochloride on poloxamer based in situ gels was studied by Orasugh et al. (2019). Cellulose was extracted from jute fibers, being then purified and processed to create the nanocrystals. The addition of cellulose nanocrystals to the poloxamer gel led to a reduced gel dissolution due to the hydrogen-bond interaction between nanocrystals and poloxamer molecules. Also, including nanocellulose allowed a corresponding increase in shear stress and a very substantial increase in gel strength. A sustained release of pilocarpine from these nanocomposite gels was observed. The nanoformulation containing 1.2 % (w/v) cellulose nanocrystals showed the best controlled release profile, indicating that the greater concentration of cellulose nanocrystals, the better the sustained drug release. Therefore, this potential non-toxic nanocomposite hydrogel can be foreseen as a competent ocular drug delivery system (Orasugh et al. 2019).

2.4.10. Dendrimers

Recently, dendrimers have been suggested as options in topical ocular drug delivery. Dendrimers are polymeric nanostructures with a star-shaped or tree-shaped highly branched 3D structure, formed by repetitive molecules surrounding a central core (Figure 15) (Reimondez-Troitiño et al. 2015; Ameeduzzafar et al. 2016). Their architecture displays a high number of controlled terminal groups, making them a suitable candidate for delivery of both hydrophilic and lipophilic drugs (Ameeduzzafar et al. 2016; Bachu et al. 2018). Therefore, dendrimers are appropriate for ocular drug delivery as their core can solubilize lipophilic and hydrophilic drugs and their terminal groups provide sustained drug release (Bachu et al. 2018). Moreover therapeutic agents can be covalently bonded onto the surface of the dendrimer as well (Ameeduzzafar et al. 2016). The drug delivery can be modified by the surface groups (e.g. amine, carboxylic or hydroxyl), the size or the molecular weight of the dendrimers (Bachu et al. 2018). Yet, in general, dendrimers increase drugs precorneal residence time, granting an improved bioavailability and a prolonged therapeutic effect (Reimondez-Troitiño et al. 2015), and may also present antimicrobial properties (Kamaleddin 2017). The performance of these carriers can be enhanced by modifying their surface using strategies such as acetylation or PEGylation (polyethylene glycol modification), which may also reduce their toxicity (Reimondez-Troitiño et al. 2015). Dendrimers consisting of polyamidoamine (PAMAM), with carboxylic and hydroxyl surface groups, improve drugs solubility and allow surface connection of the targeting ligand and/or drugs (Bachu et al. 2018). The synthesis of PAMAM dendrimers begins with a central core molecule and ‘generations’ of branches are added in a series of sequential reactions (Lancina and Yang 2017). *In vitro* studies revealed robust interactions between the ocular mucins and PAMAM dendrimers in the tear film (Bachu et al. 2018). Some dendrimers show the ability to bypass efflux transporters and enable an efficient drug transport across cellular barriers (Ameeduzzafar et al. 2016).

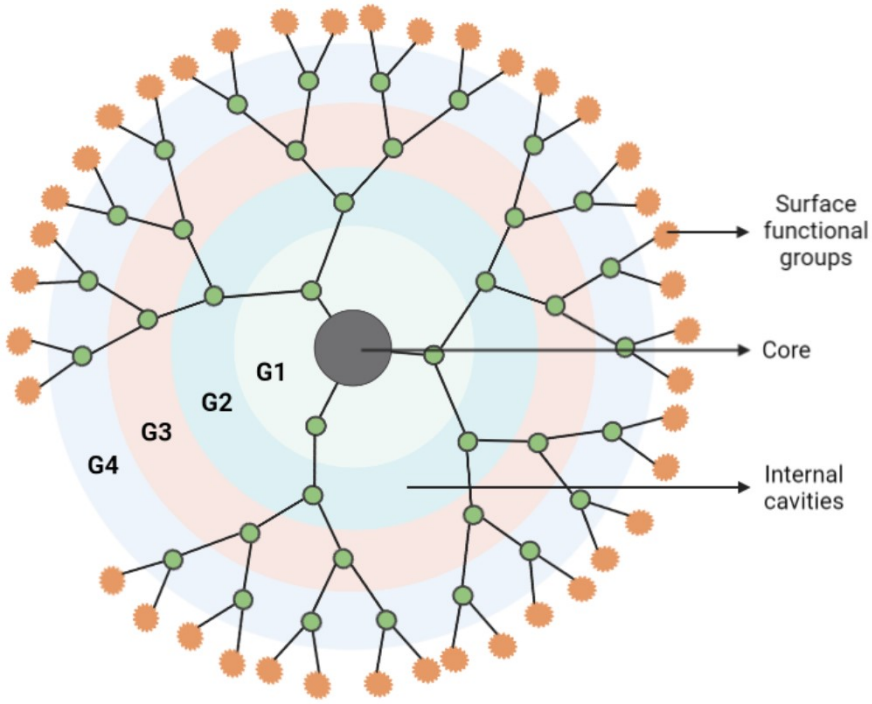

Figure 15: Schematic representation of a dendrimer's structure showing four generations of branches (G1, G2, G3 and G4) (created with BioRender.com).

Dendrimers are one of the most versatile nanoscaled drug delivery systems due to their well-defined size, tailorable structure, reproducible and optimized design, targeted delivery, and appropriate biodistribution in both anterior and posterior eye segments, addressing physicochemical limitations of the classical drugs (Ameeduzzafar et al. 2016). Vandamme and Brobeck (2005) created different types of PAMAM dendrimers to compare with Carbopol® 980 NF and hydroxypropyl methylcellulose as ophthalmic vehicles of pilocarpine nitrate and tropicamide. Dendrimers were synthesized by Dendritech® and then purified by ultrafiltration. The pH values, osmolality, refractive index, viscosity and surface tension were in the range of ophthalmic administration. Rheological results revealed that dendrimers would have the potential to prolong drugs contact time with the cornea. Dendrimers with hydroxyl groups showed greater efficiency in lowering surface tension than charged dendrimers, causing less discomfort. Yet, no dendrimers formulation caused any ocular irritation or induced any watering reflex. Dendrimers from the generation 2 with carboxylate surface groups and from generation 4 with hydroxyl surface groups presented the longest ocular residence time (comparable to Carbopol®) and greater drug bioavailability (Vandamme and Brobeck 2005). Despite dendrimers significant mucoadhesive characteristics, it is possible to improve this feature by association with bioadhesive agents. One of the first attempts was performed by Lopez et al. (2009) whose team developed PAMAM dendrimers modified with polyethylene glycol groups

(PEGylation) and investigated their performance against the common ocular pathogens *Pseudomonas aeruginosa* and *Staphylococcus aureus*. The MIC values of G3 and G5 PAMAM for both bacteria were higher than those of the most common antibiotics: ciprofloxacin, gatifloxacin, levofloxacin and moxifloxacin. On the other hand, PEGylation resulted in a reduction of the activity against *P. aeruginosa* and even an almost complete deactivation against *S. aureus*. Possibly, the charge density and the partial shielding of polyethylene glycol chains decreased the electrostatic interactions with the negatively-charged bacterial surface. However, the PEGylation was necessary, especially for G5 dendrimers, because even a low degree of PEGylation was sufficient to reduce the toxicity of PAMAM dendrimers against transformed human corneal epithelial cells to levels comparable to those of antibiotics. The study concluded that G3 dendrimers modified with a low coverage (< 10%) of relatively long polyethylene glycol chains were considered promising antimicrobial agents, with a potential advantage of developing less bacterial resistance than the standard antibiotics (Lopez et al. 2009).

More recently, Lancina et al. (2018) created DenTimol, a dendrimer-based polymeric timolol associated with polyethylene glycol, in which the drug is the outermost layer. These PAMAM dendrimers showed no signs of cytotoxicity and efficiently crossed the cornea, being this ability attributed to its hydrophilic-lipophilic balance. Because of its high dendrimer drug loading, DenTimol could be more effective in maintaining therapeutic concentrations of timolol. A single topical administration of DenTimol (10 µL of 0.5 % w/v timolol) effectively reduced the IOP of rats at a higher extent than timolol solution. Moreover, the repeated administration of DenTimol did not lead to toxicity signs or ocular irritation, which was confirmed by histological analysis (Lancina et al. 2018). PEGylated PAMAM dendrimers were also developed by Yang et al. (2019) but co-modified with cyclic RGD hexapeptide and penetratin, targeting the posterior segment of the eye. The aim was the treatment of choroidal neovascularization associated to age-related macular degeneration. Although the nanocarriers were not significantly cytotoxic, the polyethylene glycol conjugation substantially reduced the cytotoxicity of PAMAM. The cellular uptake results of RGD-modified nanocarriers showed significant affinity for integrin αvβ3, which corroborated the dendrimers targeting for the neovasculature. The penetratin modification not only improved the *in vitro* permeation and *in vivo* ocular distribution of the dendrimers, but also showed their greater distribution in the posterior segment of the eye and prolonged retention in the retina for more than 12 hours (Yang et al. 2019). These results supported the PEGylation of dendrimers as a valuable resource to both decrease dendrimers toxicity and increase their mucoadhesive potential, consequently increasing drugs intraocular bioavailability.

Another example of mucoadhesive enhancement was accomplished by Yang et al. (2012). A hybrid dendrimer hydrogel/ poly(lactic-co-glycolic acid) nanoparticle platform (HDNP)

containing both brimonidine (0.7 %) and timolol maleate (3.5 %) was created to help in glaucoma management. The formulations were considered non-toxic and physiochemically compatible with ocular administration. After 5 minutes of incubation, the nanoparticle uptake for HDNP was nearly seven times higher than that of saline solution and longer incubation resulted in more nanoparticle uptake, which ultimately would lead to increased drug absorption because drug molecules are firmly encapsulated into nanoparticles. The release of brimonidine and timolol maleate was remarkably extended by HDNP and poly(lactic-co-glycolic acid) nanoparticles, as the drug molecules were evenly released over 28 days for the poly(lactic-co-glycolic acid) nanoparticles and 35 days for the HDNP (50 % in 10 days). Moreover, both drugs were released at a similar rate, ensuring a complementary therapeutic efficacy. HDNP exhibited an extended ocular surface retention and the best IOP reduction results, with an onset at 3 hours, reducing IOP by 29.5 %, maintaining above 18 % of IOP reduction until 96 hours. Furthermore, brimonidine and timolol ocular concentrations at day 7 post-instillation were substantially higher in aqueous humor, cornea and conjunctiva when compared to other formulations, indicating that HDNP enhanced both drugs concentrations but also prevented their rapid decline in aqueous humor (Yang et al. 2012). Likewise, Bravo-Osuna et al. (2016) developed and studied hydrophilic mucoadhesive carbosilane dendrimers to carry acetazolamide intended for glaucoma treatment. All generations of anionic and cationic (except one) dendrimers were considered non-toxic by *in vitro* and *in vivo* studies. Regarding mucin interaction, a substantial part of the cationic dendrimers was permanently retained in the mucin glycoprotein layer, whereas the interaction between the anionic dendrimers and mucin was non-permanent. After a single instillation, the system containing 0.07 % of acetazolamide in 0.9 % saline and 5 μM of third-generation cationic dendrimer presented the maximum hypotensive effect, with onset at 1 hour and duration of 7 hours (Bravo-Osuna et al. 2016). Both the HDNP system and the cationic carbosilane dendrimers led to a more rapid and prolonged reduction of IOP, when compared to commercial eye drops, indicating that these mucoadhesive dendrimers could be a valid long-term alternative for glaucoma treatment and potentially other chronic diseases. More information concerning ophthalmic mucoadhesive dendrimers as summarily described in table 8.

Table 8: Mucoadhesive dendrimers with possible ophthalmological applications. Description of the studied drug, the particles main composition, and the most important results.

Drug	Materials	Essential outcomes	References
Puerarin	PAMAM (G3.5, G4, G4.5, G5)	Slow release; prolonged residence time; no corneal damage	(Yao et al. 2010)
Puerarin	PAMAM (G3)	Stability; higher transcorneal permeability; increased bioavailability	(Wang et al. 2011)
Puerarin	PAMAM (G3, G4, G5)	Substantial increase of transcorneal permeation	(Yao et al. 2011)
Timolol maleate + Brimonidine	PAMAM (G3); polyethylene glycol	Sustained release; mucoadhesive properties; increased cellular uptake and transcorneal permeation; non-cytotoxic	(Holden et al. 2012)
Acyclovir	PAMAM (G3.5); cysteamine HCl	Suitable physicochemical characteristics; sustained release; enhanced mucoadhesion	(Yandrapu et al. 2013)
Timolol maleate + Brimonidine	PAMAM; PLGA; polyethylene glycol	Increased ocular absorption and bioavailability; sustained and extended release (35 days); prolonged therapeutic effect (4 days)	(Yang and Leffler 2013)
Acetazolamide	Poly(propylene imine) (G0.5-5.0)	Stable; controlled and sustained release; increased residence time; sustained therapeutic effect	(Mishra and Jain 2014)
Dexamethasone	PAMAM (G3-G4.5)	Sustained release; improved permeation; increased drug concentration on site of action; non cytotoxic (G3 and G4)	(Yavuz et al. 2015)
Antisense oligonucleotides	PAMAM (G5); penetratin; hyaluronic acid	Increased cellular uptake and permeability; higher distribution in ocular posterior segment; enhanced retention time	(Tai et al. 2017)
Brimonidine tartrate	PAMAM (G3); methoxy-polyethylene glycol	Slow release; improved therapeutic efficacy after 3 weeks; excellent tolerance	(Lancina et al. 2017)

2.5. Conclusions and future perspectives

The effective treatment of ocular disorders remains a challenge due to the presence of ocular barriers in the anterior and posterior segments of the eye. Several approaches have been proposed for topical ocular drug delivery using the combination of nanotechnology with mucoadhesive polymers, in order to grant superior performances in the controlled and sustained drug release, while maintaining drug stability and low toxicity, which was often corroborated by *in vivo* studies. These drug carriers are able to target specific tissues and, consequently, to increase drug's therapeutic effect with lower or even absent adverse effects. However, as described along this literature review, each colloidal nanosystem has advantages and limitations in their role in ocular drug delivery. Liposomes, made from biocompatible phospholipids, can effectively entrap hydrophobic and hydrophilic drugs but have low stability. Nanoemulsions, constituted by surfactants and co-surfactants, can cause ocular irritancy. Niosomes may present ocular incompatibility depending on which non-ionic surfactant is used. Nanoparticles used for sustained drug release can permeate and be retained in intracellular structures, which in a long-term basis could be problematic. Dendrimers are the state-of-the-art colloidal systems with remarkable delivery features but their cytotoxicity is an important drawback, requiring physicochemical modifications that can decrease their performance as drug carriers. Moreover, promising innovative ophthalmic drug delivery systems should be not only effective, stable, versatile and safe but should also have a production method as simple and affordable as possible, in order to be easily reproducible and commercially viable, and avoid any physicochemical damage of the active principle. As described in several studies, the production of lipidic nanocarriers requires high temperature and/or aggressive solvents, these last also usually present in dendrimers synthesis, which could degrade fragile drug molecules. Being so, in our point of view, the colloidal nanosystem that would properly respect the great majority of the requirements for ocular drug delivery are polymeric nanoparticles, more specifically those with chitosan in their constitution. Chitosan characteristics were well explained during this review and this polymer stands out from the rest not only because it is biodegradable, biocompatible and non-toxic, but also because it is an antimicrobial and healing promoter mucoadhesive agent (Paolicelli et al. 2009; Bernkop-Schnürch and Dünnhaupt 2012). Chitosan nanoparticles can be easily produced by ionic gelation method upon the addition of sodium tripolyphosphate, with the possibility of adding surfactants and other polymers according to the nature of the drug carried, to enhance mucoadhesive and permeation effects without compromising the stability of the formulation (see section 2.8 and table 6). Chitosan nanoparticles represent an effective mean to reduce dosing frequency of ocular topical formulations, potentially reducing overall costs and improving long-term patient' compliance, which is especially important when considering chronic diseases.

In general, colloidal nanosystems with mucoadhesive properties could be a valuable tool in the treatment of complex ophthalmic diseases such as glaucoma and dry eye syndrome, as well as ocular inflammations and bacterial or fungal infections. Nevertheless, there is an urge for more and wide-ranging comparative studies between colloidal nanosystems, focusing on their ability to transport therapeutic agents to the posterior segment of the eye through topical administration. An increase in the investment made in research can be justified if the new technologies provide a substantial improvement in treatment outcomes at a similar or lower cost than classical treatments. Therefore, scientists should pursue their efforts to achieve a better understanding of pharmacokinetics, safety, and clinical efficacy of these ophthalmic mucoadhesive nanosystems, so they can proceed to clinical trials and become commercially available.

CHAPTER 3

New nanoparticles for topical ocular delivery of erythropoietin

Silva B, Marto J, Braz BS, Delgado E, Almeida AJ, Gonçalves L. New nanoparticles for topical ocular delivery of erythropoietin. Int J Pharm. 2020;576:119020. doi:10.1016/j.ijpharm.2020.119020

3.1. Abstract

Erythropoietin (EPO) is known for its neuroprotective and neuroregenerative properties. EPO topical ocular administration has not been tested yet and its bioavailability could be improved by mucoadhesive hydrogels. Thus, this study aimed to develop and evaluate a chitosan (CS) and hyaluronic acid (HA) nanoparticulate system for topical ocular delivery of EPO. Nanoparticles were prepared by ionotropic gelation using six different HAs (HA1-HA6), and characterized by size, zeta potential (ZP), polydispersity index (PDI), cytotoxicity and mucoadhesion. Encapsulation efficiency and drug loading capacity were also determined. *Ex vivo* permeation was tested using fresh porcine corneas, scleras and conjunctivas. The permeated EPO was quantified by ELISA, and its presence in the membranes was confirmed by immunohistochemistry. Nanoparticles presented size ≤ 300 nm, ZP around +30 mV and low PDI (0.167-0.539) at a 1:1 CS:HA mass ratio. The most suitable HA was HA6 (300 kDa – Eye), which had the best mucoadhesive properties. CS/HA6-EPO nanoformulation permeated more rapidly through porcine conjunctiva, followed by sclera and thirdly by cornea, as assessed by immunohistochemistry. All formulations were noncytotoxic on ARPE-19 and HaCaT cell lines, as evaluated by metabolic and membrane integrity tests. In conclusion, CS/HA6-EPOβ nanoparticles could be a promising formulation for increasing EPO ocular bioavailability by enhancing its retention time and permeation through the different ocular membranes.

3.2. Graphical Abstract

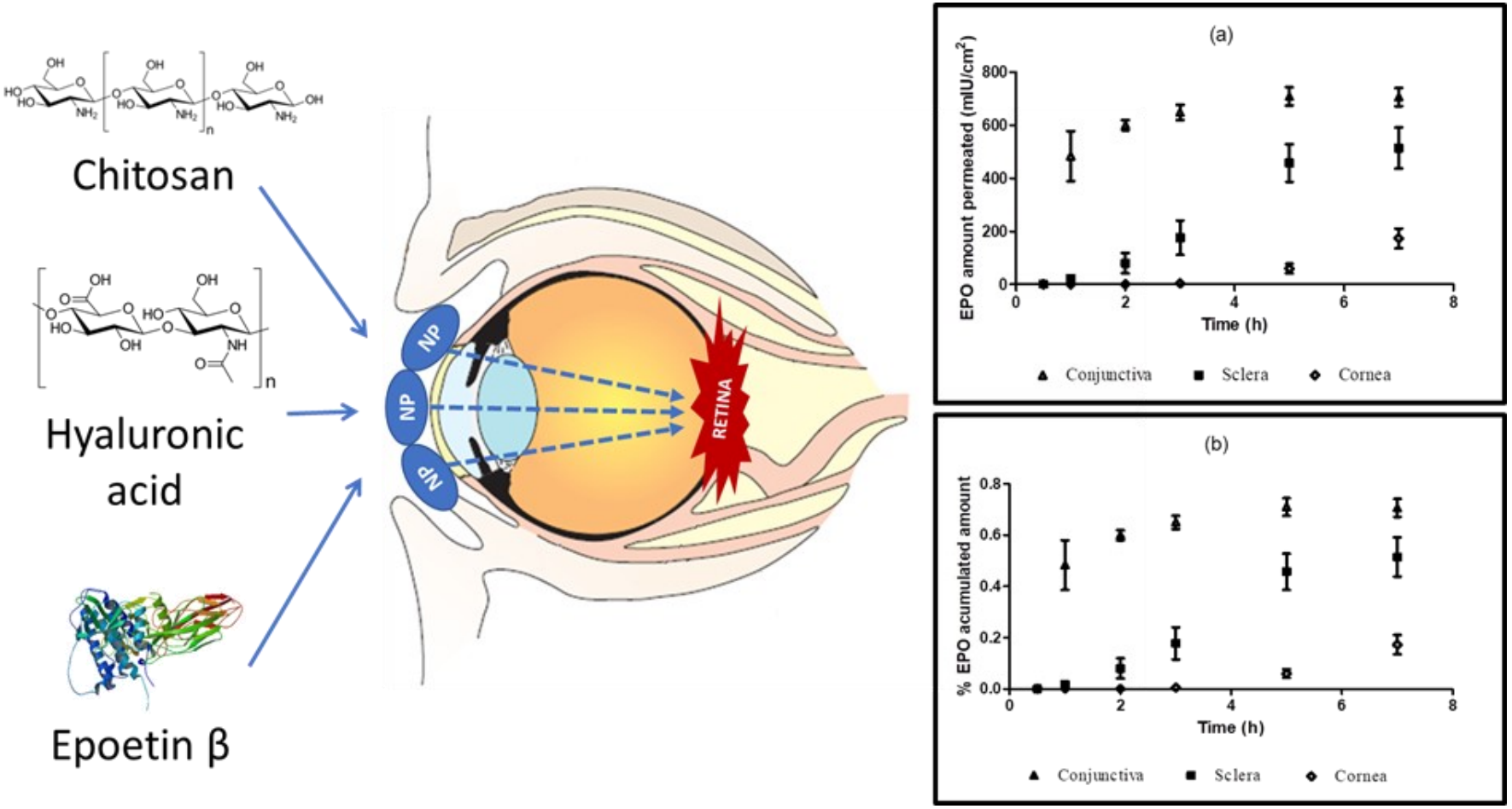

3.3. Introduction

Creating non-invasive drug delivery systems to reach the posterior segment of the eye is a difficult challenge, especially when considering retinal disease treatment. Research is evolving towards neuroprotective strategies to increase neurons survival by preserving their function and structure (Pardue and Allen 2018). Pardue and Allen (2018) recently reviewed some neuroprotective drugs for retinal diseases. For example, ursodeoxycholic acid and progesterone have anti-apoptotic and anti-inflammatory effects while neurotrophic factors can enhance synaptic strength and neuronal survival (Pardue and Allen 2018). However, some of the results are inconsistent and there is still a lack of standardized procedures, effective dose optimization and evaluation of long-term effects. Although erythropoietin (EPO) was not reviewed in that paper, this glycoprotein has significant neuroprotective and neuroregenerative properties (Lagreze et al. 2009). EPO is an hematopoietic growth factor of approximately 30.4 kDa (Abri Aghdam et al. 2016) that could be considered an interesting neuroprotective drug, since it is available in clinical practice and has a widely studied neuroprotective effect (Lagreze et al. 2009). EPO is produced mostly in adult kidneys but the central nervous system also produces it in low levels (Abri Aghdam et al. 2016). In human adults, a wide distribution of EPO and EPO receptors was reported in the brain and on the retina, suggesting autocrine or paracrine actions (Brines et al. 2004; Luo et al. 2015; Shirley Ding et al. 2016). Several models of ophthalmic and non-ophthalmic neurodegenerative diseases indicate that EPO has important neuroprotective and neuroregenerative properties due to its ability to decrease apoptosis, inflammation, oxidation and excitotoxicity (Bartesaghi et al. 2005; L. Zhong et al. 2007; Grasso et al. 2009; Bond and Rex 2014; Resende et al. 2018), and to increase the progenitor cell proliferation (Abri Aghdam et al. 2016). Therefore, EPO appears to be a valuable drug to prevent apoptosis of the retinal ganglion cells (RGCs) and can be administered by systemic, intravitreal and retrobulbar routes (Tsai et al. 2005; Zhong et al. 2008). Recent studies explored the delivery of epoetin β (recombinant human erythropoietin) to the retina by subconjunctival administration, with good results (Resende et al. 2013; Resende et al. 2016; Resende et al. 2018). This administration route avoids potential side effects related to hematopoiesis stimulation (systemic administration) and complications such as endophthalmitis, retinal detachment, uveitis or cataracts (intravitreal and retrobulbar administration) (Sahoo et al. 2008; Lagreze et al. 2009; Jordán and Ruíz-Moreno 2013). Furthermore, Resende et al. (2017) showed that epoetin β (EPOβ) can permeate porcine conjunctiva, cornea, and sclera after topical instillation in *ex vivo* conditions, which opened the window to consider this administration route as a valid option. Extrapolating from the subconjunctival route, topical ocular administration of EPOβ could be considered innocuous in the dose tested, with the advantage of being a non-invasive route, not requiring sedation or

local anesthesia. Despite these appealing features it is imperative to consider the substantial ocular barriers to be overcome.

After topical administration, the drug permeates into the ocular globe through conjunctival, corneal and scleral pathways (Mandal et al. 2018). Conjunctival intercellular spaces are more permeable to larger molecules than the cornea, being also permeable to hydrophilic drugs (Prausnitz 1998; Hosoya et al. 2005). On the other hand, only moderately charged and lipophilic small molecules can penetrate the cornea (Hosoya et al. 2005; Kim et al. 2014). Despite its network of collagen fibrils, the sclera demonstrated permeability to macromolecules up to 150 kDa (Ambati and Adamis 2002; Radhakrishnan et al. 2017). In general, corneal epithelium hydrophobicity, corneal and conjunctival tight junctions, aqueous and vitreous humors, blood-aqueous humor barrier and blood-retinal barrier are main limitations to topically applied hydrophilic and hydrophobic molecules, leading to a bioavailability of only 1 to 7%, and even lower for macromolecules (Yi et al. 2000; Ghate and Edelhauser 2008; Kalam 2016a; Peynshaert et al. 2018). Protective mechanisms of the eye such as blinking, tearing and tear dilution, tear enzymes metabolism and nasolacrimal drainage increase the difficulty of effective drug permeation (De La Fuente et al. 2008; Fabiano et al. 2015).

One way to improve drugs ocular bioavailability after topical administration is to use nanoparticulate delivery systems based on mucoadhesive polymers (Di Colo et al. 2002; Uccello-Barretta et al. 2010; Weng et al. 2017), such as chitosan and hyaluronic acid.

Chitosan (CS) functional properties are due to the exceptional high content of primary amines at the C-2 position of the glucosamine residues (Yi et al. 2005). CS is a hydrophilic biodegradable polymer with a polycationic nature that interacts with the polyanionic surface of the ocular mucosa, enhancing drug's mucoadhesion and increasing its retention time on the ocular surface (De Campos et al. 2001; Wadhwa et al. 2010; Kalam 2016a; Silva et al. 2017). It is also considered a permeation and absorption enhancer due to its capacity of widening the membranes tight junctions (Thanou et al. 2001). This cationic polysaccharide is abundant in nature and is obtained by deacetylation of chitin found in the exoskeleton of crustaceans and on fungi cell walls, making its production low cost and ecologically appealing (Peter MG 1995). In pharmaceutical applications, CS is often used as a component of hydrogels, having the advantage of promoting wound-healing and having bacteriostatic effects (Felt et al., 2009; Ueno et al., 2001).

Hyaluronic acid (HA) is a naturally occurring polysaccharide with unique viscoelastic and hygroscopic characteristics (Rah 2011). It is widely distributed throughout connective, epithelial and neural tissues and can be found in the vitreous, lacrimal gland, human tear, conjunctiva and corneal epithelium (Rah 2011). HA has second generation mucoadhesion properties through CD44 receptor-mediated binding and enhances precorneal residence time

of some drugs (Wadhwa et al. 2010). It has similar viscoelastic and biophysical properties to those of mucins, being biocompatible and biodegradable as well (Graça et al. 2018). HA also protects corneal epithelium against dehydration and reduces the associated inflammation, lubricates ocular surface and promotes corneal wound healing (Di Colo et al. 2009; Guillaumie et al. 2010), being an extremely valuable and versatile compound. The concentration of HA in commercial formulations ranges from 0.1 to 0.4 wt% and the average molecular weight varies from 155 to 1400 kDa (Guillaumie et al. 2010; Salzillo et al. 2016).

There has been some research about CS-EPO association and EPO hydrogels for diverse purposes with good results (Hirakura et al. 2010; Bulmer et al. 2012a; Zhang et al. 2014; M. et al. 2018). Taking that into consideration and due to the exceptional characteristics and reasonable production costs of CS and HA, these were considered the ideal polymers for this research. The production of nanoparticles instead of microparticles, for example, was a choice based on the assumption that nanoparticles are more likely to origin a fluid translucid formulation that avoids blurry vision and is well tolerated when in contact with the ocular surface. The coating of HA on CS nanoparticles accelerates the endocytosis of nanoparticles (Kalam 2016a) and the strong mucoadhesive characteristics of CS/HA nanoparticles will probably increase EPOβ retention time on ocular surface. Therefore, this study aimed to develop and evaluate CS/HA-EPOβ nanoparticles for topical ocular delivery. To the best of our knowledge, there is no reference in the literature about nanoparticulate systems for topical ocular administration of EPOβ.

3.4. Materials and Methods

3.4.1. Materials

The sodium hyaluronate PrimalHyal™ brand (50 kDa, 300 kDa, 1000 kDa, 3000 kDa, 1-1.4 MDa - CrystalHyal) from Soliance and the sodium hyaluronate eye drop grade quality (300 kDa – Eye) from Shandong Topscience, were a kind gift from Inquiaroma (Barcelona, Spain). Code names were attributed to the hyaluronic acids, as follows: HA1 = 50 kDa, HA2 = 300 kDa, HA3 = 1000 kDa, HA4 = 3000 kDa, HA5 = CrystalHyal and HA6 = 300 kDa – Eye. Chitosan with low molecular weight (LMW CS, 100 kDa, 92% deacetylation), mucin from porcine stomach type II, 3-(4,5-dimethyl-2-thiazolyl)-2,5-diphenyl-2H-tetrazolium bromide (MTT) and propidium iodide (PI) were obtained from Sigma Aldrich (Irvin, UK). The recombinant human erythropoietin (Epoetin beta, EPOβ) used was NeoRecormon 5000® (RocheDiagnostics GmbH, Mannheim, Germany). ARPE-19 (ATCC® CRL-2302™) a spontaneously immortalized cell line of human retinal pigment epithelium was obtained from

the American Type Cell Culture collection (Manassas, VA, USA9). HaCaT (a spontaneously immortalized human keratinocyte cell line) was obtained from CLS Cell Lines Service GmbH (Eppelheim, Germany). All the cell culture media and supplements were from Gibco (ThermoFisher Scientific, Paisley, UK). Polyclonal goat anti-EPO antibody (1:100; sc-1310), rhodamine conjugated antibody anti-goat (1:100; sc-2094) and DAPI (UltraCruz™ Mounting Medium sc-24941) were acquired from Santa Cruz Biotechnology, USA.

3.4.2. Methods

Formulation and characterization of chitosan-hyaluronic acid nanoparticles

The final goal of this study was to select the most suitable hyaluronic acid, among the six tested, to be used in further investigation towards ocular topical delivery of EPO. The unsuitable nanoformulations, therefore the unsuitable HAs, were excluded based on the results in each step of the protocol.

An adapted ionotropic gelation technique previously described was used to create the nanoparticles (Silva et al. 2017). Briefly, to the solution of chitosan at 1 mg/mL in 0.1% (v/v) of acetic acid, were added different amounts of the tested hyaluronic acid, in order to obtain 0.5:1, 1:1 and 1:2 chitosan to hyaluronic acid mass ratios. In order to encapsulate EPOβ into the nanoparticles, 1000 IU of EPOβ was added to the HA solution before the ionotropic gelation with CS. Nanoparticles were characterized by their size, polydispersity index (PDI) and zeta potential (ZP) using the dynamic light scattering method. Size was measured by a Zetasizer Nanoseries Nano S and ZP by a Zetasizer Nanoseries Nano Z (Malvern Instruments, Malvern, UK). The samples were diluted in filtered 0.22 µm purified water and analyzed at 25°C, and data was collected in triplicate.

Encapsulation efficiency and loading capacity

EPOβ encapsulation efficiency (%EE) and loading capacity (%DL) were determined using a MicroBCA Kit Assay (Pierce, UK) to measure the protein remaining in solution after separation of the nanoparticles by centrifugation in an Allegra™ 64R centrifuge (Beckman Coulter, USA) (12,000g, 15 min at 4ºC), and comparing it to the total amount added to the nanoformulation. The %EE and %DL were determined as follows:

$$\%EE = \frac{[Total\ protein] - [\text{Free Protein}]}{[Total\ protein]} \times 100 \qquad (1)$$

$$\%DL = \frac{[Total\ protein] - [\text{Free Protein}]}{[Mass\ nanoparticles]} \times 100 \qquad (2)$$

In vitro cytotoxicity

The Alamar Blue (7-hydroxy-3H-phenoxazin-3-one 10-oxide) assay, a general endpoint resazurin reduction test, and propidium iodide (PI) dye exclusion assay were performed to quantitatively measure cell viability. Both tests were adapted from previously published procedures (Silva et al. 2017). The cell lines used were HaCaT (a spontaneously immortalized human keratinocyte cell line, CLS, Germany) and ARPE-19 (human retinal pigment epithelial cell line, ATCC® CRL-2302™). Cells were seeded with a density of 2x105 cells/mL in sterile flat-bottom tissue culture plates (Greiner, Kremsmünster, Austria) with 96 wells each, in RPMI 1640 culture medium (ThermoFisher Scientific, Paisley, UK), supplemented with 10% fetal bovine serum (ThermoFisher Scientific, Paisley, UK), 100 µg/mL of streptomycin sulfate (ThermoFisher Scientific, Paisley, UK), 2 mM L-glutamine (ThermoFisher Scientific, Paisley, UK) and 100 units/mL of penicillin G (sodium salt) (Life Technologies, Paisley, UK).

Cells were incubated in an atmosphere with 5% of CO_2 at 37 °C for 24 hours. The medium was replaced by fresh medium containing samples of the different nanoformulations to be analyzed, and each sample was tested in six wells per plate. Cells were then incubated in the same conditions for 24 hours. Cells to which culture medium without nanoformulations was added served as the negative control, and the positive control were cells to which medium with sodium dodecyl sulfate (SDS) at 1 mg/mL was added. After 24 hours of exposure (contact with the samples), the medium was replaced by 0.3 µM PI in culture medium (stock solution 1.5 mM in dimethyl sulfoxide (DMSO), diluted with culture medium 1:5000). Fluorescence was measured in a FLUOstar Omega Microplate Reader (BMGLabtech, Ortenberg, Germany) at excitation and emission wavelengths of 485 nm and 590 nm, respectively. The Alamar Blue assay was performed afterwards, consisting of replacing the medium by medium with 5 mM of resazurin and, after 3 hours of incubation, the fluorescence was measured in the same microplate reader at 530 nm of excitation wavelength and 590 nm of emission wavelength. The relative cell viability (%) was calculated in comparison to the control cells, as follows:

$$\text{Cell viability}\ (\%) = \frac{[Fluorescence]sample}{[Fluorescence]control} \times 100 \quad \text{for the Alamar Blue assay} \qquad (3)$$

$$\text{Cell viability}\ (\%) = \frac{[Fluorescence]sample}{[Fluorescence]control} \quad \text{for the PI uptake assay} \qquad (4)$$

In vitro release

The three nanoformulations (HA1, HA4 and HA6) were added to a solution of simulated tear fluids (STF; NaCl 0.67 g, $NaHCO_3$ 0.20 g, $CaCl_2 \cdot 2H_2O$ 0.008 g, and purified water to 100 g) and incubated at 37ºC with agitation of 100 rpm. At specific time points, namely, 15, 30, 45, 60, 90, 120, 240 and 360 minutes after the incubation, the solution was removed and analyzed using a MicroBCA Kit Assay (Pierce, UK) for released protein.

Mucoadhesion

The interaction between mucin and the nanoparticles' formulations was assessed using two *in vitro* methods, rheology, and zeta potential determination.

Rheology

The mucoadhesion was evaluated using a controlled stress Malvern Kinexus Rheometer (Malvern Instruments, Malvern, UK) and a plate and plate geometry (pull away assay or tackiness testing), as previously published (Graça et al. 2018). Briefly, a toolkit with the conditions of 0.1 mm/s, 5 mm and 0.15 GAP was used. The mucin used in this study was hydrated with water by gentle stirring until complete dissolution to yield a dispersion of 10% (w/w). The adhesive strength of each individual component, HA1, HA4, HA6 and mucin, were measured in triplicate. The adhesive force between the pig eye and samples was measured, using the same procedure previously described (Graça et al. 2018). The pig eyes were obtained from a local slaughterhouse.

Zeta potential

The effect of mucin on the ZP of the formulations was also evaluated and it was measured before and after the incubation with mucin, as previously described (Graça et al. 2018).

Ex vivo permeation

The assay was performed as previously described by our group (Resende et al. 2017). Fresh porcine ocular tissues were used, namely the conjunctiva (n=10), the sclera (n=10) and the cornea (n=10). Those membranes were dissected from 30 pig eyes, which were collected from a slaughterhouse and properly stored until their use (immersed in PBS at low temperature for 1 h). After dissection, the ocular membranes were assembled onto the receptor area of the

Franz diffusion cells (receptor volume: 3 mL; permeation area: 1 cm^2) and immediately hydrated with 10 mM PBS (pH 7.4). All Franz diffusion cells were incubated at 37 °C and at 300 rpm until the end of the assay.

NeoRecormon 5000® (RocheDiagnostics GmbH, Mannheim, Germany), with 5000 IU of epoetin beta per 0.3 ml of solution, was used to prepare the nanoformulations. EPOβ is a globular protein with an average molecular weight of 30 kDa.

A sample of 200 µL of the CS/HA6 nanoformulation with 100 IU of EPOβ was added to the donor phase of each Franz cell. At predetermined time points during 7 hours, samples of 200 µL were withdrawn from the Franz cells receptor phase and replaced by 200 µL of PBS (10 mM, pH 7.4, 37 °C). The permeated EPOβ was quantified by ELISA (Abcam® ab119522, Cambridge, England), following the manufacturer's instructions, and the absorbance at 450 nm was measured in a microplate reader (FLUOstar Omega, BMGLabtech, Germany).
The following equation (5) was used to determine the cumulative amount of permeated EPOβ per membrane surface area (Qt, mIU/cm^2) as function of time. Vr is the volume of the receptor solution, Ct is the EPOβ concentration of the receptor solution at each sampling time, $\sum_{t=0}^{t-1} Ci$ is the sum of EPOβ concentration determined at sampling intervals 1 trough t-1 and Vs is the volume of the sample. S corresponds to the membrane area which is 1 cm^2.

$$Qt = \frac{\mathrm{Vr} \times \mathrm{Ct} + \sum_{t=0}^{t-1} Ci \times \mathrm{Vs}}{S} \qquad (5)$$

The transmembrane fluxes (J, mIU/cm^2 h) and the apparent permeability coefficients (Papp, cm/s) of EPOβ were calculated as previously published (Hahn et al. 2007).

Immunohistochemistry

At the end of the permeation assay, all ocular membranes were stored in 10% (v/v) formaldehyde in PBS (0.1 M, pH 7.4) overnight, in order to be later embedded in paraffin blocks. After the inclusion in paraffin, one cross-section of 3 µm was made per each ocular membrane, being then deparaffinized in xylol and rehydrated in alcohols and purified water. The cross-sections were processed with 0.1% Triton X-100 solution and washed in PBS, and then assembled in the cover plates and washed with PBS-Tween 20 solution, followed by incubation with 10% (v/v) normal donkey serum in PBS at room temperature for 30 min. Polyclonal goat anti-EPO antibody (1:100; sc-1310, Santa Cruz Biotechnology) was then added to all samples, except the negative controls, followed by overnight incubation at 4 °C. The positive control was a cross-section of fetal bovine kidney.

After the overnight incubation, the cross-sections were washed in PBS and incubated with rhodamine conjugated antibody anti-goat (1:100, Santa Cruz Biotechnology) at 4°C for 24 hours. Finally, the cross-sections were washed again in PBS and a drop of DAPI, a cell nucleus

marker (UltraCruzTM Mounting Medium; sc-24941, Santa Cruz Biotechnology), was placed onto them. The cross-sections were analyzed using an Axioscop 40 fluorescence microscope with an Axiocam HRc camera (Carl Zeiss, Germany). The emitted fluorescence was observed and recorded in images processed with AxioVision software (Rel. 4.8.1, Carl Zeiss).

Statistical methods

The experimental data was statistically assessed using one-way ANOVA (one-way analysis of variance) and the statistical analysis of the differences between groups was performed using Tukey's test (GraphPad Prism version 6.0, GraphPad Software, CA, USA). The established statistical significance was 95%, corresponding to a *p*-value of 0.05. Data were presented as mean ± standard deviation (SD).

3.5. Results

3.5.1. Development and optimization of nanoparticles

The effect of different hyaluronic acids

One of the critical points of nanoparticles formation using chitosan is the pH value, as this will determine the protonation of amino groups, which will allow the electrostatic interaction with the anionic groups of the hyaluronic acid chain. From previous results of our group, the best range of pH for the chitosan solution is between 4 and 5 (Caetano et al. 2016). In the present work a pH value of 5 was selected (adjusted with NaOH 1 N), while the pH of the hyaluronic acid solutions ranged from 6 to 6.9. Ionotropic gelation was performed at 1:0.5, 1:1 and 1:2 CS:HA mass ratios using HA1-6. All samples obtained with the 1:0.5 CS:HA ratio exhibited aggregation, thus were not considered valid for further assays. Nanoparticles' size, ZP and PDI were measured for the formulations obtained with 1:1 and 1:2 CS:HA mass ratios, and the results are shown in figure 16.

Based on the literature (see Discussion section) it was established a threshold of 300 nm for particle size and a ZP around +30 mV. The ideal PDI was the lowest possible to indicate a stable nanoparticle dispersion (Kalam 2016a).

Formulations HA3 and HA5 from 1:1 ratio and HA4 and HA6 from 1:2 ratio, were excluded because they led to the formation of nanoparticles larger than 300 nm (Figure 16a). Analyzing the results of HA1, HA2, HA4 and HA6 from 1:1 ratio and HA1, HA2, HA3 and HA5 from 1:2 ratio, the average particle size was 192 nm at 1:1 mass ratio and 174 nm at 1:2 ratio, yet this difference was not statistically significant. For the same formulations, the PDI values

ranged from 0.167 to 0.539 for the 1:1 ratio and from 0.258 to 0.434 for the 1:2 ratio (Figure 16b). Likewise, the difference in PDI was not statistically significant. The 1:1 CS:HA ratio presented positive ZP from +29 ± 1 mV to +39 ± 2 mV, while the 1:2 ratio had ZP from –25 ± 1 mV to +23 mV (Figure 16c), being this difference statistically significant ($p < 0.001$).

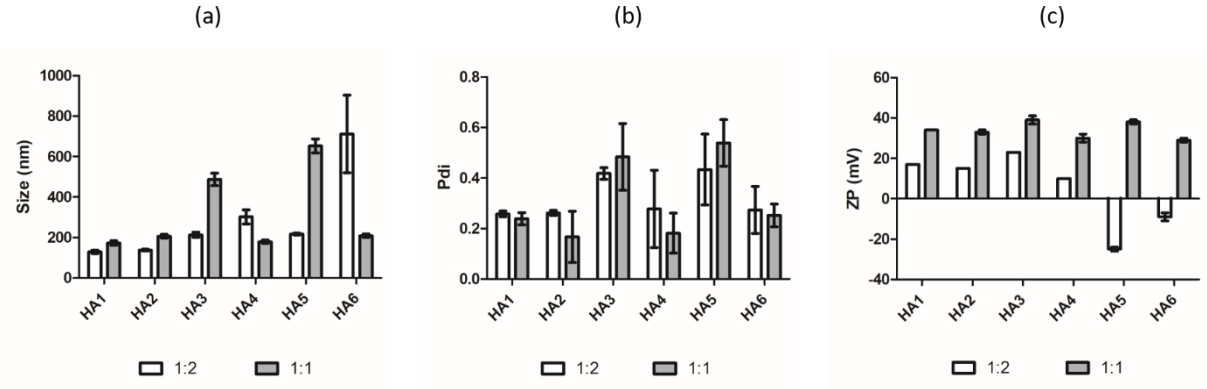

Figure 16: The effect of different hyaluronic acids and CS:HA ratios (1:2, 1:1) on nanoparticles characteristics: (a) size (nm); (b) polydispersity index – PDI; (c) Zeta potential – ZP (mV) (n = 3, mean ± SD).

All nanoparticles' formulations presenting less than 300 nm were automatically selected. Regarding the very similar PDI between 1:1 and 1:2 CS:HA mass ratios, the ZP was considered a major differentiating factor in this assay. Therefore, the 1:1 CS:HA mass ratio was selected for further tests.

The effect of salts

As the physicochemical properties of nanoparticles' dispersions may be affected by the presence of salts, a study has been devised to assess the effect of a sodium chloride solution on nanoparticles formation (Wadhwa et al. 2010; Nakai et al. 2012). For this purpose, the chitosan stock solution (10 mg/mL) was diluted in purified water and in physiological saline (0.9% NaCl) solution. Particles' size, ZP, PDI of the resulting nanoparticle dispersions were then measured (Figure 17).

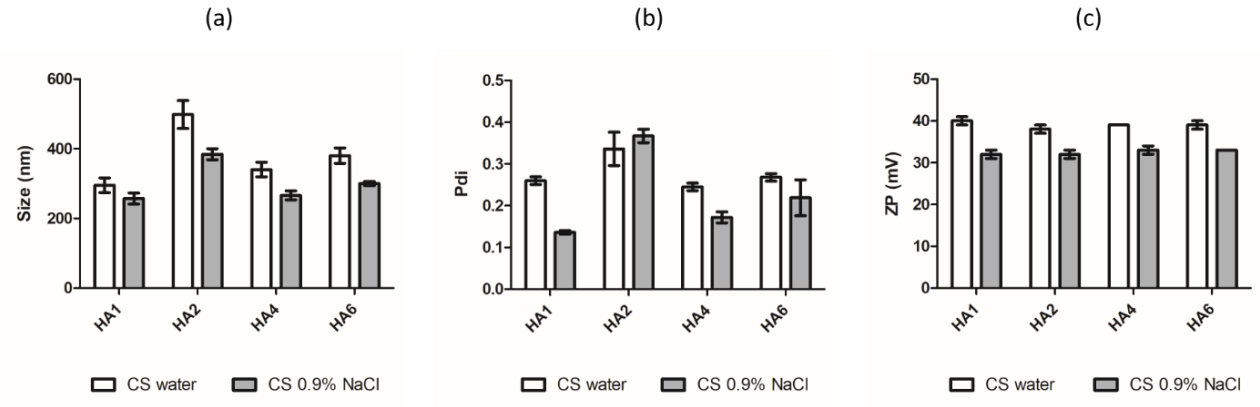

Figure 17: The effect of 0.9% NaCl on the characteristics of nanoparticles with a 1:1 CS:HA mass ratio: (a) size (nm); (b) polydispersity index – PDI; (c) Zeta potential – ZP (mV). Data presented as mean ± SD (n = 3).

Except for the HA1 formulation, there is a statistically significant difference in ZP, PDI and size between nanoparticles prepared with CS in purified water and CS in 0.9% NaCl. ZP was the only variable where this difference had the same statistical significance for all the nanoformulations ($p < 0.001$). The HA2 was excluded due to out-of-range size and PDI values. Nanoparticles prepared with CS in 0.9% NaCl presented the best results, with a size from 257 nm to 300 nm (Figure 17a), PDI values ranging from 0.136 to 0.219 (Figure 17b) and a ZP varying from to +32±1 mV to +33±1 mV (Figure 17c). Therefore, NaCl 0.9% seemed a better solvent for CS than purified water, permitting the formation of more appropriate nanoparticles.

Encapsulation of EPOβ and loading capacity

Both the encapsulation efficiency (%EE) and the drug loading capacity (%DL) are crucial aspects regarding the preparation of nanoparticles loaded with proteins. They should be as high as possible to improve intraocular bioavailability (Fabiano et al. 2015).
Ionotropic gelation was performed with HA1, HA4 and HA6 and each nanoformulation received 80 IU of EPOβ, being the mean values of EPOβ's %EE and %DL determined afterwards. There was no settled threshold for %EE and %DL.

The HA4 nanoformulation presented the highest %EE and %DL, respectively 39.9 ± 0.6% and 18.1 ± 0.3%, while the HA1 presented the lowest values (Table 9). Although the three nanoformulations had statistically significant differences for both %EE and %DL, it was decided not to exclude any from the study. The objective was to retrieve additional data that could properly support the selection of the best hyaluronic acid.

Table 9: Nanoparticles encapsulation efficiency and drug loading of EPOβ using different hyaluronic acids at 1:1 CS:HA mass ratio (n=3, mean ±SD).

Formulation	Encapsulation Efficacy (%)	Drug Loading (%)
HA1	35.2 ± 0.5	16.0 ± 0.2
HA4	39.9 ± 0.6	18.1 ± 0.3
HA6	38.4 ± 0.3	17.4 ± 0.1

5.3.2. In vitro cytotoxicity

Hyaluronic acid and chitosan are described as non-toxic and biocompatible compounds, which promote wound-healing, having broad pharmaceutical applications (Ueno et al. 2001; Rah 2011). Nevertheless, the irritant potential of the CS/HA nanoparticles was tested through cell viability assays (AlamarBlue and PI), after incubation of the cell cultures with HA1, HA4 and HA6 nanoformulations at 400 µg/ mL. Two different cell lines (HaCaT and ARPE-19) were tested. To assess ocular irritation is recommended by OECD (test guidelines TG 492) the use of keratinocytes to mimic the corneal epithelium cells of the eye.

Results show a survival rate around 100% for both HaCaT and ARPE-19 (Figure 18), with no statistically significant difference between the 3 nanoformulations (Figure 18a and 18c). The PI uptake ratio corroborates these results, as the 3 nanoformulations presented similar values to the negative control (cells in medium), for both cell lines, demonstrating a high cell survival rate (Figure 18b and 18d). Therefore, the results suggested that the 3 nanoformulations tested are safe for HaCaT and ARPE-19 cell lines.

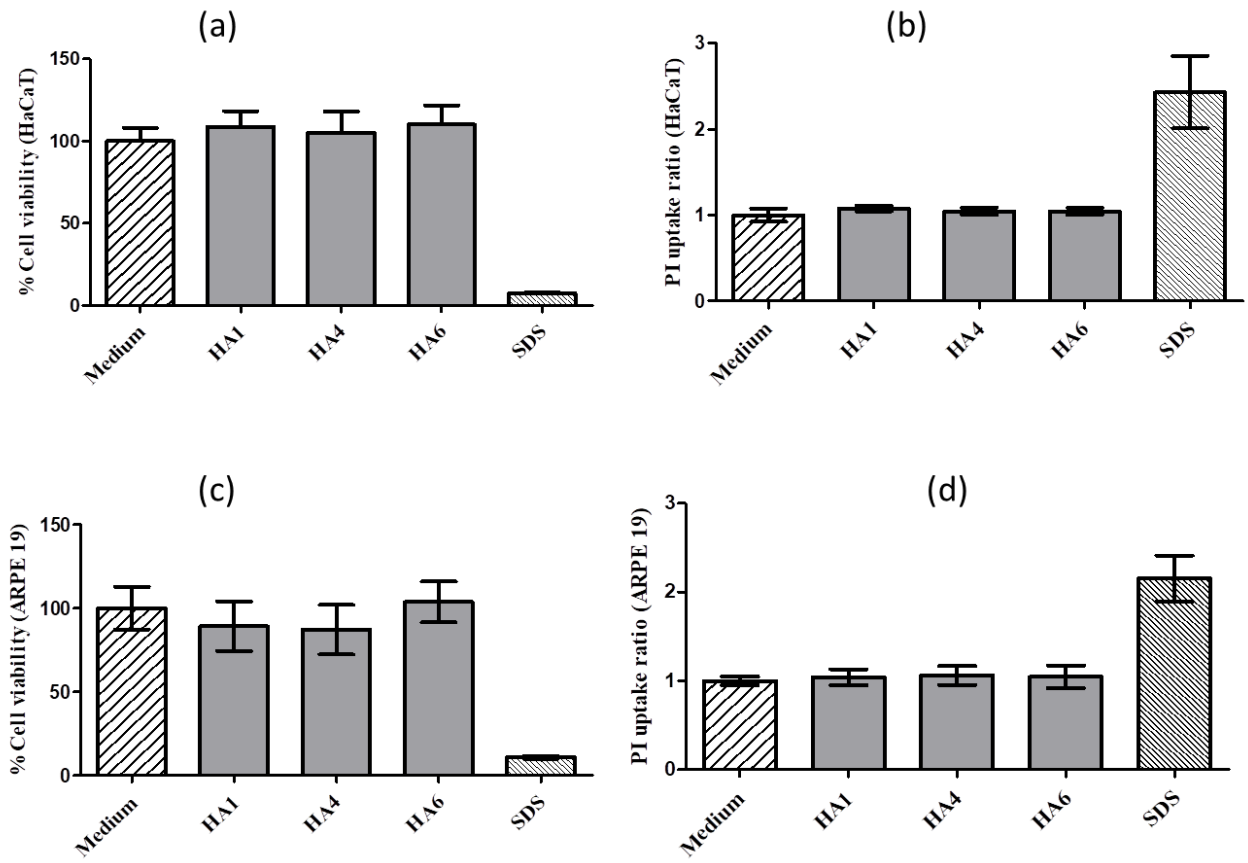

Figure 18: Cell viability of HaCaT (a,b) and ARPE-19 (c,d). Cell lines were exposed for 24 h to 400 µg/mL of formulations. Propidium iodide (PI) uptake ratio (b,d) and rezasurin reduction (a,c) results are shown (n = 8, mean ± SD).

3.5.3. In vitro release

Considering the goal of topical ophthalmic administration, an *in vitro* release assay in simulated tear fluid (STF) was performed. The release profiles of EPOβ in STF (37ºC, pH 7.4) of HA1, HA4 and HA6 nanoformulations were very similar (Figure 19). All nanoformulations presented an initial burst release, where 80% of the EPOβ was released within the first 15 minutes, followed by a slow and sustained release (Figure 19). No statistically significant differences were found among the release profiles, thus further assays were needed to select the ideal HA.

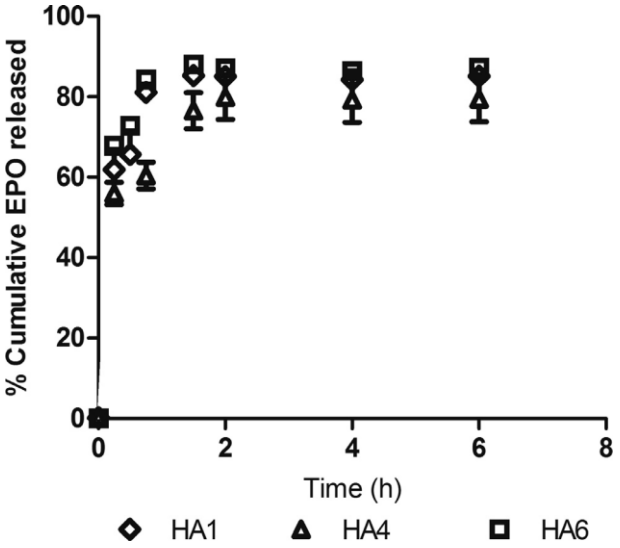

Figure 19: *In vitro* release profiles of EPOβ in STF of nanoformulations HA1, HA4 and HA6 (n = 3, mean ± SD).

3.5.4. Mucoadhesion

Although a fluid solution is better tolerated than a viscous one, a high viscosity prolongs drug's precorneal residence time (Uccello-Barretta et al. 2010), which is a desirable feature regarding the treatment of intraocular disorders by topical administration. As such, the adhesive strength of the hyaluronic acids and their interaction with the pig eyes and the mucin were studied.

Results of the tackiness testing are shown in Table 10. The HA4 + Mucin was considered the tackiest of the analyzed samples with a peak normal force of –0.201 ± 0.008 N. Comparing the HA1, HA4 and HA6 nanoformulations, the latter presented the highest peak force when tested alone (–0.177 ± 0.005 N), followed by HA4 (–0.162 ± 0.008 N) and HA1 (–0.157 ± 0.026 N), but these differences were not statistically significant. On the other hand, HA6 also showed the highest peak force when combined with the pig´s ocular surface (–0.118 ± 0.017 N), followed by HA4 (–0.072 ± 0.002) and HA1 (–0.065±0.026) with statistically significant differences ($p < 0.01$). All samples prepared with HA6 presented the highest results of the area under force-time curve, which indicates the adhesive strength: HA6 = 0.511 ± 0.047 N; HA6 + Mucin = 1.049 ± 0.028 N; Eye + HA6 = 0.487 ± 0.156 N (Table 10).

HA6 presented more suitable results compared to HA1 and HA4, being apparently the strongest HA when combined with CS. Therefore, CS/HA6 nanoparticles were incubated with mucin to determine the mucoadhesion interaction by ZP measurement, and the results are presented in Table 11. The mucin turned the ZP of the nanoformulation from positive (+39.2 ± 1.0 mV) to negative (–1.8 ± 0.1 mV), revealing a good interaction between them. H6 was selected to be in the last assays of this study.

Table 10: Rheology measurements of the different formulations tested (n=6; mean ± SD).

Nanoformulation	Peak normal force (N)	Area under force time curve (N.s)
HA1	–0.157 ± 0.026	0.387 ± 0.064
HA4	–0.162 ± 0.008	0.008 ± 0.023
HA6	–0.177 ± 0.005	0.511 ± 0.047
Mucin	–0.193 ± 0.022	0.841 ± 0.047
HA1 + Mucin	–0.199 ± 0.010	0.968 ± 0.017
HA4 + Mucin	–0.201 ± 0.008	0.989 ± 0.023
HA6 + Mucin	–0.175 ± 0.016	1.049 ± 0.028
Eye + NaCl solution 0.9%	–0.061 ± 0.014	0.313 ± 0.059
HA1 + Eye	–0.065 ± 0.019	0.322 ± 0.034
HA4 + Eye	–0.072 ± 0.0020	0.409 ± 0.0235
HA6 + Eye	–0.118 ± 0.0171	0.487 ± 0.1559

Table 11: Zeta potential of nanoparticles upon dilution 1:1 with water or mucin dispersion (n=3; mean ± SD).

Formulation	Zeta Potential (mV)
Mucin	–26.6 ± 0.6
Nanoparticles (CS:HA6, 1:1)	+39.2 ± 1.0
Nanoparticles+Mucin (1:1)	–1.8 ± 0.1

3.5.5. Ex vivo permeation

Ocular outer membranes are a major limitation to intraocular penetration of topical drugs. Thus, we performed *ex vivo* permeation assays using conjunctivas, corneas, and scleras surgically dissected from fresh pig eyes. The ocular membranes were placed into Franz diffusion cells and immediately hydrated with PBS. The ionotropic gelation was performed with chitosan and HA6, and each Franz diffusion cell received 100 IU of EPOβ.

Figures 20a and 20b illustrate the results and show that the CS/HA6-EPOβ formulation permeated more rapidly through the porcine conjunctiva, followed by the sclera and the cornea. As shown in these figures, seven hours after the instillation, EPOβ's permeated amount through the conjunctiva was 706.4 ± 34 mIU/cm^2 (0,706 ± 0.035%), through the sclera was 514.1 ± 78 mIU/cm^2 (0,515 ± 0.077%) and through the cornea was 173.4 ± 37 mIU/cm^2 (0,173 ± 0,038%). These differences were statistically significant for conjunctiva-sclera (p <

0.05) and conjunctiva-cornea ($p < 0.01$). This is supported by EPOβ fluxes and permeability coefficient (Table 12), which were higher for the conjunctiva (219 ± 13 mIU/cm^2.h; 1.22 ± 0.07×10^{-7} cm^{-1}), followed by the sclera (113 ± 13 mIU/cm^2.h; 0.64 ± 0.07×10^{-7} cm^{-1}) and the cornea (21 ± 6 mIU/cm^2.h; 0.11 ± 0.04×10^{-7} cm^{-1}). The lag time, which is the time before the formulation begins to permeate, is accordingly lower for the conjunctiva (0.22 ± 0.03 h) and higher for the cornea (2.38 ± 0.75 h) as seen in table 12.

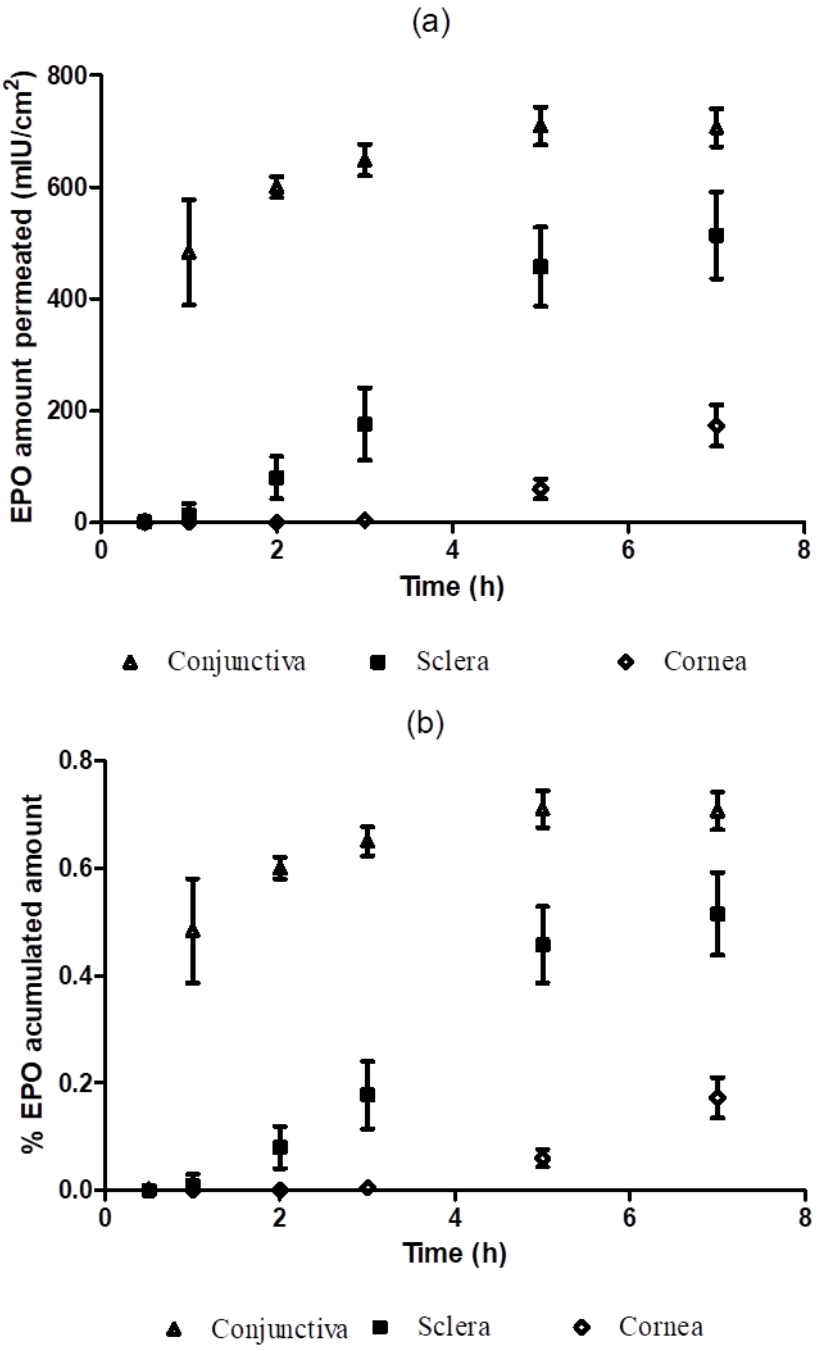

Figure 20: *Ex vivo* permeation of EPOβ in nanoformulation HA6 (mean ± SD, n = 10) (a) Accumulated permeated amount; (b) Percentage of accumulated permeated amount.

Table 12: *Ex vivo* permeation parameters of nanoencapsulated EPOβ (mean ± SD, n=10).

	Flux (mIU/cm^2.h)	Permeation coefficient (cms^{-1})	Lag Time (h)
Conjunctiva	219 ± 13	1.22 ± 0.07×10^{-7}	0.22 ± 0.03
Sclera	113 ± 13	0.64 ± 0.07×10^{-7}	1.16 ± 0.22
Cornea	21 ± 6	0.11 ± 0.04×10^{-7}	2.38 ± 0.75

3.5.6. Immunohistochemistry

Immunohistochemistry allowed the detection of EPOβ within the ocular membranes' cells. As previously described, one cross-section per each sample of porcine ocular membrane was processed to enable immunohistochemistry assessment. The cell nucleus emitted blue fluorescence while the EPOβ emitted red fluorescence.

As observed in figure 21, all the ocular membranes contained EPOβ, with a stronger red fluorescence in the porcine conjunctiva when compared to the scleral and corneal tissues. These results confirmed that EPOβ crossed over the porcine ocular membranes and that the conjunctiva was the most permeable membrane. It was also possible to observe that the EPOβ was still present in the ocular membranes 7 hours after the instillation (*Ex vivo* permeation assays) and that the nanoparticles did not block the diffusion of EPOβ across the tissues.

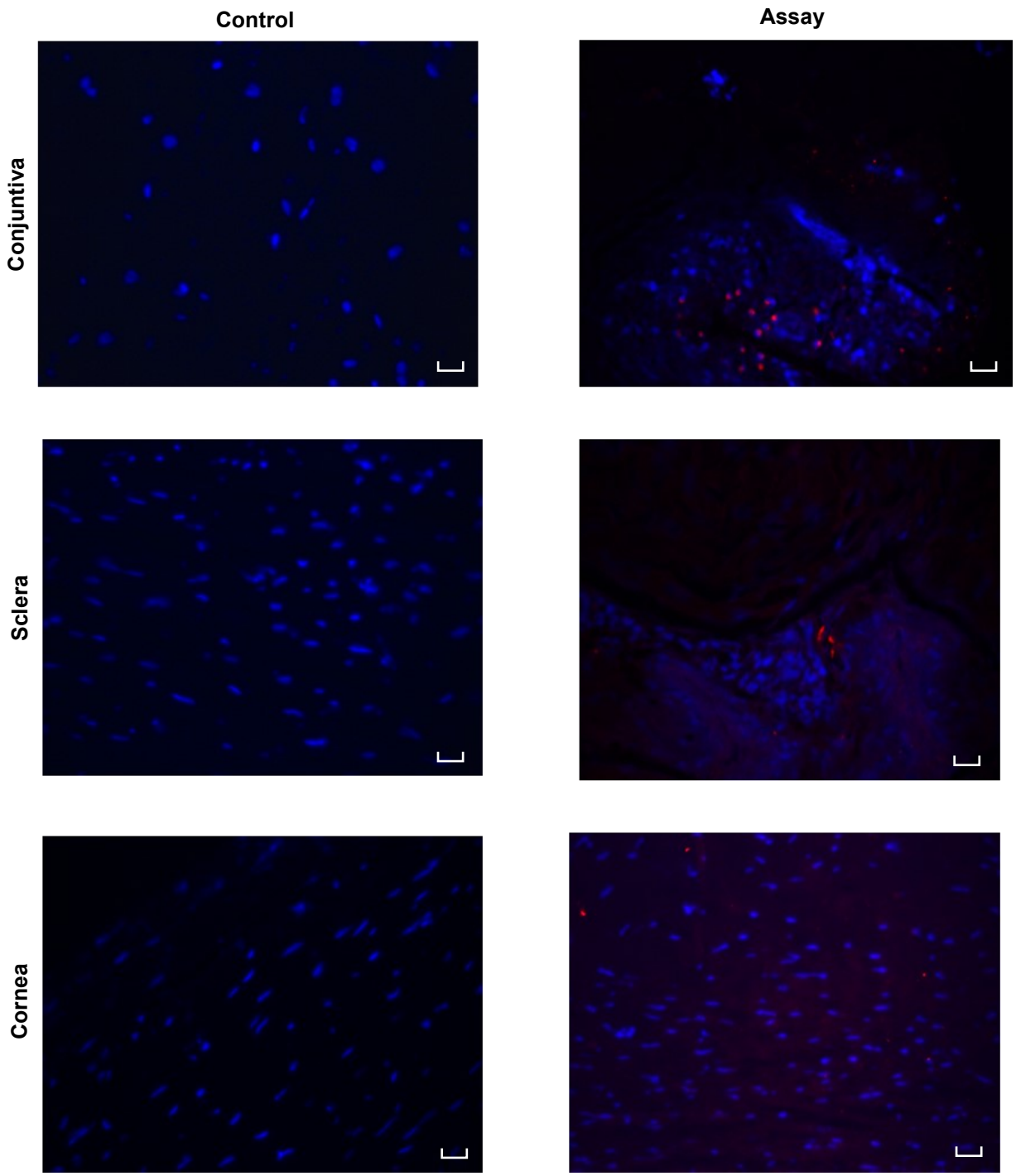

Figure 21: Immunohistochemistry for cell nucleus marker of the conjunctiva, sclera and cornea (DAPI, blue) and EPO antibody (red), 7 h after the administration into the donor phase (scale bar 20 µm).

3.6. Discussion

3.6.1. Development and optimization of nanoparticles

The effect of different hyaluronic acids

A nanoparticulate delivery system designed for ocular instillation must have a low average particle size and the lowest polydispersity index possible, in order to promote mucoadhesion and corneal uptake to enhance intraocular bioavailability (De Campos et al. 2001; Sahoo et al. 2008). The particle size that human eyes can tolerate without discomfort is < 10 μm (Kalam 2016a) and nanoparticulate systems intended for ocular use normally ranges from 50 to 400 nm (Bachu et al. 2018). A positive ZP (at least +30 mV) is required to create a stabilized colloidal system and to promote interaction between the nanoparticles and the mucin, due its negatively charged carboxyl and sulfate groups (Gonçalves et al. 2010; Graça et al. 2018). Despite the absence of HA, Miklavžin et al. (2018) loaded EPO in CS and CS-TMC nanoparticles presenting mean particle size of 300 ± 35 nm and 250 ± 20 nm, polydispersity index of 0.30 ± 0.022 and 0.31 ± 0.025, and zeta potential of +30 ± 3 mV and +35 ± 4 mV respectively. In addition, a wide variety of research studies using CS and CS/HA nanoparticles sustain the premises of an optimal ZP around +30 mV and a threshold of 300 nm for size (De Campos et al. 2001; Wadhwa et al. 2010; Caetano et al. 2016; Kalam 2016a; Silva et al. 2017). LMW CS helped to achieve this goal because it reduces the nanoparticles' size when compared with a higher molecular weight CS (De La Fuente et al. 2008).

The CS:HA mass ratio has an important role in nanoparticles' formation (Caetano et al. 2016). In our study, the 1:0.5 CS:HA mass ratio led to aggregation instead of nanoparticles in the majority of the formulations. However, Wadhwa et al. (2010) successfully produced nanoparticles with 1:0.5 CS:HA mass ratio, with a size of 319.5 ± 4.0 nm and ZP of +33.3 ± 6.1 mV, but the MW of the HA was not mentioned and the method was ionotropic gelation with sodium tripolyphosphate (TPP), so the results cannot be fully compared.

In our assays, the 1:2 CS:HA mass ratio presented inconsistent results when compared to the 1:1 ratio. The CS/HA5 nanoparticles were smaller (217±5 nm) than the CS/HA4 (302±35 nm) and the CS/HA6 (712±192 nm) ones, which seemed incoherent because the HA5 MW is higher than the HA4 and HA6 ones. We expected the CS/HA2 and CS/HA6 nanoparticles to have similar size, ZP and PDI since they have approximately the same MW (300 kDa). However, at 1:2 CS:HA mass ratio the size difference was statistically significant ($p < 0.001$). Similar results were obtained for the ZP, with statistically significant differences between HA2 and HA6 for both ratios: $p < 0.05$ for 1:1 and $p < 0.001$ for 1:2. It was also observed an inversion

of the ZP from positive to negative in HA5 and HA6 and a general lowering of the absolute ZP value. These results justified the exclusion of the 1:2 CS:HA mass ratio from the study.

The results obtained for nanoparticles made with 1:1 CS:HA mass ratio were much more reasonable, especially the ZP values, which showed more variation with the CS:HA mass ratio, independently of the HA MW. Indeed, the nanoparticles' characteristics did not seem to be influenced by the MW of the HAs tested in this study. The PDI values (0.167-0.539) denoted a sufficiently homogeneous nanoparticles' size distribution, according to the literature (Singh and Shinde 2011; Khan et al. 2013; Tamba et al. 2015).

As a note, a microscopical image of the nanoformulations would be a valuable source of information about the nanoparticles' morphology and could support the results. However, our group has already shown that this type of nanoparticles present a spherical morphology (Cadete et al. 2012), thus that was taken into account.

The effect of NaCl

The CS/HA nanoparticles physicochemical stability can be influenced by salt concentration (Kayitmazer et al. 2015). Regarding 0.9% NaCl, Na^+ cations act as counter ions on the HA anionic structure, reducing electrostatic repulsion and decreasing the absolute ZP value (Graça et al. 2018), which is consistent with the results (Figure 17c). Nanoparticles size and PDI values also decreased with 0.9% NaCl (Figure 17a and 17b), reinforcing the choice of 0.9% NaCl as CS solvent in detriment of water.

Encapsulation of EPOβ and loading capacity

The hydrogel encapsulation of proteins while preserving their pharmacological activity and stability is a focus of investigation (Hirakura et al. 2010). Encapsulation efficiency and drug loading depend on the solubility of the nanoparticles in the polymeric matrix, which is related to the drug-polymer interactions, the polymer composition, the MW and the presence of ester or carboxyl groups, among others. The drug loading capacity must be high in order to reduce the amount of excipients (Gonçalves et al. 2010). To the best of the authors knowledge, there are no published data concerning CS/HA nanoparticles loaded with EPOβ, especially when considering the ophthalmic use. Therefore, it was challenging to compare the %EE and %DL results with the literature.

In our study, %EE and %DL of EPOβ were higher for the HA with the highest MW (HA4 – 3000 kDa) and lower for the HA with the smallest MW (HA1 – 50 kDa) (Table 9). Saxena et al. (2005) found a similar relation but regarding gelatin nanoparticles: those made with higher MW gelatins presented higher %EE and %DL. The EPO %EE of HA4 was 39.9 ± 0.6%, which

was not considered high comparing to the literature. Zhang et al. (2017) created CS/TPP-EPO nanoparticles with %EE of 78.45% but with an average nanoparticles size of 485 ± 12 nm. Bulmer et al. (2012a, 2012b) presented EPO %EE of 47.97 ± 4.10% for CS/Carrageenan nanoparticles and 38.93 ± 1.48 for LMW CS/TPP nanoparticles which is very similar to our results. Bokharaei et al. (2011) results are also similar to ours, with EPO %EE of 34.5% for CS/TPP nanoparticles.

There are scarce reports about EPO %DL in NPs, especially in CS nanoparticles. Miklavžin et al. (2018) conducted a study with CS/TPP-EPO and TMC/TPP-EPO nanoparticles attaining %DL of 62% and 33%, respectively. On the other hand, Hirakura et al. (2010) entrapped EPO in cholesterol hydrogels showing a maximum %DL of 1.96 ± 0.13% but with a high %EE (83.6 ± 2.6%). Nevertheless, a recent review paper entitled "Advances on the formulation of proteins using nanotechnologies" concluded that polysaccharide-based nanoparticles have the highest protein %DL among the delivery systems indicated in that article (Santalices et al. 2017). Theoretically, both %EE and %DL calculated in this study could be improved by modification of the nanoparticle's composition or the formulation method, but that would increase the complexity of the process and could also damage the protein, compromising its activity. Our primary goal was to use methods that could produce acceptable results and, at the same time, were compatible with EPO's delicate structure.

3.6.2. In vitro cytotoxicity

In vitro cell viability tests are important steps in the development of a new drug, even when the biocompatibility and non-toxicity of chitosan and hyaluronic acid are well acknowledged. This study showed 100% of cell viability for ARPE-19 and HaCaT cell lines for the 3 nanoformulations tested, which is consistent with previous published data (De La Fuente et al. 2008; Silva et al. 2017).

3.6.3. In vitro release

EPOβ release was evaluated in STF (pH 7.4) at 37 ºC in order to mimic the extraocular conditions, as described in the literature (Lin et al. 2007; Kalam 2016a). The three nanoformulations (HA1, HA4 and HA6) did not present significant differences in the release profiles. The observed initial burst of released EPOβ could be explained by the non-encapsulated EPOβ which rapidly dissolved into the medium, as described by Lin et al. (2007) although using pilocarpine. On the other hand, the following slow release is compatible with the diffusion of EPOβ from the CS-HA nanoparticles, which is in accordance with the behavior of similar nanoparticles found in the literature (Lin et al. 2007; Kalam 2016a).

3.6.4. Mucoadhesion

The rheological characteristics of the formulations provided information to help in the selection of the optimal HA.

The nanoformulation with HA6 presented the highest adhesive strength and the highest peak force when combined with the pig eye (Table 10), being considered the strongest HA. This is apparently contradictory as the MW of HA4 is 3000 kDa while the MW of HA6 is in average 300 kDa. Salzillo et al. studied several ophthalmic commercial HA formulations and reported that an increase of the HA MW is directly proportional to an increase of its mucoadhesive strength (Salzillo et al. 2016). However, the viscosity and the surface/interfacial tensions between the polymer and the substrate substantially influence the HA mucoadhesive properties (Graça et al. 2018). Those features were not evaluated in this study so no further conclusions can be made about this matter. Besides, the hyaluronic acids were obtained from different sources which could also interfere with the mucoadhesive properties.

After the incubation of HA6 with the mucin to evaluate the mucoadhesion interaction, the ZP value decreased (Table 11) which could be attributed to the adsorption of negatively charged mucin particles onto the positively charged surface of CS/HA nanoparticles (Silva et al. 2017). This denoted a suitable ionic interaction between both components and justified the selection of HA6 for further assays. Moreover, Sadeghi et al. (2015) showed that a monodisperse suspension, characterized by particles of uniform size in a dispersed phase, have a PDI lower than 0.3 and with a single peak in the size distribution curve. HA6 follows those requirements, having an average PDI of 0.219±0.043 (Figure 17b), which reinforced its selection as the ideal HA for the CS/HA-EPOβ nanoformulation.

3.6.5. Ex vivo permeation

EPOβ faces important physical barriers after ocular topical instillation, so it is essential to assess its permeability across the conjunctiva, the cornea and the sclera. It is known that EPOβ can penetrate the sclera in *in vivo* conditions after subconjunctival injection (Resende et al. 2013; Resende et al. 2016; Resende et al. 2018) and our research group published an *ex vivo* study using porcine conjunctiva, sclera and cornea with positive permeation results, but EPOβ was not loaded in nanoparticles (Resende et al. 2017). Nanoparticles usually present a biphasic release pattern characterized by an early burst release followed by a sustained release (Bachu et al. 2018), which is compatible with our results for the 3 membranes (Figure 20). Nevertheless, there were statistically significant differences between the membranes' permeation. CS/HA6-EPOβ nanoformulation permeated more rapidly through the porcine conjunctiva, followed by the sclera and the cornea. The cornea is the thickest

membrane (≈ 500 μm in humans) constituted by an epithelium, stroma (≈ 450 μm in humans) and endothelium. The epithelium is relatively permeable to small and lipophilic molecules, while the highly organized collagen fibers of the stroma make it mainly hydrophilic (Prausnitz 1998; Kim et al. 2014). The sclera is also an important barrier but in human *ex vivo* studies, the sclera presented permeation of molecules up to 150 kDa (Kim et al. 2014). The conjunctiva is a thin layer and have wider intercellular spaces compared to the cornea, being more permeable to larger molecules (Prausnitz 1998). These are just some anatomic/histologic features that can justify the different permeation patterns and parameters observed among the ocular membranes in this assay (Figure 20 and Table 12), which are also supported by the literature (Yi et al. 2000; Ambati and Adamis 2002; Pescina et al. 2015; Kalam 2016a; Radhakrishnan et al. 2017).

The EPOβ permeated amount was higher than that observed in our previous study using 100 IU/ 200 μL of EPOβ in solution (Resende et al. 2017). Regarding the conjunctiva, the permeated amount in this study was 23.7% to 60% more than that previously obtained (Resende et al. 2017). In the sclera the difference is even higher (22.6% to 85.3%) and the cornea presented up to 2.5x more permeated amount when compared to the referred study (Resende et al. 2017). Similar differences were observed for the EPOβ fluxes, although not so significant. Therefore, it can be assumed that the CS/HA6 nanoparticles plays a significant role in EPOβ ocular permeation. CS is considered a permeation and absorption enhancer, widening the tight junctions of membranes (Thanou et al. 2001). Moreover, both CS and HA have mucoadhesive properties that increase the drug retention time on the ocular surface (De Campos et al., 2001; Kalam, 2016b; Silva et al., 2017) and HA has second generation mucoadhesion properties through CD44 receptor-mediated binding (Wadhwa et al. 2010; Contreras-Ruiz et al. 2011). These properties might justify the higher permeated amount of EPOβ observed in this study when compared to Resende et al. (2017) study, especially regarding the cornea.

The very low bioavailability of drugs to the anterior chamber after topical instillation (Yi et al. 2000; Ghate and Edelhauser 2008; Kalam 2016a; Peynshaert et al. 2018) complicate the task to reach the intraocular therapeutic dose. Shirley Ding et al. (2016) revised EPO as a treatment for ocular disorders and concluded that 10 IU of EPO, after subretinal and intravitreal administration, is enough to develop anti-apoptotic effects in RGC-induced axonal degeneration in a rat model. Thus, it is possible that by concentrating the nanoformulation developed in our study, this therapeutic level could be achieved in *in vivo* conditions. Nevertheless, additional *in vivo* research is needed to assess EPO's ocular therapeutic dose by ocular/periocular routes of administration.

3.6.6. Immunohistochemistry

Immunohistochemistry uses antibodies to detect specific proteins and has been used to identify erythropoietin in numerous tissues (L. Zhong et al. 2007; Resende et al. 2017). In this work, histological cross-sections of the 3 porcine ocular membranes were stained by immunohistochemistry and assessed by fluorescent microscopy. All the ocular membranes presented EPOβ, but the conjunctiva yielded a stronger positive immunostaining signal (Figure 21). This confirmed that porcine outer ocular membranes are permeable to EPOβ, with the conjunctiva being the most permeable, which is in accordance with the permeation results (Figure 20 and Table 12) and with our previous published study (Resende et al. 2017). It is possible to assume that EPOβ was able to slowly diffuse out of the CS/HA6 nanoparticles after the burst release because it was still present in the ocular membranes 7 hours after the instillation.

3.7. Conclusions

EPOβ can be successfully encapsulated in nanoparticles of chitosan and hyaluronic acid, creating a biologically safe formulation with suitable particle size, zeta potential, polydispersity index and mucoadhesive properties. Our goal was to choose the HA with the finest features to improve EPO's intraocular bioavailability in further *in vivo* studies. The CS:HA mass ratios and the interaction between nanoparticles and different solvents interfered in their characteristics, but the mucoadhesion was the determinant factor to select the ideal HA, which was HA6 (300 kDa – Eye). Among the studied porcine ocular membranes, the conjunctiva was the most permeable to the CS/HA6-EPOβ nanoformulation, with EPOβ being detected in all membranes by immunohistochemistry 7 hours after instillation. These results support the possibility of using these nanoparticles as a system for topical ocular delivery of EPOβ but, theoretically, the formulation's acidic pH could destabilize EPOβ's activity. Also, the ocular defense mechanisms like tear film clearance, blinking, conjunctiva/ choriocapillaris blood flow, uveoscleral outflow and IOP, among other, were not considered in this study. Therefore, further *in vivo* studies will be conducted for the evaluation of EPOβ's integrity, activity once loaded in the nanoparticles, and its pharmacodynamic and pharmacokinetic profiles after ocular topical instillation. In addition, the CS/HA6-EPOβ nanoparticles could be further optimized in order to enhance the amount of permeated EPOβ to achieve a therapeutic concentration in the retina, which would also be a focus of further investigation.

CHAPTER 4

Chitosan and hyaluronic acid nanoparticles as vehicles of epoetin beta for subconjunctival ocular delivery

Silva B, Gonçalves LM, Braz BS, Delgado E. Chitosan and Hyaluronic Acid Nanoparticles as Vehicles of Epoetin Beta for Subconjunctival Ocular Delivery. Mar Drugs. 2022;20(2):151. Published 2022 Feb 18. doi:10.3390/md20020151

4.1. Abstract

Neuroprotection in glaucoma using epoetin beta (EPOβ) has yielded promising results. Our team has developed chitosan-hyaluronic acid nanoparticles (CS/HA) designed to carry EPOβ into the ocular globe, improving the drug's mucoadhesion and retention time on the ocular surface to increase its bioavailability. In the present *in vivo* study, we explored the possibility of delivering EPOβ to the eye through subconjunctival administration of chitosan-hyaluronic acid-EPOβ (CS/HA-EPOβ) nanoparticles. Healthy Wistar Hannover rats (n = 21) were split into 7 groups and underwent complete ophthalmological examinations, including electroretinography, and microhematocrit evaluations before and after the subconjunctival administrations. CS/HA-EPOβ nanoparticles were administered to the right eye (OD), and the contralateral eye (OS) served as control. At selected timepoints, animals from each group (n = 3) were euthanized, and both eyes were enucleated for histological evaluation (immunofluorescence and HE). No adverse ocular signs, no changes in the microhematocrits (≈ 45%), and no deviations in the electroretinographies in both photopic and scotopic exams were observed after the administrations ($p > 0.05$). IOP remained in the physiological range during the assays (11-22 mmHg). EPOβ was detected in the retina by immunofluorescence 12 h after the subconjunctival administration and remained detectable until day 21. We concluded that CS/HA nanoparticles could efficiently deliver EPOβ into the retina, and this alternative was considered biologically safe. This nanoformulation could be a promising tool for treating retinopathies, namely optic nerve degeneration associated with glaucoma.

4.2. Introduction

Neurodegenerative ocular diseases, such as glaucoma, have a major impact on people's daily life, and the interest in neuroprotection as part of glaucoma treatment has been increasing (Vidal-Sanz et al. 2012). Erythropoietin (EPO) is a glycoprotein produced in adult kidneys and fetal liver that has a primary hematopoietic role of stimulating the production of erythrocytes in the bone marrow (Abri Aghdam et al. 2016). However, novel EPO secreting sites were discovered, like the brain (Marti 2004) and the retina (Hernández et al. 2006), which have also demonstrated the expression of EPO receptors (Garcia-Ramirez, Marta; Hernández, Cristina; Simó 2008; Ott et al. 2015). Recent studies demonstrated that EPO has tissue-protective properties in the brain, heart, inner ear, and retina (Luo et al. 2015), and the subconjunctival administration of EPO, as an alternative delivery method aiming at the posterior ocular segment, has been explored with promising results (Resende et al. 2013; Resende et al. 2016). Recent investigation with glaucomatous rats demonstrated that epoetin beta (EPOβ), a recombinant version of EPO, administered by subconjunctival route, reached the retina and improved its condition when compared to non-treated animals (Resende et al. 2018).

Topical administration is considered ineffective for the treatment of posterior ocular diseases; systemic administration may result in severe side effects, and intravitreal injection is invasive and may lead to side effects like increased IOP, vitreous detachment, retinal haemorrhage/ toxicity, and cataracts (Varela-Fernández et al. 2020). Subconjunctival administration is a minor-invasive procedure with few side effects and it is considered a promising alternative route of administration for the treatment of retinal diseases (Ranta and Urtti 2006). Nevertheless, despite enabling a sustained drug delivery, a percentage of the drug is always cleared out by conjunctival blood or lymphatic flow (Attar et al. 2013). Thus, it is important to improve the drug's retention time and penetration through the outer ocular layers to increase its bioavailability when administered subconjunctivally.

Mucoadhesive nanoparticles are state-of-the-art systems that can fulfil those requirements by protecting the drug while enhancing its permeation across biological barriers (Ameeduzzafar et al. 2016). Chitosan is a well-studied natural polymer with excellent mucoadhesive characteristics. Its cationic nature enables ionic interactions with the ocular mucosa (negatively charged), which improve the drug's mucoadhesion and retention time on the ocular surface (De Campos et al. 2001; Bernkop-Schnürch and Dünnhaupt 2012). Therefore, chitosan nanoparticles can reduce the frequency of ocular administrations and improve long-term patient compliance (Silva et al. 2021). Chitosan also acts like a permeation enhancer by widening the tight junctions of the cell membranes (Thanou et al. 2001). Moreover, it has a low production cost and a reduced ecological impact because it is obtained

from crustaceans exoskeletons and fungi cell walls by deacetylation of chitin (Peter MG 1995). A recent study used chitosan-coated nanoparticles for the delivery of bevacizumab to the posterior segment of the eye by subconjunctival administration, and the results showed higher drug concentration in the posterior segment and better results in the retinopathy model, compared to the topical and intravitreal administrations (Pandit et al. 2021). Chitosan can be associated with various synthetic and natural compounds, such as hyaluronic acid. Hyaluronic acid is a natural polysaccharide distributed throughout ocular tissues, such as the vitreous body, lacrimal gland, human tears, conjunctiva, and corneal epithelium (Rah 2011). When considering ophthalmic formulations, their mucins-like viscoelastic and biophysical properties and their additional mucoadhesive strength due to CD44 receptor-mediated binding are valuable features (Wadhwa et al. 2010; Graça et al. 2018).

Recently, our team has developed a system of chitosan-hyaluronic acid nanoparticles (CS/HA) designed to carry EPOβ into the ocular globe. *In vitro* and *ex vivo* testing of the physicochemical stability, cytotoxicity, and mucoadhesive strength of the chitosan-hyaluronic acid-epoetin beta (CS/HA-EPOβ) nanoparticles have been previously performed (Silva et al. 2020). Therefore, in the present study, we aimed to evaluate the behavior of the CS/HA-EPOβ nanoparticulate system *in vivo*. For that, we used Wistar Hanover rats, and we tested the subconjunctival route of administration under physiological conditions. We intended to assess the formulation's biological tolerance and safety, its local and systemic impact, its influence in retinal electrophysiology, and EPOβ's distribution in ocular tissues by immunofluorescence.

4.3. Materials and Methods

4.3.1. Materials

Adult male Wistar Hannover albino rats (n = 21) were the model selected for this study, with an average weight of 317 ± 36 g. Animals were acquired from Charles River Laboratories (Saint-Germain-Nuelles, France). Chitosan of low molecular weight (LMW CS, 100 kDa, 92% deacetylation) was obtained from Sigma Aldrich (Irvin, UK). The sodium hyaluronate eyedrop grade quality (300 kDa—Eye) from Shandong Topscience was a kind gift from Inquiaroma (Barcelona, Spain). The recombinant human erythropoietin (epoetin beta, EPOβ) used was NeoRecormon® 30000 IU (RocheDiagnostics GmbH, Mannheim, Germany). The subconjunctival administration was performed using insulin syringes with 29 G needles (Becton Dickinson® Micro-Fine Insulin Syringe 0,5 mL). The drugs used were ketamine (Ketamidor® 100 mg/mL, Richter Pharma, Wels, Austria), medetomidine (Domtor® 1mg/mL, Orion Corporation, Espoo, Finland), atipamezole (Antisedan® 5 mg/mL, Zoetis, Parsippany-

Troy Hills, NJ, USA) and sodium pentobarbital (Euthasol® 400 mg/mL, Animalcare Group, North Yorkshire, UK) available in the Faculty of Veterinary Medicine (ULisboa). The ERG equipment (RETIcom, Roland Consult, Stasche & Finger GmbH, Brandenburg, Germany), the rebound tonometer (Tonolab®, Icare, Finland), the slit lamp (Hawk Eye®, Dioptrix, France), and the PanOptic® ophthalmoscope (WelchAllyn-Hillrom, USA) belonged to the Faculty of Veterinary Medicine (ULisboa). The positively charged microscope slides used were Epredia™ SuperFrost Plus™ Adhesion slides (ThermoFisher Scientific, Waltham, MA, USA). Cover plates and immunostaining rack (Epredia™ Shandon™ Sequenza™, ThermoFisher Scientific, Waltham, MA, USA) and Thermo Scientific™ Gemini™ AS (Waltham, MA, USA) slide stainer for hematoxylin and eosin stain belonged to the Faculty of Veterinary Medicine (ULisboa). HepG2 human-derived liver hepatocellular carcinoma cell line (ATCC® HB-8065™). All the cell culture media and supplements were from Gibco (ThermoFisher Scientific, Waltham, MA, USA). UltraCruz® Blocking Reagent (sc-516214) was from Santa Cruz Biotechnology (Texas, USA). EPO monoclonal primary antibody 4F11 (MA5-15684) and goat anti-mouse IgG (H+L) secondary antibody DyLight 488 (35502) were from Invitrogen (ThermoFisher Scientific, Waltham, MA, USA). The mounting medium used was UltraCruz® Aqueous Mounting Medium with DAPI (sc-2494; Santa Cruz Biotechnology, Dallas, TX, USA). Axioscop 40 fluorescence microscope with an Axiocam HRc camera (Carl Zeiss, Germany) and the Zetasizer Nanoseries Nano S and Nano Z (Malvern Instruments, Malvern, UK).

4.3.2. Methods

Animals and Timepoints

Wistar Hannover rats (n = 21) were split into 7 groups (n = 3). Each group of rats were housed in a type IV cage (1875 cm^2 of floor area) with a stainless-steel wire cover. Food pellets and water were offered ad libitum, and the room environment was maintained in a 12 h cycle of light/ darkness, at 20 ± 2 °C and an average humidity of 50–60%.

Each group corresponded to a specific time point as follows: Group A (n = 3) corresponding to 12 h after the injection; Group B (n = 3) to 1 day; Group C (n = 3) to 3 days; Group D (n = 3) to 7 days; Group E (n = 3) to 14 days; Group F (n = 3) to 21 days; and finally, Group G (n = 3) corresponding to 28 days. These specific time points correspond to the time of euthanasia after the subconjunctival administration of CS/HA-EPOβ nanoparticles. This study was performed in accordance with animal ethical requirements, and it was approved by the Organ Responsible for Animal Welfare (Órgão Responsável pelo Bem-Estar dos Animais—ORBEA) of the Faculty of Veterinary Medicine, University of Lisbon, and by the

national entity General Directorate of Food and Veterinary (Direção Geral de Alimentação e Veterinária—DGAV).

Ophthalmological Examination

Figure 22 summarizes the occurrence of the events. All animals (n = 21) underwent a complete ophthalmological examination prior to being included in the study, including measurement of the intraocular pressure (IOP) with a rebound tonometer (Tonolab®, Icare, Finland), biomicroscopic examination of the anterior segment with a slit lamp (Hawk Eye®, Dioptrix, France), and posterior segment examination with PanOptic® ophthalmoscope (WelchAllyn-Hillrom, Skaneateles Falls, NY, USA). Complete ophthalmological examinations were then performed periodically after the subconjunctival administration of CS/HA-EPOβ nanoparticles: 1 h, 12 h and 1, 2, 3, 7, 14, 21, and 28 days after.

Figure 22: Sequence of procedures performed in each animal (n = 21). Oph Exam – Ophthalmological examination; Htc – blood collection for microhematocrit; ERG – electroretinography; CS/HA-EPOβ – subconjunctival administration of the nanoformulation.

Electroretinography

Flash electroretinography (ERG) was performed in all animals at two periods of time: the first ERG preceded the administration of CS/HA-EPOβ nanoparticles, and the second ERG preceded euthanasia. The ERG procedure was based on previously published protocols [13] in which rods and cones activity were recorded as a-wave and b-wave amplitudes (μV) in response to luminous stimuli. Animals were kept in the dark for 12 h before the exam. General anesthesia was required for a total immobilization of the animal. A combination of ketamine (70 mg/ kg) and medetomidine (0.8 mg/ kg) was administered intraperitoneally to induce anesthesia. Active electrodes with wired silver tips were placed on both corneas (Figure 23a) after one drop of oxybuprocaine hydrochloride (Anestocil®, Edol, Lisbon, Portugal) followed by one drop of a carbomer-based gel (Lubrithal®, Dechra, Northwich, United Kingdom). Reference electrodes were placed subcutaneously, and the tip of the electrode was located between the ear and lateral cantus of both sides, and the ground electrode was placed at the base of the tail (Figure 23b). A heating pad was used to maintain the animal's body temperature, which was periodically checked. For light stimulation, a MiniGanzfeld was placed

on the animal's head (Figure 23c). Signals were recorded independently for each eye and the impedance < 5 kohms at 0.1–1000 Hz frequency (0 dB = 3 cds/m^2). Each ERG examination lasted 75 min and was divided into 5 parts. The first part was the scotopic luminance response (SLR) which consisted of 9 intensities of light flashes from –35 dB to +5 dB, delivered three times at 0.1 Hz. The next part was the photopic adaptation (PA), in which the flashes intensity was calculated at the maximum b-wave amplitude of the SLR. Flashes were delivered three times at 1.3 Hz at 0, 2, 4, 8, and 16 min of light adaptation. Then, the photopic luminance response (PLR) used light flashes of 9 intensities from –35 dB to +5 dB, delivered three times at 1.3 Hz. After 10 min of light adaptation, the photopic flicker delivered flashes of 0, –5, –10, and –15 dB at 6.3 Hz. Lastly, the scotopic adaptation (SA) used white dim flashes delivered three times at 1.3 Hz at 0, 2, 4, 8, 16, and 32 min of dark adaptation. Rod function was tested by stimulating the retina with dim flashes in scotopic conditions (–35 dB = –3.02 log cds/m^2), while cone function was assessed by retinal stimulation with bright flash's (+5 dB = 0.98 log cds/m^2) and 6.3 Hz flicker in photopic conditions.

(a) (b) (c)

Figure 23: Pictures the ERG set: (a) active electrodes (red) with silver tips placed on corneas; (b) reference electrodes (blue) placed next to the ears and the ground electrode (black) at the base of the tail; (c) head positioning inside the MiniGanzfeld stimulator.

Hematocrit

A blood sample was retrieved from each animal during the anesthesia for the ERG to assess microhematocrits. The rat tail was immersed in warm water (≈ 40 °C) for 3 to 5 min, and the blood was collected from a lateral vein by a needle punch (23 G needle) with the aid of a capillary tube. Samples were centrifuged in a capillary centrifuge at 10,000 rpm for 5 min, and microhematocrits were read using a proper scale. This procedure was performed twice before the first ERG and before the second ERG.

Nanoparticles' Preparation

The formulation was prepared on the day of the experimental procedures, based on previously published methods (Wadhwa et al. 2010; Graça et al. 2018) which consist of a modified ionotropic gelation technique. All reagents were previously sterilized using a 0.22 μm sterile filter in a laminar flow cabinet, and the nanoparticles were produced with EPOβ (CS/HA-EPOβ nanoparticles; 1000 IU of EPOβ), and without EPOβ (empty CS/HA nanoparticles) in a laminar flow cabinet following the previously published procedure (Silva et al. 2020). Firstly, the chitosan solution at 2 mg/mL in 0.1% (v/v) of acetic acid was diluted in NaCl 0.9% in 1:1 (v/v) ratio (CS-NaCl; 1 mg/mL). Separately, the hyaluronic acid solution at 2 mg/mL in purified water was mixed with 1000 IU of EPOβ (NeoRecormon®) at a 1:1 (v/v) ratio (HA-EPOβ; 1 mg/mL). Finally, HA-EPOβ was slowly added to CS-NaCl, and the formation of the nanoparticles occurred instantly by self-assembly. For the empty CS/HA formulation (without EPOβ), the same volume of purified water was added to the hyaluronic acid instead of EPOβ. The formulation was aspirated with a sterilized insulin syringe to be further administered subconjunctivally.

Subconjunctival Administration

At the end of the first ERG, during anesthesia, all animals underwent subconjunctival administration of 80 μL of CS/HA-EPOβ nanoparticles (1000 IU of EPOβ) in the right eye (OD); and 80 μL of empty CS/HA nanoparticles (without EPOβ) were administered in the left eye (OS), which served as a negative control. The subconjunctival administration (Figure 24) was performed with an insulin syringe with a 29 G needle at 3 different subconjunctival sites, using a binocular magnifier. Anesthesia was reverted with subcutaneous atipamezole (2.5 mg/ kg).

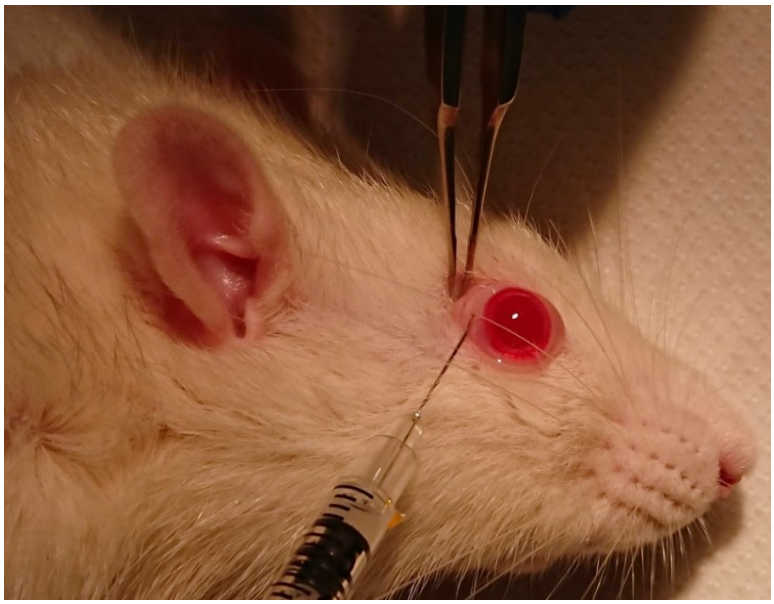

Figure 24: Photo of the subconjunctival administration of the C/HA-EPOβ in the OD of a rat, under general anesthesia.

Euthanasia and Enucleation

At 12 h (n = 3), 1 day (n = 3), 3 days (n = 3), 7 days (n = 3), 14 days (n = 3), 21 days (n = 3) and 28 days (n = 3) after the administration of the CS/HA-EPOβ formulation, euthanasia was performed with intraperitoneal sodium pentobarbital (150 mg/kg). Before euthanasia, a second blood sampling for microhematocrit evaluation and a second ERG was performed. Immediately after euthanasia, both eyes were enucleated and painted with tissue dyes in the optic nerve and the lateral, medial, dorsal, and ventral sides, as shown in figure 25, to allow for correct orientation of the histological sections. Eyes were stored in 10% (v/v) formaldehyde in PBS (0.1 M, pH 7.4) and further included in paraffin blocks.

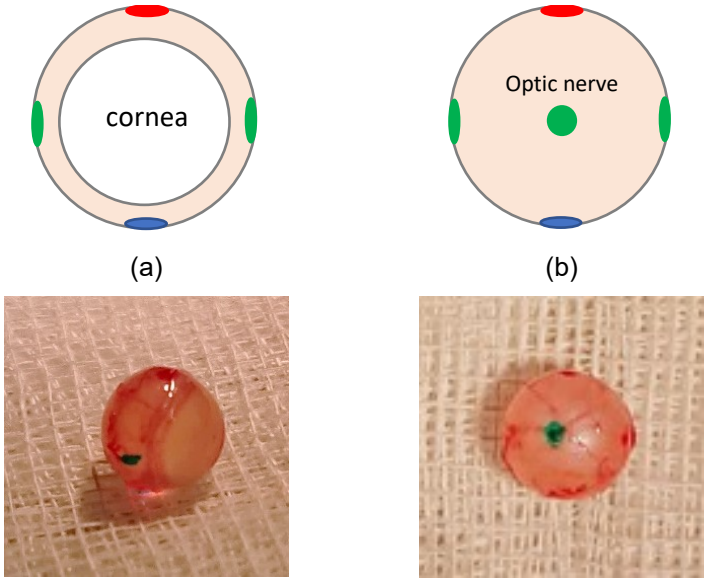

.

Figure 25: Representation of a rat ocular globe painted with tissue dyes: (a) frontal view; (b) caudal view. Photo of a rat ocular globe painted with tissue dyes: (c) lateral view; (d) caudal view, in green we can identify the transected optic nerve.

Histologic Evaluation

After including the ocular globes in paraffin blocks, immunofluorescence and hematoxylin and eosin (HE) stains were performed. From the OD and the OS, cross-sections of 3 µm each were made using a microtome, 4 cross-sections per eye were used for immunofluorescence, and 4 cross-sections per eye were used for HE staining. For immunofluorescence, sections were placed in adhesion slides and deparaffinized in xylol for 15′ + 5′, rehydrated in alcohol from 100° to 70° (3′ each) and purified water (3′ + 15′). A sequence of washing steps with Triton X-100 solution (0.1% v/v in PBS) and Tween 20 solution (0.1% v/v in PBS) was performed, followed by assembling of the slides in cover plates. Sections were incubated with UltraCruz® Blocking Reagent at room temperature for 60′. Then, EPO monoclonal primary antibody 4F11 (1:400) was added, followed by overnight incubation at 4 °C. On the following day, cross-sections were washed with Tween 20 solution (0.1% v/v in PBS) and incubated with goat anti-mouse secondary antibody DyLight 488 (1:1000) in the dark, at room temperature, for 60′. Cross-sections were washed again in PBS, and the slides were carefully disassembled from the cover plates. A small amount of UltraCruz® mounting medium with DAPI was added in each slide, and a coverslip was placed on the top, followed by sealing with varnish. Sections were analyzed using an Axioscop 40 fluorescence microscope with an Axiocam HRc camera (Carl Zeiss, Germany). The emitted fluorescence

was observed and recorded in images processed with AxioVision software (Rel.4.8.1, Carl Zeiss). Negative controls were the OS, and the positive controls were HepG2 cell cultures because they naturally express EPO. These cell cultures were submitted to a hypoxic environment for 120′ at 37 °C and then fixed in 10% (v/v) formaldehyde in PBS for 15′ at room temperature in the dark. HepG2 cells were washed with Triton X-100 solution (0.1% v/v in PBS) for 5′. From this step on, the protocol was the same as the cross-sections. For HE, all sections were placed in regular slides and processed in the multi-tasking stainer Gemini™ AS.

Statistical Methods

The experimental data were statistically assessed using GraphPad Prism version 6.0 (GraphPad Software, San Diego, CA, USA) and Microsoft Office Excel (Microsoft, Albuquerque, NM, USA) by one-way ANOVA and t-test to detect significant differences between means. The established statistical significance was 95%, corresponding to a *p*-value of 0.05. Data were presented as mean ± standard deviation (SD).

4.4. Results

4.4.1. Ophthalmological Examinations

On day 1 after the subconjunctival administration, a discrete reddish discharge in the ocular medial canthus of both eyes was observed in 3 rats (one from group B and two from group C), but apart from that, no other ocular changes were detected, namely conjunctival hyperemia, corneal oedema or aqueous flare. Therefore, ophthalmological examinations of both eyes were considered normal for all animals (n = 21). Moreover, animals exhibited a completely normal behavior and showed no signs of pain or discomfort throughout the entire study.

Before the subconjunctival administration, the mean IOP was 17 ± 2 mmHg for the OD and 18 ± 3 mmHg for the OS when the animals were awake. Immediately after the subconjunctival administration (day 0; Figure 26), when animals were still anesthetized, the mean IOP was 11 ± 2 mmHg for the OD and 11 ± 1 mmHg for the OS. The mean IOP of the OD was not significantly different from the OS (control) within groups ($p > 0.05$), but it was different between groups when comparing day 0 with the following timepoints ($p < 0.05$). Nevertheless, the mean IOP of both eyes remained within the physiological range during the whole study, with a minimum IOP of 11 mmHg and a maximum of 22 mmHg (Figure 26).

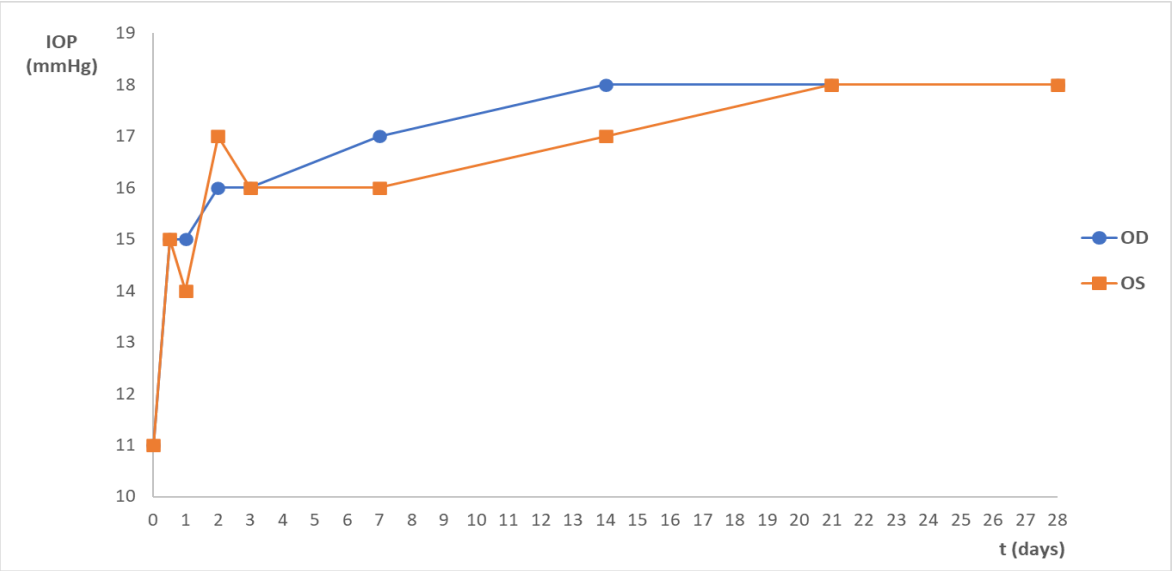

Figure 26: Mean IOP (mmHg) variation during the study after the subconjunctival administration of the nanoparticles. Data represent all groups.

4.4.2. Hematocrit

The hematocrit of rats was not affected by the subconjunctival administration of the nanoformulation. Considering all animals, the mean microhematocrit before the nanoparticles administration was 44.3 ± 3.1%, and after the administration (before euthanasia), it was 44.8 ± 3.6%. As shown in table 13, no statistically significant differences were detected in hematocrit values before and after subconjunctival administration ($p > 0.05$), so no significant influence in erythropoiesis was observed as an EPOβ side effect. There were significant statistical differences between groups ($p < 0.05$), which were considered physiological variability as the results were within reference values.

Table 13: Each group's hematocrit (Htc) was obtained from the microhematocrit measurement before and after the CS/HA-EPOβ nanoparticles administration (mean ± SD; %). After–before euthanasia.

		Group A (12 h)	Group B (1 day)	Group C (3 days)	Group D (7 days)	Group E (14 days)	Group F (21 days)	Group G (28 days)
Htc (%)	Before	42.0 ± 1.0	48.0 ± 2.6	47.0 ± 1.7	44.0 ± 2.6	42.7 ± 2.5	42.3 ± 2.5	45.5 ± 2.6
	After	42.7 ± 1.5	49.0 ± 2.6	47.7 ± 3.2	44.3 ± 4.0	42.7 ± 2.1	42.3 ± 2.5	45.4 ± 2.8

4.4.3. Electroretinography

Assessment of the retinal function was achieved by flash ERG, in which the curves and the amplitudes of the a-wave and the b-wave (mean ± SD [min; max]) were analyzed. All groups (from A to F) showed a similar retinal response in both eyes (OU) before and after the subconjunctival administration of the CS/HA-EPOβ nanoparticles. Also, there were no significant differences between the OD and the OS in the different parts of the ERG exam. At the end of the scotopic luminescence response (SLR) with 5 dB of light intensity, before the CS/HA-EPOβ nanoparticles administration, the mean a-wave of the OD was 236 ± 75 [110; 375] μV and the b-wave was 619 ± 147 [379; 1010] μV. After the administration, the OD showed a mean a-wave of 219 ± 62 [110; 311] μV and a mean b-wave of 569 ± 119 [349; 831] μV. No statistically significant differences ($p > 0.05$) were found between the mean amplitudes of the a and b waves of the OD before and after the administration. Concerning the OS, again no significant differences ($p > 0.05$) were detected before (a-wave: 239 ± 68 [114; 346] μV; b-wave: 600 ± 137 [349; 859] μV) and after (a-wave: 228 ± 61 [114; 323] μV; b-wave: 624 ± 118 [391; 844] μV) the administrations, or between OS and OD, at any timepoint. Figure 27 illustrates the variation of the a and b waves according to light stimuli, and both waves increased their amplitude when the light intensity increased. Figure 28 is a real representation of the SLR.

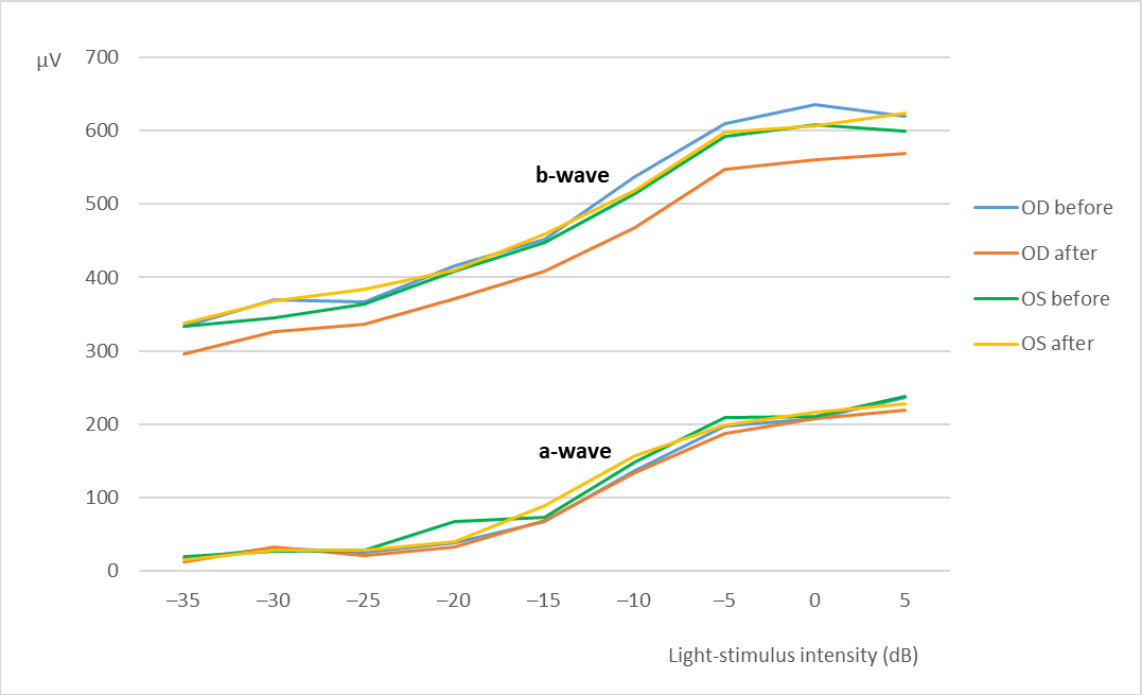

Figure 27: Scotopic luminesce response-mean amplitudes of the a-wave and the b-wave (μV) recorded from the OD and OS in response to increscent light-stimulus intensities (dB). Values correspond to

before and after the administration of the nanoparticles (after = before euthanasia). Data represent all groups.

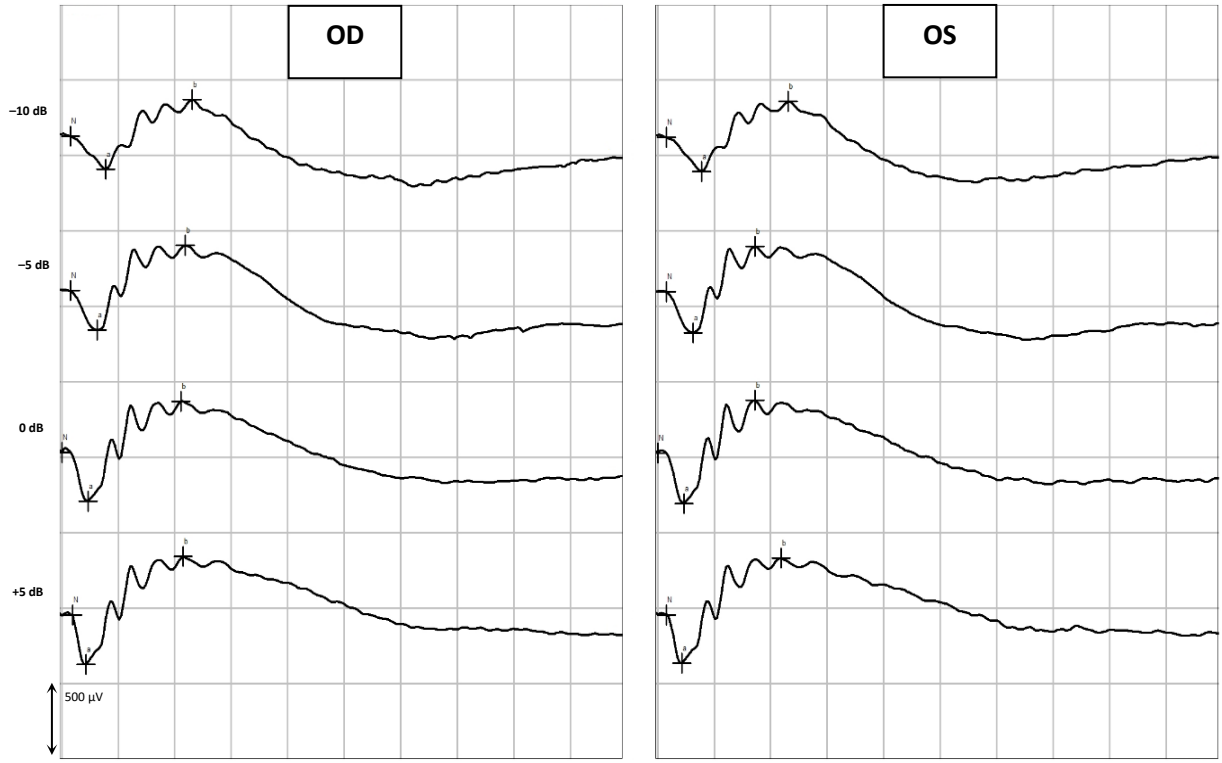

Figure 28: Example of the scotopic luminesce response. The retinal response was recorded from the OD and OS of a rat (group C) before euthanasia in response to crescent light-stimulus intensities (in this example, from –10 dB to +5 dB).

The photopic adaptation (PA) results are shown in table 14 and reveal no statistically significant difference ($p > 0.05$) between treated and control eyes and among the groups. At 16 min of light adaptation, the mean wave amplitudes for the OD before the administration was 16 ± 12 [2; 37] µV for the a-wave and 200 ± 40 [135; 264] µV for the b-wave, and after the administration, it was 16 ± 11 [1; 35] µV for the a-wave and 212 ± 44 [107; 294] µV for the b-wave. Regarding the OS, the mean a-wave before administration was 19 ± 14 [3; 39] µV and the b-wave was 201 ± 44 [135; 294] µV, and after the administration, it corresponded to 18 ± 12 [1; 37] µV for the a-wave and to 201 ± 46 [117; 294] µV for the b-wave. Waves did not seem to increase or decrease with light stimuli.

Table 14: Photopic adaptation-mean amplitudes of the a-wave and the b-wave (μV) recorded from the OD and OS in response to light-stimuli at 0, 2, 4, 8, and 16 min of light adaptation. Values correspond to before and after the administration of the nanoparticles

		a-wave (μV)		b-wave (μV)	
	min	**OD**	**OS**	**OD**	**OS**
Before	0	19 ± 12	16 ± 13	212 ± 36	211 ± 59
	2	20 ± 16	20 ± 13	201 ± 36	193 ± 43
	4	13 ± 12	14 ± 11	198 ± 50	199 ± 44
	8	18 ± 16	17 ± 12	202 ± 46	214 ± 53
	16	16 ± 12	19 ± 14	200 ± 40	201 ± 44
After	0	19 ± 18	21 ± 18	216 ± 45	213 ± 52
	2	20 ± 14	19 ± 12	204 ± 38	193 ± 41
	4	14 ± 11	20 ± 18	214 ± 48	192 ± 37
	8	16 ± 9	16 ± 14	208 ± 42	202 ± 47
	16	16 ± 11	18 ± 12	212 ± 44	201 ± 46

The results of the photopic luminescence response (PLR) are illustrated in figure 29, where the b-wave clearly increases with light intensity, unlike the a-wave, whose amplitudes maintained somewhat constant. Nevertheless, mean amplitudes of a and b waves were similar before and after the administration of the nanoparticles, for the OD and OS, and between OD and OS, in all groups. At 5 dB of light intensity, before the administration of the nanoparticles, the OD presented a-wave of 16 ± 13 [5; 51] μV and b-wave of 224 ± 50 [99; 315] μV, while the OS had a-wave of 16 ± 14 [3; 59] μV and a b-wave of 229 ± 42 [167; 343] μV. After the administration, the a-wave and b-wave were, respectively, 14 ± 6 [3; 29] μV and 212 ± 54 [100; 343] μV for the OD; and 14 ± 15 [3; 60] μV and 205 ± 53 [115; 333] μV for the OS. Thus, no statistically significant differences ($p > 0.05$) were observed among those results.

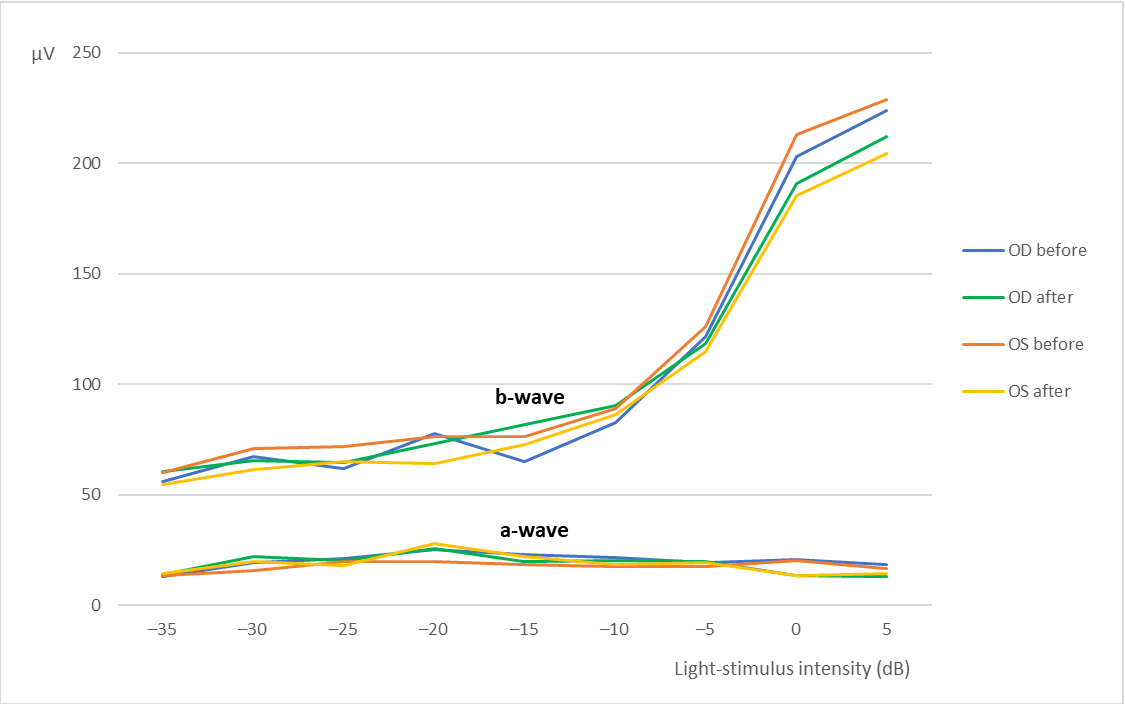

Figure 29: Photopic luminesce response-mean amplitudes of the a-wave and the b-wave (µV) recorded from the OD and OS in response to increscent light-stimulus intensities (dB). Values correspond to before and after the administration of the nanoparticles (after – before euthanasia). Data represent all groups.

Photopic flicker (PF) results have a graphic representation in figure 30. Before the administration of the nanoparticles, after 10 min of light exposure, the a and b waves recorded at 0 dB were, respectively, 6 ± 4 [1; 13] µV and 227 ± 61 [108; 353] µV for the OD; and 8 ± 4 [3; 18] µV and 227 ± 44 [177; 354] µV for the OS. After the administration, the OD had a-wave of 6 ± 3 [1; 12] µV and b-wave of 229 ± 59 [111; 338] µV; and the OS had a-wave of 6 ± 3 [2; 14] µV and b-wave of 234 ± 43 [139; 318] µV. Differences in these results were not statistically significant ($p > 0.05$). While the b-wave tends to decrease with the decreasing light stimuli, the a-wave tends to increase.

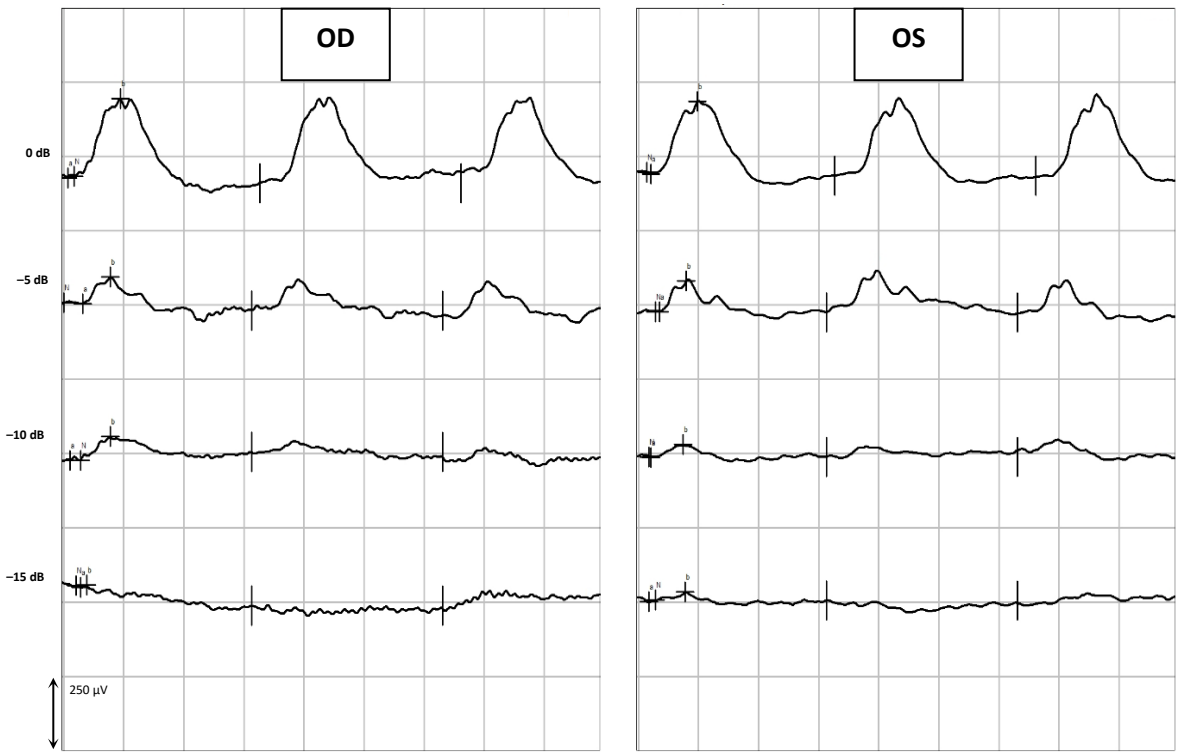

Figure 30: Example of a photopic flicker exam. The retinal response was recorded from the OD and OS of a rat (group D) before euthanasia in response to decrescent light-stimulus intensities (from 0 dB to –15 dB), after 10 min of continuous light exposure.

The last part of the ERG exam was the scotopic adaptation (SA), whose results are presented in figure 31, while figure 32 shows an example of a SA curve. The longer the dark adaptation, the more the retina appears to respond to light stimuli, as both a and b waves show a tendency to increase with time. That behavior was observed in all groups. At the end of the SA (32 min), the OD before the administration had a mean a-wave of 111 ± 33 [53; 170] µV and a b-wave of 398 ± 60 [303; 514] µV; while after the administration, the a and b waves of the OD were 92 ± 37 [43; 145] µV and 425 ± 60 [307; 510] µV, respectively. At the same time, the OS a and b wave values were, respectively, 93 ± 33 [52; 171] µV and 407 ± 72 [239; 532] µV before administration; and 97 ± 35 [56; 169] µV and 422 ± 56 [309; 499] µV after administration. No statistically significant differences ($p > 0.05$) were detected between OD and OS before and after the administration of the CS/HA-EPOβ.

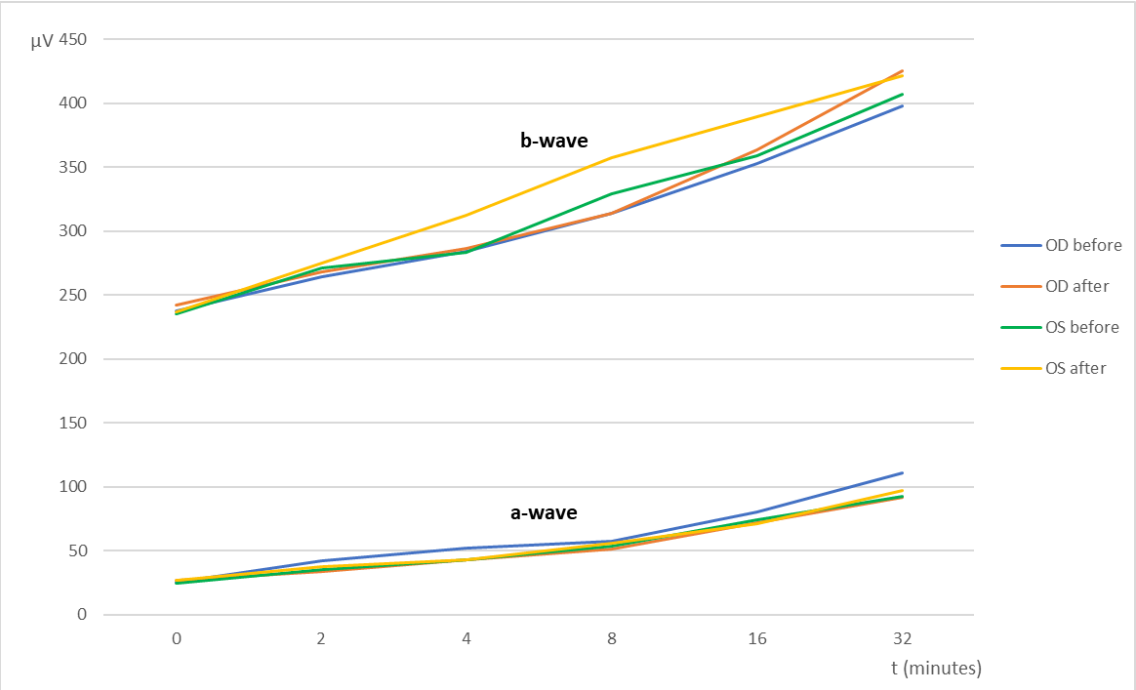

Figure 31: Scotopic Adaptation-mean amplitudes of the a-wave and the b-wave (µV) recorded from the OD and OS in response to light-stimulus after t minutes of dark adaptation (from 0 to 32 min). Values correspond to before and after the administration of the nanoparticles (after – before euthanasia). Data represent all groups.

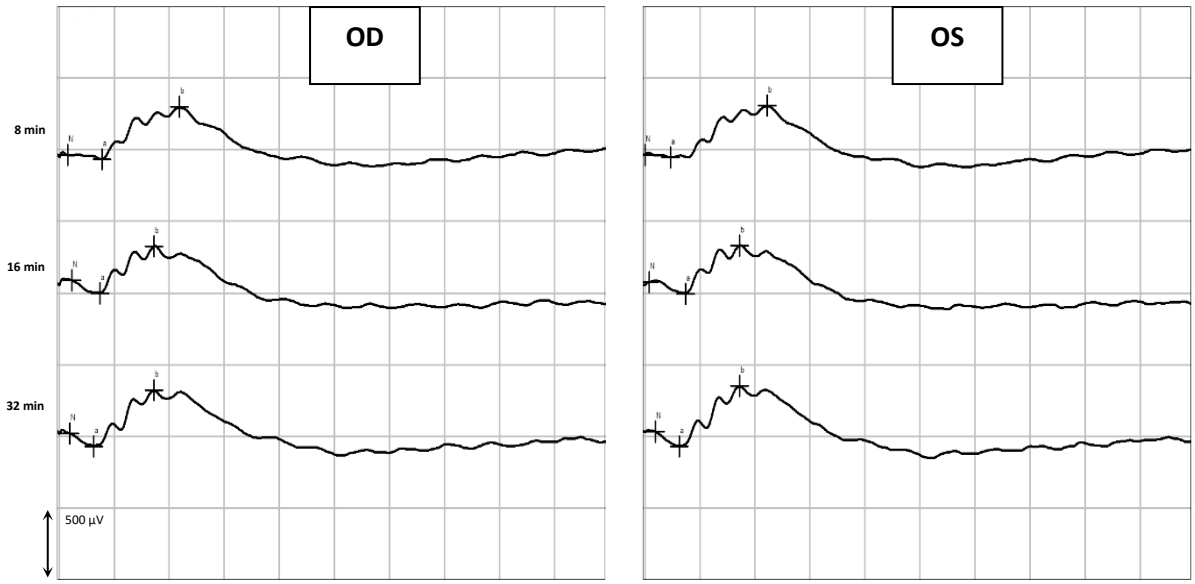

Figure 32: Example of a Scotopic Adaptation exam. The retinal response was recorded from the OD and the OS of a rat (group E) before euthanasia in response to light-stimulus after 0 to 32 min of dark adaptation. This figure shows timepoints 8, 16, and 32 min.

To sum up, no statistically significant differences were detected in the ERGs before and after the subconjunctival administration of the nanoparticles or between treated and control eyes. Therefore, the CS/HA nanoformulation did not seem to have a negative influence in the retina, either with or without encapsulated EPOβ.

4.4.4. Histologic Evaluation

The last step of this study was the histologic evaluation of cross-sections of the ocular globes preserved in paraffin blocks. Immunofluorescence was performed to detect if EPOβ had reached the retinal layers while HE staining was used to evaluate the cellular structure.

Regarding the immunofluorescence findings, 12 hours after the administration of the nanoformulation (group A), we detected EPOβ in the corneal endothelium, ciliary body, posterior capsule of the lens, vitreous, sclera, and the ganglion cell layer (GCL) of the OD. From group B to group F, EPOβ was most commonly detected throughout the retinal cell layers, and secondly in the vitreous, choroid, and sclera, among other tissues. The strength and number of fluorescent signals (EPOβ) decreased with time, and at day 21 (group F), fewer fluorescent dots remained detectable. Figure 33 shows fluorescent signals corresponding to EPOβ distributed throughout the retinal layers. On day 28 (group G), no EPOβ was observed in any ocular tissue. Interestingly, Group E (14 days) revealed an unexpected number of fluorescent signals in the vitreous chamber, in comparison with previous groups, indicating a possible delay in EPOβ absorption from the subconjunctival area. Additionally, EPOβ was not detected in any of the control eyes (OS) of all groups. HepG2 cells served as positive controls (Figure 34) to guarantee the accuracy of the immunofluorescence technique.

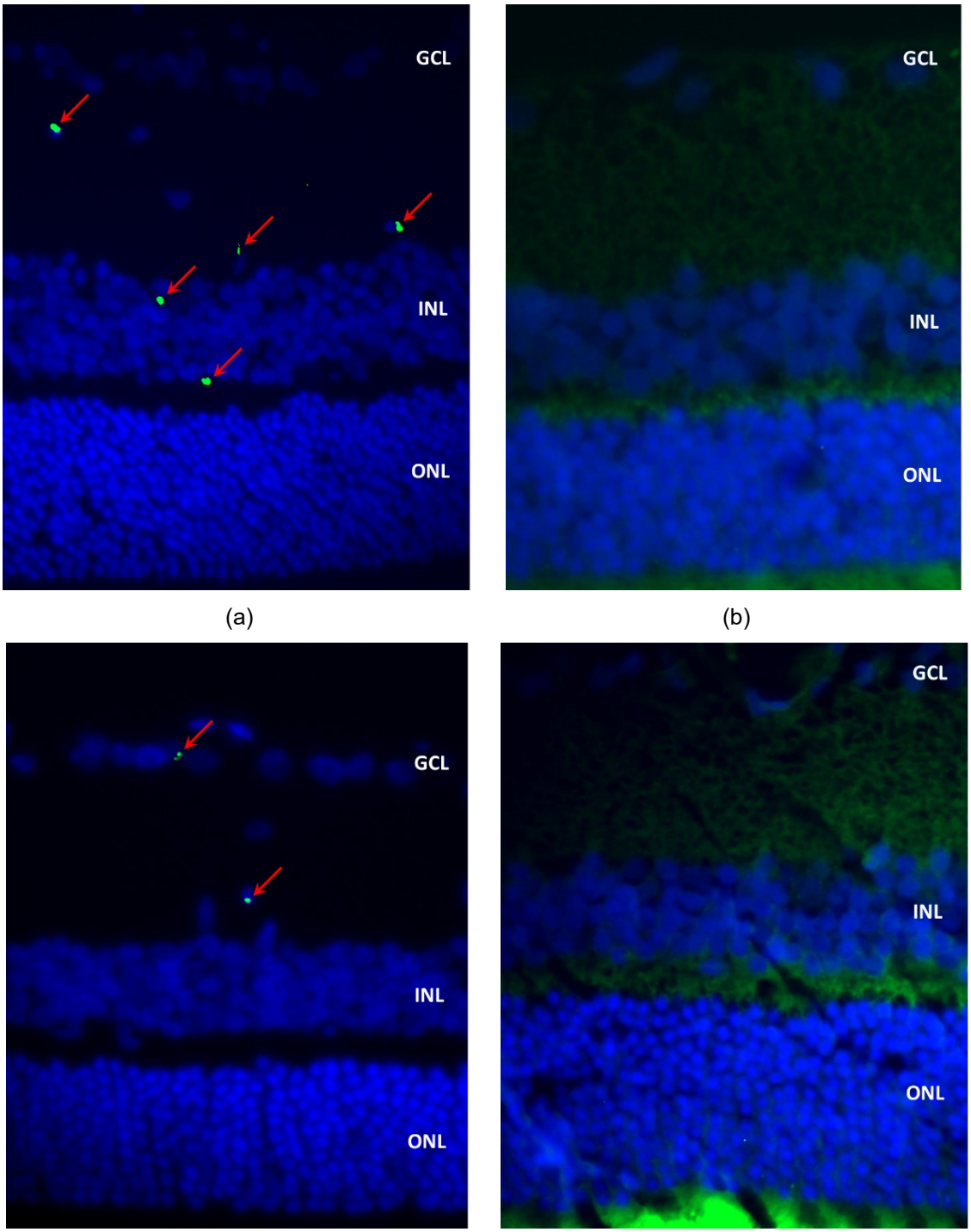

Figure 33: Immunofluorescence image showing a cross-section of the retina after CS/HA-EPOβ administration: (a) OD from group A; (b) OS from group A (control); (c) OD from group F; (d) OS from group F (control). Green and blue channels were merged, and green tissue auto-fluorescence is visible in (b) and (d). Red arrows indicate EPOβ and cell nuclei are blue (DAPI) (40×). GCL, ganglion cell layer; INL, inner nuclear layer; ONL, outer nuclear layer.

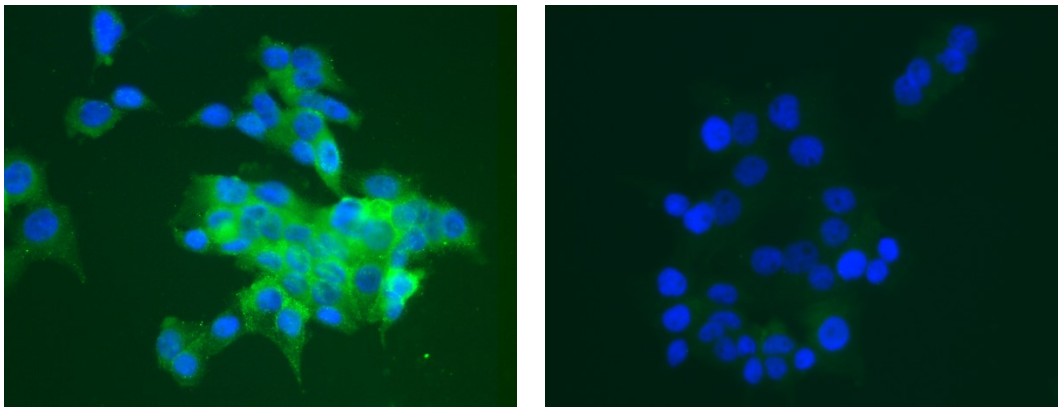

(a) (b)

Figure 34: Immunofluorescence image of the HepG2 cells: (a) positive control showing EPO in green and nuclei in blue; (b) negative control showing a very light green (auto-fluorescence) surrounding the nuclei in blue. Green and blue channels were merged (40×).

Regarding the cellular structural evaluation through the HE staining, no signs of cellular damage or morphology changes were observed, and no differences were detected between the OD and the OS in any group. Figure 35 represents the microscopic view of OD ocular tissues stained with HE, including the retina, in more detail.

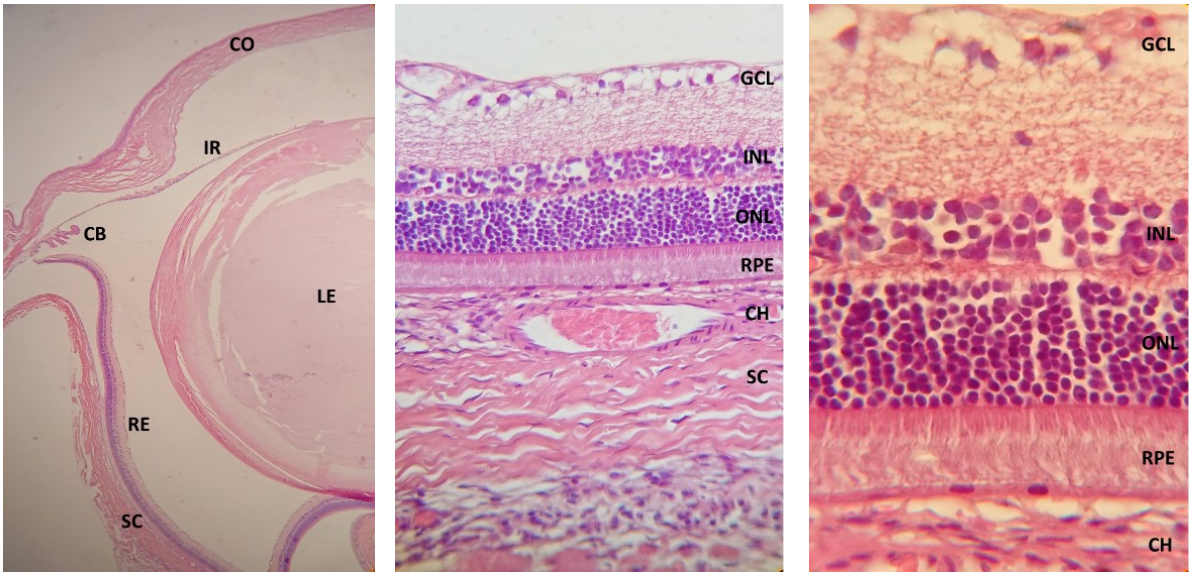

(a) (b) (c)

Figure 35: Photomicrographs of the treated eye cross-sections after CS/HA-EPOβ administration stained with hematoxylin and eosin: (a) ocular globe from group C (magnification 4×); CO, cornea; IR, iris; CB, ciliary body; LE, lens; RE, retina; SC, sclera. (b) cross-section from a rat's retina from group D (magnification 40×); CH, choroid; GCL, ganglion cell layer; INL, inner nuclear layer; ONL, outer nuclear layer; RPE, retinal pigment epithelium. (c) cross-section from a rat's retina from group E (magnification 100×).

4.5. Discussion

Chitosan and hyaluronic acid are well-known polymers with remarkable mucoadhesive characteristics, along with excellent biocompatibility and versatility in use (Peter MG 1995; De Campos et al. 2001; Thanou et al. 2001; Wadhwa et al. 2010; Rah 2011; Bernkop-Schnürch and Dünnhaupt 2012; Graça et al. 2018; Silva et al. 2021). Our team already described CS/HA nanoparticles carrying EPOβ designed for ocular use, and the empty nanoparticles presented size of 300 ± 6 nm; polydispersity index (PDI) of 0.219 ± 0.043; and zeta potential (ZP) of 33 ± 1 mV. Nanoparticles with 1000 IU of EPOβ were not significantly different from empty nanoparticles in terms of size (289 ± 3 nm), PDI (0.126 ± 0.085), and ZP (39 ± 1 mV), and they were noncytotoxic for both ARPE-19 and HaCaT cells. The CS/HA-EPOβ nanoparticles *in vitro* release in simulated tear fluid (37 °C, pH 7.4) showed that 60–70% of the EPOβ was released within the first 15 min, followed by sustained release of about 90% within 6 hours. Moreover, the drug loading was 17.4 ± 0.1%, and the encapsulation efficiency was 38.4 ± 0.3% (Silva et al. 2020).

EPOβ, a recombinant human EPO, was chosen as an active principle due to its potential neuroprotective and neuroregenerative qualities, with the perspective of helping in glaucoma treatment. A recent review article describes the antiapoptotic, angiogenic, anti-inflammatory, antioxidant, and neuroprotective effects of EPO in the ocular tissues, including the retina (Feizi et al. 2021). Subconjunctival administration of EPOβ in solution (NeoRecormon®) in rats was already performed by our team, which proved that EPOβ reached the inner layers of the retina with one single dose (Resende et al. 2013; Resende et al. 2016; Resende et al. 2018). Due to the minor-invasive nature of this route of administration, it was selected to administer CS/HA-EPOβ nanoparticles to rats to assess its safety and ocular penetration in healthy animals.

Considering the results, one day after the administration, 3 rats showed a bilateral discrete reddish discharge in the ocular medial canthus, with no other ocular signs of disease. Chromodacryorrhea is the excessive production of porphyrin-pigmented tears secreted by the harderian gland (Mans and Donnelly 2013). It can be due to stress and considering the small amount of discharge presented and the fact that it disappeared after one day, this ocular sign was not considered relevant. Animals presented normal behavior and normal ophthalmological examinations in both eyes. The variations in IOP values after the subconjunctival administration shown in Figure 26 were between the physiological range, according to the literature (Wang et al. 2005), and no significant differences were observed between the OD and the OS. On day 0, IOP was measured when the animals were still anesthetized, which justifies the lower IOP values when compared with the following time points. These findings denote the high tolerance and safety of the nanoformulation.

It is known that EPO stimulates red blood cell production in bone marrow (Abri Aghdam et al. 2016). Although it was reported that EPOβ did not alter the hematocrit of rats when administered by the subconjunctival route (Resende et al. 2013), in this study, EPOβ is coated with chitosan and hyaluronic acid, and there were no reports until the moment on how these substances would interact together. Thus, the microhematocrit assessment was necessary to evaluate the systemic impact of subconjunctival CS/HA-EPOβ nanoparticles. No statistically significant differences ($p > 0.05$) were detected in the mean hematocrit values before and after the subconjunctival administration, which was around 45% (Table 13). Although differences in the mean values between groups existed, it was attributed to individual variability. Hematocrit results were within the physiological range, which is between 45 ± 6% and 50 ± 2% for rats with 6 to 12 months old (Jacob Filho et al. 2018), which exclude a significant influence of CS/HA-EPOβ nanoparticles in erythropoiesis.

Flash ERG is the recommended procedure to evaluate retinal function in rats. The recorded waveforms following light stimulation represent a range of cell responses (Weymouth and Vingrys 2008). Photoreceptors' hyperpolarization is shown as a negative deflection following the flash onset, and it is called an a-wave (Rosolen et al. 2005). Under photopic conditions, a-wave represents cone function, and under scotopic conditions, it indicates rod function (Skaat et al. 2011). The b-wave is a positive wave that represents the activity of the bipolar and Müller cells (Rosolen et al. 2005). Figures 28, 30, and 32 are good ERG examples retrieved from our assays, where no statistically significant differences were found between treated and control eyes. Although protocols from other studies may differ from ours, both the photopic and the scotopic ERGs recorded in this study have comparable waveforms, in terms of shape and amplitude, to those described in the literature for healthy albino rats (Rosolen et al. 2005; An et al. 2012). The mean a and b waves of the SLR and the SA were comparable to the scotopic ERG results of a study that utilized silver electrodes and the Ganzfeld stimulator (Bayer et al. 2001). The same study performed light-adapted ERG, and the mean b-waves were similar to our PA results. A-wave amplitudes in the PLR were quite constant while b-waves increased, which matches what is described in the literature, as the a-wave cannot be produced when the stimulus exceeds a certain intensity (Green 1973). Regarding PF, our results showed similarities to those found in the literature (An et al. 2012), which indicates that cone function was preserved. Considering the totality of the ERG results, no influence of the CS/HA-EPOβ nanoparticles was detected in retinal cells electrophysiological responses, which corroborates the local safety of this nanoformulation.

Immunofluorescence was effective in detecting EPOβ in ocular tissues. The fluorescent signal in the treated eye (OD) became gradually weaker and was completely absent at the end of the study (28 days). It is clear that CS/HA nanoparticles administered by the subconjunctival route efficiently delivered EPOβ to the retina. The nanoparticles allowed EPOβ to trespass the

outer layers of the ocular globe to reach the inner layers after only 12 hours. This fast delivery to the retina might be attributed to the hydrophilic nature of EPOβ, due to its high degree of glycosylation (Cowper et al. 2020), which means that the preferential route of EPOβ absorption would be the conjunctival-scleral pathway, as it is more successful to the posterior segment delivery (Hosoya et al. 2005). In previous studies, EPOβ was also detected in the retina after subconjunctival administration of a commercial solution (NeoRecormon®) (Resende et al. 2013; Resende et al. 2016). Moreover, in this study, EPOβ was likewise detected in the corneal endothelium and ciliary body, and the conjunctival-scleral absorption would be unlikely to contribute to this finding due to the presence of the blood-aqueous barrier (Nayak and Misra 2018). Possibly, EPOβ reached the anterior ocular tissues coming from the corneal pathway due to some amount of nanoformulation that overflew from the subconjunctival bubble. This means that EPOβ could diffuse from the CS/HA nanoparticles and trespass the cornea, which is in accordance with our previous *ex vivo* results using porcine ocular tissues (Silva et al. 2020). Another study from our team had already demonstrated *ex vivo* corneal permeability to EPOβ using a commercial aqueous solution (NeoRecormon®) (Resende et al. 2017).

Another interesting result was that a larger number of fluorescent signals were observed in the vitreous chamber on day 14 compared to previous time points. Considering the high mucoadhesive strength of CS/HA nanoparticles and the corneal permeation due to the formulation's overflow from the conjunctiva, it would be plausible to deduce that nanoformulation remained in the subconjunctival area and/or in the cornea and enabled a delayed EPOβ permeation. A smooth fluorescent signal was still present at day 21 after the subconjunctival administration, indicating that EPOβ could have a mid-term therapeutic effect with one single dose of 1000 IU. A long-term effect would probably require additional administrations of CS/HA-EPOβ because no EPOβ was detected on day 28 after the administration. As no cellular damage or structural modifications were detected by observing ocular cross-sections stained with HE, and no differences were observed between test and control eyes, the safety of the CS/HA nanoparticles with and without EPOβ is sustained, as already verified in our previous *in vitro* studies (Silva et al. 2020). Besides, it also indicates that EPOβ is safe when administered by the subconjunctival route using this formulation. The safety of the subconjunctival sole administration of EPO solution has already been demonstrated (Resende et al. 2013; Resende et al. 2016).

In conclusion, CS/HA nanoparticles are an innovative ocular delivery system for EPOβ that was considered biologically safe since they did not cause any local or systemic adverse side effects. These nanoparticles allowed for a sustained EPOβ retinal delivery during 21 days using a minor invasive route of administration. This nanoformulation could target neuroprotection in cases of retinal diseases such as glaucoma and other retinopathies. Further

research to assess EPOβ pharmacokinetics and pharmacodynamics after ocular administration should also be considered.

CHAPTER 5

Topical ocular delivery of epoetin beta in nanoparticles: *in vivo* study using Wistar Hannover rats

B. Silva, L. Gonçalves, B. São Braz, E. Delgado. Topical ocular delivery of nanoparticles with epoetin beta in Wistar Hannover rats. Sci Rep 13, 1559 (2023). https://doi.org/10.1038/s41598-023-28845-0.

5.1. Abstract

Epoetin beta (EPOβ) as a neuroprotective agent in glaucoma has been recently under research. This study explores the potential delivery of EPOβ in chitosan-hyaluronic acid (CS/HA-EPOβ) nanoparticles to the posterior segment of the eye by topical route of administration. Nanoparticles' physicochemical characteristics were already published. Complete ophthalmological examinations, followed by electroretinography, and microhematocrit evaluations, were performed in Wistar Hannover rats (n=18), before and after the topical administration of the nanoparticles. The right eye (OD) received CS/HA-EPOβ, and the left eye received CS/HA without EPOβ (control). Animals were split into 6 groups and at designated timepoints, all animals from each group (n=3) were euthanized and both eyes were enucleated. Immunofluorescence staining was performed afterwards. After the topical administration, results show no effect in microhematocrits (≈ 45%) nor in electroretinographies, in both photopic and scotopic tests, and no adverse ocular signs. During the study, intraocular pressure (IOP) of both eyes was between 11 and 22 mmHg, with no abnormal fluctuations. Immunofluorescence enabled the identification of EPOβ in ocular tissues, which was detected in the retina by 12 hours after the topical administration and was still detectable until day 21. In conclusion, CS/HA nanoparticles could efficiently deliver EPOβ into the retina of Wistar Hannover rats through topical instillation and they were considered biologically safe. Considering that glaucoma is a neurodegenerative disease and present therapeutic is based on IOP management only, CS/HA-EPOβ nanoformulation could be a feasible neuroprotective adjuvant in glaucoma treatment, and the topical administration would be valuable to increase long-term patients' compliance.

5.2. Introduction

Glaucoma is a neurodegenerative disease that is one of the leading causes of blindness worldwide. The use of neuroprotective drugs targeting the retina as part of the glaucoma treatment has been a compelling field of study (Vidal-Sanz et al. 2012). It is known that erythropoietin (EPO) acts like a protective agent in organs and tissues, such as the brain, the heart, the inner ear and the retina, and the recombinant forms of EPO, like epoetin beta (EPOβ), are currently of great interest in ophthalmology research (Luo et al. 2015). EPOβ has revealed beneficial effects in the retina of rats with glaucoma after subconjunctival administration (Resende et al. 2018). Recently, our team developed chitosan-hyaluronic acid nanoparticles conceived to carry EPOβ into the ocular medium (Silva et al. 2020) and already tested this nanoformulation in Wistar Hannover rats by subconjunctival administration (Silva et al. 2022). Topical administration of EPOβ would be a very interesting approach because it has never been tested and has the advantages of being user friendly and potentially lead to fewer side effects than other routes of administration. When considering the treatment of posterior ocular segment diseases, intravitreal, systemic, and subconjunctival routes of administration are usual choices. However, intravitreal injection is an invasive procedure and it is related to side effects like intraocular haemorrhage, endophthalmitis, cataracts, vitreous detachment, increased intraocular pressure (IOP) and retinal toxicity (Varela-Fernández et al. 2020). Subconjunctival administration is less invasive and have minor side effects (Ranta and Urtti 2006) but patients cooperation and/or a light sedation are still required. Systemic administration demands high drug doses which may result in critical secondary effects (Varela-Fernández et al. 2020). Therefore, despite mechanisms like blinking, nasolacrimal drainage and tear turnover, that hinder drugs permeation through ocular tissues, topical instillation of drugs targeting the posterior ocular segment is an expanding area of research (De Campos et al. 2004; Nayak and Misra 2018).

Mucoadhesive nanoparticles are a way of enhancing drugs permeation across biological ocular barriers, while protecting them from the ocular environment, therefore increasing drugs intraocular concentration and bioavailability. They play an important role as vehicles in topical ocular administration, due to their connection with the ocular mucosa (Ameeduzzafar et al. 2016). Chitosan is a mucoadhesive natural polymer with cationic nature, that establish ionic interactions with the negatively charged ocular mucosa and also widen the tight junctions of the cell membranes (De Campos et al. 2001; Thanou et al. 2001; De Campos et al. 2004; Bernkop-Schnürch and Dünnhaupt 2012). Recent studies using chitosan based nanoparticles, applied by topical route of administration in rats/ rabbits, observed a greater permanence of the nanoparticles on the ocular surface (Yu et al. 2020; Varela-Fernández et al. 2021), and also a higher therapeutic activity (anti-inflammatory/ antimicrobial) than the

control formulations (Alqurshi et al. 2019; Bin-Jumah et al. 2020). Thus, chitosan can increase drugs pre-corneal retention time, which might reduce the frequency of the administration and improve patients compliance (De Campos et al. 2001; Bernkop-Schnürch and Dünnhaupt 2012; Silva et al. 2021). In addition, chitosan mucoadhesiveness can be enhanced by association with hyaluronic acid, which is a natural polymer found in ocular tissues like vitreous, lacrimal gland, conjunctiva, corneal epithelium and also in human tears (Rah 2011). Hyaluronic acid is widely used in ophthalmic formulations due to its viscoelasticity and mucoadhesiveness associated to CD44 receptors located in corneal epithelium and endothelium (Wadhwa et al. 2010; Guter and Breunig 2017; Graça et al. 2018). Being so, chitosan-hyaluronic acid nanoparticles are able to improve drugs retention time on ocular surface when and their penetration through the ocular tissues, potentially increasing their bioavailability (Silva et al. 2021).

The nanoparticulate system of chitosan-hyaluronic acid-epoetin beta (CS/HA-EPOβ) created by our team was already analyzed in terms of physicochemical stability, cytotoxicity and mucoadhesive strength by *in vitro* and *ex vivo* tests (Silva et al. 2020). In the present study, we aimed to explore the biological impact of this nanoformulation in healthy Wistar Hanover rats, using the topical ocular route of administration. We proposed to evaluate the *in vivo* tolerance, safety, systemic and local impacts, the effect in the retinal electrophysiology, and the EPOβ ocular distribution by immunohistochemistry. Our team is committed to pursuit this promising line of research by using CS/HA-EPOβ nanoparticles as a non-invasive neuroprotective/ neuroregenerative co-adjuvant treatment targeting the retina of glaucomatous animals.

5.3. Materials and Methods

5.3.1. Materials

Animals used in this study were Wistar Hannover albino male rats (n=18), weighting 330±24 g, acquired from Charles River Laboratories (Saint-Germain-Nuelles, France). Ophthalmological equipment belonged to the Faculty of Veterinary Medicine (ULisboa), namely, the slit lamp (Hawk Eye®, Dioptrix, France), and the PanOptic® ophthalmoscope (WelchAllyn – Hillrom, USA), the rebound tonometer (Tonolab®, Icare, Finland) and the ERG device (RETIcom, Roland Consult, Stasche & Finger GmbH, Brandenburg, Germany). NeoRecormon® 30000 IU (RocheDiagnostics GmbH, Mannheim, Germany) was the epoetin beta (EPOβ) used in the nanoparticles. Low molecular weight chitosan (LMW CS, 100 kDa, 92% deacetylation) was purchased from Sigma Aldrich (Irvin, UK). The eye grade quality hyaluronic acid, with an average Mw of 300 kDa, from Shandong Topscience, were a kind gift

from Inquiaroma (Barcelona, Spain). Ketamine (Ketamidor® 100 mg/mL, Richter Pharma, Wels, Austria) and medetomidine (Domtor® 1mg/mL, Orion Corporation, Espoo, Finland) was used to anesthetize the animals, and atipamezole was used to revert it (Antisedan® 5 mg/mL, Zoetis, New Jersey, USA). Oxybuprocaine hydrochloride for topical anesthesia (Anestocil®, Edol, Lisbon, Portugal) and a carbomer based gel for corneal lubrification (Lubrithal®, Dechra, Northwich, United Kingdom). For euthanasia, sodium pentobarbital (Euthasol® 400 mg/mL, Animalcare Group, North Yorkshire, UK) was used. All these drugs were available in the Faculty of Veterinary Medicine (ULisboa). Epredia™ SuperFrost Plus™ Adhesion slides (ThermoFisher Scientific, Massachusetts, USA) were used to immunofluorescence assays. The cover plates, the immunostaining rack (Epredia™ Shandon™ Sequenza™, ThermoFisher Scientific, Massachusetts, USA) and the slide stainer for hematoxylin and eosin stain (Thermo Scientific™ Gemini™ AS, Massachusetts, USA) belonged to the Faculty of Veterinary Medicine (ULisboa). HepG2 human derived liver hepatocellular carcinoma cell line (ATCC® HB-8065™) was used as immunofluorescence control. All cell culture media and supplements were from Gibco (ThermoFisher Scientific, Massachusetts, USA). EPO monoclonal primary antibody 4F11 (MA5-15684) and goat anti-mouse IgG (H+L) secondary antibody DyLight 488 (35502) were from Invitrogen (ThermoFisher Scientific, Massachusetts, USA). The blocking reagent (sc-516214) and the aqueous mounting medium with DAPI (sc-2494) were from UltraCruz® (Santa Cruz Biotechnology, Texas, USA). Axioscop 40 fluorescence microscope with an Axiocam HRc camera (Carl Zeiss, Germany) belonged to the Faculty of Pharmacy (ULisboa).

5.3.2. Methods

The procedures performed in each animal (n=18) in this study were carried out in a sequence, as follows: 1st. Ophthalmological examination; 2nd. Blood collection for microhematocrit; 3rd. Electroretinography; 4th. Topical administration of the CS/HA-EPOβ nanoparticles to the OD and CS/HA empty nanoparticles to the OS; 5th. Ophthalmological examination; 6th. Blood collection for microhematocrit; 7th. Electroretinography; 8th. Euthanasia and bilateral enucleation; 9th. Histological processing and analysis. Procedures are fully described below.

Animals

Animals used in this study were Wistar Hannover male rats (n=18) which were randomly split into 6 groups of 3 animals each. Animals were housed in type IV cages (1875 cm^2 of floor area) with a stainless-steel wire cover, one group (n=3) per cage, with food pellets

and water ad libitum. The room was maintained in a 12 hours light/ darkness cycle and the temperature (20 ± 2 ºC) and the humidity (50-60%) were constantly controlled. Timepoints were selected after the topical administration of CS/HA-EPOβ nanoparticles to perform euthanasia, as follows: 12 hours (group A), 1 day (group B), 3 days (group C), 7 days (group D), 14 days (group E) and 21 days (group F). This study was performed in accordance with animal ethical requirements, and it was approved by the Organ Responsible for Animal Welfare (Órgão Responsável pelo Bem-Estar dos Animais – ORBEA) of the Faculty of Veterinary Medicine, University of Lisbon, approval date February 13, 2020, code 005/ 2020; and by the national entity General Directorate of Food and Veterinary (Direção Geral de Alimentação e Veterinária – DGAV), approval date January 8, 2021, code 0421/ 000/ 000/ 2020.

Ophthalmological examination

A complete ophthalmological examination was performed in every animal before the study, which included the biomicroscopic examination of the anterior segment with slit lamp (Hawk Eye®, Dioptrix, France), posterior segment examination with PanOptic® ophthalmoscope (WelchAllyn – Hillrom, U.S.A.) and the measurement of the IOP with rebound tonometer (Tonolab®, Icare, Finland). Complete ophthalmological examinations were also performed 1 hour, 12 hours and 1, 2, 3, 7, 14 and 21 days after the topical administration of CS/HA-EPOβ nanoparticles.

Preparation of nanoparticles

Nanoparticles were prepared before the first electroretinography. Reagents were previously sterilized by filtration in a laminar flow cabinet, using a 0.22 µm filter. Nanoparticles were also prepared in a laminar flow cabinet, to maintain their sterility, by a modified ionotropic gelation technique based on a previously described protocol (Wadhwa et al. 2010; Graça et al. 2018) and already published by our group (Silva et al. 2020). To the chitosan solution at 1 mg/mL in NaCl 0.9% was added 1000 IU of EPOβ (NeoRecormon®) in hyaluronic acid solution (1 mg/mL). The empty CS/HA nanoparticles (without EPOβ), which were used in the negative controls, were prepared following the same protocol, by adding purified water instead to EPOβ. Both the CS/HA-EPOβ and the CS/HA formulations were aspirated with sterilized insulin syringes and kept at room temperature until the topical administration.

Hematocrit

General anesthesia combining 70 mg/ kg of ketamine and 0.8 mg/ kg of medetomidine was administered intraperitonially to allow the electroretinography (ERG) procedure. Right after the anesthesia induction, a blood sample was collected from a lateral vein of the tail with a capillary tube, and then centrifuged at 10000 rpm for 5 min. Hematocrit was read using a proper scale. This was performed before the first and before the second ERG.

Electroretinography

Flash ERG essentially records rods and cones activity as a-wave and b-wave amplitudes (μV) in response to different intensities and frequencies of luminous stimuli. All animals underwent an ERG before the administration of CS/HA-EPOβ nanoparticles, to assess the previous status of the retina, and before euthanasia, to assess the outcome of the nanoparticles' topical administration. The ERG protocol was adapted from a previously published method (Rosolen et al. 2005), and a scotopic adaptation of 12 hours before the ERG exam was mandatory. General anesthesia allowed a complete immobilization of the animal. A heating pad was used to prevent hypothermia and the animal's body temperature was periodically checked. One drop of oxybuprocaine hydrochloride (Anestocil®, Edol, Lisbon, Portugal) and one drop of a carbomer based gel (Lubrithal®, Dechra, Northwich, United Kingdom) was instilled on both corneas, and on each one was placed an active electrode with a silver tip (Figure 36). Reference electrodes (blue) were placed subcutaneously on both sides of the head, so that the tip of the electrode was between the ear and lateral cantus (Figure 36). At the base of the tail, a ground electrode (black) was placed and a MiniGanzfeld was the light-stimulation device that was placed on the animal's head. The luminescence equivalency for 0 dB was 3 cds/m^2, the reference impedance was < 5 kohms and the frequency applied was between 0.1 and 1000 Hz. ERG results were independent for each eye, but they were recorded simultaneously. An ERG exam was split in five steps, with a total duration of 75 minutes. The scotopic luminance response (SLR) was the first step and consisted in delivering light flashes of nine intensities from –35 dB (–3.02 log cds/m^2) to +5 dB (0.98 log cds/m^2), three times per intensity level, at a 0.1 Hz rate. The photopic adaptation (PA) used the maximum b-wave amplitude of the SLR to calculate the intensity of the light flashes delivered after 0, 2, 4, 8 and 16 minutes of light adaptation (3 times, 1.3 Hz). Following, the photopic luminance response (PLR) used nine intensities light flashes, from –35 dB to +5 dB, delivered three times at 1.3 Hz. The photopic flicker (PF) delivered flashes of 0, –5, –10 and –15 dB, at 6.3 Hz, after 10 minutes of light adaptation. At last, the scotopic adaptation (SA) used white dim flashes delivered after 0, 2, 4, 8, 16 and 32 min of dark adaptation (3 times, 1.3 Hz). The stimulation

of the retina with dim flashes in scotopic conditions intended to test rod function, while the stimulation with bright flashes and 6.3 Hz flicker in photopic conditions was used to test cone function. The anesthesia was then reverted with atipamezole (2.5 mg/ kg) by intramuscular administration.

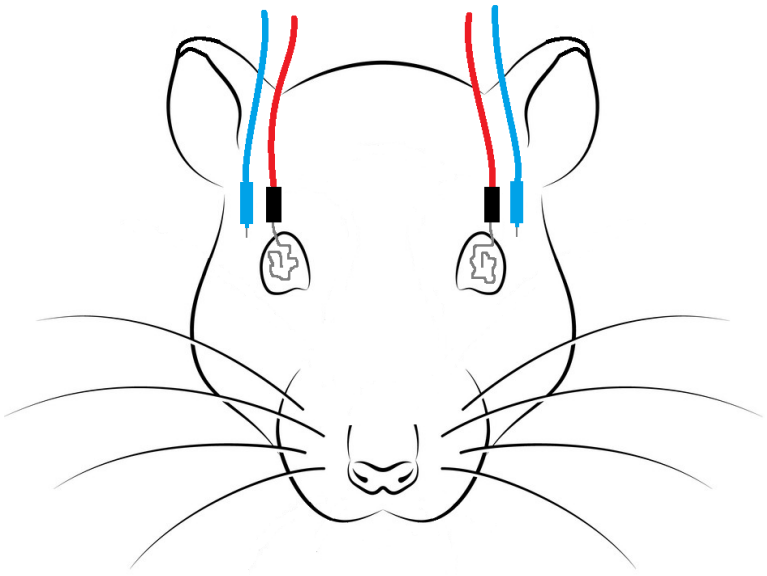

Figure 36: Representation of the ERG setup: active electrodes (red) with silver tips placed on corneas, and reference electrodes (blue) placed between the ears and the lateral canthus.

Topical administration of nanoparticles

The topical ocular administration of the nanoparticles was initiated immediately after the first ERG, at a rate of one drop every 5 minutes until a total amount of 80 µL/ eye (6 drops in average). The right eye (OD) received CS/HA-EPOβ nanoparticles corresponding to 1000 IU of EPOβ. The left eye (OS) received empty CS/HA nanoparticles (without EPOβ) and was the negative control.

Euthanasia and enucleation

At 12 hours (group A), 1 day (group B), 3 days (group C), 7 days (group D), 14 days (group E) and 21 days (group F) after the administration of the CS/HA-EPOβ formulation, euthanasia was executed in all animals of each group, immediately after the second ERG, by intraperitoneal injection of sodium pentobarbital (150 mg/kg). Both ocular globes were enucleated right after the euthanasia and the optic nerve and the lateral, medial, dorsal and ventral sides were painted with tissue dyes to facilitate the orientation for paraffin inclusion and

histological sections (Figure 37). Ocular globes were preserved in 10% (v/v) formaldehyde in PBS (0.1 M, pH 7.4) and then processed to be included in paraffin blocks.

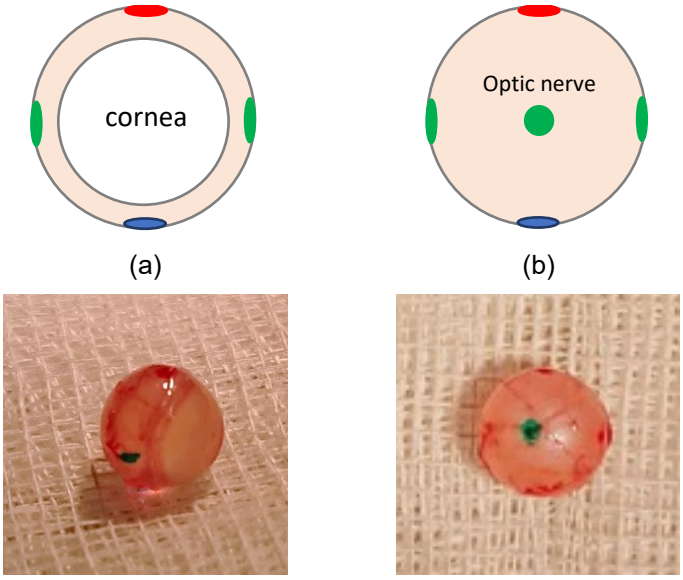

Figure 37: Representation of a rat ocular globe painted with tissue dyes: (a) frontal view; (b) caudal view. Photo of a rat ocular globe painted with tissue dyes: (c) lateral view; (d) caudal view, in green we can identify the transected optic nerve.

Histological assessment

Immunofluorescence and hematoxylin and eosin (HE) stains were performed in both ocular globes of all animals. After paraffin inclusion, 8 cross sections (3 µm) per eye were made using a microtome. Four sections were placed in adhesion slides for immunofluorescence and four sections were placed in regular slides for HE staining. All slides were put in an incubator for one hour at 60º C and then overnight at 37º C. On the following day, sections for HE were processed in the multi-tasking stainer Gemini™ AS. The immunofluorescence slides were deparaffinized in xylol for 15 min plus 5 min, and gradual rehydrated in alcohol from 100º to 70º (3 min each) and purified water (3 min + 15 min). Following, washing with Triton X-100 solution (0.1% v/v in PBS) and Tween 20 solution (0.1% v/v in PBS) was performed and then assembling of the slides in cover plates. Simultaneously, HepG2 cells (positive control) were previously in a hypoxic environment for 2 hours at 37º C and were fixed in 10% (v/v) formaldehyde in PBS in the dark for 15 min at room temperature. They were washed with Triton X-100 solution (0.1% v/v in PBS) for 5 min and then followed the same protocol as the cross sections. Sections were incubated with UltraCruz® Blocking Reagent for one hour at room temperature, followed by another washing step and incubation with EPO monoclonal primary antibody 4F11 (1:400), overnight at 4 °C. On the next day, another washing step was made with Tween 20 solution (0.1% v/v in PBS), followed by

incubation with goat anti-mouse secondary antibody DyLight 488 (1:1000) in the dark, for one hour at room temperature. After washing with PBS, slides were cautiously disassembled from the cover plates, each slide received 2-3 drops of UltraCruz® mounting medium with DAPI and was covered by a coverslip, being then sealed with varnish. The analysis of the sections was performed using an Axioscop 40 fluorescence microscope with an Axiocam HRc camera (Carl Zeiss, Germany), in which the recorded images were processed with AxioVision software (Rel.4.8.1, Carl Zeiss). The observed EPOβ fluorescence was green (OD), the negative control was the OS and the positive control to ensure, the quality of the immunofluorescence technique, were HepG2 cells.

Statistical methods

Statistical assessment was performed with GraphPad Prism version 6.0 (GraphPad Software, CA, USA) and Microsoft Office Excel (Microsoft, Washington, USA), using one-way ANOVA and t-test to detect significant differences between means. The statistical significance was 95%, which corresponds to a *p*-value of 0.05, and data was presented as mean ± standard deviation (SD).

5.4. Results

5.4.1. Ophthalmological examinations

All animals showed very good tolerance to the CS/HA nanoparticles, with EPOβ (OD) and without EPOβ (OS). After the instillation of the nanoformulation, no signs of discomfort or pain were observed, and all animals exhibited normal behavior throughout the entire study. Likewise, no abnormal ocular signs were observed, such as epiphora, blepharospasm, conjunctival hyperemia, corneal oedema or ulcerations, keratitis, etc. Therefore, ophthalmological examinations of both eyes were considered normal for all groups (n=18) after the administration of the nanoparticles.

Regarding the IOP, mean values for the OD and the OS before the topical administration were 18 ± 1 mmHg and 19 ± 2 mmHg, respectively. Figure 38 represent the mean IOP variation of both eyes after the instillation. There are statistically significant differences ($p < 0.05$) between the mean IOP measured immediately after the administration (t=0) and the IOP of the following days, from 12 hours (t=0.5) to day 7 (t=7). These differences were no longer evident at day 14 and 21. These differences were solely attributed to individual variability at the moment of the measurement, as values are comparable to the reference IOP

values for healthy conscious Wistars Hannover rats (Wang et al. 2005). Comparing the OD (treatment) and the OS (control), no statistically significant differences ($p > 0.05$) were detected between the mean IOP of both eyes in any of the groups/ timepoints, meaning that the CS/HA nanoparticles, with and without EPOβ, did not influence the ocular physiology.

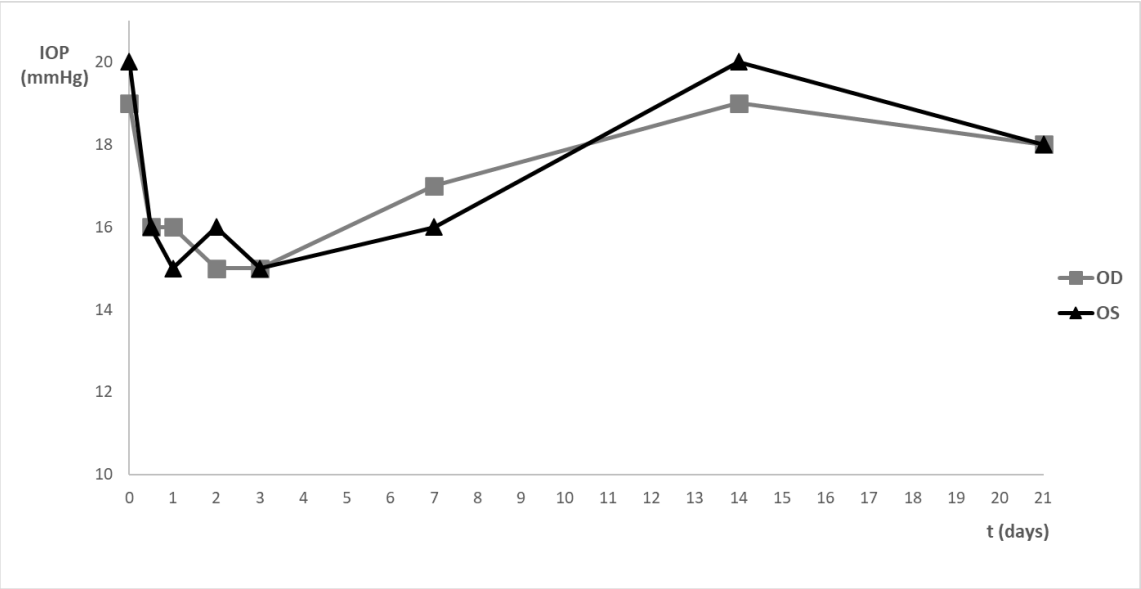

Figure 38: Variation of the mean IOP (mmHg) through time after topical administration of CS/HA-EPOβ nanoparticles to the right eye (OD) and empty CS/HA nanoparticles to the left eye (OS). Values represent all groups.

5.4.2. Hematocrit

Hematocrits of rats were stable during the entire study and were within the reference range for Wistar Hannover rats between 6 to 12 months of age (Jacob Filho et al. 2018). The mean microhematocrit before and after the topical administration of the CS/HA-EPOβ nanoparticles, were 45.3 ± 2.5% and 45.2 ± 2.8%, respectively (Figure 39). No significant variations in the microhematocrit were detected between before and after the topical administration ($p > 0.05$), which means that the impact of CS/HA-EPOβ nanoparticles in the erythropoiesis was inconsiderable.

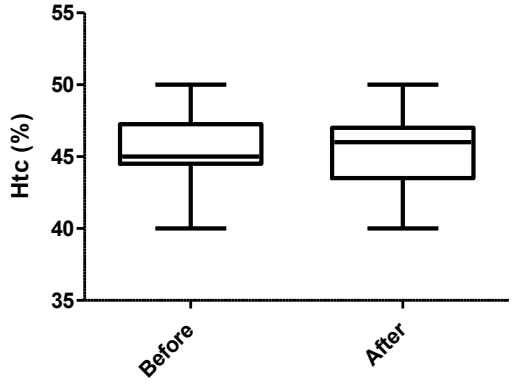

Figure 39: Hematocrit (Htc) of all groups obtained from microhematocrit measurement, before and after the topical administration of the CS/HA-EPOβ nanoparticles (mean ± SD; %). After = before euthanasia.

5.4.3. Electroretinography

Flash electroretinography (ERG) was performed to evaluate the retinal response to the CS/HA-EPOβ nanoparticulate system, in which the waveforms and the amplitudes of a and b waves were studied. Figure 40 is a plot representation of each ERG part recorded in this study, whose results are detailed described below as mean ± SD [min; max] μV.

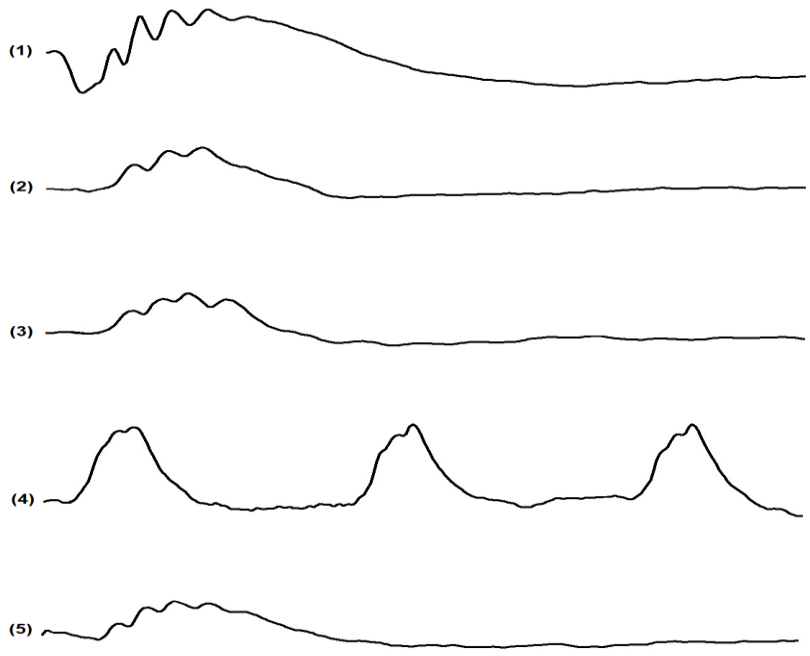

Figure 40: Example of ERG waveforms recorded in this study: (1) Scotopic luminesce response at 5 dB; (2) Photopic adaptation at 16 min; (3) Photopic luminescence response at 5 dB; (4) Photopic flicker at 0 dB; (5) Scotopic adaptation at 32 min.

In the scotopic luminescence response (SLR), the amplitudes of both a and b waves increased with light intensity. Before CS/HA-EPOβ administration, at –35 dB of light (–3.02 log cds/m^2) the a-wave was 22 ± 9 [3; 43] µV for the OD and 25 ± 17 [3; 64] µV for the OS; and the b-wave amplitude was 278 ± 83 [137; 471] µV for the OD and 288 ± 87 [151; 445] µV for the OS. At a light intensity of 5 dB (0.98 log cds/m^2), the a-wave was 268 ± 67 [159; 356] µV for the OD and 263 ± 47 [173; 323] µV for the OS; while the b-wave was 653 ± 128 [349; 858] µV for the OD and 628 ± 83 [478; 763] µV for the OS. A and b waves mean amplitudes, before and after the topical administration, were not significantly different (p > 0.05) between both eyes or among groups. For instance, after the topical administration, at 5 dB, the mean a-wave for the OD was 215 ± 79 [114; 375] µV and the b-wave was 585 ± 113 [443; 789] µV Additionally, the OS showed a mean a-wave of 247 ± 57 [159; 326] µV and a b-wave of 612 ± 103 [399; 766] µV. Figure 41 illustrates the mean a and b waves amplitudes for both the OD and the OS, considering the 9 different light intensities of the SLR.

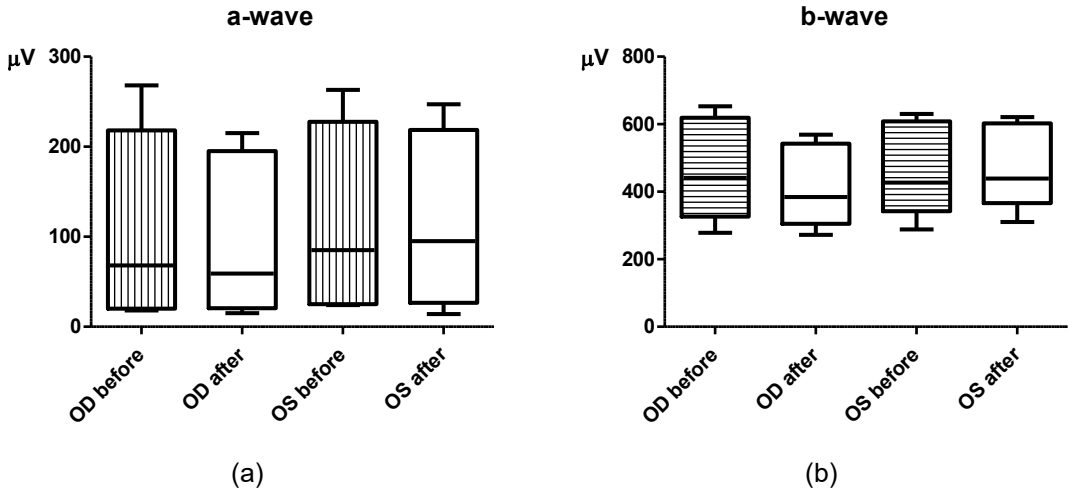

(a) (b)

Figure 41: Mean amplitudes of the a-wave (a) and b-wave (b) recorded from the OD and OS in the scotopic luminesce response, before and after topical administration of the nanoparticles (after = before euthanasia). Data is presented in µV as mean ± SD and represent all groups.

No statistically significant differences (p > 0.05) were observed in the photopic adaptation (PA) between treated (OD) and control (OS) eyes, and there were also no substantive changes among groups. At the end of this phase (16 min of light adaptation), before the administration, the OD presented mean a and b waves of 18 ± 16 [2;61] µV and 220 ± 52 [135; 312] µ, respectively. The OS had mean a-waves of 17±15 [1;54] µV and b-waves of 240 ± 59 [164; 357] µ. After the topical administration, the mean a-wave was 15 ± 12 [1; 39] µV for the OD and 17 ± 16 [2; 66] µV for the OS; while the b-wave was 200 ± 35 [145; 254] µV

for the OD and 224 ± 49 [153; 357] μV for the OS. Results in figure 42 correspond to the mean waves considering the five steps of light adaptation.

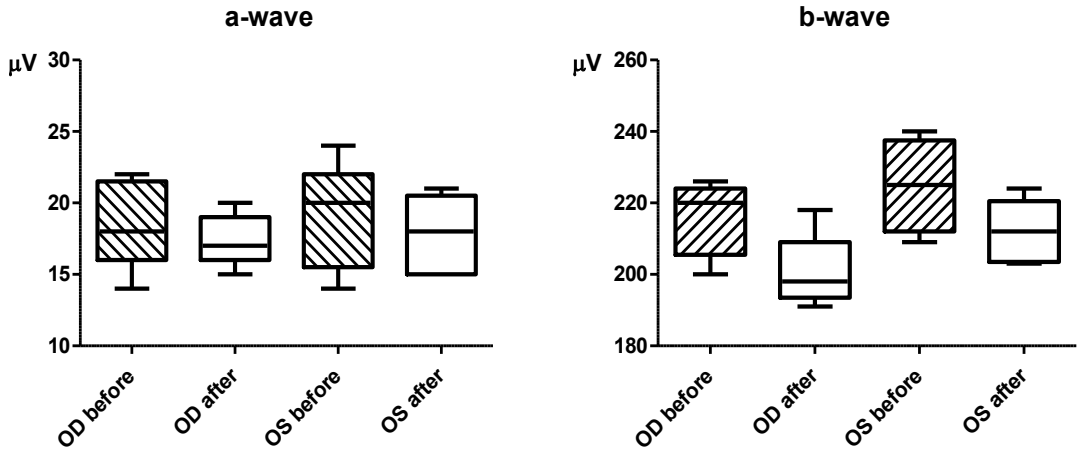

(a) (b)

Figure 42: Photopic adaptation – a (a) and b (b) waves recorded from the OD and the OS in the five phases of light adaptation (μV; mean ± SD), before and after the topical administration of the nanoparticles (after = before euthanasia). Results correspond the sum of the results from all groups.

Photopic luminescence response (PLR) results show that the b-wave amplitude increases with light intensity, while the a-wave amplitude was nearly constant (Figure 43). No statistically significant differences ($p > 0.05$) were noticed among groups or between OD and OS, as the mean amplitudes of the a-waves and b-waves were comparable before and after the topical administration of the nanoparticles. At 5 dB of light intensity, the OD showed a mean a-wave of 15 ± 14 [2; 51] μV and a b-wave of 250 ± 40 [186; 323] μV before the administration; and a-wave of 16 ± 14 [2; 58] μV and a b-wave of 222 ± 52 [124; 371] μV after the administration. On the other hand, before the administration, the OS presented a mean a-wave of 18 ± 17 [1; 60] μV and a b-wave of 231 ± 61 [99; 369] μV; and after the administration, the a-wave and b-wave were, respectively, 14 ± 12 [4; 49] μV and 218 ± 47 [111; 304] μV.

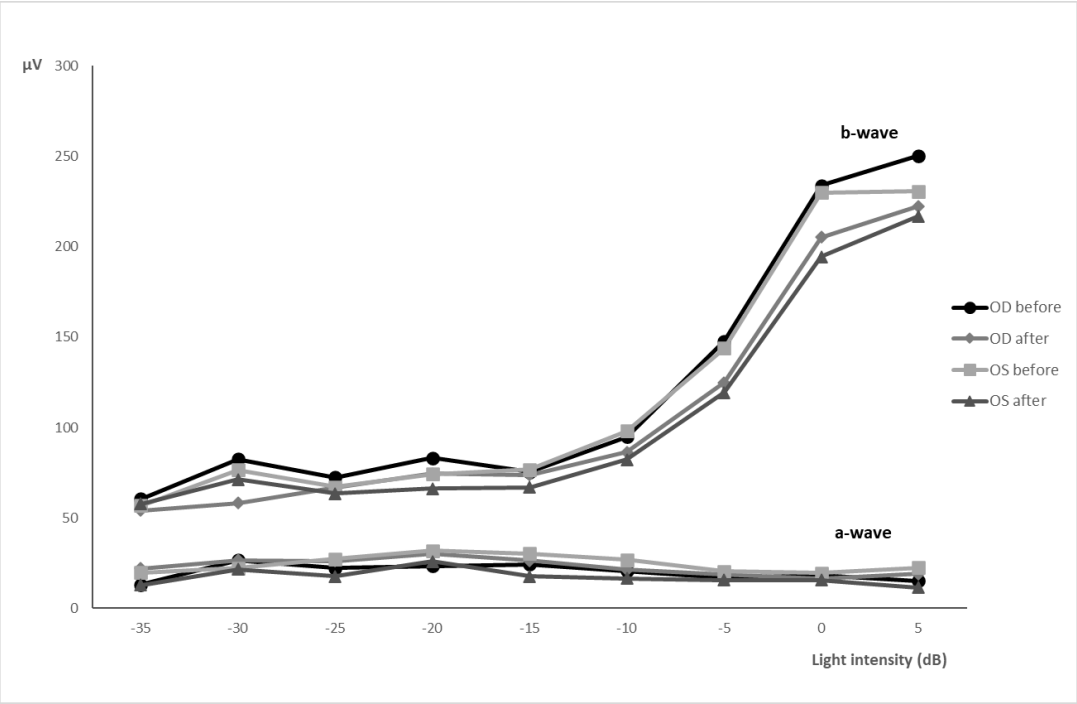

Figure 43: Representation of the a and b waves mean amplitudes recorded from the OD and OS during the photopic luminesce response, before and after the topical administration of the nanoparticles (after = before euthanasia). Data represent all groups (µV; mean ± SD).

Photopic flicker (PF) results are presented in table 15, which show no statistically significant differences ($p > 0.05$) between OD and OS, before or after topical administration. The a and b waves recorded at 0 dB, before the administration were, respectively, 6 ± 3 [2; 14] µV and 236 ± 55 [108; 348] µV for the OD; and 7±3 [3; 15] µV and 231 ± 36 [164; 294] µV for the OS. After the administration, the a and b waves were, respectively, 5 ± 4 [1; 18] µV and 230 ± 48 [148; 354] µV for the OD; and 7 ± 4 [2; 18] µV and 249 ± 69 [139; 387] µV for the OS.

Table 15: Photopic flicker-mean amplitudes of the a-wave and b-wave (µV; mean ± SD) recorded from the OD and OS in response to decrescent light-stimuli (0, –5, –10 and –15 dB). Values correspond to before and after administration of nanoparticles (after – before euthanasia). Data represent all groups.

Light (dB)	b-wave (µV)				a-wave (µV)			
	OD		OS		OD		OS	
	Before	After	Before	After	Before	After	Before	After
0	236±55	230±48	231±36	249±69	6±3	5±4	7±3	7±4
-5	127±38	135±52	130±36	121±42	18±15	16±22	15±11	18±15
-10	73±19	76±38	80±27	78±33	18±14	13±13	14±8	14±9
-15	65±38	59±45	74±53	66±42	19±11	16±12	14±8	20±13

Figure 44 represent the scotopic adaptation (SA) results, which is the last step of the ERG exam. In all groups, both a and b waves show an increase in their amplitudes (μV) after the dark adaptation period (t; minutes). At 32 minutes of dark adaptation, before the topical administration, the mean a-wave was 91 ± 43 [34; 207] μV for the OD and 87 ± 31 [46; 140] μV for the OS; while the mean b-wave was 395 ± 109 [277; 685] μV for the OD and 414 ± 67 [293; 541] μV for the OS. After the administration, the a and b wave were, respectively, 109 ± 43 [34; 198] μV and 455 ± 49 [339; 553] μV for the OD and 100±36 [53; 170] μV and 421 ± 74 [241; 532] μV for the OS. Likewise, there was no significant differences in results observed (p > 0.05) before and after the administration of the nanoparticles, and between the OD and the OS, in every group.

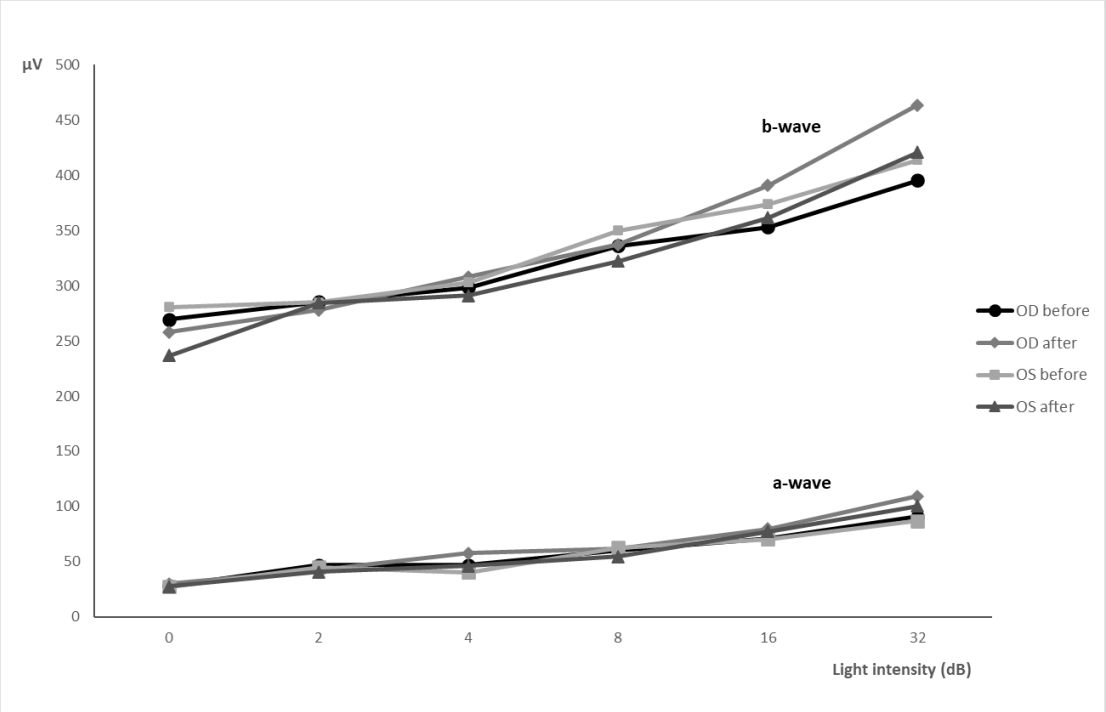

Figure 44: Scotopic Adaptation – a and b waves mean amplitudes (μV) recorded from the OD and the OS in response to light-stimuli after 0 to 32 minutes of dark adaptation (t). Data represent all groups, before and after administration of nanoparticles (after – before euthanasia).

Considering the results from the five steps of the ERG exam, the CS/HA nanoparticles with and without encapsulated EPOβdid not cause any adverse side effects in the electrical retinal activity when applied topically, because no statistically significant differences were observed between the retinal response of the OD and the OS in any group (from A to F), in any step of the ERG (p > 0.05). Also, results before and after the administration of the nanoparticles were comparable for both eyes (p > 0.05).

5.4.4. Histologic evaluation

At the end of this study, immunofluorescence was performed to evaluate EPOβ's distribution throughout the ocular globe and the hematoxylin and eosin (HE) staining was used to assess cellular structure of the ocular tissues. Immunofluorescence results show that EPOβ was detected in the retina, more precisely at the retinal ganglion cell layer, of the OD of all animals from group A, which correspond to 12 hours after the topical administration of the nanoformulation. At that specific timepoint, it was also observed EPOβ in the corneal stroma, corneal endothelium, ciliary body, posterior capsule of the lens, vitreous, sclera and retina of the OD. In the remaining timepoints, EPOβ was most frequently detected in the different retinal cell layers, followed by the vitreous, choroid and sclera. In the group E (14 days) EPOβ was still detected in the corneal stroma, denoting a sustained transcorneal permeation. The intensity and amount of fluorescent dots (EPOβ) declined with time, and at day 21 (group F) only fluorescent remnants were observed in the retina. Figure 45 shows EPOβ distributed throughout the retinal layers of group B and E, while figure 46 shows a retinal section of a control eye (OS) of group E. No EPOβ was observed in the control eyes (OS) in any of the animals. Regarding the HE staining, cross sections of the ocular globes were analyzed in terms of cellular damage and alterations in cell/ tissue morphology, after the topical administration of the nanoparticles. No significant histological changes were observed in any of the ocular globes, and all groups presented comparable characteristics between the OD and the OS, meaning that the CS/HA nanoparticles, with and without EPOβ, seem innocuous. Figure 47 represent the cross section of ocular tissues from an OD from Group E after CS/HA-EPOβ topical administration, stained with HE.

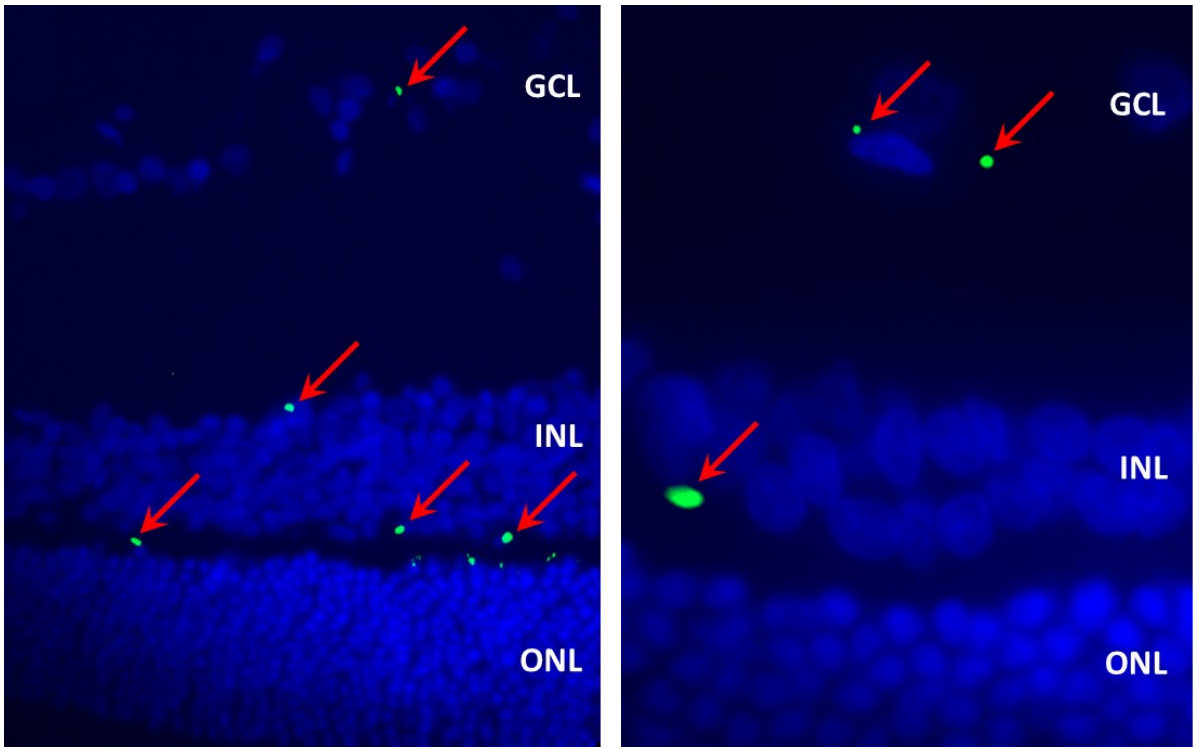

(a) (b)

Figure 45: Immunofluorescence images showing cross sections of the retina after CS/HA-EPOβ topical administration: (a) OD from group B (magnification 40×); (b) OD from group E (magnification 100×). Images show the merging of the green and the blue filters. Red arrows indicate EPOβ and cell nuclei are stained in blue by DAPI. GCL, ganglion cell layer; INL, inner nuclear layer; ONL, outer nuclear layer.

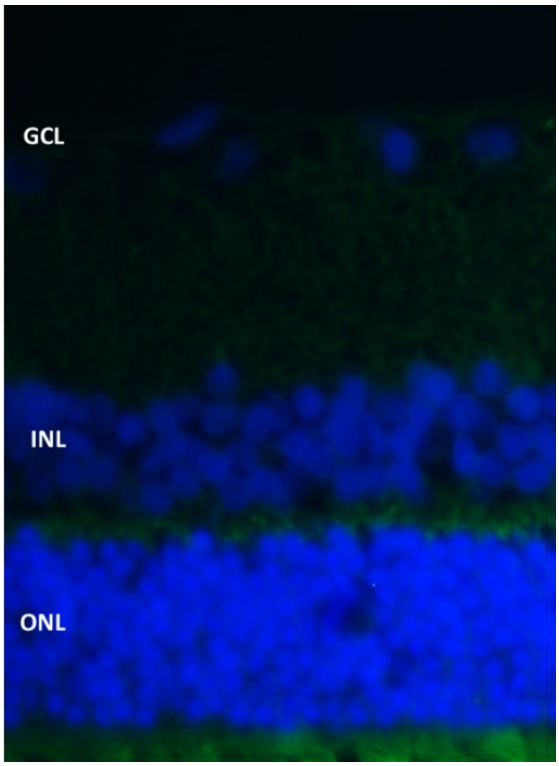

Figure 46: Immunofluorescence image showing a cross section of the retina of a control eye (OS) from group E after CS/HA topical administration (magnification 40×). Green and blue channels were merged. Basal auto-fluorescence stained in green is mostly visible under INL and ONL, and cell nuclei are stained in blue with DAPI. GCL, ganglion cell layer; INL, inner nuclear layer; ONL, outer nuclear layer.

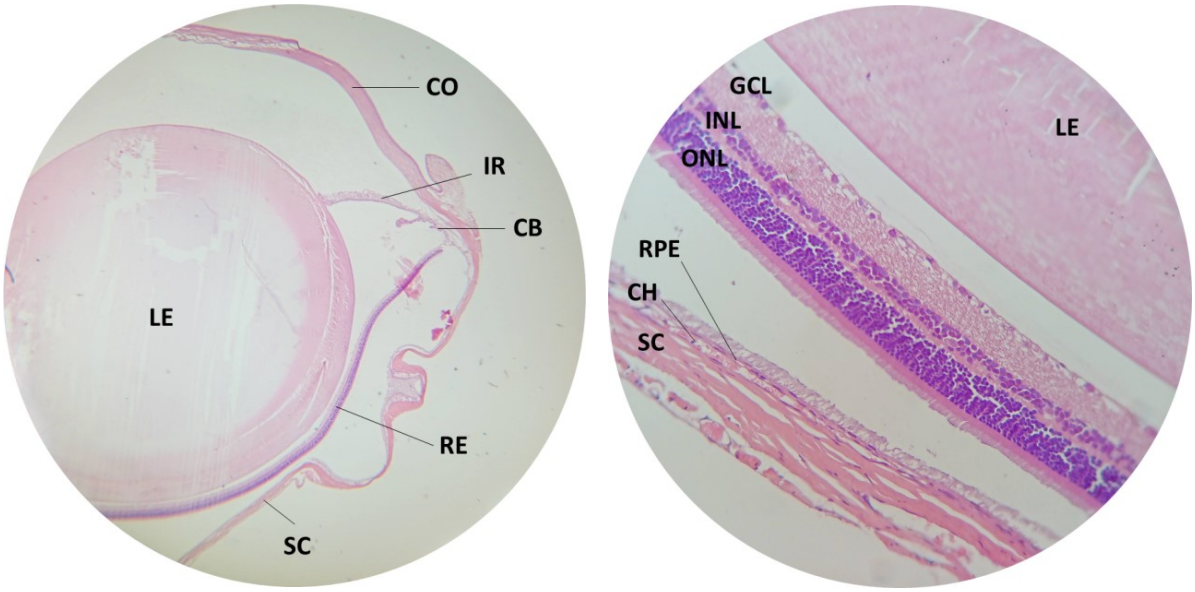

(a) (b)

Figure 47: Cross sections of the OD from group E after CS/HA-EPOβ topical administration: (a) CO, cornea; IR, iris; CB, ciliary body; LE, lens; RE, retina; SC, sclera (HE, 4x magnification); (b) LE, lens; GCL, ganglion cell layer; INL, inner nuclear layer; ONL, outer nuclear layer; RPE, retinal pigment epithelium; CH, choroid; SC, sclera (HE, 40x magnification).

5.5. Discussion

In the past, erythropoietin was considered solely an hematopoietic cytokine produced by the fetal liver and adult kidney but, in the last decades, several studies support other roles in different tissues (A. K. Junk et al. 2002). The brain (Marti 2004) and the retina (Hernández et al. 2006), for instance, were reported as new EPO secreting sites that also express EPO receptors (García-Ramírez et al. 2008; Ott et al. 2015). A recent review article describes the antiapoptotic, angiogenic, anti-inflammatory, antioxidant and neuroprotective effects of EPO in the ocular tissues, including the retina (Feizi et al. 2021). As EPOβ is a recombinant human EPO commonly used in medical practice, it was selected for this study with the perspective of contributing for glaucoma treatment as a neuroprotective agent.

Chitosan and hyaluronic acid are biocompatible polymers with notable mucoadhesive characteristics, that have a wide range of medical applications and were extensively studied throughout these last decades for ophthalmological use (De Campos et al. 2001; Thanou et al. 2001; De Campos et al. 2004; Wadhwa et al. 2010; Rah 2011; Bernkop-Schnürch and Dünnhaupt 2012; Ameeduzzafar et al. 2016; Guter and Breunig 2017; Graça et al. 2018; Silva et al. 2021) Our team developed chitosan and hyaluronic acid nanoparticles (CS/HA) designed to carry EPOβ into the ocular environment, and described their physicochemical characteristics, *in vitro* safety and, *ex vivo* permeation, among other features. Empty nanoparticles had 300 ± 6 nm, with a polydispersity index of 0.219 ± 0.043 and a zeta potential of 33 ± 1 mV, while nanoparticles with 1000 IU of EPOβ presented a size of 289 ± 3 nm, polydispersity index of 0.126 ± 0.085, and zeta potential of 39 ± 1 mV. The nanoparticles' drug loading was 17.4 ± 0.1%, and the encapsulation efficiency was 38.4 ± 0.3%. In the *in vitro* release assay in simulated tear fluid (37 °C, pH 7.4), 60 to 70% of EPOβ was released within the first 15 minutes, followed by a controlled release of nearly 90% of EPOβ in 6 hours. *Ex vivo* permeation results showed that the conjunctiva was the most permeable ocular tissue to EPOβ, followed by the sclera and the cornea. Moreover, CS/HA-EPOβ nanoparticles were noncytotoxic for ARPE-19 and HaCaT cells (Silva et al. 2020). These promising results encouraged our team to proceed to the *in vivo* studies, beginning with assessing the *in vivo* effects of the CS/HA-EPOβ nanoparticulate system when administered through the subconjunctival route in Wistar Hannover rats, which enabled the conclusion that the nanoformulation was biologically safe and enabled a sustained EPOβ retinal delivery during 21 days in the rats eyes (Silva et al. 2022). Topical administration of CS/HA-EPOβ nanoparticles was chosen for the following *in vivo* evaluation, due to its non-invasive nature that can lead to a safe and less expensive therapeutic approach.

Despite mechanisms like blinking, nasolacrimal drainage, and tear turnover, that hinder drugs permeation through ocular tissues, topical instillation of drugs targeting the posterior ocular segment is an expanding area of research. Topical administration of the nanocarriers through eyedrops could represent a safe and low-cost therapy that could render neuroprotection accessible to a large number of patients suffering from vision threatening diseases caused by retinal degenerative diseases.

All animals exhibited completely normal behavior during the study, as no signs of stress were observed, like obsessive-compulsive behavior, apathy, alopecia, or other skin lesions. No discrepancies in food and water intake, nor abnormal changes in body weight were detected. Moreover, ophthalmic examinations were always within the normal range. Thus, no signs of ocular lesions, discomfort or pain were observed after the topical administration of the CS/HA-EPOβ nanoparticles, which is in accordance with our subconjunctival study (Silva et al. 2022). Likewise, ophthalmological examinations were considered normal for all rats of every group throughout the study. Animals' tolerance to the nanoparticles applied topically was considered good since no animal reacted to the moment of instillation, and no ocular changes were observed afterwards, like epiphora, conjunctival hyperemia, conjunctival oedema, corneal oedema, keratitis, or pruritus. IOP values after the topical administration were always within the physiological range for both eyes, which corresponds to 18.4 ± 0.1 mm Hg (Wang et al. 2005), with no significant differences between OD and OS. These findings indicate that these nanocarriers are safe and well tolerable, which corroborate the results of the previous subconjunctival study (Silva et al. 2022).

EPO stimulates erythropoiesis and the microhematocrit assessment was important to evaluate EPOβ's systemic impact when administered through CS/HA nanoparticles by topical route. No significant changes were observed in hematocrit values, which were always within reference values (Jacob Filho et al. 2018). Therefore, this nanoformulation appears to be systemically innocuous, which is in accordance with previous results (Silva et al. 2022).

One of the ways of evaluating retinal physiology is the flash ERG, in which the retinal response to light stimulation is recorded as waveforms and represent the activity of different retinal cells (Weymouth and Vingrys 2008). The a-wave corresponds to the hyperpolarization of photoreceptors and it is the first negative deflection after the flash beginning, while the b-wave is a positive deflection that follows the a-wave and represents the activity of the bipolar and Müller cells (Rosolen et al. 2005). In the photopic ERG, a-waves represent cone function, while in the scotopic ERG, a-waves indicate rod function (Skaat et al. 2011). Despite the different ERG protocols found in the literature, our results from the photopic and the scotopic ERG performed in treated rats showed similar wave amplitudes and shapes to those recorded in controls and also in previous studies using healthy Wistar Hannover rats (Rosolen et al. 2005; An et al. 2012). The scotopic ERG results (SLR and SA) were comparable to the results

of Bayer et al. (2001), using silver electrodes and the Ganzfeld stimulator in Wistar rats (Bayer et al. 2001). In that study, the b-wave amplitudes of the scotopic phase oscillated from approximately 250 μV to 550 μV (Bayer et al. 2001), which is within the same range of values recorded in our ERGs. On the other hand, the a-wave varied from around 110 μV to 150 μV (Bayer et al. 2001), which is in the mean range of both SA and SLR responses observed in our study. Considering the light-adapted ERG, the same study presents a b-wave between 200 μV and 250 μV (Bayer et al. 2001), which is comparable to our PA and PLR results. Moreover, the PLR results show that the b-wave increased with light intensity while the a-wave stayed nearly constant, which is understandable because when the light stimulus is excessive, the a-wave is not produced (Green 1973). The PF results presented similarities to those found in the literature (An et al. 2012; Resende et al. 2018), supporting that cone function was maintained. Since no statistically significant changes in the ERGs wave forms or amplitudes were observed before and after topical administration of the CS/HA-EPOβ nanoparticles, and no differences were detected between OD and OS, it is reasonable to affirm that this nanoformulation did not influence retinal cells responses, which reinforces its local safety.

Immunofluorescence findings indicate that EPOβ was detected in all the treated eyes (OD, n=18) and no EPOβ was observed in any control eye (OS, n=18). CS/HA nanoparticles topically administered efficiently delivered EPOβ to the retina. The fluorescent signal (EPOβ) was detected in the RGC of treated eyes (OD) 12 hours after administration (Group A). Considering that EPOβ is highly soluble (Cowper et al. 2020), it could be firstly absorbed by the conjunctival-scleral route until the posterior segment of the eye (Hosoya et al. 2005), which justifies the presence of EPOβ in the retina only 12 hours after its topical instillation. In the subconjunctival study, EPOβ was also observed in the retina 12 h after injection (Group A) (Silva et al. 2022), which reinforces the hypothesis of the conjunctival-scleral absorption pathway. In previous studies from our team, using a commercial aqueous solution of EPOβ (NeoRecormon®), the protein was also detected in the retina 12 hours after its subconjunctival administration (Resende et al. 2013; Resende et al. 2016). In this study, EPOβ was also observed in the corneal stroma, corneal endothelium and ciliary body, suggesting that EPOβ diffused from the CS/HA nanoparticles and permeate the cornea instead of following a conjunctival-scleral pathway, due to the blood-aqueous barrier (Nayak and Misra 2018). Furthermore, EPOβ was still detected in the corneal stroma after 14 days (Group E), indicating a sustained trans-corneal absorption, where nanoparticles persisted in the pre-corneal area and allowed a delayed EPOβ permeation. Trans-corneal permeation of EPOβ after topical administration of the CS/HA-EPOβ nanoparticles matches our previous *ex vivo* permeation results using porcine ocular tissues, which showed a slower EPOβ permeation across the cornea, when compared to the sclera and the conjunctiva (Silva et al. 2020). In addition, our

team had already proved the trans-corneal *ex vivo* permeation of EPOβ using solely a commercial solution (NeoRecormon®) (Resende et al. 2017).

Fluorescence declined with time and at day 21 there were still some fluorescent signals in the retina, meaning that 3 days of topical instillation of CS/HA-EPOβ were enough to deliver EPOβ to the retina for as long as 3 weeks. When comparing the grade of fluorescence with the subconjunctival study (Silva et al. 2022), fewer fluorescent signals were observed in all ocular tissues when eyedrops were used, which is understandable considering the ocular barriers to overcome after topical administration. HE staining revealed no cellular or structural modifications in any ocular globes, which reinforces the biological safety of the CS/HA-EPOβ nanoparticles at ocular level. This had already been shown both *in vitro* by cytotoxicity assays (Silva et al. 2020), and *in vivo* in the subconjunctival study (Silva et al. 2022).

5.6. Conclusion

We propose to develop a patient-friendly drug delivery system of EPOβ to the retina using eyedrops with nanocarriers. This nanoparticulate system based on CS/HA nanoparticles was effective in delivering EPOβ to the retina by topical route of administration, allowing for a sustained EPOβ retinal delivery for 21 days. *In vivo* tests assessing the local and the systemic impact of this nanoformulation demonstrated that the CS/HA nanoparticles, with or without encapsulated EPOβ, were biologically safe, since no changes in ocular morphology or physiology were detected. The nanoformulation was very well tolerated by the animals after its topical instillation, which precludes a favorable patient's acceptance as eyedrops.

The non-invasive route of administration, the high tolerance and the efficient EPOβ delivery to the retina renders the nanoparticulate system CS/HA-EPOβ a promising formulation aiming the neuroprotection in retinal diseases, such as glaucoma and other retinopathies. Current glaucoma therapy is solely based on managing aqueous humor outflow and inflow, and it lacks a targeted and effective way to prevent visual loss. Neuroprotection is growing in the scope of scientific research and CS/HA-EPOβ nanoparticles create an opportunity to a topical ocular neuroprotective therapeutic, to increase patient's quality of life. Nevertheless, future research directions should include pharmacokinetic and pharmacodynamic studies of EPOβ after topical administration, and also the perspective of testing the effects of this nanoformulation in an animal model of retinal disease.

CHAPTER 6

Topical administration of a nanoformulation of chitosan-hyaluronic acid-epoetin beta in a rat model of glaucoma

B. Silva, L. Gonçalves, B. São Braz, E. Delgado. Topical Administration of a Nanoformulation of Chitosan-Hyaluronic Acid-Epoetin Beta in a Rat Model of Glaucoma. Pharmaceuticals 2023, 16, 164. https://doi.org/10.3390/ph16020164.

6.1. Abstract

A nanoformulation containing mucoadhesive nanoparticles of chitosan-hyaluronic acid-epoetin beta (CS/HA-EPOβ) has been previously developed and administered through subconjunctival and topical routes in healthy rats, allowing EPOβ delivery to the retina. The present study aimed to evaluate the effects of this nanoformulation after topical administration in a rat model of glaucoma. Wistar Hannover rats (n=24) were submitted to a complete ophthalmological examination and electroretinography, followed by experimental induction of glaucoma in their right eye (OD). Topical administration of CS/HA nanoparticles with EPOβ (n=12, treatment group (T)) and without EPOβ (n=12, control group (C)) was performed. Electroretinography was repeated on day 3 (n=24) and before euthanasia on day 7 (n=8), 14 (n=8) and 21 (n=8). Bilateral enucleation precluded *post-mortem* ocular assessment through hematoxylin-eosin staining (structural evaluation) and immunofluorescence (EPOβ detection). Animals showed good tolerance to the nanoformulation. The maximum IOP of the right eye occurred shortly after glaucoma induction (T = 62.6 ± 8.3 mmHg; C = 63.6 ± 7.9 mmHg), with an increase in IOP values of 3.6 folds. Treated animals presented a tendency for faster recovery of retinal electrical activity, although differences between groups were not statistically significant ($p > 0.05$). EPOβ presence was detected by immunofluorescence in the retina of all treated rats. Hematoxylin-eosin staining confirmed that animals from the control group had thinner retinas compared to the treated ones (Treatment = 145.6 ± 22 µm; Control = 120.2 ± 10.6 µm; $p < 0.05$). Apoptosis was identified in the neuroretina solely in the control group at 7 days, and not in any treated animal. We concluded that the topical ocular administration of CS/HA-EPOβ nanoparticles enabled EPOβ delivery to the retina of glaucomatous rats, and promoted an earlier retinal recovery, confirming EPOβ's neuroprotective effects. This preclinical study offers new insights into the field of ocular drug delivery targeting the posterior

segment of the eye, opening the window for topical administration of neuroprotective compounds.

6.2. Introduction

Neurodegenerative ocular diseases, such as glaucoma, have a substantial impact in people's daily life, as they can cause major visual impairment, and ultimately blindness. Glaucoma is a group of ocular disorders with an unclear pathophysiology, that is accompanied by degeneration and death of the retinal ganglion cells (RGC), which leads to optic neuropathy (Vidal-Sanz et al. 2012). The principal risk factor is the high intraocular pressure (IOP), in which the current glaucoma therapy is focused to manage by increasing aqueous humor outflow and by decreasing its production, to prevent disease's progression (Ghate and Edelhauser 2008). However, the ophthalmology research is shifting towards neuroprotection as a complementary approach to glaucoma treatment, and several neuroprotective strategies are under study, such as the use of progesterone, neurotrophic factors (Pardue and Allen 2018), asiatic acid (W. Huang et al. 2018), and gene therapy (Rhee and Shih 2021).

Erythropoietin (EPO) is a well-known glycoprotein that, apart from its hematopoietic role, can protect the retina by attenuating inflammatory responses, stimulating neurotrophin expression and up-regulating neurotrophic factors, amongst other features (Luo et al. 2015). The **antiapoptotic effects** of EPO in the RGC include the down-regulation of caspase-3 through the PI3K/AKT pathway, the up-regulation of Bcl-xl (Sullivan et al. 2012), the suppression of the cytochrome C mitochondrial release and the intracellular calcium regulation (Sullivan et al. 2011). Epoetin beta (EPOβ), a recombinant variant of EPO, was previously tested in glaucomatous rats using the subconjunctival route, revealing positive effects in the retina through the improvement of retinal electric responses and decrease in cellular damage of the retina (Resende et al. 2018).

Following this line of research, our team developed a nanoparticulate system with chitosan and hyaluronic acid (CS/HA) to act as an EPOβ ocular delivery system (Silva et al. 2020) and studied the *in vivo* safety of this nanoformulation in healthy Wistar Hannover rats after subconjunctival (Silva et al. 2022) and topical (Chapter 5) administrations. Both chitosan and hyaluronic acid are natural polymers with excellent mucoadhesive features, which can be enhanced through mutual association. Chitosan interacts with the ocular mucosa by ionic forces and is capable of widen cellular tight junctions (De Campos et al. 2001; De Campos et al. 2004; Bernkop-Schnürch and Dünnhaupt 2012), while hyaluronic acid mucoadhesive power is associated to CD44 receptors located both in the corneal epithelium and endothelium (Wadhwa et al. 2010; Guter and Breunig 2017; Graça et al. 2018). Therefore, despite the

natural ocular defense mechanisms that delay drugs permeation (De Campos et al. 2004; Nayak and Misra 2018), CS/HA nanoparticles could enhance the retention time of drugs on the ocular surface, potentially increasing their penetration and intraocular bioavailability (Silva et al. 2021).

Our team has also demonstrated that after topical instillation of CS/HA-EPOβ nanoparticles in Wistar rats, EPOβ could permeate through the outer layers of the eye and reach the retina after 12 hours, its presence still being confirmed 21 days later (Chapter 5). These results led us to consider the topical route of administration as an option to deliver a neuroprotective/neuroregenerative treatment targeting the retina in an experimental model of retinal disease. As far as we know, this innovative approach has never been reported in the literature before. Thus, in the present preclinical study, we intended to evaluate the effects of this newly developed CS/HA-EPOβ nanoformulation administered through topical ocular route using a rat model of glaucoma.

6.3. Materials and Methods

6.3.1. Materials

Wistar Hannover male rats from Charles River Laboratories (Saint-Germain-Nuelles, France) (n=24) were used, with an average weight of 329±53 g. Ophthalmological equipment and surgical instruments were available at the Faculty of Veterinary Medicine (ULisboa): Slit Lamp (Hawk Eye®, Dioptrix, France), Indirect ophthalmoscope (PanOptic®, WelchAllyn, Hillrom, USA), rebound tonometer (Tonolab®, Icare, Finland), Electroretinograph (RETIcom, Roland Consult, Stasche & Finger GmbH, Brandenburg, Germany), Surgical microscope (OPMI Lumera i®, Carl Zeiss Surgical GmbH, Germany), Phacoemulsification apparatus (Laureate® World Phaco System, Alcon Laboratories) and Optical microscope (Olympus® CX 22 RFS1, Olympus, Tokyo, Japan). The epoetin beta used in the nanoformulation was NeoRecormon® 30000 IU (RocheDiagnostics GmbH, Mannheim, Germany). Hyaluronic acid (eye grade quality; 300 kDa) from Shandong Topscience, was a kind gift from Inquiaroma (Barcelona, Spain). Chitosan of low molecular weight (100 kDa, 92% deacetylation) was acquired from Sigma Aldrich (Irvin, UK). All used drugs were available at the Faculty of Veterinary Medicine (ULisboa), namely meloxicam (Metacam® 5 mg/mL injectable and Meloxidyl® 0.5 mg/mL oral suspension) ketamine (Ketamidor® 100 mg/ mL, Richter Pharma, Wels, Austria), medetomidine (Domtor® 1mg/mL, Orion Corporation, Espoo, Finland), atipamezole (Antisedan® 5 mg/mL, Zoetis, New Jersey, USA), sodium pentobarbital (Euthasol® 400 mg/mL, Animalcare Group, North Yorkshire, UK), oxybuprocaine hydrochloride (Anestocil®,

Edol, Lisbon, Portugal) and carbomer based gel (Lubrithal®, Dechra, Northwich, United Kingdom). 9-0 Vicryl® (Johnson & Johnson®, New Jersey, USA) suture was available at the Faculty of Veterinary Medicine (ULisboa). Primary antibody rabbit anti-cleaved caspase-3 Asp175 (#9661), Cell Signaling Technology EnVision+ (EnVision System™, Dako®, Glostrup, Denmark) and horseradish peroxidase (HRP) labelled polymer anti-rabbit chromogen 3,3′-Diaminobenzidine (DAB) (Dako®, Glostrup, Denmark) were used in the immunohistochemistry for activated caspase-3 detection by the Pathology Laboratory of the Instituto Gulbenkian Ciência (IGC). The slide stainer for hematoxylin and eosin (HE) staining was Thermo Scientific Gemini™ AS (Massachusetts, USA). For immunofluorescence (IF), adhesion slides SuperFrost Plus™ and cover plates (Epredia™, ThermoFisher Scientific, Massachusetts, USA) were used. EPO monoclonal primary antibody 4F11 (MA5-15684) and goat anti-mouse IgG (H+L) secondary antibody DyLight 488 (35502) were from Invitrogen (ThermoFisher Scientific, Massachusetts, USA). The blocking reagent (sc-516214) and the aqueous mounting medium with DAPI (sc-2494) were from UltraCruz® (Santa Cruz Biotechnology, Texas, USA). The immunofluorescence control used was HepG2 cell cultures (human derived liver hepatocellular carcinoma cell line; ATCC® HB-8065™). Cell culture media and supplements were from Gibco (ThermoFisher Scientific, Massachusetts, USA). Histology laboratory devices and reagents were available at the Faculty of Veterinary Medicine (ULisboa). Axioscop 40 fluorescence microscope with an Axiocam HRc camera (Carl Zeiss, Germany) belonged to the Faculty of Pharmacy (ULisboa).

6.3.2. Methods

Previous to glaucoma induction, all animals (n=24) underwent a complete ophthalmological examination and an ERG. After glaucoma induction, CS/HA-EPOβ nanoparticles were administered through the topical route and 3 days later a control ERG was performed. At selected timepoints, another ERG was made followed by euthanasia and bilateral enucleation. Histological analysis and apoptosis quantification were the last steps of this study. Procedures are described in detail below.

Animals

Our **sample size** was calculated by power analysis for unpaired t test, with power of test of 80% and significance level of 0.05, using the software GraphPad StatMate 2 (GraphPad® Software, CA, USA). We chose a sample size of 4 per each timepoint of euthanasia based on a SD of 70 μV for ERG, which was an estimate from the physiological studies (Silva et al. 2022; Chapter 5), and considering the experience in ERG acquired through the assays. Thus, for

n=4 we had 80% power to detect a difference between means of approximately 164 μV with a significance level of 0.05 (two-tailed), which we considered suitable, also accounting for ethical issues of animal experimentation.

Wistar Hannover male rats (n = 24) were randomly split into 6 groups with 4 animals each (n=4), 3 treated groups (T) and 3 control groups (C). According to duration of the experiment, each group was respectively labelled as T7/C7 (one week duration), T14/C14 (two weeks duration) and T21/C21 (three weeks duration). Each group was housed in a conventional EU type IV polycarbonate cage (floor area = 1875 cm^2) with a stainless-steel wire lid, with food pellets and water *ad libitum*. Room environment was maintained at 20 ± 2 ºC and 50-60% of relative humidity. Luminosity and darkness phases were of 12 hours each. This study was performed in accordance with animal ethical requirements, and it was approved by the Organ Responsible for Animal Welfare (Órgão Responsável pelo Bem-Estar dos Animais – ORBEA) of the Faculty of Veterinary Medicine, University of Lisbon, approval date February 13, 2020, code 005/ 2020; and by the national entity General Directorate of Food and Veterinary (Direção Geral de Alimentação e Veterinária – DGAV), approval date January 8, 2021, code 0421/ 000/ 000/ 2020.

Ophthalmological examination

At the beginning of the study, all animals (n = 24) underwent a complete ophthalmological examination. The neuroophthalmological examination consisted in the evaluation of the palpebral, corneal, pupillary (direct and indirect) and dazzle reflexes, as well as visual acuity through a maze test response. The assessment of the anterior segment was done with a portable Biomicroscope (Hawk Eye®, Dioptrix, France) and the posterior segment was assessed with a PanOptic® Ophthalmoscope (WelchAllyn, Hillrom, U.S.A.). The IOP measurement was performed with a rebound tonometer (Tonolab®, Icare, Finland). These procedures were repeated immediately after glaucoma induction, and then after 1 h, 3 h, and 1, 2, 3, 5 and 7 days in all groups, and at 14 and 21 days in cases where applied.

Electroretinography

In order to evaluate the condition of the retina, animals underwent a flash ERG, which records the activity of rods and cones in response to luminous stimuli. This procedure was performed 3 times in each animal (n=24). The first time was before glaucoma induction, to confirm the previous normal functioning of the retina. The second was 3 days after glaucoma induction, to guarantee that the IOP raise had caused cellular damage to the retinal cells. The third was at 7 days (Groups T7/ C7), 14 days (Groups T14/ C14) or 21 days (Groups T21/ C21)

after glaucoma induction to assess the potential effects of the CS/HA-EPOβ nanoparticles. After the third ERG, euthanasia and enucleation were performed.

The ERG protocol was adapted from previously published procedures (Rosolen et al. 2005), which demanded a prior scotopic adaptation of 12 hours. General anesthesia was mandatory, and a combination of ketamine (70 mg/ kg) and medetomidine (0.8 mg/ kg) was administered through intraperitoneal injection. To avoid hypothermia, the animal was placed over a heating pad and its body temperature was periodically measured. One drop of oxybuprocaine hydrochloride (Anestocil®, Edol, Lisbon, Portugal) and one drop of a carbomer based gel (Lubrithal®, Dechra, Northwich, United Kingdom) was applied onto each cornea. Active silver electrodes were placed in contact with both corneas (Figure 48); reference electrodes were placed between the ear and lateral cantus, subcutaneously (Figure 48); and a ground electrode was placed at the tail base. Retinal responses were recorded simultaneously from both eyes. Light stimulation was achieved by means of a MiniGanzfeld device over the animal's head, with a base luminescence of 3 cds/m^2 (0 dB). The reference impedance was < 5 kohms and the light frequency was between 0.1 and 1000 Hz.

The ERG examination was divided in 5 parts and rod function was tested using dim flashes in scotopic conditions, while cone function was tested using bright flashes and flicker in photopic conditions. In the scotopic luminance response (SLR), light flashes of 9 intensities from –35 dB (–3.02 log cds/m^2) to +5 dB (0.98 log cds/m^2) were delivered 3 times per each intensity level, at a frequency of 0.1 Hz. In the photopic adaptation (PA) step, flashes were delivered 3 times after 0, 2, 4, 8 and 16 minutes of light adaptation, at a frequency of 1.3 Hz, and the intensity was calculated using the maximum b-wave amplitude of the SLR. The photopic luminance response (PLR) used light flashes of 9 intensities, varying from –35 dB to +5 dB, delivered 3 times at a frequency of 1.3 Hz. The photopic flicker (PF) delivered flashes of 0, –5, –10 and –15 dB, at a frequency of 6.3 Hz, after 10 minutes of light adaptation. Lastly, the scotopic adaptation (SA) used white dim flashes after 0, 2, 4, 8, 16 and 32 min of dark adaptation, delivered 3 times, at a frequency of 1.3 Hz. The entire ERG exam lasted for 75 minutes and anesthesia was reverted with an intramuscular injection of atipamezole (2.5 mg/ kg).

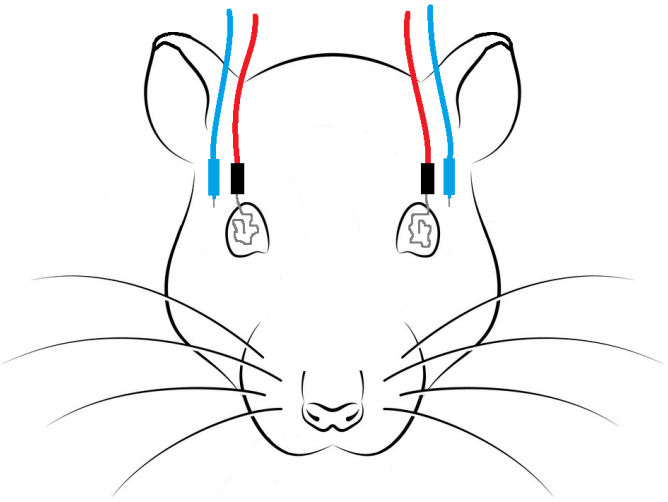

Figure 48: Representation of the ERG setup: active electrodes (red) with silver tips placed on corneas, and reference electrodes (blue) placed between the ears and the lateral canthus ipsilateral to the tested eye.

Preparation of the nanoformulation

Nanoparticles were prepared before glaucoma induction. In a laminar flow cabinet, reagents were sterilized by filtration, using a 0.22 µm filter, and nanoparticles were prepared by a modified ionotropic gelation procedure, based on published protocols (Wadhwa et al. 2010; Graça et al. 2018) and previously described by our group (Silva et al. 2020). Briefly, to the hyaluronic acid (HA) solution at 1 mg/mL, 1000 IU of EPOβ (NeoRecormon®) was added, at room temperature. Then, the HA-EPOβ was added to the chitosan (CS) solution at 1 mg/mL in NaCl 0.9%, creating CS/HA-EPOβ nanoparticles. Nanoparticles without EPOβ were called "empty nanoparticles" and were prepared following the same protocol by addition of purified water instead of EPOβ. Empty nanoparticles were administered to the control animals. CS/HA-EPOβ and CS/HA formulations were aspirated with sterilized insulin syringes and kept at room temperature until the topical ocular administration.

Glaucoma experimental induction

After the first ERG, animals underwent glaucoma induction in the right eye (OD), while the left eye (OS) was kept intact to remain the control for IOP values. Glaucoma induction was achieved by the cauterization of 3 episcleral veins, whose locations are schematically illustrated in figure 49. This microsurgical technique was performed using a surgical microscope, under general anesthesia with ketamine (70 mg/ kg) and medetomidine (0.8 mg/ kg) and using microsurgical instrumentation. Before the surgical procedure a drop of oxybuprocaine hydrochloride (Anestocil®, Edol, Lisbon, Portugal) was applied on the OD and

then a small incision of approximately 2 mm in length was made in the bulbar conjunctiva and Tenon's capsule, adjacent to the sclero-corneal limbus. Two small radial incisions were made at the edges of the first incision to expose the underlying extraocular muscle, which was gently handled with a clamp to enable the cauterization of the underlying episcleral vein (Figure 50b). Cauterization was performed at the vein bifurcation with the micro-electrocautery attached to the Phacoemulsification apparatus, leading to an immediate iris congestion (Figure 51). This procedure was uniquely performed in the OD, on two dorsal and one lateral veins, and allowed blockage of the respective venous drainage area, leading to an abrupt IOP increase. IOP was measured, on both eyes, immediately before and after the cauterization, to attest if the blockage had been successful. Each conjunctival incision was closed with absorbable 9-0 Vicryl® suture. Continuous hydration of the cornea was performed during the procedure with sterile NaCl 0.9%, and Lubrithal® was applied in the end for corneal lubrication and again 1 hour later. For analgesia, meloxicam (1 mg/ kg) was administered by subcutaneous route, followed by 1 mg/ kg of meloxicam oral suspension on the day after. After the cauterization of 3 episcleral veins, anesthesia was reverted with an intramuscular injection of atipamezole (2.5 mg/ kg) and animals were kept in separate cages until full anesthesia recovery. Along with the post-surgical ophthalmological examinations, the presence of discomfort or pain was assessed using the Rat Grimace Scale.

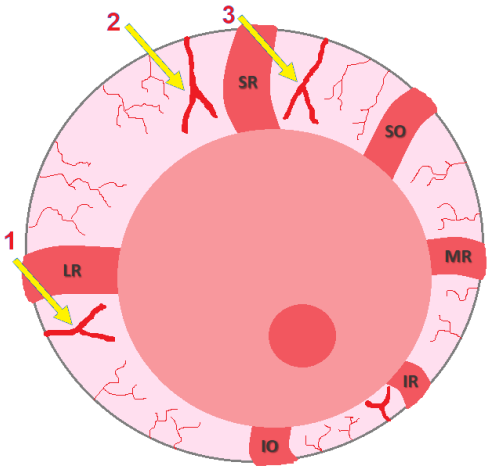

Figure 49: Representation of a rat ocular globe: yellow arrows indicate the cauterized episcleral veins; 1) lateral vein, 2) dorso-lateral vein, 3) dorso-medial vein. Extraocular muscles: SR, superior rectus; SO, superior oblique; MR, medial rectus; IR, inferior rectus; IO, inferior oblique; LR, lateral rectus.

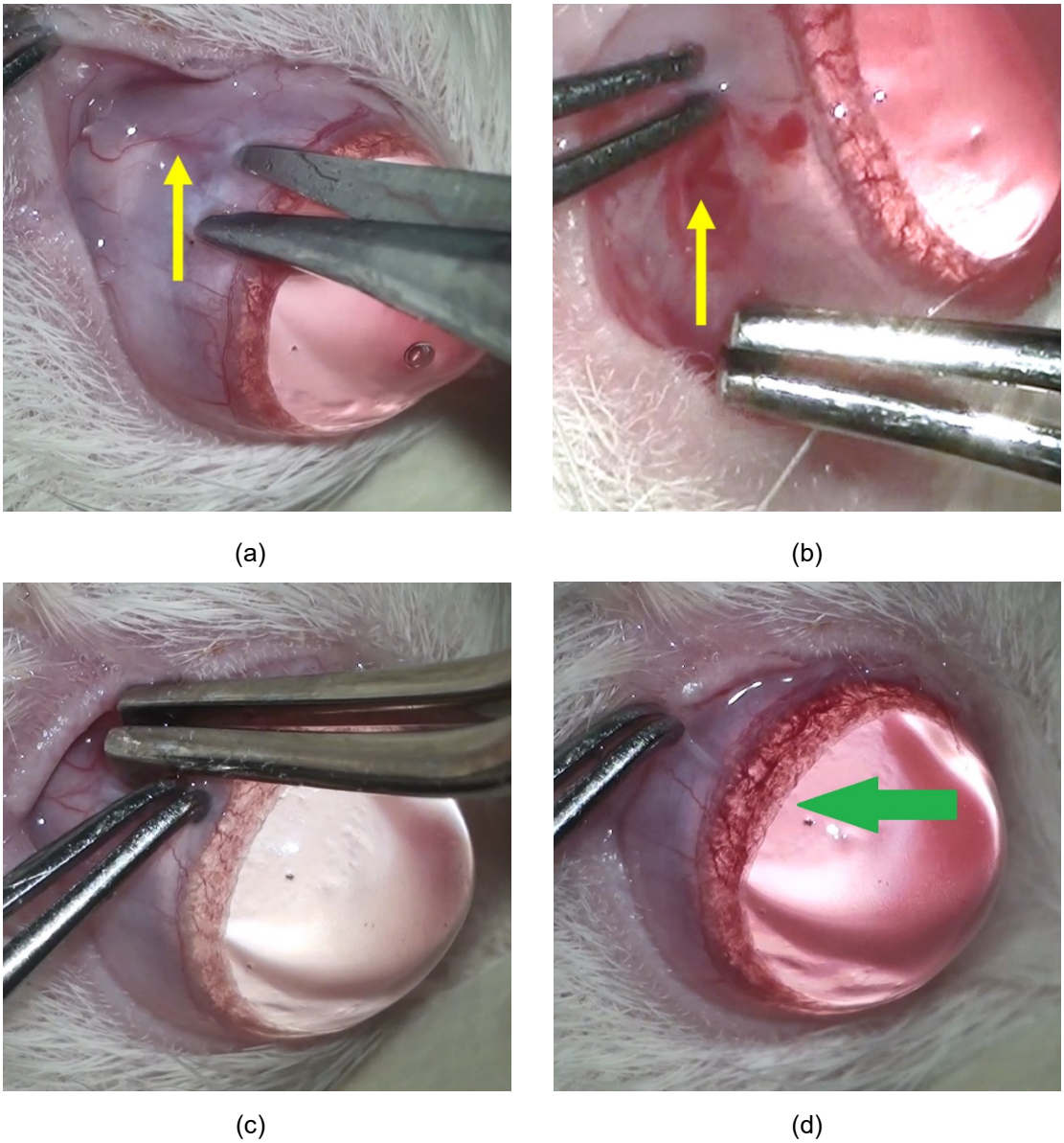

(a) (b)

(c) (d)

Figure 50: Photos of a rat ocular globe during the microsurgical procedure: (a) yellow arrow indicates a dorsal episcleral vein before conjunctiva incision; (b) yellow arrow indicates a lateral episcleral vein after the conjunctival incision; (c) before the cauterization of the dorsal episcleral vein, showing normal iris vascularization; (d) after the cauterization of the dorsal episcleral vein, showing an evident iris congestion (green arrow)..

Topical administration of nanoparticles

Topical ocular administration of the nanoformulation in the OD was initiated immediately after glaucoma induction with a frequency of one drop 3 times daily during a period of 3 days, to simulate an average frequency of administration of an eyedrop. Groups T7, T14 and T21 received CS/HA-EPOβ nanoparticles transporting EPOβ, while groups C7, C14 and C21 received empty CS/HA nanoparticles. No eyedrop was applied in the contralateral eye (OS).

Euthanasia and enucleation

On day 7 (T7/ C7), day 14 (T14/ C14) and day 21 (T21/ C21) after topical administration of the nanocarriers, a third ERG was performed followed by euthanasia with an intraperitoneal injection of sodium pentobarbital (150 mg/kg). Then, both ocular globes were enucleated and painted with tissue dyes at the optic nerve area (green) and also at the lateral (green), medial (green), dorsal (red) and ventral (blue) poles to facilitate eye orientation during paraffin inclusion and histological sections (Figure 52). Ocular globes were fixated in 10% (v/v) formaldehyde diluted in PBS (0.1 M, pH 7.4), included in paraffin blocks and processed.

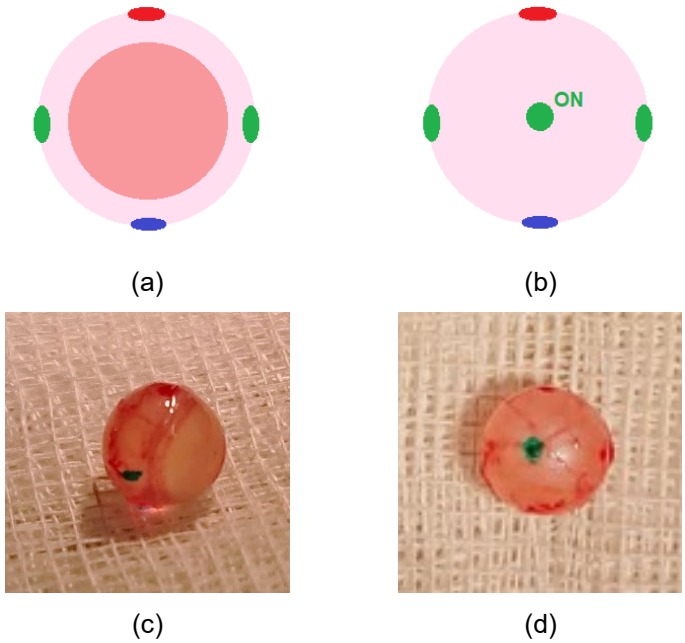

Figure 51: Representation of a rat ocular globe painted with tissue dyes: (a) frontal view; (b) caudal view. Photographs of a rat ocular globe painted with tissue dyes: (c) lateral view; (d) caudal view. In green we can identify the transected optic nerve. ON, optic nerve.

Histological assessment

After paraffin inclusion, cross sections measuring 3 μm were made with a microtome, in a total of 4 sections for immunofluorescence and 4 sections for hematoxylin and eosin (HE) staining. Slides were kept at 60° C for 1 hour and then overnight at 37° C. HE slides were processed in the multi-tasking stainer Gemini™ AS, and then observed in an optical microscope (Olympus® CX 22 RFS1, Olympus, Tokyo, Japan) in order to evaluate cellular structure and perform measurements of the retinal thickness from a distance of 500 μm until 1500 μm away from the optic nerve, which corresponds approximately to two microscopic view fields. Pictures were taken from each field at 40× magnification and, posteriorly, 10 measurements of the retinal thickness from the inner limiting membrane (ILM) to the outer limiting membrane (OLM) were performed in each picture using the ImageJ® Software.

Immunofluorescence slides followed a more complex protocol, starting from being deparaffinized in xylol, and gradually rehydrated in alcohol from 100° to 70° and finally in purified water. Sections were washed with Triton X-100 solution (0.1% v/v in PBS) and Tween 20 solution (0.1% v/v in PBS), followed by setting the slides in cover plates. Meanwhile, HepG2 cells (positive control for immunofluorescence) were submitted to a hypoxic environment during 2 hours at 37° C, then fixated in 10% (v/v) formaldehyde in PBS and washed with Triton X-100 solution. From that point on, HepG2 cells followed the same protocol as the cross sections. Sections were incubated with UltraCruz® Blocking Reagent for 1 hour at room temperature, followed by a washing step and incubation with EPO monoclonal primary antibody 4F11 (1:400) overnight at 4 °C. Then, another washing step was made, followed by incubation with goat anti-mouse secondary antibody DyLight 488 (1:1000) in the dark for 1 hour, at room temperature. Slides were carefully disassembled from the cover plates and received a small amount of UltraCruz® mounting medium with DAPI, followed by a coverslip and varnish sealing. The immunofluorescence analysis was performed using an Axioscop 40 fluorescence microscope with an Axiocam HRc camera (Carl Zeiss, Germany), and images were processed with the AxioVision software (Rel.4.8.1, Carl Zeiss). EPOβ fluorescence was detected in green, the negative control being the OS and the positive control for the immunofluorescence technique being the HepG2 cells.

Caspase-3 activity evaluation

Immunohistochemistry using chromogen DAB (3,3′-Diaminobenzidine) for activated caspase-3 was performed to determine the location and distribution of caspase-3 in retinal cells. This procedure was performed in all OD from the treatment and control groups, which were preserved in paraffin, by the Pathology Laboratory of the Instituto Gulbenkian Ciência

(IGC). Cross sections were deparaffinized and hydrated. Antigen retrieval was done with citrate buffer, following 3% hydrogen peroxide and Protein Block solutions. Cell Signaling Technology EnVision+ used primary antibody rabbit anti-cleaved caspase-3 Asp175 and HRP-labeled polymer anti-rabbit DAB. Positive results were determined with the presence of intracytoplasmic brown staining material, while negative results did not present that finding.

Statistical methods

Statistical analysis was performed with GraphPad Prism version 6.0 (GraphPad Software, CA, USA) and Microsoft Office Excel (Microsoft, Washington, USA), using one-way ANOVA and paired t-test to detect significant differences between group means. The statistical significance was 95%, corresponding to a *p*-value of 0.05. Results were presented as mean ± standard deviation (SD).

6.4. Results

6.4.1. Ophthalmological signs and behavior

Animals demonstrated a high tolerance to the nanoformulation, both to empty (control groups) and EPOβ loaded (treatment groups) CS/HA nanoparticles. Behavior was monitored throughout the study according to the Rat Grimace Scale, whose results were the same for all animals, as follows: orbital tightening “0”, nose flattening “0”, ear changes “0” and whisker change “0”. Thus, signs of pain or discomfort were absent, meaning that analgesia was effective. Moreover, no animal reacted with discomfort during the topical administrations.

Ophthalmological examinations revealed no severely abnormal ocular signs, such as blepharospasm, epiphora, purulent discharge, moderate/severe conjunctival hyperemia, corneal oedema, hyphemia, or others. Neuroophthalmological and fundoscopic exams showed no alterations (n=24). Biomicroscopic exams revealed that one rat from group T7 and one rat from group T21 exhibited superficial keratitis in the OD, and one rat from group C14 developed bilateral superficial keratitis, confirmed by fluorescein test. All rats recovered completely in 48 hours and no therapy was necessary. These cases could be justified by the exposure keratitis during anesthesia since the blinking reflex is abolished. In addition, on the day after glaucoma induction, mild conjunctival hyperemia (rated 1/3) was present in the OD of all animals and a discrete amount of bilateral chromodacryorrhea was observed in 14/24 rats, from both treatment and control groups. These ocular signs were expectable when taking into account the surgery itself and the postsurgical stress.

Figure 53 shows pictures of one rat 1 hour after the glaucoma induction (a), and 3 days later (b). The ocular symmetry is evident on both timepoints, showing that the IOP raise apparently had no impact in the conformation of the right ocular globe. The same was noted for the rest of the animals.

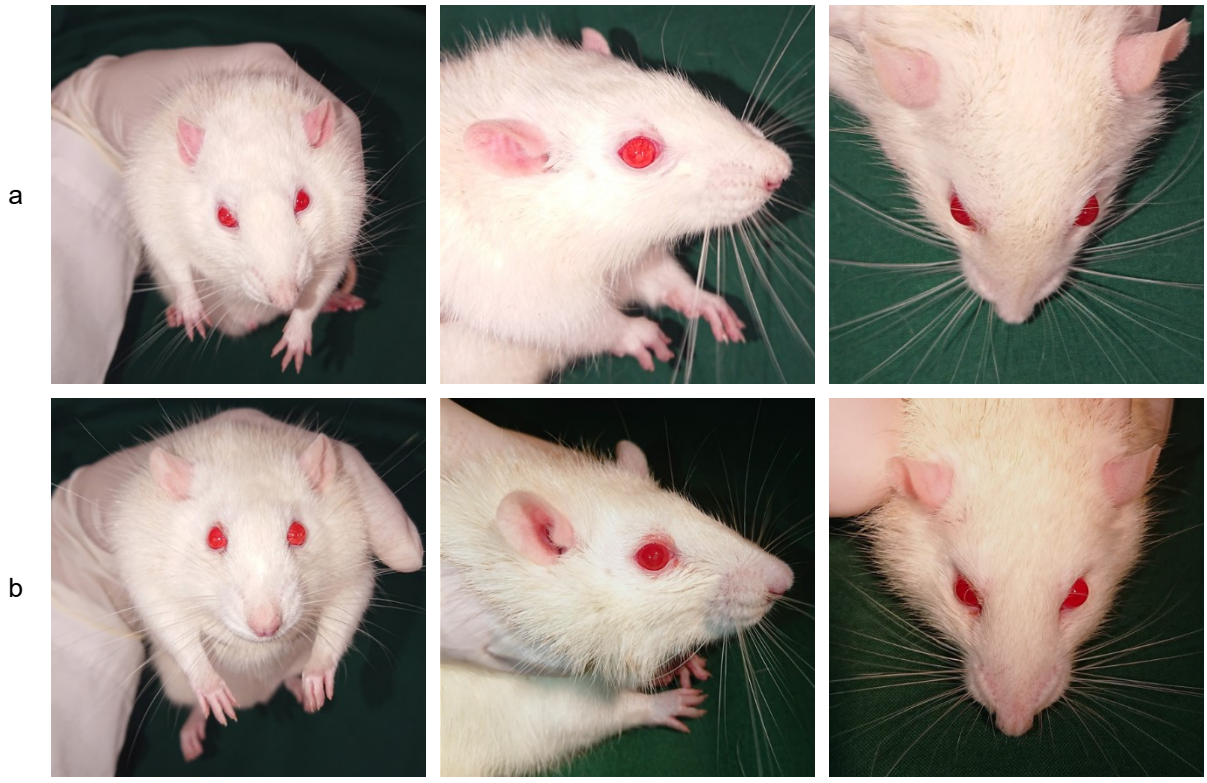

Figure 52: Pictures of a rat 1 hour (a) and 3 days (b) after the cauterization of the episcleral veins of the OD. The animal shows symmetry between both ocular globes and no signs of discomfort.

6.4.2 Intraocular pressure

The average IOP of conscious rats, at the beginning of the study, was OD = 17.2 ± 1.4 mmHg and OS = 17.2 ± 0.9 mmHg for treatment groups, and OD = 17.4 ± 1.3 mmHg and OS = 17.3 ± 1.4 mmHg for control groups, with no statistically significant differences between groups ($p > 0.05$). Those values were in accordance with the reference IOP for healthy Wistars Hannover rats (Wang et al. 2005).

Table 16 shows the IOP measurements before and after (T=0) glaucoma induction, denoting that the difference between IOP values before and after glaucoma induction was statistically significant for all animals ($p < 0.05$). This validates this technique and means that

the cauterization of three episcleral veins was an effective procedure for raising the IOP of the OD, with no indirect effects in the OS.

Table 16: IOP measurements (mmHg) for both eyes, before and after (T=0) glaucoma induction, in treatment (n=12) and control groups (n=12). OD, right eye; OS, left eye.

	Treatment		Control	
	Before	After (T=0)	Before	After (T=0)
OD	10.9 ± 0.8 mmHg	62.6 ± 8.3 mmHg*	11.1 ± 0.8 mmHg	63.6 ± 7.9 mmHg*
OS	10.8 ± 0.7 mmHg	10.7 ± 7.9 mmHg*	10.8 ± 0.7 mmHg	11.0 ± 1.2 mmHg*

*Significance level of 0.05

Figure 54 represents the IOP variation for the treatment (a) and the control groups (b) from the time of glaucoma induction (T0) till the end of the study (T21). The IOP of the OS varied between 10 mmHg and 22 mmHg, with an average of 15.4 ± 2.8 mmHg for treated animals and 16.1 ± 2.8 mmHg for control animals, which were within the reference range (Wang et al. 2005). Considering the OD, the maximum IOP measured were at T0 (Figure 54) with statistically significant differences between OD and OS ($p < 0.05$). No difference was observed between groups in the average IOP at T0 ($p > 0.05$), being 62.6 ± 8.3 mmHg for the treatment group and 63.6 ± 7.9 mmHg for the control group (Table 16). In both groups, the IOP of the OD raised in average 3.6 folds from the physiological baseline but rapidly decreased in the following days, reaching physiological values at day 7 (Figure 54). Treatment and control groups did not show any significant differences in the average IOP measurements ($p > 0.05$), meaning that EPOβ did not seem to influence IOP.

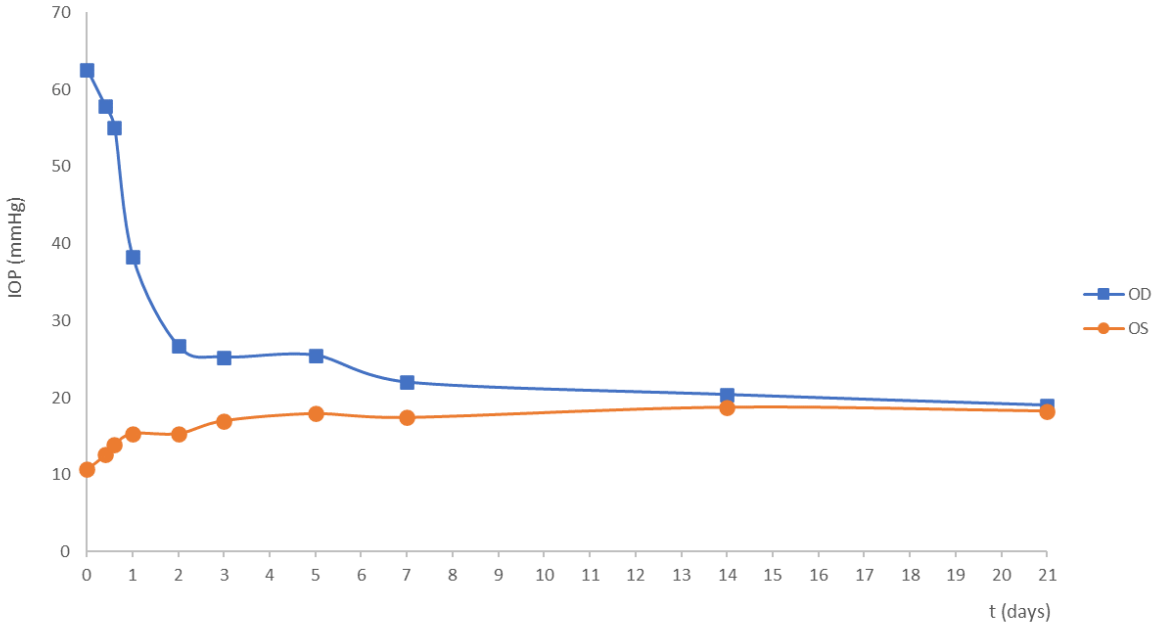

(a)

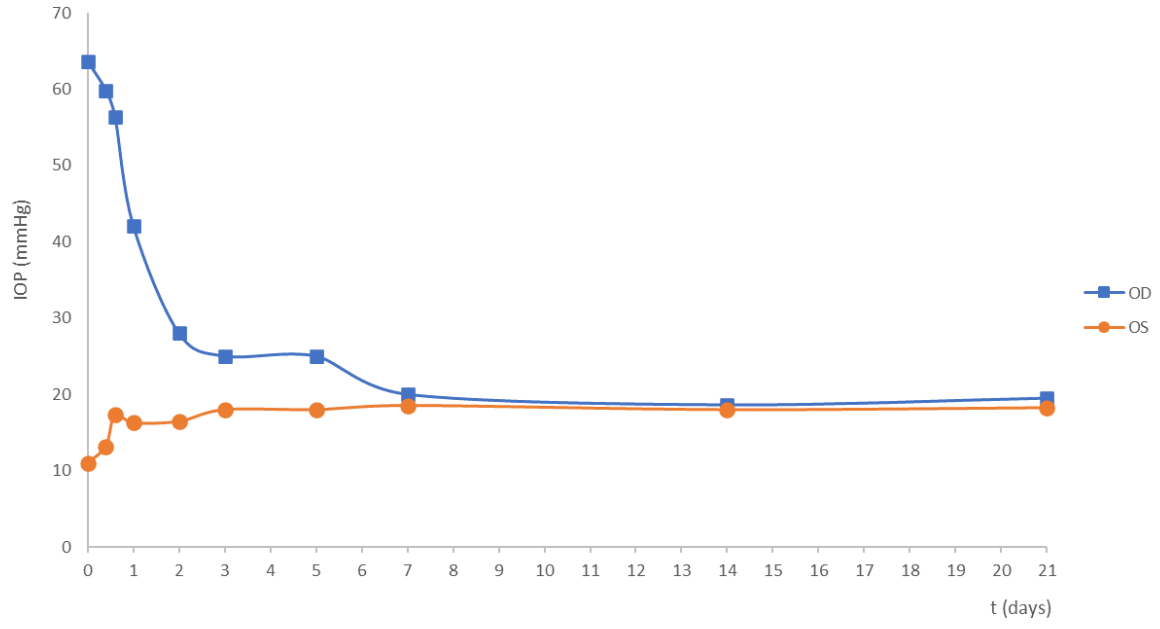

(b)

Figure 53: Mean IOP from the OD (orange) and from the OS (blue) since the day of glaucoma induction (t = 0) until 21 days later, in the treatment (a) and the control (b) groups. IOP is presented in mmHg.

6.4.3. Electroretinography

Three flash electroretinographies per animal were performed to evaluate the changes in retinal function after glaucoma induction and to assess retinal response to treatment with CS/HA-EPOβ nanoparticles. Waveforms and amplitudes of a and b waves were analyzed and the results (presented in μV as mean ± SD [min; max]) are fully described below.

Efficacy of the glaucoma induction

As mentioned before, a previous ERG was performed in all animals before glaucoma induction. In order to assess the retinal damage of the OD due to the increased IOP, an ERG was performed 3 days after glaucoma induction. The analysis of the changes in retinal electrical activity sustained that the cauterization of 3 episcleral veins successfully led to retinal impairment in the OD, as statistically significant differences ($p < 0.05$) were observed in the majority of recordings, in both treatment and control groups (Table 17). In both groups, SLR and SA showed statistically significant differences in both a and b waves, while PA, PLR, and PF presented significant differences only in the b-wave, as shown in table 17. No statistically significant differences ($p > 0.05$) were detected between treatment and control groups, indicating that the episcleral veins cauterization was performed similarly in all groups of animals. For instance, within the treatment group the SLR at 5 dB presented an a-wave of 263 ± 36 [180; 312] μV before glaucoma induction and 46 ± 27 [8; 90] μV at day 3; while the b-wave was 618 ± 15 [440; 891] μV before the microsurgery and 124 ± 66 [19; 208] μV at day 3 (Table 17). Likewise, for the control group, the SLR at 5 dB presented an a-wave of 266 ± 31 [203; 300] μV before the surgical procedure and 45 ± 15 [19; 74] μV at day 3; and the b-wave was 626 ± 12 [349; 810] μV before the microsurgery and 123 ± 47 [67; 227] μV at day 3 (Table 17). Table 17 summarizes the ERG results of treatment and control groups, before and 3 days after glaucoma induction in the OD.

Figure 55 illustrates the waveforms recorded from the OD before the procedure and at day 3, where it is visible the flattening of the waves as a result of decreased retinal electric response. On the other hand, the a and b waves recorded from the OS showed no statistically significant differences ($p > 0.05$) between day 0 and 3 days after the surgery, in neither the treatment nor in the control groups. For example, in the treated group, the SA of the OS at 32 min before the glaucoma induction had mean a and b waves of, respectively, 84 ± 49 [30; 212] μV and 394 ± 14 [158; 695] μV; while 3 days later they corresponded to 87 ± 39 [31; 223] μV and 400 ± 16 [139; 795] μV, respectively. Before the procedure, the control group presented an a-wave of 90 ± 34 [39; 145] μV and a b-wave of 386 ± 85 [216; 515] μV while 3 days later,

the mean a-wave was 87 ± 53 [36; 195] µV and the b-wave corresponded to 399 ± 10 [206; 575] µV.

Table 17: ERG results from the OD – a-waves and b-waves recorded during the five ERG components. Results are presented as mean ± SD in microvolts (µV). ERGs were performed in the treatment and control groups, before glaucoma induction and again 3 days later. Results show statistically significant differences between timepoints (*) with $p < 0.05$.

		Treatment (µV)				Control (µV)			
		Before		3 days		Before		3 days	
		a-wave	b-wave	a-wave	b-wave	a-wave	b-wave	a-wave	b-wave
SLR	-35 (dB)	18 ± 4*	293 ± 110*	5 ± 4*	41 ± 24*	18 ± 4*	296 ± 76*	7 ± 3*	43 ± 28*
	-30	22 ± 10*	324 ± 107*	10 ± 5*	78 ± 41*	21 ± 10*	326 ± 85*	10 ± 6*	72 ± 31*
	-25	26 ± 11*	336 ± 122*	11 ± 6*	80 ± 46*	28 ± 8*	341 ± 91*	12 ± 8*	78 ± 51*
	-20	41 ± 13*	380 ± 119*	14 ± 7*	86 ± 51*	37 ± 15*	391 ± 78*	14 ± 8*	86 ± 28*
	-15	76 ± 31*	419 ± 140*	17 ± 20*	90 ± 53*	79 ± 18*	428 ± 82*	17 ± 13*	89 ± 54*
	-10	152 ± 69*	488 ± 126*	28 ± 22*	93 ± 55*	156 ± 39*	496 ± 80*	29 ± 17*	91 ± 59*
	-5	204 ± 51*	578 ± 144*	33 ± 17*	96 ± 69*	210 ± 24*	579 ± 99*	34 ± 14*	97 ± 68*
	0	231 ± 68*	602 ±159*	48 ± 20*	124 ± 73*	240 ± 31*	612 ± 114*	43 ± 15*	121 ± 46*
	5	263 ± 36*	618 ± 145*	46 ± 27*	124 ± 67*	266 ± 31*	627 ± 119*	45 ± 15*	123 ± 47*
PA	0 (min)	18 ± 9	202 ± 48*	12 ± 8	71 ± 29*	17 ± 13	206 ± 60*	10 ± 9	68 ± 28*
	2	23 ± 20	211 ± 37*	16 ± 10	75 ± 41*	22 ± 15	198 ± 36*	15 ± 9	77 ± 40*
	4	18 ± 13	213 ± 41*	13 ± 6	79 ± 56*	21 ± 13	199 ± 42*	14 ± 10	75 ± 23*
	8	22 ± 15	212 ± 49*	14 ± 16	71 ± 38*	22 ± 15	200 ± 42*	14 ± 13	73 ± 26*
	16	28 ± 16	205 ± 53*	16 ± 13	64 ± 24*	27 ± 17	199 ± 49*	16 ± 9	67 ± 23*
PLR	-35 (dB)	19 ± 12	70 ± 24*	13 ± 12	41 ± 21*	17 ± 9*	71 ± 25*	11 ± 9*	42 ± 22*
	-30	25 ± 11*	73 ± 36*	12 ± 11*	45 ± 19*	25 ± 13*	79 ± 42*	12 ± 13*	47 ± 23*
	-25	27 ± 14	82 ± 30*	20 ± 15	49 ± 23*	27 ± 15*	85 ± 39*	11 ± 7*	49 ± 19*
	-20	25 ± 13	84 ± 29*	15 ± 13*	49 ± 22*	26 ± 14*	89 ± 35*	14 ± 4*	52 ± 20*
	-15	22 ± 15	94 ± 32*	17 ± 12*	51 ± 18*	21 ± 14	89 ± 37*	21 ± 8	53 ± 14*
	-10	17 ± 13	107 ± 36*	17 ± 11	56 ± 28*	21 ± 18	110 ± 32*	14 ± 15	55 ± 16*
	-5	27 ± 25	127 ± 40*	13 ± 11	58 ± 23*	24 ± 23	128 ± 50*	20 ± 14	61 ± 21*
	0	24 ± 22	198 ± 64*	12 ± 9	59 ± 24*	27 ± 22	202 ± 80*	13 ± 9	60 ± 23*
	5	23 ± 30	227 ± 53*	10 ± 11	71 ± 19*	22 ± 28	218 ± 96*	12 ± 15	73 ± 21*
PF	0 (dB)	7 ± 4	229 ± 47*	5 ± 4	51 ± 23*	8 ± 6	239 ± 59*	6 ± 4	52 ± 10*
	-5	13 ± 9	134 ± 33*	9 ± 5	47 ± 21*	18 ± 8*	122 ± 41*	11 ± 6*	47 ± 22*
	-10	19 ± 13	81 ± 32*	13 ± 8	44 ± 13*	20 ± 17	85 ± 30*	13 ± 8	43 ± 16*
	-15	18 ± 9	61 ± 24*	16 ± 8	40 ± 12*	23 ± 15	71 ± 24*	14 ± 9	39 ± 15*
SA	0 (min)	25 ± 14*	243 ± 52*	13 ± 8*	55 ± 23*	25 ± 13*	241 ± 70*	12 ± 9*	53 ± 28*
	2	42 ± 24*	265 ± 53*	16 ± 8*	57 ± 30*	41 ± 20*	266 ± 44*	17 ± 8*	60 ± 34*
	4	47 ± 30*	291 ± 57*	18 ± 13*	67 ± 30*	46 ± 23*	285 ± 72*	18 ± 10*	62 ± 35*
	8	61 ± 43*	333 ± 67*	19 ± 9*	69 ± 36*	57 ± 32*	329 ± 80*	19 ± 11*	72 ± 40*
	16	71 ± 48*	365 ± 41*	28 ± 16*	79 ± 31*	80 ± 46*	355 ± 76*	26 ± 13*	77 ± 51*
	32	91 ± 49*	403 ± 52*	39 ± 26*	82 ± 59*	85 ± 56*	405 ± 123*	39 ± 26*	83 ± 38*

* Statistically significant differences ($p < 0.05$)

SLR, scotopic luminescence response; PA, photopic adaptation; PLR, photopic luminescence response; PF, photopic flicker; SA, scotopic adaptation; dB, decibel; min, minutes.

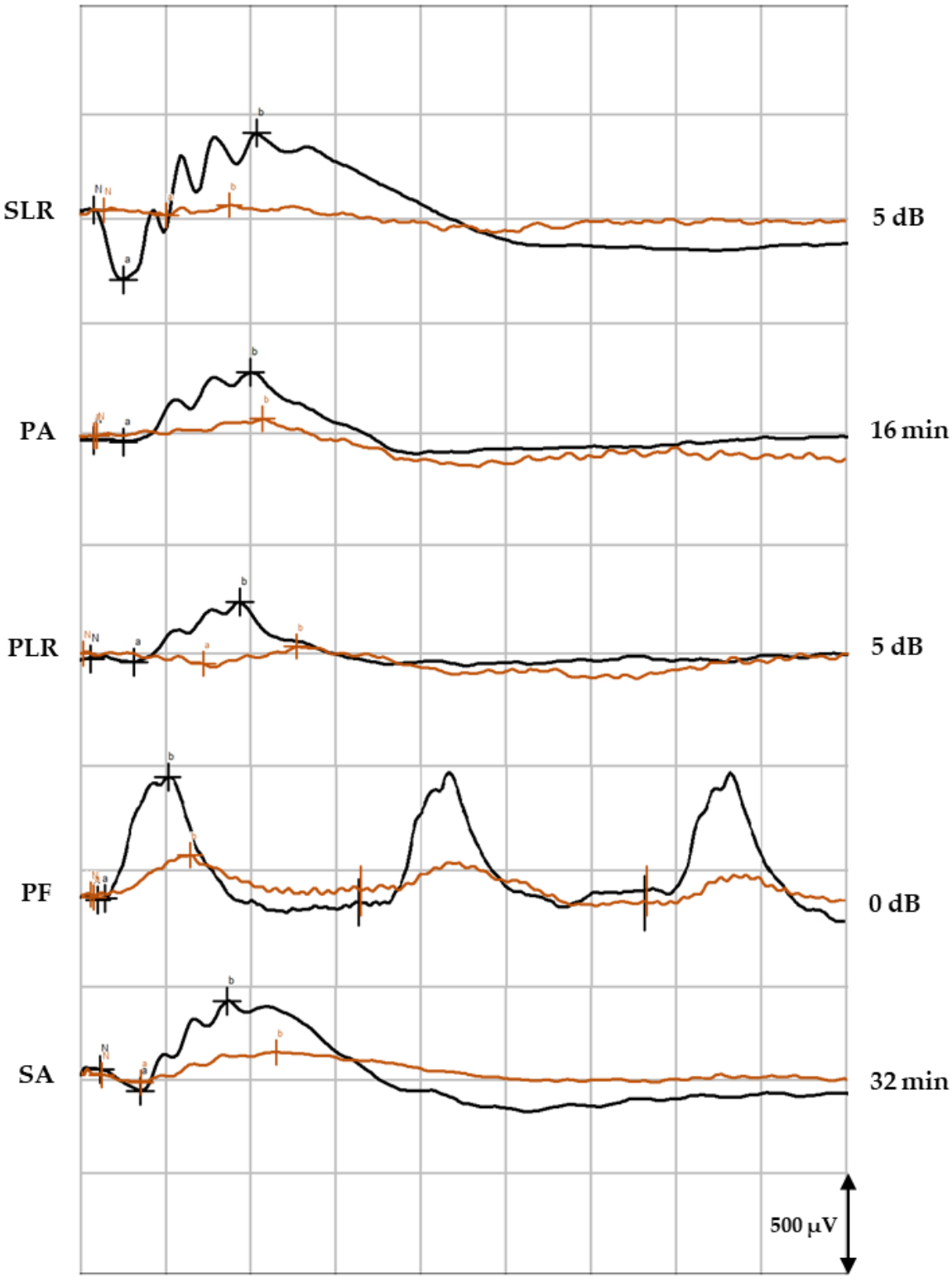

Figure 54: Example of ERG waveforms recorded from the OD at the beginning of the study (black) and at day 3 after the glaucoma induction (orange). SLR, scotopic luminescence response; PA, photopic adaptation; PLR, photopic luminescence response; PF, photopic flicker; SA, scotopic adaptation; dB, decibel; min, minutes.

Effects of CS/HA- EPOβ nanoparticles

ERG was also used to evaluate the evolution of the retinal electrical activity after glaucoma induction, performed in timepoints 3, 7, 14 and 21 days, both in treated and in control groups, in order to assess the neuroprotective effects of CS/HA-EPOβ nanoparticles in the retina. Analyzing the results (Table 18), it is noticeable that the treated group (T) had higher b-wave amplitudes than the control group (C) from day 7 till day 21, although these differences were not statistically significant ($p > 0.05$). Differences were more evident at the end of the study (21 days) particularly in scotopic conditions. The mean b-wave of the SLR (5 dB) was 341 ± 55 μV in the treatment group and 257 ± 80 μV in the control group, while the mean b-wave of the SA (32 min) was 198 ± 51 μV in the treatment group and 145 ± 39 μV in the control group.

Table 18: ERG results of the OD after glaucoma induction: b-wave mean amplitudes recorded in a single step of each ERG part, presented as mean ± SD in microvolts (μV). ERGs performed in the treatment (T) and control (C) groups 3, 7, 14 and 21 days after glaucoma induction.

	b-wave (μV)							
	3 days		7 days		14 days		21 days	
	T	C	T	C	T	C	T	C
SLR (5 dB)	124 ± 66	123 ± 47	216 ± 90	212 ± 97	247 ± 91	233 ± 80	341 ± 55	244 ± 80
PA (16 min)	64 ± 24	67 ± 23	95 ± 25	82 ± 18	104 ± 24	102 ± 46	125 ± 50	115 ± 68
PLR (5 dB)	71 ± 19	73 ± 21	93 ± 48	84 ± 23	118 ± 59	107 ± 35	129 ± 42	118 ± 32
PF (0 dB)	51 ± 23	52 ± 17	76 ± 51	58 ± 33	89 ± 19	82 ± 43	97 ± 52	94 ± 29
SA (32 min)	82 ± 59	83 ± 38	125 ± 45	103 ± 40	162 ± 32	135 ± 44	176 ± 65	139 ± 41

SLR, scotopic luminescence response; PA, photopic adaptation; PLR, photopic luminescence response; PF, photopic flicker; SA, scotopic adaptation; dB, decibel; min, minutes.

When studying the differences between the timepoints T3 (retinal damage baseline), T7, T14 and T21, significant differences between treated and control groups were found. Mean values were analyzed (n=4 per group/ timepoint) and statistically significant differences ($p < 0.05$) were checked in each step of the ERG. Table 19 summarizes the comparison between groups/ timepoints.

Comparing day 3 with day 7, statistically significant differences ($p < 0.05$) were detected in the treatment group in the majority of the SLR exams (from –25 dB to 5 dB), while in the control group the difference was significant only at –5 dB and 0 dB. Also, the treated group

showed significant differences ($p < 0.05$) in almost all SA exams (from 0 to 16 min), while in the control group the differences were significant at steps 0, 2 and 4 min.

Comparing day 3 and day 14, statistically significant differences ($p < 0.05$) in the SLR were maintained between –25 dB to 5 dB in the treated group, and in the control group the significance was observed from –10 dB to 0 dB. Both groups presented statistically significant differences at 0 dB in the PF. In the SA step, significant differences ($p < 0.05$) in the treated group were found during the entire procedure (0-32 min), and in the control group throughout the majority of the protocol (0-16 min).

Finally, comparing day 3 with day 21, the treated group presented significant differences ($p < 0.05$) in the whole SLR step (from –35 dB to 5 dB), while in the control group the difference was significant from –25 to –5 dB. Both groups presented significant differences ($p < 0.05$) in all SA examinations (0-32 min). Considering photopic conditions, treated groups showed statistically significant differences ($p < 0.05$) in the PA (8 and 16 min), in the PLR (0 and 5 dB) and PF (0, –5, –10 dB), while the control group solely maintained the significant differences in PF at 0 dB.

Table 19: ERG comparison between timepoints T3 and T7, T14 and T21 after glaucoma induction in the OD, both in treated and control groups. Results show the ERG steps (in dB or min) with statistically significant differences ($p < 0.05$) between timepoints, regarding the b-wave.

ERG steps	3-7 days		3-14 days		3-21 days	
	T	C	T	C	T	C
SLR (dB)	–25 –20 –15 –10 –5 0 5	–5 0	–25 –20 –15 –10 –5 0 5	–10 –5 0	–35 –30 –25 –20 –15 –10 –5 0 5	–25 –20 –15 –10 –5
PA (min)	NS	NS	NS	NS	8 16	NS
PLR (dB)	NS	NS	NS	NS	0 5	NS
PF (dB)	NS	NS	0	0	0 –5 –10	0
SA (min)	0 2 4 8 16	0 2 4	0 2 4 8 16 32	0 2 4 8 16	0 2 4 8 16 32	0 2 4 8 16 32

NS - No statistically significant differences

T, treated groups; C, control groups; SLR, scotopic luminescence response; PA, photopic adaptation; PLR, photopic luminescence response; PF, photopic flicker; SA, scotopic adaptation; dB, decibel; min, minutes.

Even though overall results showed in table 18 presented no statistically significant differences ($p < 0.05$) between the treated and the control groups, there was a tendency for b-wave amplitudes to increase with time, with the treatment group presenting higher values than the control group. The treatment group demonstrated more consistent results towards retinal improvement, and maintained a tendency for faster retinal recovery in both scotopic and photopic conditions (Table 19). Although no significant differences ($p > 0.05$) were found in the a-wave between timepoints, the same tendency for an increase in a-wave's amplitude and quicker retinal improvement was observed in the treated group. Figure 56 illustrates some examples of b-waves from the treatment group at 3 days and at 21 days after glaucoma induction.

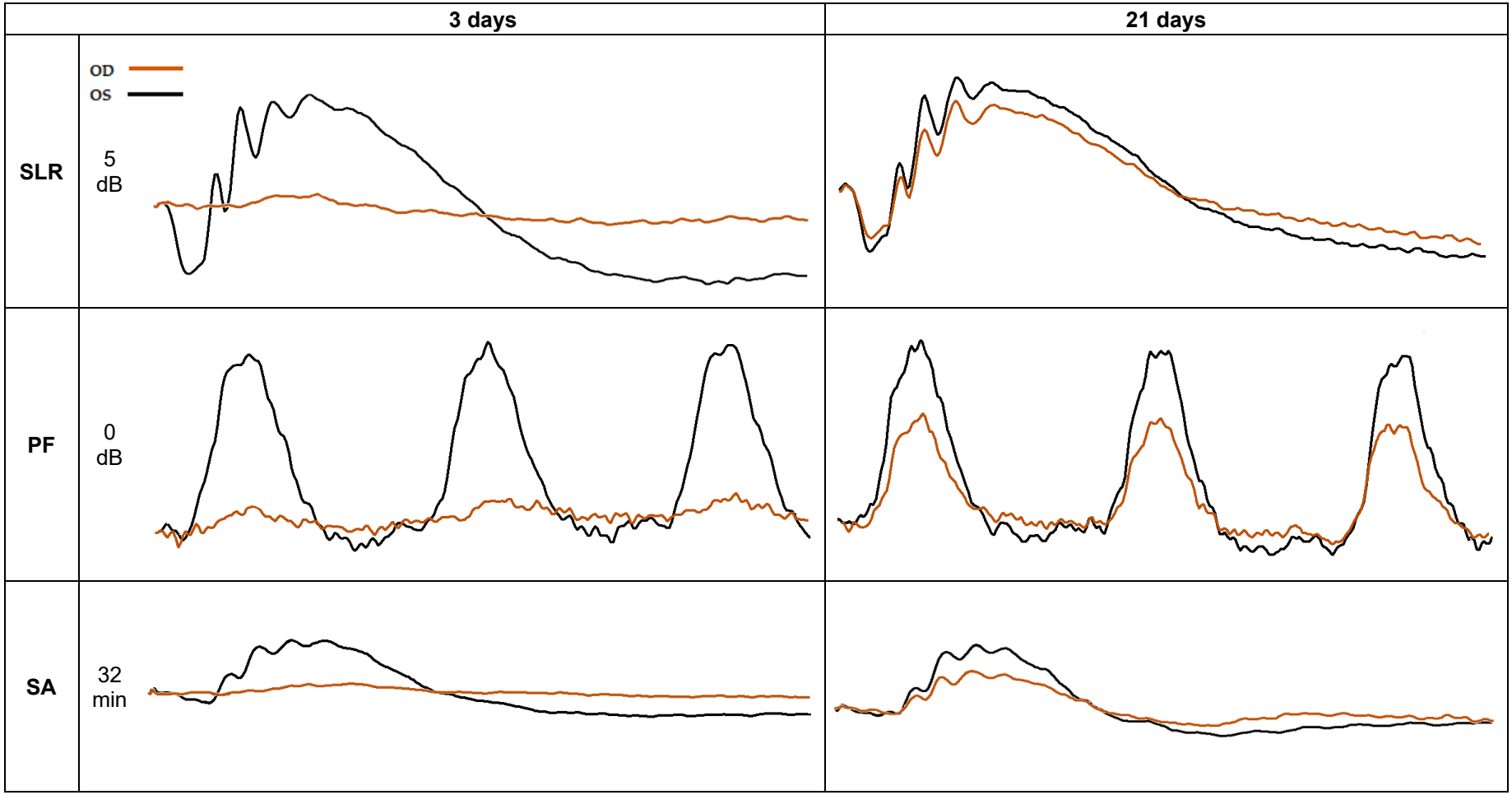

Figure 55: ERG waveforms of the OD (orange) and the OS (black) recorded at day 3 and day 21 after the glaucoma induction, from the treatment group. SLR, scotopic luminescence response; PF, photopic flicker; SA, scotopic adaptation; OD, right eye; OS, left eye.

6.4.4. Histologic evaluation

Retinal thickness

Measurements of retinal thickness were performed in OD cross sections stained with HE and results are presented in table 20 and in figure 57. There was a gradual improvement in retinal thickness in treatment and control groups from day 7 to day 21, which might indicate a process of retinal regeneration in both groups. Yet, animals from the treatment group presented a more pronounced recovery in retinal thickness when compared to the control group, these differences being statistically significant ($p < 0.05$). Overall, histological evaluation yielded a more expressive retinal recovery in the treated group versus the control group.

Table 20: Retinal thickness measurements (µm) of the OD from treatment and control groups at 7, 14 and 21 measured in a distance between 500 µm and 1500 µm from the optic nerve ($p < 0.05$).

	Treatment	Control
7 days	104.3 ± 21.1 µm	92.3 ± 13.3 µm
14 days	122.2 ± 13.2 µm	110.8 ± 7.0 µm
21 days	145.6 ± 22 µm	120.2 ± 10.6 µm

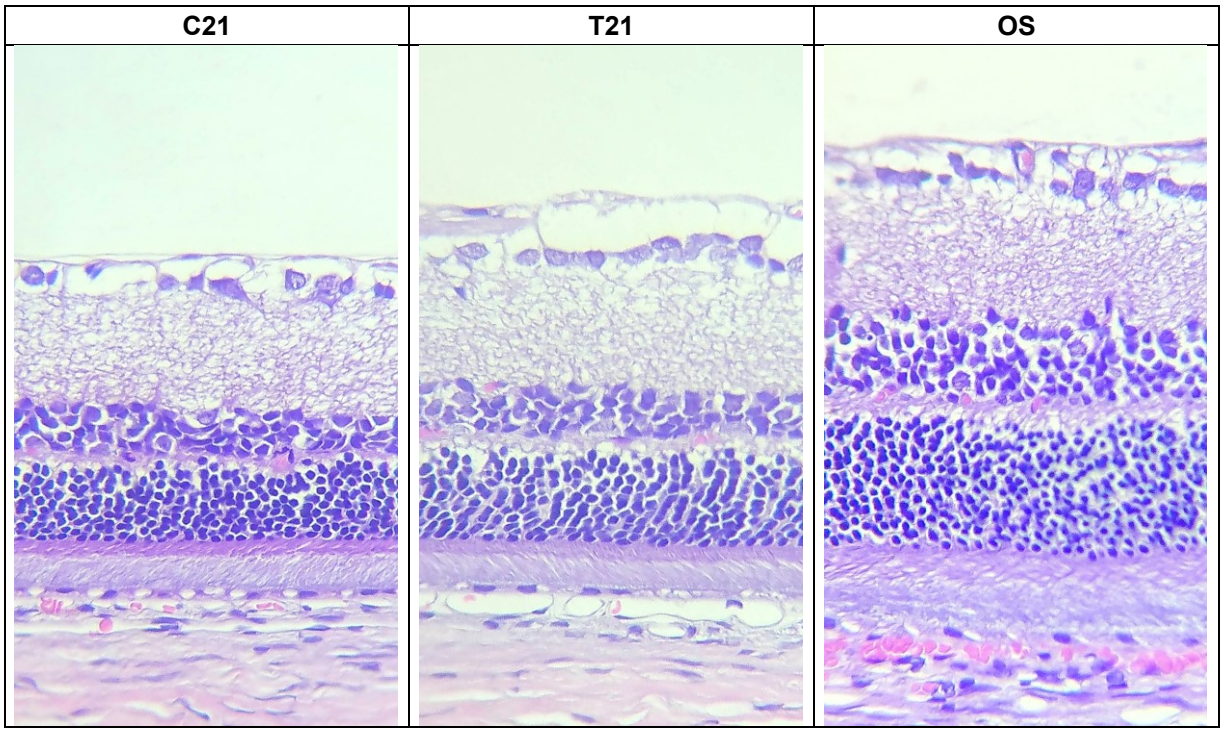

Figure 56: Photomicrographs of retinal sections from the OD, 21 days after glaucoma induction, from control (C21) and treatment (T21) groups, and from a non-glaucomatous eye (OS). We can observe

that the recovery in retinal damage was more pronounced in the treated group. Hematoxylin and eosin staining, 40× magnification.

Immunofluorescence

Immunofluorescence was performed in cross sections from the OD and OS of the treatment group. EPOβ was detected only in the OD, no EPOβ being observed in the OS of any animal. The number of fluorescent dots (EPOβ) in the ocular tissues was fairly stable throughout the study, although it presented a slight decrease in group T21. EPOβ was detected in the retina from groups T7, T14 and T21, distributed in the GCL, INL and ONL (Figure 58). EPOβ was also observed in the corneal stroma (T14), corneal endothelium, ciliary body (T21), vitreous and sclera. The presence of EPOβ in the corneal stroma and in the anterior ocular segment denoted a transcorneal permeation of EPOβ and the signal was still present 21 days after the administration of the nanoformulation, which suggests a sustained delivery of EPO with this nanoformulation.

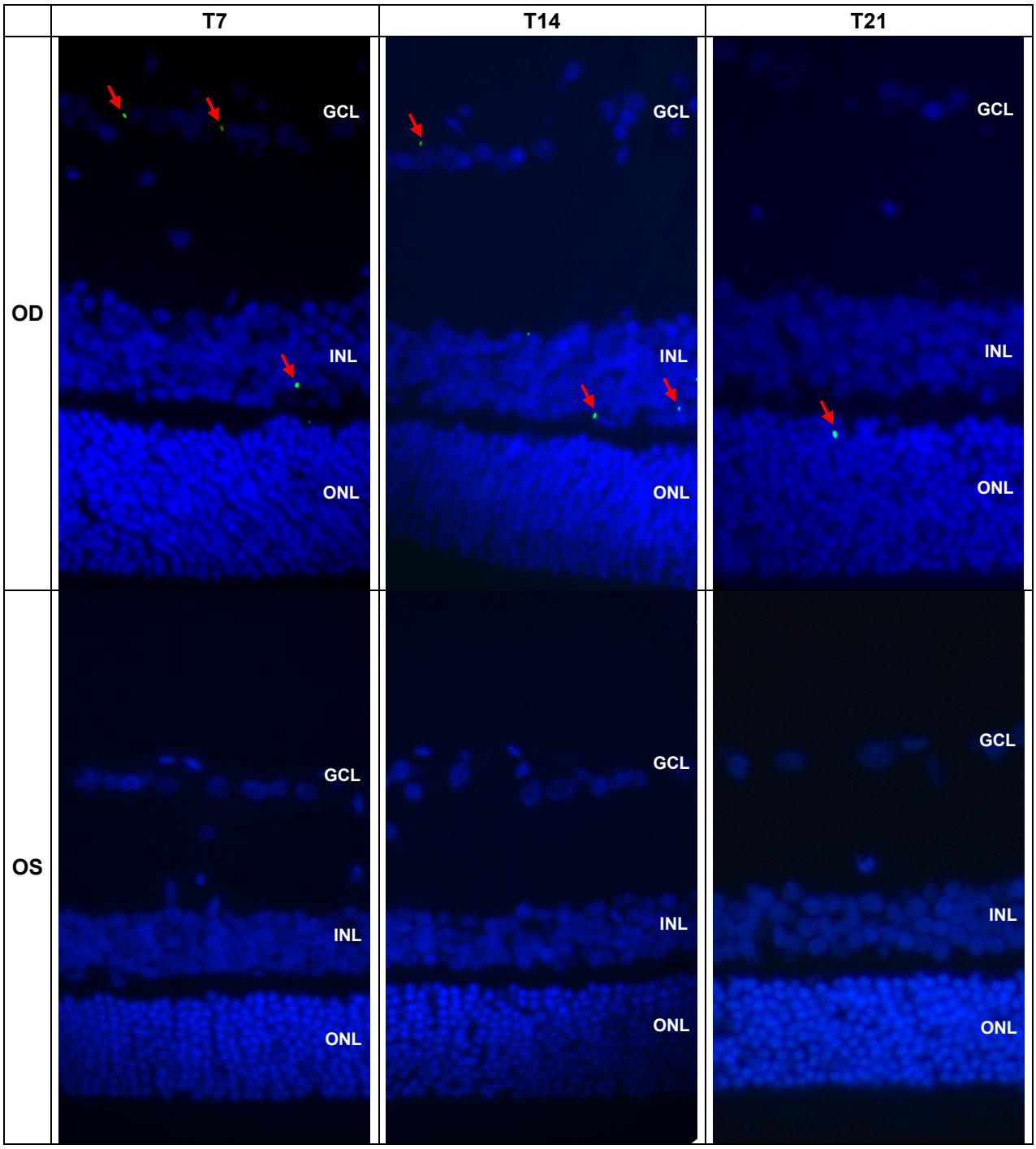

Figure 57: Immunofluorescence photomicrographs showing cross sections of the OD (treated eye) and OS (control eye) in the treatment groups T7, T14 and T21 (magnification 40×). Images show the merging of green and blue filters. Red arrows indicate EPOβ stained in green and cell nuclei are stained in blue with DAPI. GCL, ganglion cell layer; INL, inner nuclear layer; ONL, outer nuclear layer.

Apoptosis

The retina was the only ocular tissue to present positive results corresponding to brown intracytoplasmic staining in the apoptosis evaluation. The cleaved caspase-3-positive cells were diffusely located in the neurosensory retina of group C7 (n=4), in the ganglion cell layer (GCL), outer nuclear layer (ONL), and inner nuclear layer (INL), this last layer being the one with the highest number of positive cells (Figure 55). Thus, we could only detect apoptosis in the animals from the control group, with non-treated glaucoma, which could mean that EPO decreased the rate of apoptosis in the treated group. Nevertheless, the obtained results are not expressive enough to draw this conclusion.

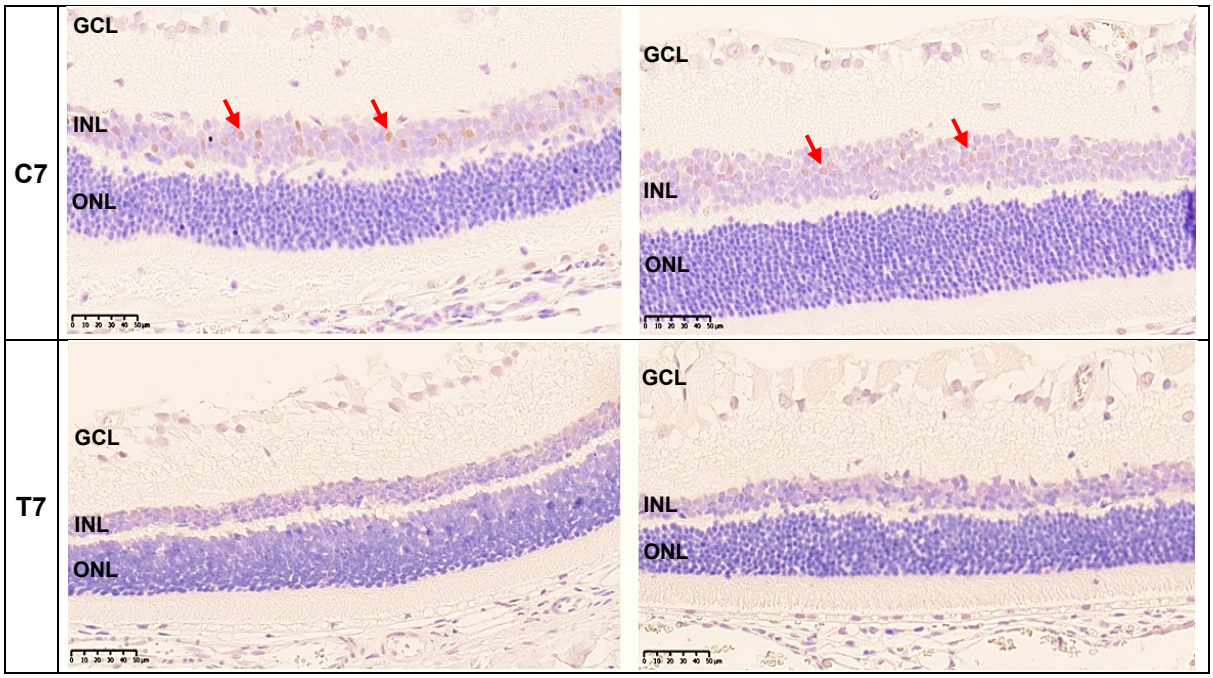

Figure 58: Photomicrographs of retinal sections submitted to immunohistochemistry for apoptosis detection (cleaved caspase-3) from treatment (T7) and control (C7) groups, at day 7 after the glaucoma induction, at 40× magnification. Intracytoplasmic brown material (red arrows) indicates a positive result. GCL, ganglion cell layer; ONL, outer nuclear layer; INL, inner nuclear layer.

6.5. Discussion

Current glaucoma management is based on pharmacological agents and surgical procedures to decrease aqueous humor production or increase its outflow. Yet, research direction is shifting towards neuroprotection as a state-of-the-art glaucoma adjuvant therapy. EPO's neuroprotective and antiapoptotic effects in ocular tissues were recently described in a comprehensive review article (Feizi et al. 2021) but before that other studies have also supported additional functions for EPO other than the classical hematopoietic role (A. K. Junk et al. 2002). Additionally the retina has been described as an EPO secreting location with the expression of EPO receptors (Hernández et al. 2006) (García-Ramírez et al. 2008; Ott et al. 2015). Moreover, EPOβ in aqueous solution has already revealed neuroprotective effects in the retina of glaucomatous rats after its subconjuctival injection (Resende et al. 2018).

All these data challenged our team and we decided to put our efforts in the development of a nanoformulation based on mucoadhesive compounds to transport EPOβ into the ocular medium. To accomplish this goal, we developed CS/HA-EPOβ nanoparticles and tested the nanoformulation in healthy Wistar Hannover rats using both the subconjunctival (Silva et al. 2022) and topical (Chapter 5) routes of administration, paving the way for the next logical step of this research: topical administration of EPO through a non-invasive, accessible to all and easy to administer eyedrop system. In this study we aimed to evaluate the effects of our new nanoformulation in an animal model of glaucoma. In this pre-clinical study, we topically administered CS/HA-EPOβ nanoparticles in order to evaluate the permeation of EPO in glaucoma conditions as well as the neuroprotective and neuroregenerative effects of the nanoformulation at retinal level.

Glaucoma is a painful condition, so the use of analgesia was mandatory to assure animal wellbeing. Meloxicam was selected due to its extended action of pain relieving for 24 hours, and the absence of contra-indications in the literature that could compromise our results. Pain assessment according to the Rat Grimace Scale was classified as not present "0" in all parameters. Animals demonstrated a completely normal behavior throughout the study, suggesting that the analgesic protocol was effective. Furthermore, according to our previous subconjunctival (Silva et al. 2022) and topical (Chapter 5) studies, the nanocarriers were well tolerated and safe. This led us to believe that the discrete ophthalmological signs observed corresponding to superficial keratitis, mild degree of conjunctival hyperemia in the operated eyes for 24 to 48 hours and the moderate chromodacryorrhea observed right after the vein coagulation were probably adverse side effects related to glaucoma induction and not due to the nanoformulation administration.

At the beginning of the study, the mean IOP value for both groups was 17.3 ± 1.3 mmHg, which is within reference range for healthy Wistars Hannover rats (18.4 ± 0.1 mmHg)

(Wang et al. 2005). Immediately after glaucoma induction, IOP of the OD increased on average 3.6 folds above physiological values, so cauterization of the three episcleral veins was effective in inducing glaucoma in both treatment and control groups, as previously described (Shareef et al. 1995; Pang and Clark 2007). The raise in IOP values was remarkable in both groups, yet values returned to normal earlier than expected, which could be due to a sudden increase in blood outflow in the remaining episcleral vein, promoting the drainage of the aqueous humor. The cauterization of 4 episcleral veins (Shareef et al. 1995) or other methods described in the literature, such as the circumlimbal suture (Liu et al. 2015), could be considered in the future to enable a more sustained IOP increase. The IOP of the OS was not influenced by the glaucoma induction in the OD, as mentioned in other studies (Shareef et al. 1995; Pang and Clark 2007; Johnson and Tomarev 2010). Moreover, the average IOP measurements were similar in both the treatment and control groups, meaning that EPOβ did not influence IOP values, as already had been reported before (Resende et al. 2016; Resende et al. 2018).

ERG traces were an indirect way of proving that glaucoma induction had been effective, since they represent the activity of different retinal cells to light stimuli (Weymouth and Vingrys 2008), indicating the grade of retinal impairment. The currently used ERG protocol has already been described by others (Rosolen et al. 2005; An et al. 2012) and our team has already used it in previous studies (Silva et al. 2022; Chapter 5). In the dark-adapted ERG in rats, retinal response to dim flashes is mainly composed by negative potentials thought to be originated in the inner retina, next to the bipolar cells (Bui and Fortune 2004). This response is called scotopic threshold response (STR) and is dominated by the retinal ganglion cells (RGC), which also contribute to the photopic b-wave. RGC damage is directly related to STR and photopic b-wave diminishing (Bui and Fortune 2004). One study reports a STR for rats at $\phi \approx 5 \times 10^{-3}$ (-2.30 log cds/m^{-2}) (Naarendorp et al. 2001), which could be theoretically feasible for us to measure since our SLR begins at -3.02 log cds/m^{-2}. However, the ERG protocol used in this study was not developed to detect the STR, therefore the photopic b-wave was a more suitable tool to assess the RGC status. Simplifying the ERG interpretation, the b-wave corresponds to the activity of the bipolar and Müller cells, and the a-wave corresponds to hyperpolarization of cones in the photopic steps and rods in the scotopic steps of the exam (Rosolen et al. 2005; Skaat et al. 2011). The considerably low a and b waves recorded from the OD after the microsurgery (day 3) confirmed retinal damage in both groups and, consequently, the success of glaucoma induction. As both waves substantially declined, it indicated that damage occurred in the inner as well as in the outer retina of glaucomatous eyes, which is in accordance with the literature (Ou et al. 2022). ERG recordings from the OS were kept within normal range after the cauterization, showing no influence of the procedure on the contralateral eye, as previously reported (Johnson and Tomarev 2010). In addition, both treatment and control groups

presented similar changes in amplitudes and waveforms, denoting the accuracy of the microsurgical procedure.

To assess the effects of the CS/HA-EPOβ nanoparticles in retinal electric activity, ERG measurements were performed at timepoints 7, 14 and 21 days after glaucoma induction. Overall, electrical retinal response increased with time in both treatment and control groups. Despite the treatment group presenting a higher a-wave and b-wave amplitudes compared to the control group, especially in the scotopic exams, those differences were not statistically significant. However, there were significant differences between day 3 and day 7, 14 and 21, especially in the b-wave from the scotopic exams, precluding that retinal improvement happened earlier and more consistently in the treated animals. In the photopic exams, statistically significant differences were observed only in few steps of PF, PA and PLR and, once again, earlier on in the treatment group. Thus, a tendency for faster retinal recovery was seen in the treatment group and the lack of statistical significance might be explained by the reduced sample size at each timepoint (n=4). Although this number was considered suitable regarding ethical requirements, the statistical power (80%) and the significance level (0.05; two-tailed), we believe that by adding 2 animals in each group (n=6) we could have obtained more statistically significant results without major implications in animal welfare. Moreover, IOP lowering after the cauterization might have contributed to the retinal recovery also observed in the control group. It has been reported by others that in rats very short-term retinal injury caused by an elevated IOP can be completely reversible within 3 weeks (Abbott et al. 2014). Taking this into consideration, in future studies we could modify our glaucoma inducing technique to better mimic the chronic disease evaluating CS/HA-EPOβ nanoparticles neuroprotective and neuroregenerative effects on a more long-term basis.

The precocious IOP dropping might also justify the differences found between the photopic and scotopic exams. It is known that the b-wave represents the activity of rod-bipolar cells (RBC) and Müller cells in scotopic conditions (Gallego-Ortega et al. 2020) and RGC in photopic conditions (Bui and Fortune 2004), while a-wave in photopic conditions indicates the activity of cone-bipolar cells (CBC) (Gallego-Ortega et al. 2020). Studies concluded that RBC are less susceptible to acute IOP increases when compared to RGC and CBC. Thus, photopic ERG exams are particularly affected by acute IOP elevations, where CBC and RGC show more cell loss and slower recovery than RBC (Bui and Fortune 2004; He et al. 2006; Gallego-Ortega et al. 2020). This is consistent with our ERG results, in which the photopic responses showed less improvement than the scotopic ones, being this last one probably related to the RBC recovery.

Glaucoma causes death of retinal cells, specially of the RGC (Cordeiro et al. 2004), whose apoptotic process culminates in cell atrophy, chromatin condensation and nuclear DNA fragmentation (Kroemer et al. 2007), potentially leading to a decrease in retinal thickness

(Abbott et al. 2014). In this study, the retinas of the operated eyes presented a generalized thinning compatible with the disease process. Retinas progressively recovered thickness throughout the experiment in both treatment and control groups, although in the treated rats this improvement was significantly more marked than in the control group ($p < 0.05$), representing a greater retinal regeneration. This improvement in retinal thickness is in agreement with previous studies that used EPOβ in aqueous solution through subconjunctival administration in glaucomatous rats (Resende et al. 2018). Likewise, these findings are consistent with the faster retinal improvement observed in the ERG and apoptosis results of the treated group. EPO is being studied in other models of ocular diseases, such as diabetic retinopathy, retinal vein occlusion, optic neuritis and ischemic optic neuropathy, also aiming at retinal and optic nerve protection and regeneration (Feizi et al. 2021).

Regarding the immunofluorescence assays, the amount of EPOβ detected in the OD was rather constant through time and EPOβ was still present in the retina in group T21. In previous topical physiological study, CS/HA-EPOβ nanoparticles were administered during 30 minutes, 1 drop every 5 minutes (Chapter 5), while in this topical glaucoma study, nanoparticles were administered during 3 days (1 drop, 3 times a day). Thus, it is understandable that EPOβ permeation followed a more sustained pattern in the present study. In addition, the amount of EPOβ observed in ocular tissues in this study was lesser than the timepoints 7, 14 and 21 days in the topical physiological study (Chapter 5). Some factors could contribute to this difference. Not only the topical route of administration lead to considerable drug loss (Agrahari et al. 2016), but also glaucoma causes breakdown of blood-ocular barriers (BAB and BRB) which could amplify the clearance of EPOβ, resulting in lower intraocular EPOβ concentration when compared to non-glaucomatous animals (Shen et al. 2014; Agrahari et al. 2016). Moreover, the microsurgery for glaucoma induction might have enhanced the natural ocular defense mechanisms, such as reflex blinking and tear production/ turnover (Ghate and Edelhauser 2008), which would promote a washout effect, decreasing EPOβ permeation. In addition, considering that we proved that EPOβ can reach the retina in 12 hours after topical administration of CS/HA-EPOβ nanoparticles (Chapter 5), a large amount of EPOβ could be lost in 7 days, which is the first euthanasia timepoint in the glaucoma study. EPOβ was observed in several ocular tissues, including the retinal GCL, INL and ONL, similarly to our physiological study (Chapter 5). This reinforces the present ERG, apoptosis and retinal measurement results, indicating that the effect of the CS/HA-EPOβ nanoparticles in the retina observed in the treatment group were due to the presence of EPOβ. Likewise, Resende et al. (2018) concluded that EPOβ promoted beneficial effects in the retina of glaucomatous animals by subconjunctival route (Resende et al. 2018). A transcorneal and sustained permeation of EPOβ through 21 days was observed in the present study, as EPOβ was detected in the corneal stroma in group T14 and in the anterior segment in the group T21. This was also found

in our physiological study (Chapter 5), and supports the mucoadhesive power of the CS/HA-EPOβ nanoparticles. Lastly, no EPOβ was observed in the OS of any animal, which is in accordance with our previous studies (Chapter 5), meaning that the hypertensive condition did not cause a contralateral absorption of EPOβ.

Apoptosis is a complex mechanism of cell death in glaucoma, occurring by intrinsic and extrinsic pathways, that culminate in cell atrophy, chromatin condensation and DNA fragmentation (Kroemer et al. 2007). The intrinsic intracellular pathway involves mitochondrial permeabilization and the release of cytochrome C (Kroemer et al. 2007), whose presence outside the mitochondria enables the activation of caspase-9, which catalyzes the proteolytic activation of caspases-3, -6, and -7 (Cain et al. 2002). Cleaved caspase-3 is a standard apoptotic marker for RGC and, in a study using a rat model of retinal ischemia and reperfusion injury, positive cells for cleaved caspase-3 were found diffusely in the GCL, INL and ONL (Tan et al. 2020). This is accordance with our results, in which the cleaved caspase-3-positive cells were identified in the retina of animals from group C1 (7 days) with non-treated glaucoma. Although apoptosis was solely identified in that group, this is in accordance with our ERG results, indicating that the control group seemed to exhibit a delay in retinal recovery when compared to the treatment group. Therefore, these findings might corroborate the antiapoptotic effects of EPOβ. A recent review article on the ophthalmological applications of EPO describes several neuroprotective effects of this protein by means of anti-apoptotic, anti-inflammatory and antioxidant mechanisms (Feizi et al. 2021).

6.6. Conclusion

Beforehand our team has developed CS/HA-EPOβ nanoparticles and administered them through both subconjunctival and topical ocular routes in healthy rats, allowing for EPOβ retinal delivery in physiological conditions. Being so, we considered opportune to explore the topical route of CS/HA-EPOβ nanoparticles administration in glaucomatous rats and assess their safety and potential neuroprotective effects. The present study revealed that ocular topical administration of this nanoformulation allowed for EPOβ permeation, inclusive through the transcorneal pathway, and ultimately reaching the inner retina. Improvements in retinal electrical activity, in retinal thickness and apoptosis reduction happened earlier and more expressively in the treated animals. Not only did we prove that EPOβ could be delivered to the retina, in glaucomatous rats, by topical administration of CS/HA-EPOβ nanoparticles, but we have also demonstrated that EPOβ elicited neuroprotective effects in these experimental conditions.

No other studies on topical ocular administration of nanocarriers with neuroprotective drugs in a glaucoma animal model have been reported so far in the literature. Although adjustments in the experimental design should be addressed to lead to more statistically significant differences between treated and control groups, results of this preclinical study were promising and contribute to innovative insights into the field of ocular drug delivery. Our results open the window to the possibility of delivering neuroprotective compounds by topical route of administration targeting the posterior segment of the eye, which could become a user-friendly, cheap, safe and effective way to help preserving visual acuity in ischemic or degenerative retinopathies, namely in glaucoma, both in Man and in animals.

CHAPTER 7

General discussion, study limitations and future perspectives

General discussion

Glaucoma is considered a public health problem since it is a chronic and uncurable neurodegenerative disease, remaining one of the leading causes of blindness worldwide (Kingman 2004). The underlying mechanisms of RGC degeneration and death are intricate, and the IOP, when increased, is considered not only the most important risk factor, but also the only controllable one (Quigley 2011). Therefore, presently glaucoma treatment is based on the balance between the aqueous humor outflow and inflow, by means of pharmacological and surgical procedures, yet not preventing retinal degeneration, which ultimately may progress until blindness (Almasieh et al. 2012). To avoid the neurodegeneration associated to glaucoma, other therapeutic approaches should be considered, namely neuroprotective strategies.

Neuroprotection involves the preservation of neuronal structure and function, in order to maintain or even improve visual function. When RGCs are damaged, photoreceptors may be stimulated by light but the visual information does not reach the midbrain for processing and interpretation (Pardue and Allen 2018). Neuroprotective therapies may hinder apoptosis of RGCs and optic nerve damage normally associated to glaucoma, by preventing oxidative damage and ischemia (Vishwaraj et al. 2022). Neuroprotection could provide months or years of visual capacity, allowing people to maintain or regain independence and quality of life (Pardue and Allen 2018). Despite the hematopoietic role of EPO, this glycoprotein demonstrated neuroprotective effects in ophthalmic diseases, denoting anti-inflammatory, antioxidant and anti-apoptotic properties. EPO is able to preserve glia cells, to decrease glutamate and ROS, to enhance blood flow into damaged tissues, to recruit stem cells, to prevent caspase-3-like activities and the release of inflammatory cytokines, amongst other features (Tsai et al. 2007; Wang et al. 2009; Shirley Ding et al. 2016; Feizi et al. 2021). Ophthalmological disorders such as diabetic retinopathy, retinal vein occlusion, optic neuritis and ischemic optic neuropathy, are under research using EPO as part of the therapeutic approach (Feizi et al. 2021)

Based on the fact that our team had already pursued a line of investigation based on the use of EPOβ as a neuroprotective strategy in glaucoma (Resende et al. 2018), we considered opportune to defy some concepts on ocular drug delivery and explore a non-invasive route of administration for EPOβ – the topical route. Considering the challenges of

topical ocular administration targeting the posterior segment of the eye, our team acknowledged the need to increase the intraocular bioavailability of EPOβ. Since we had already proven that EPOβ could permeate porcine conjunctiva, sclera and cornea *ex vivo* (Resende et al. 2017), the most feasible approach seemed to be the improvement of EPOβ's contact time with the ocular surface after topical administration, in an attempt to enable a sustained EPOβ permeation through ocular membranes. Mucoadhesion seemed an interesting and achievable option to enhance pre-corneal resident time of EPOβ, characterized by attractive forces between a compound and mucus or mucous membrane (Smart 2005).

To achieve the therapeutic effect with eye drops, a frequent administration of highly concentrated solutions is required to counterbalance the diluting effect caused by tears, the mechanical removal cause by blinking, among other ocular defense mechanisms (Achouri et al. 2013). Also, local and systemic side effects may come from frequent instillation of highly concentrated drugs (Ludwig 2005). On the other hand, topical ocular drug delivery using nanotechnology and mucoadhesive polymers promotes a controlled and sustained drug release, while maintaining drug stability and low toxicity. Colloidal nanosystems, such as liposomes, noisome, nano emulsions, dendrimers and nanoparticles, have advantages and limitations in their pharmacological use and their production methods. Therefore, amongst the wide range of nanosystems and mucoadhesive materials, the selection of CS and HA for the development of nanoparticles was based on studies that proved their excellent biocompatibility, stability, versatility and mucoadhesive strength (Silva et al. 2021), and their potential synergic effect (Silva et al. 2017). Colloidal nanosystems with bioadhesive properties are the ultimate technology designed to surpass the drug delivery challenges in ophthalmology, as they protect the drug from the surroundings and increase its permeation across ocular tissues (Ameeduzzafar et al. 2016). In chronic and progressive diseases, such as glaucoma, this feature is even more valuable, as the patients' compliance may fade with continuous treatment and the mucoadhesive nanosystem might decrease the frequency of administration and even enhance its therapeutic effect.

Bearing this in mind, our team aimed to develop a nanoparticulate system with CS and HA to carry EPOβ to the ocular medium (Silva et al. 2020). The ionic gelation method, chosen to produce the nanoparticles, was the simplest possible to avoid alterations in EPOβ's structure. The most suitable HA was selected to create nanoparticles with size, ZP and PDI compatible with physicochemical stability and *in vivo* tolerance, as well as high mucoadhesive power. The *ex vivo* permeation study indicated a higher permeation of EPOβ when using the nanoformulation CS/HA-EPOβ compared to the commercial solution NeoRecormon®, whose *ex vivo* permeation study has already been conducted by our team (Resende et al. 2017). These results motivated us to proceed to the *in vivo* assays using in healthy Wistar Hannover rats. Both subconjunctival and topical routes of ocular administration of the newly developed

nanoformulation were effective, allowing EPOβ permeation through the ocular membranes, reaching the retina, without adverse side effects (Silva et al. 2022; Chapter 5). Moreover, the topical study also demonstrated that there was *in vivo* transcorneal EPOβ permeation (Chapter 5).

These results motivated us to pursue to our final goal. In the following study, glaucoma was surgically induced in Wistar Hannover rats by microsurgical cauterization of three episcleral veins in one eye and afterwards CS/HA-EPOβ nanocarriers were applied through the topical route. ERG and apoptosis results of this pre-clinical study indicated a tendency for faster retinal recovery in the treated group when compared to the control group, which received empty CS/HA nanoparticles. Retinal thickness has clearly increased more pronouncedly in the treatment group after the initial phase of retinal atrophy, reinforcing the potential neuroprotective effects of EPOβ. Moreover, EPOβ signal was detected by immunofluorescence in all retinal layers, corroborating the permeation of the protein after topical administration of the nanoformulation. Sustained permeation was also confirmed by the presence of EPOβ in the ciliary body 21 days after glaucoma induction, denoting the mucoadhesive power of the CS/HA-EPOβ nanoparticles. To our knowledge this was the first pre-clinical study involving topical ocular administration of a nanoformulation carrying a neuroprotective compound that could reach the retina and exert its neuroprotective effects, lifting the veil for the possibility of new forms of topical drug delivery to the posterior segment of the eye.

In conclusion, our team managed to develop a stable, non-toxic and mucoadhesive system of CS/HA-EPOβ nanoparticles designed for ocular drug delivery, that showed a better performance in the *ex vivo* permeation study than the EPOβ aqueous solution alone. We demonstrated that this nanoparticulate system with 1000 IU of EPOβ, administered through subconjunctival and topical ocular routes in healthy Wistar Hannover rats, could efficiently deliver EPOβ to all retinal layers, with no local or systemic secondary effects. We also proved that there was transcorneal permeation of EPOβ after topical instillation and that the vitreous was not a relevant barrier to the intraocular distribution of EPOβ in rats. Finally, we discovered that topical administration of CS/HA-EPOβ nanoparticles enabled the delivery of EPOβ to all retinal layers in rats with induced glaucoma. Moreover, by this route of administration, EPOβ's neuroprotective/ antiapoptotic effects in the retina were observed through ERG, apoptosis detection and histological assessments. These promising results could preclude the search for new drug delivery methods to the posterior ocular segment through topical ocular administration.

Study limitations and future perspectives

In spite of the valuable information retrieved from this research, that are some issues that could be managed in the attempt to achieve better results. The %DL of the CS/HA-EPOβ nanoparticles was 17.4±0.1 %, which is in the range of the average values for %DL found in the literature for CS based nanoparticles produced by self-assembling (Quiñones et al. 2018). For instance, the %DL of CS nanoparticles carrying ibuprofen and dipyridamole were 14.18% and 13.03%, respectively (Liu and Zhao 2013); paclitaxel loaded modified glycol-CS nanoparticles had %DL from 9.8 to 23.9 % (Saravanakumar et al. 2009); cholesterol-CS nanoparticles loaded with epirubicin presented %DL around 14% (Wang et al. 2007). However, the %EE achieved in our study, 38.4 ± 0.3 %, was slightly under the average to be considered a high %EE. For example, nanoparticles of CS-Dextran sulfate-polyelectrolyte complexes containing insulin presented %EE varying from 72 ± 3% to 85.4 ± 0.5% depending on CS/ Dextran mass ratio (Sarmento et al. 2006). Also, nanoparticles made of carboxymethyl-CS-polyelectrolyte complexes combining ionotropic gelation and complex coacervation, had %EE around 70.5% (Mourya et al. 2010). On the other hand, vitamin B2 loaded nanoparticles created by ionotropic pre-gelation of alginate followed by complexation with CS showed %EE of 56 ± 6% but %DL of 2.2 ± 0.6% (Azevedo et al. 2014). Moreover, CS nanoparticles carrying L-ascorbic acid and thymoquinone separately presented %EE of, respectively, 22.8 ± 3.2% and 35.6 ± 3.6% (Othman et al. 2018). Therefore, regarding our CS/HA-EPOβ nanoparticles, we consider that the optimization of the %EE would be more pertinent than increase the %DL, to allow for a more sustained release profile of EPOβ, but not mandatory. The formation of CS nanoparticles by ionotropic gelation is affected by the MW of CS, its degree of deacetylation and concentration, the type and amount of crosslinking agent (in our case, the HA), the mixing procedure and conditions, like pH and temperature (Warsito and Agustiani 2021). All these variables were considered and carefully managed in this study, for instance, the degree of CS deacetylation is already high (92%) which increases the %EE; the CS MW is low to facilitate the stability of the formulation; we experimented HA of different MW; we tested different CS:HA mass ratios, different solvents for HA, different pH values, until the particles had the aimed criteria. Nevertheless, we are always open for further optimization. An increase in the formulation viscosity could be feasible, but always considering the potential entrapment of the active principle in the nanoparticles.

Another issue is the number of animals per group, that could be increased to diminish the variability, allowing for the obtention of statistically significant differences between treatment and control groups in the glaucoma study. We have chosen n=4 per each timepoint of euthanasia based on the power analysis using GraphPad StatMate 2 (GraphPad® Software,

CA, USA): sample size for unpaired *t* test, with power of test of 80%, significance level of 0.05 and SD for ERG of 70 μV, which was estimated based on the physiological studies (Silva et al. 2022; Chapter 5), and considering the experience in ERG acquired along the experiments. Thus, for n=4 we had 80% power to detect a difference between means of approximately 164 μV with a significance level of 0.05 (two-tailed), which we considered adequate, also taking into consideration ethical issues of animal experimentation. However, by increasing the sample size in 2 animals (n=6) we could have obtained more significant results without major implications in animal welfare.

Regarding the glaucoma induction technique, we followed the procedure described in the literature by Shareef et al. (1995) who performed cauterization of 1 to 4 episcleral veins in rats (Shareef et al. 1995). In that study, with the cauterization of 3 episcleral veins, IOP elevated values faced a decline during the first week, followed by a plateau above physiological values for 2 months, corresponding to a mean value of nearly 29 mmHg at 2 months (Shareef et al. 1995). Also, the authors observed a selective retinal ganglion cell death in the histological assessment (Shareef et al. 1995), which helped in the decision of choosing this technique for our study. More recently, Resende et al. (2016 and 2018) used the same technique of 3 episcleral veins cauterization to induce glaucoma and despite the IOP reaching physiological values, or nearly, after a week, the decline in IOP was not so abrupt as in our study (Resende et al. 2016). To better simulate the chronic disease and allow for a follow-up beyond 21 days after treatment, the cauterization of 4 episcleral veins could be performed, but as Shareef et al. (1995) described pronounced proptosis, with consequent exposure keratopathy and corneal oedema secondary to the marked IOP elevation (Shareef et al. 1995), that procedure could lead to a counter-productive decompensation of the eye. An alternative method applied in rats by Liu et al. (2015) is the circumlimbal suture, which consists in a 8/0 nylon suture tied around the equator of the ocular globe, behind the limbus. The suture produced a mild chronic IOP elevation for 15 weeks (average increase of 65 ± 5%), and from 8 weeks on the alterations in the ERG related to RGCs loss were considerable (Liu et al. 2015). This technique seems feasible for future studies as it is minimally invasive and appears to produce low levels of inflammation, but it will require training and optimization.

Concerning the protein PK/ PD, PK ocular studies are classically performed in rabbits due to a higher similarity to human eyes than rodents (Löscher et al. 2022). In PK ocular studies, samples of tears, aqueous humor, vitreous, retina or other ocular fluids/ tissues are retrieved, in one or more timepoints depending on the samples characteristics, to determine drug's ocular concentration and distribution (Salama et al. 2016; Löscher et al. 2022). Despite the classical use of rabbits, in our research, we could have collected some ocular samples from the rats to better understand the PK of CS/HA-EPOβ nanoparticles, however, our focus was proving that EPOβ could reach the retina by topical instillation of CS/HA nanoparticles

and contribute with neuroprotection. Considering a long-term study, a prolonged administration of CS/HA-EPOβ nanoparticles for more than 3 days or in clustered administrations could be considered, nevertheless many studies use one single administration as models (Jiang et al. 2020; Rathore et al. 2020; Xing et al. 2021). In terms of PD, a larger amount of EPOβ in the CS/HA nanoparticles could be tested, first in physiological conditions and then in glaucomatous animals, in order to establish a dose-effect relations.

Our team believe that the outcome of this project will contribute with innovative insights into the field of Advanced Technologies for Drug Delivery in Ophthalmology. Also, the clinical approach of glaucomatous patients would clearly benefit from a user-friendly non-invasive neuroprotective treatment, that could avoid or hinder vision loss and improve visual acuity. Patients' compliance to a long-term treatment is a major issue in chronic diseases, and glaucoma is no exception. Therefore, topical instillation of neuroprotective agents targeting the posterior segment of the eye has proven to be a promising line of research, that is worth to pursue in the upcoming future.

References

Abbott CJ, Choe TE, Lusardi TA, Burgoyne CF, Wang L, Fortune B. 2014. Evaluation of retinal nerve fiber layer thickness and axonal transport 1 and 2 weeks after 8 hours of acute intraocular pressure elevation in rats. Investig Ophthalmol Vis Sci. doi:10.1167/iovs.13-12811.

Abdel-Rashid RS, Helal DA, Omar MM, El Sisi AM. 2019. Nanogel loaded with surfactant based nanovesicles for enhanced ocular delivery of acetazolamide. Int J Nanomedicine. doi:10.2147/IJN.S201891.

Abdelbary A, Salem HF, Khallaf RA, Ali AMA. 2017. Mucoadhesive niosomal in situ gel for ocular tissue targeting: in vitro and in vivo evaluation of lomefloxacin hydrochloride. Pharm Dev Technol. doi:10.1080/10837450.2016.1219916.

Abdelbary G. 2011. Ocular ciprofloxacin hydrochloride mucoadhesive chitosan-coated liposomes. Pharm Dev Technol. doi:10.3109/10837450903479988.

Abed N, Couvreur P. 2014. Nanocarriers for antibiotics: A promising solution to treat intracellular bacterial infections. Int J Antimicrob Agents. 43(6):485–496. doi:10.1016/j.ijantimicag.2014.02.009.

Abrego G, Alvarado H, Souto EB, Guevara B, Bellowa LH, Parra A, Calpena A, Garcia ML. 2015. Biopharmaceutical profile of pranoprofen-loaded PLGA nanoparticles containing hydrogels for ocular administration. Eur J Pharm Biopharm. doi:10.1016/j.ejpb.2015.01.026.

Abri Aghdam K, Soltan Sanjari M, Ghasemi Falavarjani K. 2016. Erythropoietin in ophthalmology: A literature review. J Curr Ophthalmol. 28(1):5–11. doi:10.1016/j.joco.2016.01.008. http://dx.doi.org/10.1016/j.joco.2016.01.008.

Achouri D, Alhanout K, Piccerelle P, Andrieu V. 2013. Recent advances in ocular drug delivery. Drug Dev Ind Pharm. 39(11):1599–617. doi:10.3109/03639045.2012.736515.

Adachi K, Kashii S, Masai H, Ueda M, Morizane C, Kaneda K, Kume T, Akaike A, Honda Y. 1998. Mechanism of the pathogenesis of glutamate neurotoxicity in retinal ischemia. Graefe's Arch Clin Exp Ophthalmol. doi:10.1007/s004170050156.

Adibkia K, Omidi Y, Siahi MR, Javadzadeh AR, Barzegar-Jalali M, Barar J, Maleki N, Mohammadi G, Nokhodchi A. 2007. Inhibition of endotoxin-induced uveitis by methylprednisolone acetate nanosuspension in rabbits. J Ocul Pharmacol Ther. doi:10.1089/jop.2007.0039.

Adibkia K, Shadbad MRS, Nokhodchi A, Javadzedeh A, Barzegar-Jalali M, Barar J, Mohammadi G, Omidi Y. 2007. Piroxicam nanoparticles for ocular delivery: Physicochemical characterization and implementation in endotoxin-induced uveitis. J Drug Target. doi:10.1080/10611860701453125.

Aggarwal D, Kaur IP. 2005. Improved pharmacodynamics of timolol maleate from a mucoadhesive niosomal ophthalmic drug delivery system. Int J Pharm. 290(1–2):155–159. doi:10.1016/j.ijpharm.2004.10.026.

Aggarwal D, Pal D, Mitra AK, Kaur IP. 2007. Study of the extent of ocular absorption of acetazolamide from a developed niosomal formulation, by microdialysis sampling of aqueous humor. Int J Pharm. doi:10.1016/j.ijpharm.2007.01.019.

Agibayeva LE, Kaldybekov DB, Porfiryeva NN, Garipova VR, Mangazbayeva RA, Moustafine RI, Semina II, Mun GA, Kudaibergenov SE, Khutoryanskiy V V. 2020. Gellan gum and its methacrylated derivatives as in situ gelling mucoadhesive formulations of pilocarpine: In vitro and in vivo studies. Int J Pharm. doi:10.1016/j.ijpharm.2020.119093.

Ahmad I, Pandit J, Sultana Y, Mishra AK, Hazari PP, Aqil M. 2019. Optimization by design of etoposide loaded solid lipid nanoparticles for ocular delivery: Characterization, pharmacokinetic and deposition study. Mater Sci Eng C. doi:10.1016/j.msec.2019.03.060.

Ahuja M, Dhake AS, Sharma SK, Majumdar DK. 2011. Diclofenac-loaded Eudragit

S100 nanosuspension for ophthalmic delivery. J Microencapsul. doi:10.3109/02652048.2010.523794.

Ahuja M, Verma P, Bhatia M. 2015. Preparation and evaluation of chitosan–itraconazole co-precipitated nanosuspension for ocular delivery. J Exp Nanosci. doi:10.1080/17458080.2013.822108.

Akhter S, Anwar M, Siddiqui MA, Ahmad I, Ahmad J, Ahmad MZ, Bhatnagar A, Ahmad FJ. 2016. Improving the topical ocular pharmacokinetics of an immunosuppressant agent with mucoadhesive nanoemulsions: Formulation development, in-vitro and in-vivo studies. Colloids Surfaces B Biointerfaces. 148:19–29. doi:10.1016/j.colsurfb.2016.08.048.

Akhter S, Talegaonkar S, Khan ZI, Jain GK, Khar RK, Ahmad FJ. 2011. Assessment of ocular pharmacokinetics and safety of ganciclovir loaded nanoformulations. J Biomed Nanotechnol. doi:10.1166/jbn.2011.1241.

Aksungur P, Demirbilek M, Denkbaş EB, Vandervoort J, Ludwig A, Ünlü N. 2011. Development and characterization of Cyclosporine A loaded nanoparticles for ocular drug delivery: Cellular toxicity, uptake, and kinetic studies. J Control Release. doi:10.1016/j.jconrel.2011.01.010.

Allen RS, Olsen TW, Sayeed I, Cale HA, Morrison KC, Oumarbaeva Y, Lucaciu I, Boatright JH, Pardue MT, Stein DG. 2015. Progesterone treatment in two rat models of ocular ischemia. Investig Ophthalmol Vis Sci. doi:10.1167/iovs.14-16070.

Allen RS, Sayeed I, Oumarbaeva Y, Morrison KC, Choi PH, Pardue MT, Stein DG. 2016. Progesterone treatment shows greater protection in brain vs. retina in a rat model of middle cerebral artery occlusion: Progesterone receptor levels may play an important role. Restor Neurol Neurosci. doi:10.3233/RNN-160672.

Almasieh M, Wilson AM, Morquette B, Cueva Vargas JL, Di Polo A. 2012. The molecular basis of retinal ganglion cell death in glaucoma. Prog Retin Eye Res. doi:10.1016/j.preteyeres.2011.11.002.

Almeida H, Lobão P, Frigerio C, Fonseca J, Silva R, Quaresma P, Lobo JMS, Amaral MH. 2016. Development of mucoadhesive and thermosensitive eyedrops to improve the ophthalmic bioavailability of ibuprofen. J Drug Deliv Sci Technol. doi:10.1016/j.jddst.2016.04.010.

Almeida H, Lobão P, Frigerio C, Fonseca J, Silva R, Sousa Lobo JM, Amaral MH. 2017. Preparation, characterization and biocompatibility studies of thermoresponsive eyedrops based on the combination of nanostructured lipid carriers (NLC) and the polymer Pluronic F-127 for controlled delivery of ibuprofen. Pharm Dev Technol. doi:10.3109/10837450.2015.1125922.

Alqurshi A, Hanafy AF, Abdalla AM, Guda TK, Gabr KE, Royall PG. 2019. Ocular anti-inflammatory activity of prednisolone acetate loaded chitosan-deoxycholate self-assembled nanoparticles. Int J Nanomedicine. doi:10.2147/IJN.S195892.

Alvarez-Trabado J, López-García A, Martín-Pastor M, Diebold Y, Sanchez A. 2018. Sorbitan ester nanoparticles (SENS) as a novel topical ocular drug delivery system: Design, optimization, and in vitro/ex vivo evaluation. Int J Pharm. doi:10.1016/j.ijpharm.2018.05.015.

Ambati J, Adamis AP. 2002. Transscleral drug delivery to the retina and choroid. Prog Retin Eye Res. 21(2):145–151. doi:10.1016/S1350-9462(01)00018-0.

Ambati J, Canakis CS, Miller JW, Gragoudas ES, Edwards A, Weissgold DJ, Kim I, Delori FC, Adamis AP. 2000. Diffusion of high molecular weight compounds through sclera. Investig Ophthalmol Vis Sci.

Ameeduzzafar A, Ali J, Fazil M, Qumbar M, Khan N, Ali A. 2016. Colloidal drug delivery system: Amplify the ocular delivery. Drug Deliv. doi:10.3109/10717544.2014.923065.

del Amo EM, Rimpelä AK, Heikkinen E, Kari OK, Ramsay E, Lajunen T, Schmitt M,

Pelkonen L, Bhattacharya M, Richardson D, et al. 2017. Pharmacokinetic aspects of retinal drug delivery. Prog Retin Eye Res. doi:10.1016/j.preteyeres.2016.12.001.

An J, Guo Q, Li L, Zhang Z. 2012. Properties of Flicker ERGs in Rat Models with Retinal Degeneration. ISRN Ophthalmol. doi:10.5402/2012/346297.

Anand N. 2015. Target Intraocular Pressure. In: Glaucoma: Second Edition.

Andersen JK. 2004. Oxidative stress in neurodegeneration: Cause or consequence? Nat Rev Neurosci. doi:10.1038/nrn1434.

Attar M, Brassard JA, Kim AS, Matsumoto S, Ramos M, Vangyi C. 2013. Safety Evaluation of Ocular Drugs. In: A Comprehensive Guide to Toxicology in Preclinical Drug Development.

Aung MH, na Park H, Han MK, Obertone TS, Abey J, Aseem F, Thule PM, Michael Iuvone P, Pardue MT. 2014. Dopamine deficiency contributes to early visual dysfunction in a rodent model of type 1 diabetes. J Neurosci. doi:10.1523/JNEUROSCI.3483-13.2014.

Aytekin E, Öztürk N, Vural İ, Polat HK, Çakmak HB, Çalış S, Pehlivan SB. 2020. Design of ocular drug delivery platforms and in vitro - in vivo evaluation of riboflavin to the cornea by non-interventional (epi-on) technique for keratoconus treatment. J Control Release. doi:10.1016/j.jconrel.2020.05.017.

Azevedo MA, Bourbon AI, Vicente AA, Cerqueira MA. 2014. Alginate/chitosan nanoparticles for encapsulation and controlled release of vitamin B2. Int J Biol Macromol. doi:10.1016/j.ijbiomac.2014.05.036.

Bachu RD, Chowdhury P, Al-Saedi ZHF, Karla PK, Boddu SHS. 2018. Ocular drug delivery barriers—role of nanocarriers in the treatment of anterior segment ocular diseases. Pharmaceutics. 10(1):1–31. doi:10.3390/pharmaceutics10010028.

Badr MY, Abdulrahman NS, Schatzlein AG, Uchegbu IF. 2021. A polymeric aqueous tacrolimus formulation for topical ocular delivery. Int J Pharm. doi:10.1016/j.ijpharm.2021.120364.

Bai Y, Xu J, Brahimi F, Zhuo Y, Sarunic M V., Uri Saragovi H. 2010. An agonistic TrKb mAb causes sustained TrkB activation, delays RGC death, and protects the retinal structure in optic nerve axotomy and in glaucoma. Investig Ophthalmol Vis Sci. doi:10.1167/iovs.09-5032.

Balguri SP, Adelli GR, Majumdar S. 2016. Topical ophthalmic lipid nanoparticle formulations (SLN, NLC) of indomethacin for delivery to the posterior segment ocular tissues. Eur J Pharm Biopharm. doi:10.1016/j.ejpb.2016.10.015.

Bartesaghi S, Marinovich M, Corsini E, Galli CL, Viviani B. 2005. Erythropoietin: A novel neuroprotective cytokine. Neurotoxicology. 26(5):923–928. doi:10.1016/j.neuro.2005.01.016.

Bayer AU, Cook P, Brodie SE, Maag KP, Mittag T. 2001. Evaluation of different recording parameters to establish a standard for flash electroretinography in rodents. Vision Res. doi:10.1016/S0042-6989(01)00103-1.

Bazán Henostroza MA, Curo Melo KJ, Nishitani Yukuyama M, Löbenberg R, Araci Bou-Chacra N. 2020. Cationic rifampicin nanoemulsion for the treatment of ocular tuberculosis. Colloids Surfaces A Physicochem Eng Asp. doi:10.1016/j.colsurfa.2020.124755.

Bernkop-Schnürch A. 2005. Thiomers: A new generation of mucoadhesive polymers. Adv Drug Deliv Rev. doi:10.1016/j.addr.2005.07.002.

Bernkop-Schnürch A, Dünnhaupt S. 2012. Chitosan-based drug delivery systems. Eur J Pharm Biopharm. doi:10.1016/j.ejpb.2012.04.007.

Bhardwaj P, Tripathi P, Gupta R, Pandey S. 2020. Niosomes: A review on niosomal research in the last decade. J Drug Deliv Sci Technol. doi:10.1016/j.jddst.2020.101581.

Bhatta RS, Chandasana H, Chhonker YS, Rathi C, Kumar D, Mitra K, Shukla PK. 2012. Mucoadhesive nanoparticles for prolonged ocular delivery of natamycin: In vitro and pharmacokinetics studies. Int J Pharm. doi:10.1016/j.ijpharm.2012.04.060.

Bin-Jumah M, Gilani SJ, Jahangir MA, Zafar A, Alshehri S, Yasir M, Kala C, Taleuzzaman M, Imam SS. 2020. Clarithromycin-loaded ocular chitosan nanoparticle: Formulation, optimization, characterization, ocular irritation, and antimicrobial activity. Int J Nanomedicine. doi:10.2147/IJN.S269004.

Böcker-Meffert S, Rosenstiel P, Röhl C, Warneke N, Held-Feindt J, Sievers J, Lucius R. 2002. Erythropoietin and VEGF promote neural outgrowth from retinal explants in postnatal rats. Investig Ophthalmol Vis Sci.

Bodoki E, Vostinaru O, Samoila O, Dinte E, Bodoki AE, Swetledge S, Astete CE, Sabliov CM. 2019. Topical nanodelivery system of lutein for the prevention of selenite-induced cataract. Nanomedicine Nanotechnology, Biol Med. doi:10.1016/j.nano.2018.09.016.

Bokharaei M, Margaritis A, Xenocostas A, J. Freeman D. 2011. Erythropoietin Encapsulation in Chitosan Nanoparticles and Kinetics of Drug Release. Curr Drug Deliv. doi:10.2174/156720111794479862.

Bonanno JA. 2012. Molecular mechanisms underlying the corneal endothelial pump. Exp Eye Res. doi:10.1016/j.exer.2011.06.004.

Bond WS, Rex TS. 2014. Evidence that erythropoietin modulates neuroinflammation through differential action on neurons, astrocytes, and microglia. Front Immunol. 5(OCT):1–9. doi:10.3389/fimmu.2014.00523.

Botla R, Spivey JR, Aguilar H, Bronk SF, Gores GJ. 1995. Ursodeoxycholate (UDCA) inhibits the mitochondrial membrane permeability transition induced by glycochenodeoxycholate: A mechanism of UDCA cytoprotection. J Pharmacol Exp Ther.

Boyd BJ. 2008. Past and future evolution in colloidal drug delivery systems. Expert Opin Drug Deliv. 5(1):69–85. doi:10.1517/17425247.5.1.69.

Brannigan RP, Khutoryanskiy V V. 2017. Synthesis and evaluation of mucoadhesive acryloyl-quaternized PDMAEMA nanogels for ocular drug delivery. Colloids Surfaces B Biointerfaces. doi:10.1016/j.colsurfb.2017.04.050.

Bravo-Osuna I, Vicario-De-La-Torre M, Andrés-Guerrero V, Sánchez-Nieves J, Guzmán-Navarro M, De La Mata FJ, Gómez R, De Las Heras B, Argüeso P, Ponchel G, et al. 2016. Novel water-soluble mucoadhesive carbosilane dendrimers for ocular administration. Mol Pharm. doi:10.1021/acs.molpharmaceut.6b00182.

Brines M, Grasso G, Fiordaliso F, Sfacteria A, Ghezzi P, Fratelli M, Latini R, Xie Q -w., Smart J, Su-Rick C -j., et al. 2004. Erythropoietin mediates tissue protection through an erythropoietin and common -subunit heteroreceptor. Proc Natl Acad Sci. 101(41):14907–14912. doi:10.1073/pnas.0406491101.

Bucolo C, Maltese A, Maugeri F, Busà B, Puglisi G, Pignatello R. 2004. Eudragit RL100 nanoparticle system for the ophthalmic delivery of cloricromene. J Pharm Pharmacol. doi:10.1211/0022357023835.

Bucolo C, Maltese A, Puglisi G, Pignatello R. 2002. Enhanced ocular anti-inflammatory activity of ibuprofen carried by an eudragit RS100® nanoparticle suspension. Ophthalmic Res. doi:10.1159/000065608.

Budai L, Hajdu M, Budai M, Grof P, Beni S, Noszal B, Klebovich I, Antal I. 2007. Gels and liposomes in optimized ocular drug delivery: Studies on ciprofloxacin formulations. Int J Pharm. 343(1–2):34–40. doi:10.1016/j.ijpharm.2007.04.013.

Bui B V., Fortune B. 2004. Ganglion cell contributions to the rat full-field electroretinogram. J Physiol. doi:10.1113/jphysiol.2003.052738.

Bulmer C, Margaritis A, Xenocostas A. 2012a. Encapsulation and Controlled Release of Recombinant Human Erythropoietin from Chitosan-Carrageenan Nanoparticles. Curr Drug Deliv. 9(5):527–537. doi:10.2174/156720112802650680.

Bulmer C, Margaritis A, Xenocostas A. 2012b. Production and characterization of novel chitosan nanoparticles for controlled release of rHu-Erythropoietin. Biochem Eng J. 68:61–69. doi:10.1016/j.bej.2012.07.007. http://dx.doi.org/10.1016/j.bej.2012.07.007.

Cadete A, Figueiredo L, Lopes R, Calado CCR, Almeida AJ, Gonalves LMD. 2012. Development and characterization of a new plasmid delivery system based on chitosan-sodium deoxycholate nanoparticles. Eur J Pharm Sci. 45(4):451–458. doi:10.1016/j.ejps.2011.09.018. http://dx.doi.org/10.1016/j.ejps.2011.09.018.

Caetano LA, Almeida AJ, Gonçalves LMD. 2016. Effect of experimental parameters on alginate/chitosan microparticles for BCG encapsulation. Mar Drugs. 14(5). doi:10.3390/md14050090.

Cain K, Bratton SB, Cohen GM. 2002. The Apaf-1 apoptosome: A large caspase-activating complex. Biochimie. doi:10.1016/S0300-9084(02)01376-7.

Cairns EA, Baldridge WH, Kelly MEM. 2016. The Endocannabinoid System as a Therapeutic Target in Glaucoma. Neural Plast. doi:10.1155/2016/9364091.

Calvo P, Vila-Jato JL, Alonso MJ. 1997. Evaluation of cationic polymer-coated nanocapsules as ocular drug carriers. Int J Pharm. doi:10.1016/S0378-5173(97)00083-5.

De Campos AM, Diebold Y, Carvalho ELS, Sánchez A, Alonso MJ. 2004. Chitosan nanoparticles as new ocular drug delivery systems: In vitro stability, in vivo fate, and cellular toxicity. Pharm Res. doi:10.1023/B:PHAM.0000026432.75781.cb.

De Campos AM, Sánchez A, Alonso MJ. 2001. Chitosan nanoparticles: A new vehicle for the improvement of the delivery of drugs to the ocular surface. Application to cyclosporin A. Int J Pharm. 224(1–2):159–168. doi:10.1016/S0378-5173(01)00760-8.

Caprara C, Britschgi C, Samardzija M, Grimm C. 2014. The erythropoietin receptor is not required for the development, function, and aging of rods and cells in the retinal periphery. Mol Vis.

Cayouette M, Gravel C. 1997. Adenovirus-mediated gene transfer of ciliary neurotrophic factor can prevent photoreceptor degeneration in the retinal degeneration (rd) mouse. Hum Gene Ther. doi:10.1089/hum.1997.8.4-423.

Chaiyasan W, Praputbut S, Kompella UB, Srinivas SP, Tiyaboonchai W. 2017. Penetration of mucoadhesive chitosan-dextran sulfate nanoparticles into the porcine cornea. Colloids Surfaces B Biointerfaces. doi:10.1016/j.colsurfb.2016.10.032.

Chaiyasan W, Srinivas SP, Tiyaboonchai W. 2013. Mucoadhesive chitosan-dextran sulfate nanoparticles for sustained drug delivery to the ocular surface. J Ocul Pharmacol Ther. doi:10.1089/jop.2012.0193.

Chaiyasan W, Srinivas SP, Tiyaboonchai W. 2015. Crosslinked chitosan-dextran sulfate nanoparticle for improved topical ocular drug delivery. Mol Vis.

Chan JR, Phillips LJ, Glaser M. 1998. Glucocorticoids and progestins signal the initiation and enhance the rate of myelin formation. Proc Natl Acad Sci U S A. doi:10.1073/pnas.95.18.10459.

Chang JN. 2010. Recent Advances in Ophthalmic Drug Delivery. In: Handbook of Non-Invasive Drug Delivery Systems.

Chao De La Barca JM, Simard G, Amati-Bonneau P, Safiedeen Z, Prunier-Mirebeau D, Chupin S, Gadras C, Tessier L, Gueguen N, Chevrollier A, et al. 2016. The metabolomic signature of Leber's hereditary optic neuropathy reveals endoplasmic reticulum stress. Brain. doi:10.1093/brain/aww222.

Chen H, Pan H, Li P, Wang H, Wang X, Pan W, Yuan Y. 2016. The potential use of novel chitosan-coated deformable liposomes in an ocular drug delivery system. Colloids Surfaces B Biointerfaces. 143:455–462. doi:10.1016/j.colsurfb.2016.03.061.

Chen J, Connor KM, Aderman CM, Smith LEH. 2008. Erythropoietin deficiency decreases vascular stability in mice. J Clin Invest. doi:10.1172/JCI33813.

Chen J, Matias I, Dinh T, Lu T, Venezia S, Nieves A, Woodward DF, Di Marzo V. 2005. Finding of endocannabinoids in human eye tissues: Implications for glaucoma. Biochem Biophys Res Commun. doi:10.1016/j.bbrc.2005.03.095.

Cheng T, Li J, Cheng Y, Zhang X, Qu Y. 2019. Triamcinolone acetonide-chitosan coated liposomes efficiently treated retinal edema as eye drops. Exp Eye Res.

doi:10.1016/j.exer.2019.107805.

Chetoni P, Burgalassi S, Monti D, Tampucci S, Tullio V, Cuffini AM, Muntoni E, Spagnolo R, Zara GP, Cavalli R. 2016. Solid lipid nanoparticles as promising tool for intraocular tobramycin delivery: Pharmacokinetic studies on rabbits. Eur J Pharm Biopharm. doi:10.1016/j.ejpb.2016.10.006.

Chhonker YS, Prasad YD, Chandasana H, Vishvkarma A, Mitra K, Shukla PK, Bhatta RS. 2015. Amphotericin-B entrapped lecithin/chitosan nanoparticles for prolonged ocular application. Int J Biol Macromol. doi:10.1016/j.ijbiomac.2014.10.014.

Colella P, Iodice C, Di Vicino U, Annunziata I, Surace EM, Auricchio A. 2011. Non-erythropoietic erythropoietin derivatives protect from light-induced and genetic photoreceptor degeneration. Hum Mol Genet. doi:10.1093/hmg/ddr115.

Di Colo G, Zambito Y, Burgalassi S, Serafini A, Saettone MF. 2002. Effect of chitosan on in vitro release and ocular delivery of ofloxacin from erodible inserts based on poly(ethylene oxide). Int J Pharm. 248(1–2):115–122. doi:10.1016/S0378-5173(02)00421-0.

Di Colo G, Zambito Y, Zaino C, Sans M. 2009. Selected polysaccharides at comparison for their mucoadhesiveness and effect on precorneal residence of different drugs in the rabbit model. Drug Dev Ind Pharm. doi:10.1080/03639040802713460.

Contreras-Ruiz L, de la Fuente M, Párraga JE, López-García A, Fernández I, Seijo B, Sánchez A, Calonge M, Diebold Y. 2011. Intracellular trafficking of hyaluronic acid-chitosan oligomer-based nanoparticles in cultured human ocular surface cells. Mol Vis. 17(September 2010):279–90. http://www.ncbi.nlm.nih.gov/pubmed/21283563%0Ahttp://www.pubmedcentral.nih.gov/articlerender.fcgi?artid=PMC3030601.

Cordeiro MF, Guo L, Luong V, Harding G, Wang W, Jones HE, Moss SE, Sillito AM, Fitzke FW. 2004. Real-time imaging of single nerve cell apoptosis in retinal neurodegeneration. Proc Natl Acad Sci U S A. doi:10.1073/pnas.0405479101.

Costa JR, Silva NC, Sarmento B, Pintado M. 2015. Potential chitosan-coated alginate nanoparticles for ocular delivery of daptomycin. Eur J Clin Microbiol Infect Dis. doi:10.1007/s10096-015-2344-7.

Cowper B, Lavén M, Hakkarainen B, Mulugeta E. 2020. Glycan analysis of erythropoiesis-stimulating agents. J Pharm Biomed Anal. doi:10.1016/j.jpba.2019.113031.

Crish SD, Sappington RM, Inman DM, Horner PJ, Calkins DJ. 2010. Distal axonopathy with structural persistence in glaucomatous neurodegeneration. Proc Natl Acad Sci U S A. doi:10.1073/pnas.0913141107.

Cumurcu T, Bulut Y, Demir HD, Yenisehirli G. 2007. Aqueous humor erythropoietin levels in patients with primary open-angle glaucoma. J Glaucoma. doi:10.1097/IJG.0b013e31804a5eb3.

D. Lukasiewicz P. 2005. Synaptic mechanisms that shape visual signaling at the inner retina. Prog Brain Res. doi:10.1016/S0079-6123(04)47016-2.

Daruich A, Picard E, Guégan J, Jaworski T, Parenti L, Delaunay K, Naud MC, Berdugo M, Boatright JH, Behar-Cohen F. 2022. Comparative Analysis of Urso-and Tauroursodeoxycholic Acid Neuroprotective Effects on Retinal Degeneration Models. Pharmaceuticals. doi:10.3390/ph15030334.

Das S, Suresh PK. 2011. Nanosuspension: A new vehicle for the improvement of the delivery of drugs to the ocular surface. Application to amphotericin B. Nanomedicine Nanotechnology, Biol Med. doi:10.1016/j.nano.2010.07.003.

Das SK, Tucker IG, Hill DJT, Ganguly N. 1995. Evaluation of Poly(isobutylcyanoacrylate) Nanoparticles for Mucoadhesive Ocular Drug Delivery. I. Effect of Formulation Variables on Physicochemical Characteristics of Nanoparticles. Pharm Res An Off J Am Assoc Pharm Sci. doi:10.1023/A:1016249812466.

Dasilva MA, Grieve KL, Cudeiro J, Rivadulla C. 2012. Endocannabinoid CB1

receptors modulate visual output from the thalamus. Psychopharmacology (Berl). doi:10.1007/s00213-011-2412-3.

De TK, Rodman DJ, Holm BA, Prasad PN, Bergey EJ. 2003. Brimonidine formulation in polyacrylic acid nanoparticles for ophthalmic delivery. J Microencapsul. doi:10.1080/0265204031000093591.

Debatin KM, Krammer PH. 2004. Death receptors in chemotherapy and cancer. Oncogene. doi:10.1038/sj.onc.1207558.

Diebold Y, Calonge M. 2010. Applications of nanoparticles in ophthalmology. Prog Retin Eye Res. doi:10.1016/j.preteyeres.2010.08.002.

Digicaylioglu M, Lipton SA. 2001. Erythropoietin-mediated neuroprotection involves cross-talk between Jak2 and NF-κB signalling cascades. Nature. doi:10.1038/35088074.

Dilbaghi N, Kaur H, Ahuja M, Kumar S. 2013. Evaluation of tropicamide-loaded tamarind seed xyloglucan nanoaggregates for ophthalmic delivery. Carbohydr Polym. doi:10.1016/j.carbpol.2013.01.054.

Djebaili M, Guo Q, Pettus EH, Hoffman SW, Stein DG. 2005. The neurosteroids progesterone and allopregnanolone reduce cell death, gliosis, and functional deficits after traumatic brain injury in rats. J Neurotrauma. doi:10.1089/neu.2005.22.106.

Dong Y, Dong P, Huang D, Mei L, Xia Y, Wang Z, Pan X, Li G, Wu C. 2015. Fabrication and characterization of silk fibroin-coated liposomes for ocular drug delivery. Eur J Pharm Biopharm. doi:10.1016/j.ejpb.2015.01.018.

Drew PD, Chavis JA. 2000. Female sex steroids: Effects upon microglial cell activation. J Neuroimmunol. doi:10.1016/S0165-5728(00)00386-6.

Durrani AM, Davies NM, Thomas M, Kellaway IW. 1992. Pilocarpine bioavailability from a mucoadhesive liposomal ophthalmic drug delivery system. Int J Pharm. doi:10.1016/0378-5173(92)90340-8.

El-Nabarawi MA, Abd El Rehem RT, Teaima M, Abary M, El-Mofty HM, Khafagy MM, Lotfy NM, Salah M. 2019. Natamycin niosomes as a promising ocular nanosized delivery system with ketorolac tromethamine for dual effects for treatment of candida rabbit keratitis; in vitro/in vivo and histopathological studies. Drug Dev Ind Pharm. doi:10.1080/03639045.2019.1579827.

Elmotasem H, Awad GEA. 2020. A stepwise optimization strategy to formulate in situ gelling formulations comprising fluconazole-hydroxypropyl-beta-cyclodextrin complex loaded niosomal vesicles and Eudragit nanoparticles for enhanced antifungal activity and prolonged ocular delivery. Asian J Pharm Sci. doi:10.1016/j.ajps.2019.09.003.

Emad Eldeeb A, Salah S, Ghorab M. 2019. Proniosomal gel-derived niosomes: an approach to sustain and improve the ocular delivery of brimonidine tartrate; formulation, in-vitro characterization, and in-vivo pharmacodynamic study. Drug Deliv. doi:10.1080/10717544.2019.1609622.

Fabiano A, Chetoni P, Zambito Y. 2015. Mucoadhesive nano-sized supramolecular assemblies for improved pre-corneal drug residence time. Drug Dev Ind Pharm. 41(12):2069–2076. doi:10.3109/03639045.2015.1066798.

Fabiano A, Piras AM, Guazzelli L, Storti B, Bizzarri R, Zambito Y. 2019. Impact of different mucoadhesive polymeric nanoparticles loaded in thermosensitive hydrogels on transcorneal administration of 5-fluorouracil. Pharmaceutics. doi:10.3390/pharmaceutics11120623.

Faktorovich EG, Steinberg RH, Yasumura D, Matthes MT, LaVail MM. 1990. Photoreceptor degeneration in inherited retinal dystrophy delayed by basic fibroblast growth factor. Nature. doi:10.1038/347083a0.

Feizi S, Alemzadeh-Ansari M, Karimian F, Esfandiari H. 2021. Use of erythropoietin in ophthalmology: a review. Surv Ophthalmol. doi:10.1016/j.survophthal.2021.06.002.

Felt O, Carrel A, Baehni P, Buri P, Gurny R. 2009. Chitosan as Tear Substitute: A Wetting Agent Endowed with Antimicrobial Efficacy. J Ocul Pharmacol Ther. 16(3):261–

270. doi:10.1089/jop.2000.16.261.

Fetih G. 2016. Fluconazole-loaded niosomal gels as a topical ocular drug delivery system for corneal fungal infections. J Drug Deliv Sci Technol. doi:10.1016/j.jddst.2016.06.002.

Fitzgerald P, Hadgraft J, Kreuter J, Wilson CG. 1987. A γ-scintigraphic evaluation of microparticulate ophthalmic delivery systems: liposomes and nanoparticles. Int J Pharm. doi:10.1016/0378-5173(87)90050-0.

Fleitas MFG, Dorfman D, Rosenstein RE. 2022. A novel viewpoint in glaucoma therapeutics: Enriched environment. Neural Regen Res. doi:10.4103/1673-5374.330594.

Froger N, Cadetti L, Lorach H, Martins J, Bemelmans AP, Dubus E, Degardin J, Pain D, Forster V, Chicaud L, et al. 2012. Taurine Provides Neuroprotection against Retinal Ganglion Cell Degeneration. PLoS One. doi:10.1371/journal.pone.0042017.

Fu QL, Wu W, Wang H, Li X, Lee VWH, So KF. 2008. Up-regulated endogenous erythropoietin/erythropoietin receptor system and exogenous erythropoietin rescue retinal ganglion cells after chronic ocular hypertension. Cell Mol Neurobiol. doi:10.1007/s10571-007-9155-z.

Fuchs C, Forster V, Balse E, Sahel JA, Picaud S, Tessier LH. 2005. Retinal-cell-conditioned medium prevents TNF-α-induced apoptosis of purified ganglion cells. Investig Ophthalmol Vis Sci. doi:10.1167/iovs.04-1177.

Gai X, Cheng L, Li T, Liu D, Wang Y, Wang T, Pan W, Yang X. 2018. In vitro and In vivo Studies on a Novel Bioadhesive Colloidal System: Cationic Liposomes of Ibuprofen. AAPS PharmSciTech. doi:10.1208/s12249-017-0872-4.

Gallarate M, Chirio D, Bussano R, Peira E, Battaglia L, Baratta F, Trotta M. 2013. Development of O/W nanoemulsions for ophthalmic administration of timolol. Int J Pharm. doi:10.1016/j.ijpharm.2012.10.015.

Gallego-Ortega A, Norte-Muñoz M, Miralles de Imperial-Ollero JA, Bernal-Garro JM, Valiente-Soriano FJ, de la Villa Polo P, Avilés-Trigueros M, Villegas-Pérez MP, Vidal-Sanz M. 2020. Functional and morphological alterations in a glaucoma model of acute ocular hypertension. In: Progress in Brain Research.

Garcia-Ramirez, Marta; Hernández, Cristina; Simó R. 2008. Expression of Erythropoietin and Its Receptor in the Human Retina. Diabetes Care. 31(6):1189–94. doi:10.2337/dc07-2075.Additional.

García-Ramírez M, Hernández C, Simó R. 2008. Expression of erythropoietin and its receptor in the human retina: A comparative study of diabetic and nondiabetic subjects. Diabetes Care. doi:10.2337/dc07-2075.

Gelatt KN, MacKay EO. 2004. Secondary glaucomas in the dog in North America. Vet Ophthalmol. doi:10.1111/j.1463-5224.2004.04034.x.

Ghate D, Edelhauser HF. 2008. Barriers to glaucoma drug delivery. J Glaucoma. 17(2):147–156. doi:10.1097/IJG.0b013e31814b990d.

Ghoumari AM, Ibanez C, El-Etr M, Leclerc P, Eychenne B, O'Malley BW, Baulieu EE, Schumacher M. 2003. Progesterone and its metabolites increase myelin basic protein expression in organotypic slice cultures of rat cerebellum. J Neurochem. doi:10.1046/j.1471-4159.2003.01881.x.

Goel M, Picciani RG, Lee RK, Bhattacharya SK. 2010. Aqueous humor dynamics: a review. Open Ophthalmol J. doi:10.2174/1874364101004010052.

Gómez-Vicente V, Lax P, Fernández-Sánchez L, Rondón N, Esquiva G, Germain F, De La Villa P, Cuenca N. 2015. Neuroprotective effect of tauroursodeoxycholic acid on n-methyl-daspartate-induced retinal ganglion cell degeneration. PLoS One. doi:10.1371/journal.pone.0137826.

Gonçalves C, Pereira P, Gama M. 2010. Self-assembled hydrogel nanoparticles for drug delivery applications. Materials (Basel). 3(2):1420–1460. doi:10.3390/ma3021420.

Gonzalez-Mira E, Egea MA, Garcia ML, Souto EB. 2010. Design and ocular tolerance of flurbiprofen loaded ultrasound-engineered NLC. Colloids Surfaces B Biointerfaces. doi:10.1016/j.colsurfb.2010.07.029.

Gonzalez-Mira E, Nikolić S, Calpena AC, Egea MA, Souto EB, García ML. 2012. Improved and safe transcorneal delivery of flurbiprofen by NLC and NLC-based hydrogels. J Pharm Sci. doi:10.1002/jps.22784.

González SL, Labombarda F, González Deniselle MC, Guennoun R, Schumacher M, De Nicola AF. 2004. Progesterone up-regulates neuronal brain-derived neurotrophic factor expression in the injured spinal cord. Neuroscience. doi:10.1016/j.neuroscience.2004.02.024.

Goyal R, Macri LK, Kaplan HM, Kohn J. 2016. Nanoparticles and nanofibers for topical drug delivery. J Control Release. doi:10.1016/j.jconrel.2015.10.049.

Graça A, Gonçalves LM, Raposo S, Ribeiro HM, Marto J. 2018. Useful in vitro techniques to evaluate the mucoadhesive properties of hyaluronic acid-based ocular delivery systems. Pharmaceutics. 10(3). doi:10.3390/pharmaceutics10030110.

Grasso G, Sfacteria A, Meli F, Passalacqua M, Fodale V, Giambartino F, Iacopino DG, Tomasello F. 2009. The role of erythropoietin in neuroprotection: Therapeutic perspectives. Drug News Perspect. doi:10.1358/dnp.2007.20.5.1120219.

Green DG. 1973. Scotopic and photopic components of the rat electroretinogram. J Physiol. doi:10.1113/jphysiol.1973.sp010112.

Griffiths M, Neal JW, Gasque P. 2007. Innate Immunity and Protective Neuroinflammation: New Emphasis on the Role of Neuroimmune Regulatory Proteins. Int Rev Neurobiol. doi:10.1016/S0074-7742(07)82002-2.

Guan Y, Cui L, Qu Z, Lu L, Wang F, Wu Y, Zhang J, Gao F, Tian H, Xu L, et al. 2013. Subretinal Transplantation of Rat MSCs and Erythropoietin Gene Modified Rat MSCs for Protecting and Rescuing Degenerative Retina in Rats. Curr Mol Med. doi:10.2174/15665240113139990071.

Gui D, Li Y, Chen X, Gao D, Yang Y, Li X. 2015. HIF1 signaling pathway involving iNOS, COX2 and caspase9 mediates the neuroprotection provided by erythropoietin in the retina of chronic ocular hypertension rats. Mol Med Rep. doi:10.3892/mmr.2014.2859.

Guillaumie F, Furrer P, Felt-Baeyens O, Fuhlendorff BL, Nymand S, Westh P, Gurny R, Schwach-Abdellaoui K. 2010. Comparative studies of various hyaluronic acids produced by microbial fermentation for potential topical ophthalmic applications. J Biomed Mater Res - Part A. 92(4):1421–1430. doi:10.1002/jbm.a.32481.

Gupta H, Aqil M, Khar RK, Ali A, Bhatnagar A, Mittal G. 2010. Sparfloxacin-loaded PLGA nanoparticles for sustained ocular drug delivery. Nanomedicine Nanotechnology, Biol Med. doi:10.1016/j.nano.2009.10.004.

Gupta H, Aqil M, Khar RK, Ali A, Bhatnagar A, Mittal G. 2013. Nanoparticles laden in situ gel of levofloxacin for enhanced ocular retention. Drug Deliv. doi:10.3109/10717544.2013.838712.

Guresh AM, Horvath SJ, Gemensky-Metzler A, Miller E, Yildiz V, Myers J V., Newbold GM. 2021. The effect of central corneal thickness on intraocular pressure values using various tonometers in the dog. Vet Ophthalmol. doi:10.1111/vop.12873.

Guter M, Breunig M. 2017. Hyaluronan as a promising excipient for ocular drug delivery. Eur J Pharm Biopharm. doi:10.1016/j.ejpb.2016.11.035.

Güven UM, Yenilmez E. 2019. Olopatadine hydrochloride loaded Kollidon ® SR nanoparticles for ocular delivery: Nanosuspension formulation and in vitro–in vivo evaluation. J Drug Deliv Sci Technol. doi:10.1016/j.jddst.2019.03.016.

Hafner A, Lovrić J, Romić MD, Juretić M, Pepić I, Cetina-Čižmek B, Filipović-Grčić J. 2015. Evaluation of cationic nanosystems with melatonin using an eye-related bioavailability prediction model. Eur J Pharm Sci. doi:10.1016/j.ejps.2015.04.003.

Hagigit T, Abdulrazik M, Valamanesh F, Behar-Cohen F, Benita S. 2012. Ocular

antisense oligonucleotide delivery by cationic nanoemulsion for improved treatment of ocular neovascularization: An in-vivo study in rats and mice. J Control Release. doi:10.1016/j.jconrel.2011.11.022.

Hahn SK, Kim JS, Shimobouji T. 2007. Injectable hyaluronic acid microhydrogels for controlled release formulation of erythropoietin. J Biomed Mater Res - Part A. doi:10.1002/jbm.a.30997.

Halliwell B. 2006. Oxidative stress and neurodegeneration: Where are we now? J Neurochem. doi:10.1111/j.1471-4159.2006.03907.x.

Hamdi Y, Lallemand F, Benita S. 2015. Drug-loaded nanocarriers for back-of-the-eye diseases- formulation limitations. J Drug Deliv Sci Technol. doi:10.1016/j.jddst.2015.09.010.

Handelman GJ, Levin NW. 2008. Iron and anemia in human biology: A review of mechanisms. Heart Fail Rev. doi:10.1007/s10741-008-9086-x.

Hare WA, Wheeler L. 2009. Experimental glutamatergic excitotoxicity in rabbit retinal ganglion cells: Block by memantine. Investig Ophthalmol Vis Sci. doi:10.1167/iovs.08-2103.

Hassan EE, Gallo JM. 1990. A Simple Rheological Method for the in Vitro Assessment of Mucin-Polymer Bioadhesive Bond Strength. Pharm Res An Off J Am Assoc Pharm Sci. doi:10.1023/A:1015812615635.

He Z, Bui B V., Vingrys AJ. 2006. The rate of functional recovery from acute IOP elevation. Investig Ophthalmol Vis Sci. doi:10.1167/iovs.06-0590.

Heijl A, Leske MC, Bengtsson Bo, Hyman L, Bengtsson Boel, Hussein M. 2002. Reduction of intraocular pressure and glaucoma progression: Results from the Early Manifest Glaucoma Trial. Arch Ophthalmol. doi:10.1001/archopht.120.10.1268.

Hernández C, Fonollosa A, García-Ramírez M, Higuera M, Catalán R, Miralles A, García-Arumí J, Simó R. 2006. Erythropoietin is expressed in the human retina and it is highly elevated in the vitreous fluid of patients with diabetic macular edema. Diabetes Care. doi:10.2337/dc06-0556.

Herrero-Vanrell R, Cardillo JA. 2010. Ocular pharmacokinetic, drug bioavailability, and intraocular drug delivery systems. In: Retinal Pharmacotherapy.

Herrero-Vanrell R, Vicario De La Torre M, Andrés-Guerrero V, Barbosa-Alfaro D, Molina-Martínez IT, Bravo-Osuna I. 2013. Nano and microtechnologies for ophthalmic administration, an overview. J Drug Deliv Sci Technol. doi:10.1016/S1773-2247(13)50016-5.

Herzog KH, Von Bartheld CS. 1998. Contributions of the optic tectum and the retina as sources of brain- derived neurotrophic factor for retinal ganglion cells in the chick embryo. J Neurosci. doi:10.1523/jneurosci.18-08-02891.1998.

Hirakura T, Yasugi K, Nemoto T, Sato M, Shimoboji T, Aso Y, Morimoto N, Akiyoshi K. 2010. Hybrid hyaluronan hydrogel encapsulating nanogel as a protein nanocarrier: New system for sustained delivery of protein with a chaperone-like function. J Control Release. 142(3):483–489. doi:10.1016/j.jconrel.2009.11.023. http://dx.doi.org/10.1016/j.jconrel.2009.11.023.

Holden CA, Tyagi P, Thakur A, Kadam R, Jadhav G, Kompella UB, Yang H. 2012. Polyamidoamine dendrimer hydrogel for enhanced delivery of antiglaucoma drugs. Nanomedicine Nanotechnology, Biol Med. doi:10.1016/j.nano.2011.08.018.

Horvát G, Budai-Szucs M, Berkó S, Szabó-Révész P, Soós J, Facskó A, Maroda M, Mori M, Sandri G, Bonferoni MC, et al. 2015. Comparative study of nanosized cross-linked sodium-, linear sodium- and zinc-hyaluronate as potential ocular mucoadhesive drug delivery systems. Int J Pharm. doi:10.1016/j.ijpharm.2015.08.024.

Hosoya KI, Lee VHL, Kim KJ. 2005. Roles of the conjunctiva in ocular drug delivery: A review of conjunctival transport mechanisms and their regulation. Eur J Pharm Biopharm. 60(2):227–240. doi:10.1016/j.ejpb.2004.12.007.

Hu LM, Luo Y, Zhang J, Lei X, Shen J, Wu Y, Qin M, Unver YB, Zhong Y, Xu GT, et al. 2011. EPO reduces reactive gliosis and stimulates neurotrophin expression in Muller cells. Front Biosci - Elit. doi:10.2741/e355.

Hu Y, Cho S, Goldberg JL. 2010. Neurotrophic effect of a novel TrkB agonist on retinal ganglion cells. Investig Ophthalmol Vis Sci. doi:10.1167/iovs.09-4450.

Huang D, Chen YS, Rupenthal ID. 2018. Overcoming ocular drug delivery barriers through the use of physical forces. Adv Drug Deliv Rev. doi:10.1016/j.addr.2017.09.008.

Huang HY, Wang MC, Chen ZY, Chiu WY, Chen KH, Lin IC, Yang WCV, Wu CC, Tseng CL. 2018. Gelatin–epigallocatechin gallate nanoparticles with hyaluronic acid decoration as eye drops can treat rabbit dry-eye syndrome effectively via inflammatory relief. Int J Nanomedicine. doi:10.2147/IJN.S173198.

Huang W, Gao F, Hu F, Huang J, Wang M, Xu P, Zhang R, Chen J, Sun X, Zhang S, et al. 2018. Asiatic acid prevents retinal ganglion cell apoptosis in a rat model of glaucoma. Front Neurosci. doi:10.3389/fnins.2018.00489.

Ibrahim HK, El-Leithy IS, Makky AA. 2010. Mucoadhesive nanoparticles as carrier systems for prolonged ocular delivery of gatifloxacin/prednisolone bitherapy. Mol Pharm. doi:10.1021/mp900279c.

Ibrahim MM, Abd-Elgawad A-EH, Soliman OA-E, Jablonski MM. 2015. Natural Bioadhesive Biodegradable Nanoparticle-Based Topical Ophthalmic Formulations for Management of Glaucoma. Transl Vis Sci Technol. doi:10.1167/tvst.4.3.12.

Ibrahim MM, Jablonski MM. 2019. The impact of R-801 nanoparticles as a long acting topical glaucoma therapy. J Biomed Nanotechnol. doi:10.1166/jbn.2019.2817.

In Jung K, Hyun Kim J, Kee Park C. 2015. α2-Adrenergic modulation of the glutamate receptor and transporter function in a chronic ocular hypertension model. Eur J Pharmacol. doi:10.1016/j.ejphar.2015.08.035.

De Iongh RU, Abud HE, Hime GR. 2006. WNT/Frizzled signaling in eye development and disease. Front Biosci. doi:10.2741/1982.

Iqbal MA, Md S, Sahni JK, Baboota S, Dang S, Ali J. 2012. Nanostructured lipid carriers system: Recent advances in drug delivery. J Drug Target. doi:10.3109/1061186X.2012.716845.

Ishrat T, Sayeed I, Atif F, Hua F, Stein DG. 2010. Progesterone and allopregnanolone attenuate blood-brain barrier dysfunction following permanent focal ischemia by regulating the expression of matrix metalloproteinases. Exp Neurol. doi:10.1016/j.expneurol.2010.08.023.

Jacob Filho W, Lima CC, Paunksnis MRR, Silva AA, Perilhão MS, Caldeira M, Bocalini D, de Souza RR. 2018. Reference database of hematological parameters for growing and aging rats. Aging Male. doi:10.1080/13685538.2017.1350156.

Jain GK, Pathan SA, Akhter S, Jayabalan N, Talegaonkar S, Khar RK, Ahmad FJ. 2011. Microscopic and spectroscopic evaluation of novel PLGA-chitosan Nanoplexes as an ocular delivery system. Colloids Surfaces B Biointerfaces. doi:10.1016/j.colsurfb.2010.09.010.

Jain K, Kumar R, Sood S, Dhyanandhan G. 2013. Betaxolol Hydrochloride Loaded Chitosan Nanoparticles for Ocular Delivery and their Anti-glaucoma Efficacy. Curr Drug Deliv. doi:10.2174/1567201811310050001.

Jelkmann W. 2007. Erythropoietin after a century of research: Younger than ever. Eur J Haematol. doi:10.1111/j.1600-0609.2007.00818.x.

Jiang G, Jia H, Qiu J, Mo Z, Wen Yifeng, Zhang Y, Wen Yuqin, Xie Q, Ban J, Lu Z, et al. 2020. Plga nanoparticle platform for trans-ocular barrier to enhance drug delivery: A comparative study based on the application of oligosaccharides in the outer membrane of carriers. Int J Nanomedicine. doi:10.2147/IJN.S272750.

Johnson T V., Tomarev SI. 2010. Rodent models of glaucoma. Brain Res Bull. doi:10.1016/j.brainresbull.2009.04.004.

Jordán J, Ruíz-Moreno JM. 2013. Advances in the understanding of retinal drug disposition and the role of blood–ocular barrier transporters. Expert Opin Drug Metab Toxicol. 9(9):1181–1192. doi:10.1517/17425255.2013.796928.

Ju WK, Kim KY, Angert M, Duong-Polk KX, Lindsey JD, Ellisman MH, Weinreb RN. 2009. Memantine blocks mitochondrial OPA1 and cytochrome c release and subsequent apoptotic cell death in glaucomatous retina. Investig Ophthalmol Vis Sci. doi:10.1167/iovs.08-2499.

Junk Anna K., Mammis A, Savitz SI, Singh M, Roth S, Malhotra S, Rosenbaum PS, Cerami A, Brines M, Rosenbaum DM. 2002. Erythropoietin administration protects retinal neurons from acute ischemia-reperfusion injury. Proc Natl Acad Sci U S A. doi:10.1073/pnas.152321399.

Junk A. K., Mammis A, Savitz SI, Singh M, Roth S, Malhotra S, Rosenbaum PS, Cerami A, Brines M, Rosenbaum DM. 2002. Erythropoietin administration protects retinal neurons from acute ischemia-reperfusion injury. Proc Natl Acad Sci. 99(16):10659–10664. doi:10.1073/pnas.152321399.

Jurišić Dukovski B, Juretić M, Bračko D, Randjelović D, Savić S, Crespo Moral M, Diebold Y, Filipović-Grčić J, Pepić I, Lovrić J. 2020. Functional ibuprofen-loaded cationic nanoemulsion: Development and optimization for dry eye disease treatment. Int J Pharm. doi:10.1016/j.ijpharm.2019.118979.

Kalam MA. 2016a. Development of chitosan nanoparticles coated with hyaluronic acid for topical ocular delivery of dexamethasone. Int J Biol Macromol. doi:10.1016/j.ijbiomac.2016.04.070.

Kalam MA. 2016b. The potential application of hyaluronic acid coated chitosan nanoparticles in ocular delivery of dexamethasone. Int J Biol Macromol. doi:10.1016/j.ijbiomac.2016.05.016.

Kamaleddin MA. 2017. Nano-ophthalmology: Applications and considerations. Nanomedicine Nanotechnology, Biol Med. doi:10.1016/j.nano.2017.02.007.

Karki R, Meena M, Prakash T, Rajeswari T, Goli D, Kumar S. 2011. Reduction in drop size of ophthalmic topical drop preparations and the impact of treatment. J Adv Pharm Technol Res. doi:10.4103/2231-4040.85540.

Kaskoos R. 2014. Investigation of moxifloxacin loaded chitosan-dextran nanoparticles for topical instillation into eye: In-vitro and ex-vivo evaluation. Int J Pharm Investig. doi:10.4103/2230-973x.143114.

Kass MA, Heuer DK, Higginbotham EJ, Johnson CA, Keltner JL, Philip Miller J, Parrish RK, Roy Wilson M, Gordon MO. 2002. The Ocular Hypertension Treatment Study: A randomized trial determines that topical ocular hypotensive medication delays or prevents the onset of primary open-angle glaucoma. Arch Ophthalmol. doi:10.1001/archopht.120.6.701.

Katara R, Majumdar DK. 2013. Eudragit RL 100-based nanoparticulate system of aceclofenac for ocular delivery. Colloids Surfaces B Biointerfaces. doi:10.1016/j.colsurfb.2012.10.056.

Katavetin P, Tungsanga K, Eiam-Ong S, Nangaku M. 2007. Antioxidative effects of erythropoietin. Kidney Int. doi:10.1038/sj.ki.5002482.

Kaur H, Ahuja M, Kumar S, Dilbaghi N. 2012. Carboxymethyl tamarind kernel polysaccharide nanoparticles for ophthalmic drug delivery. Int J Biol Macromol. doi:10.1016/j.ijbiomac.2011.11.017.

Kaur IP, Aggarwal D, Singh H, Kakkar S. 2010. Improved ocular absorption kinetics of timolol maleate loaded into a bioadhesive niosomal delivery system. Graefe's Arch Clin Exp Ophthalmol. doi:10.1007/s00417-010-1383-0.

Kaur IP, Kanwar M. 2002. Ocular preparations: the formulation approach. Drug Dev Ind Pharm. 28(5):473–493. doi:10.1081/DDC-120003445.

Kawakami M, Sekiguchi M, Sato K, Kozaki S, Takahashi M. 2001. Erythropoietin

Receptor-mediated Inhibition of Exocytotic Glutamate Release Confers Neuroprotection during Chemical Ischemia. J Biol Chem. doi:10.1074/jbc.M105832200.

Kayitmazer AB, Koksal AF, Kilic Iyilik E. 2015. Complex coacervation of hyaluronic acid and chitosan: Effects of pH, ionic strength, charge density, chain length and the charge ratio. Soft Matter. 11(44):8605–8612. doi:10.1039/c5sm01829c.

Khan MS, Vishakante GD, Bathool A. 2013. Development and characterization of pilocarpine loaded eudragit nanosuspensions for ocular drug delivery. J Biomed Nanotechnol. 9(1):124–131. doi:10.1166/jbn.2013.1475.

Khutoryanskaya O V., Morrison PWJ, Seilkhanov SK, Mussin MN, Ozhmukhametova EK, Rakhypbekov TK, Khutoryanskiy V V. 2014. Hydrogen-bonded complexes and blends of poly(acrylic acid) and methylcellulose: Nanoparticles and mucoadhesive films for ocular delivery of riboflavin. Macromol Biosci. doi:10.1002/mabi.201300313.

Kim DH, Kim HS, Ahn MD, Chun MH. 2004. Ganglion cell death in rat retina by persistent intraocular pressure elevation. Korean J Ophthalmol. doi:10.3341/kjo.2004.18.1.15.

Kim YC, Chiang B, Wu X, Prausnitz MR. 2014. Ocular delivery of macromolecules. J Control Release. doi:10.1016/j.jconrel.2014.06.043.

Kimura A, Namekata K, Guo X, Harada C, Harada T. 2016. Neuroprotection, growth factors and BDNF-TRKB signalling in retinal degeneration. Int J Mol Sci. doi:10.3390/ijms17091584.

Kimura A, Namekata K, Guo X, Noro T, Harada C, Harada T. 2015. Valproic acid prevents NMDA-Induced retinal ganglion cell death via stimulation of neuronal TrkB receptor signaling. Am J Pathol. doi:10.1016/j.ajpath.2014.11.005.

King CE, Rodger J, Bartlett C, Esmaili T, Dunlop SA, Beazley LD. 2007. Erythropoietin is both neuroprotective and neuroregenerative following optic nerve transection. Exp Neurol. 205(1):48–55. doi:10.1016/j.expneurol.2007.01.017.

Kingman S. 2004. Glaucoma is second leading cause of blindness globally. Bull World Health Organ. doi:/S0042-96862004001100019.

Kirchhof S, Goepferich AM, Brandl FP. 2015. Hydrogels in ophthalmic applications. Eur J Pharm Biopharm. doi:10.1016/j.ejpb.2015.05.016.

Klöcker N, Kermer P, Weishaupt JH, Labes M, Ankerhold R, Bähr M. 2000. Brain-derived neurotrophic factor-mediated neuroprotection of adult rat retinal ganglion cells in vivo does not exclusively depend on phosphatidyl-inositol-3'-kinase/protein kinase B signaling. J Neurosci. doi:10.1523/jneurosci.20-18-06962.2000.

Knox DL, Eagle RC, Green WR. 2007. Optic nerve hydropic axonal degeneration and blocked retrograde axoplasmic transport: Histopathologic features in human high-pressure secondary glaucoma. Arch Ophthalmol. doi:10.1001/archopht.125.3.347.

Ko ML, Hu DN, Ritch R, Sharma SC. 2000. The combined effect of brain-derived neurotrophic factor and a free radical scavenger in experimental glaucoma. Investig Ophthalmol Vis Sci.

Kretz A, Happold CJ, Marticke JK, Isenmann S. 2005. Erythropoietin promotes regeneration of adult CNS neurons via Jak2/Stat3 and PI3K/AKT pathway activation. Mol Cell Neurosci. doi:10.1016/j.mcn.2005.04.009.

Krishnan G, Chatterjee N. 2015. Anandamide rescues retinal barrier properties in Müller glia through nitric oxide regulation. Neuroscience. doi:10.1016/j.neuroscience.2014.10.020.

Kroemer G, Galluzzi L, Brenner C. 2007. Mitochondrial membrane permeabilization in cell death. Physiol Rev. doi:10.1152/physrev.00013.2006.

de la Fuente M, Seijo B, Alonso MJ. 2008. Bioadhesive hyaluronan-chitosan nanoparticles can transport genes across the ocular mucosa and transfect ocular tissue. Gene Ther. doi:10.1038/gt.2008.16.

De La Fuente M, Seijo B, Alonso MJ. 2008. Novel hyaluronic acid-chitosan nanoparticles for ocular gene therapy. Investig Ophthalmol Vis Sci. 49(5):2016–2024. doi:10.1167/iovs.07-1077.

Lagreze WA, Feltgen N, Bach M, Jehle T. 2009. Feasibility of intravitreal erythropoietin injections in humans. Br J Ophthalmol. 93(12):1667–1671. doi:10.1136/bjo.2008.156794. http://bjo.bmj.com/cgi/doi/10.1136/bjo.2008.156794.

Lakhani P, Patil A, Wu KW, Sweeney C, Tripathi S, Avula B, Taskar P, Khan S, Majumdar S. 2019. Optimization, stabilization, and characterization of amphotericin B loaded nanostructured lipid carriers for ocular drug delivery. Int J Pharm. doi:10.1016/j.ijpharm.2019.118771.

Lalu L, Tambe V, Pradhan D, Nayak K, Bagchi S, Maheshwari R, Kalia K, Tekade RK. 2017. Novel nanosystems for the treatment of ocular inflammation: Current paradigms and future research directions. J Control Release. doi:10.1016/j.jconrel.2017.07.035.

Lancina MG, Singh S, Kompella UB, Husain S, Yang H. 2017. Fast Dissolving Dendrimer Nanofiber Mats as Alternative to Eye Drops for More Efficient Antiglaucoma Drug Delivery. ACS Biomater Sci Eng. doi:10.1021/acsbiomaterials.7b00319.

Lancina MG, Wang J, Williamson GS, Yang H. 2018. DenTimol as A Dendrimeric Timolol Analogue for Glaucoma Therapy: Synthesis and Preliminary Efficacy and Safety Assessment. Mol Pharm. doi:10.1021/acs.molpharmaceut.8b00401.

Lancina MG, Yang H. 2017. Dendrimers for ocular drug delivery. Can J Chem. doi:10.1139/cjc-2017-0193.

Lau D, McGee LH, Zhou S, Rendahl KG, Manning WC, Escobedo JA, Flannery JG. 2000. Retinal degeneration is slowed in transgenic rats by AAV-mediated delivery of FGF-2. Investig Ophthalmol Vis Sci.

LaVail MM, Unoki K, Yasumura D, Matthes MT, Yancopoulos GD, Steinberg RH. 1992. Multiple growth factors, cytokines, and neurotrophins rescue photoreceptors from the damaging effects of constant light. Proc Natl Acad Sci U S A. doi:10.1073/pnas.89.23.11249.

Lax P, Esquiva G, Altavilla C, Cuenca N. 2014. Neuroprotective effects of the cannabinoid agonist HU210 on retinal degeneration. Exp Eye Res. doi:10.1016/j.exer.2014.01.019.

Lee D, Shim MS, Kim KY, Noh YH, Kim H, Kim SY, Weinreb RN, Ju WK. 2014. Coenzyme Q10 inhibits glutamate excitotoxicity and oxidative stress-mediated mitochondrial alteration in a mouse model of glaucoma. Investig Ophthalmol Vis Sci. doi:10.1167/iovs.13-12564.

Leske MC, Heijl A, Hussein M, Bengtsson B, Hyman L, Komaroff E. 2003. Factors for glaucoma progression and the effect of treatment: The early manifest glaucoma trial. Arch Ophthalmol. doi:10.1001/archopht.121.1.48.

Li J, Liu D, Tan G, Zhao Z, Yang X, Pan W. 2016. A comparative study on the efficiency of chitosan-N-acetylcysteine, chitosan oligosaccharides or carboxymethyl chitosan surface modified nanostructured lipid carrier for ophthalmic delivery of curcumin. Carbohydr Polym. doi:10.1016/j.carbpol.2016.03.079.

Li J, Tan G, Cheng B, Liu D, Pan W. 2017. Transport mechanism of chitosan-N-acetylcysteine, chitosan oligosaccharides or carboxymethyl chitosan decorated coumarin-6 loaded nanostructured lipid carriers across the rabbit ocular. Eur J Pharm Biopharm. doi:10.1016/j.ejpb.2017.08.013.

Li N, Zhuang C, Wang M, Sun X, Nie S, Pan W. 2009. Liposome coated with low molecular weight chitosan and its potential use in ocular drug delivery. Int J Pharm. doi:10.1016/j.ijpharm.2009.06.020.

Li X, Muller RH, Keck CM, Bou-Chacra NA. 2016. Mucoadhesive dexamethasone acetate-polymyxin B sulfate cationic ocular nanoemulsion - Novel combinatorial formulation concept. Pharmazie. 71(6):327–333. doi:10.1691/ph.2016.5190.

Li Y, Zhang Y, Li P, Mi G, Tu J, Sun L, Webster TJ, Shen Y. 2017. Ion-paired pirenzepine-loaded micelles as an ophthalmic delivery system for the treatment of myopia. Nanomedicine Nanotechnology, Biol Med. doi:10.1016/j.nano.2017.05.001.

Lin HR, Yu SP, Kuo CJ, Kao HJ, Lo YL, Lin YJ. 2007. Pilocarpine-loaded chitosan-PAA nanosuspension for ophthalmic delivery. J Biomater Sci Polym Ed. doi:10.1163/156856207779116739.

Lin Jing, Wu H, Wang Y, Lin Jianhong, Chen Q, Zhu X. 2016. Preparation and ocular pharmacokinetics of hyaluronan acid-modified mucoadhesive liposomes. Drug Deliv. doi:10.3109/10717544.2014.991952.

Liu D, Wu Q, Chen W, Lin H, Zhu Y, Liu Y, Liang H, Zhu FM. 2019. A novel FK506 loaded nanomicelles consisting of amino-terminated poly(ethylene glycol)-block-poly(D,L)-lactic acid and hydroxypropyl methylcellulose for ocular drug delivery. Int J Pharm. doi:10.1016/j.ijpharm.2019.03.022.

Liu HH, Bui B V., Nguyen CTO, Kezic JM, Vingrys AJ, He Z. 2015. Chronic ocular hypertension induced by circumlimbal suture in rats. Investig Ophthalmol Vis Sci. doi:10.1167/iovs.14-16009.

Liu P, Zhao X. 2013. Facile preparation of well-defined near-monodisperse chitosan/sodium alginate polyelectrolyte complex nanoparticles (CS/SAL NPs) via ionotropic gelification: A suitable technique for drug delivery systems. Biotechnol J. doi:10.1002/biot.201300093.

Liu R, Liu Z, Zhang C, Zhang B. 2012. Nanostructured lipid carriers as novel ophthalmic delivery system for mangiferin: Improving in vivo ocular bioavailability. J Pharm Sci. doi:10.1002/jps.23251.

Liu S, Dozois MD, Chang CN, Ahmad A, Ng DLT, Hileeto D, Liang H, Reyad MM, Boyd S, Jones LW, et al. 2016. Prolonged ocular retention of mucoadhesive nanoparticle eye drop formulation enables treatment of eye diseases using significantly reduced dosage. Mol Pharm. doi:10.1021/acs.molpharmaceut.6b00445.

Liu X, Xie W, Liu P, Duan M, Jia Z, Li W, Xu J. 2006. Mechanism of the cardioprotection of rhEPO pretreatment on suppressing the inflammatory response in ischemia-reperfusion. Life Sci. doi:10.1016/j.lfs.2005.09.053.

Lopez AI, Reins RY, McDermott AM, Trautner BW, Cai C. 2009. Antibacterial activity and cytotoxicity of PEGylated poly(amidoamine) dendrimers. Mol Biosyst. doi:10.1039/b904746h.

Lopez VM, Decatur CL, Stamer WD, Lynch RM, McKay BS. 2008. L-DOPA is an endogenous ligand for OA1. PLoS Biol. doi:10.1371/journal.pbio.0060236.

Löscher M, Seiz C, Hurst J, Schnichels S. 2022. Topical Drug Delivery to the Posterior Segment of the Eye. Pharmaceutics. doi:10.3390/pharmaceutics14010134.

Lu N, Li C, Cheng Y, DU AL. 2008. Protective effects of progesterone against high intraocular pressure-induced retinal ischemia-reperfusion in rats. Nan Fang Yi Ke Da Xue Xue Bao.

Ludwig A. 2005. The use of mucoadhesive polymers in ocular drug delivery. Adv Drug Deliv Rev. 57(11):1595–1639. doi:10.1016/j.addr.2005.07.005.

Luis de Redín I, Boiero C, Recalde S, Agüeros M, Allemandi D, Llabot JM, García-Layana A, Irache JM. 2019. In vivo effect of bevacizumab-loaded albumin nanoparticles in the treatment of corneal neovascularization. Exp Eye Res. doi:10.1016/j.exer.2019.107697.

Luo Q, Zhao J, Zhang X, Pan W. 2011. Nanostructured lipid carrier (NLC) coated with Chitosan Oligosaccharides and its potential use in ocular drug delivery system. Int J Pharm. doi:10.1016/j.ijpharm.2010.10.013.

Luo W, Hu L, Wang F. 2015. The protective effect of erythropoietin on the retina. Ophthalmic Res. 53(2):74–81. doi:10.1159/000369885.

Lütfi G, Müzeyyen D. 2013. Preparation and characterization of polymeric and lipid

nanoparticles of pilocarpine HCl for ocular application. Pharm Dev Technol. doi:10.3109/10837450.2012.705298.

Lyttle DP, Johnson LN, Margolin EA, Madsen RW. 2016. Levodopa as a possible treatment of visual loss in nonarteritic anterior ischemic optic neuropathy. Graefe's Arch Clin Exp Ophthalmol. doi:10.1007/s00417-015-3191-z.

M. Rezazadeh, N. J, V. A, M. A, M. T, M. M, M. Rostami. 2018. A mucoadhesive thermosensitive hydrogel containing erythropoietin as a potential treatment in oral mucositis: in vitro and in vivo studies. Drug Deliv Transl Res. 8(5):1226–1237. doi:10.1007/s13346-018-0566-9.
http://www.embase.com/search/results?subaction=viewrecord&from=export&id=L623634701%0Ahttp://dx.doi.org/10.1007/s13346-018-0566-9.

Ma YT, Hsieh T, Forbes ME, Johnson JE, Frost DO. 1998. BDNF injected into the superior colliculus reduces developmental retinal ganglion cell death. J Neurosci. doi:10.1523/jneurosci.18-06-02097.1998.

Maes C, Carmeliet G, Schipani E. 2012. Hypoxia-driven pathways in bone development, regeneration and disease. Nat Rev Rheumatol. doi:10.1038/nrrheum.2012.36.

Maged A, Mahmoud AA, Ghorab MM. 2016. Nano spray drying technique as a novel approach to formulate stable econazole nitrate nanosuspension formulations for ocular use. Mol Pharm. doi:10.1021/acs.molpharmaceut.6b00167.

Mahmoud AA, El-Feky GS, Kamel R, Awad GEA. 2011. Chitosan/sulfobutylether-β-cyclodextrin nanoparticles as a potential approach for ocular drug delivery. Int J Pharm. 413(1–2):229–36. doi:10.1016/j.ijpharm.2011.04.031.

Makhlof A, Werle M, Takeuchi H. 2008. Mucoadhesive drug carriers and polymers for effective drug delivery. J Drug Deliv Sci Technol. doi:10.1016/S1773-2247(08)50075-X.

Manchanda S, Sahoo PK. 2017. Topical delivery of acetazolamide by encapsulating in mucoadhesive nanoparticles. Asian J Pharm Sci. doi:10.1016/j.ajps.2017.04.005.

Mandal A, Pal D, Agrahari V, Trinh HM, Joseph M, Mitra AK. 2018. Ocular delivery of proteins and peptides: Challenges and novel formulation approaches. Adv Drug Deliv Rev. doi:10.1016/j.addr.2018.01.008.

Mans C, Donnelly TM. 2013. Rats. In: Clinical Veterinary Advisor. Elsevier. p. 242–252. https://linkinghub.elsevier.com/retrieve/pii/B9781416039693001384.

Mantopoulos D, Murakami Y, Comander J, Thanos A, Roh M, Miller JW, Vavvas DG. 2011. Tauroursodeoxycholic acid (TUDCA) protects photoreceptors from cell death after experimental retinal detachment. PLoS One. doi:10.1371/journal.pone.0024245.

Marsicano G, Goodenough S, Monory K, Hermann H, Eder M, Cannich A, Azad SC, Cascio MG, Ortega-Gutiérrez S, Van der Stelt M, et al. 2003. CB1 cannabinoid receptors and on-demand defense against excitotoxicity. Science (80-). doi:10.1126/science.1088208.

Marti HH. 2004. Erythropoietin and the hypoxic brain. J Exp Biol. doi:10.1242/jeb.01049.

Martin KRG, Quigley HA, Valenta D, Kielczewski J, Pease ME. 2006. Optic nerve dynein motor protein distribution changes with intraocular pressure elevation in a rat model of glaucoma. Exp Eye Res. doi:10.1016/j.exer.2005.11.025.

McKay BS, Schwartz SG. 2016. Pigmentation and macular degeneration: Is there a role for GPR143? J Ocul Pharmacol Ther. doi:10.1089/jop.2016.29007.bsm.

McLellan GJ, Miller PE. 2011. Feline glaucoma-a comprehensive review. Vet Ophthalmol. doi:10.1111/j.1463-5224.2011.00912.x.

Mehanna MM, Elmaradny HA, Samaha MW. 2010. Mucoadhesive liposomes as ocular delivery system: Physical, microbiological, and in vivo assessment. Drug Dev Ind

Pharm. doi:10.3109/03639040903099751.

Mehlen P, Bredesen DE. 2004. The dependence receptor hypothesis. Apoptosis. doi:10.1023/B:APPT.0000012120.66221.b2.

Miklavžin A, Cegnar M, Kerč J, Kristl J. 2018. Effect of surface hydrophobicity of therapeutic protein loaded in polyelectrolyte nanoparticles on transepithelial permeability. Acta Pharm. 68(3):275–293. doi:10.2478/acph-2018-0032.

Miller L, Hunt JS. 1998. Regulation of TNF-alpha production in activated mouse macrophages by progesterone. J Immunol.

Mishra V, Jain NK. 2014. Acetazolamide encapsulated dendritic nano-architectures for effective glaucoma management in rabbits. Int J Pharm. doi:10.1016/j.ijpharm.2013.11.043.

Mittal N, Kaur G. 2019. Leucaena leucocephala (Lam.) galactomannan nanoparticles: Optimization and characterization for ocular delivery in glaucoma treatment. Int J Biol Macromol. doi:10.1016/j.ijbiomac.2019.08.107.

Moiseev R V., Morrison PWJ, Steele F, Khutoryanskiy V V. 2019. Penetration enhancers in ocular drug delivery. Pharmaceutics. doi:10.3390/pharmaceutics11070321.

Mokbel TH, Ghanem AA, Kishk H, Arafa LF, El-Baiomy AA. 2010. Erythropoietin and soluble CD44 levels in patients with primary open-angle glaucoma. Clin Exp Ophthalmol. doi:10.1111/j.1442-9071.2010.02318.x.

Morrison PWJ, Khutoryanskiy V V. 2014a. Anatomy of the Eye and the Role of Ocular Mucosa in Drug Delivery. In: Mucoadhesive Materials and Drug Delivery Systems.

Morrison PWJ, Khutoryanskiy V V. 2014b. Enhancement in corneal permeability of riboflavin using calcium sequestering compounds. Int J Pharm. doi:10.1016/j.ijpharm.2014.06.007.

Morsi N, Ghorab D, Refai H, Teba H. 2016. Ketoroloac tromethamine loaded nanodispersion incorporated into thermosensitive in situ gel for prolonged ocular delivery. Int J Pharm. doi:10.1016/j.ijpharm.2016.04.021.

Morsi N, Ibrahim M, Refai H, El Sorogy H. 2017. Nanoemulsion-based electrolyte triggered in situ gel for ocular delivery of acetazolamide. Eur J Pharm Sci. doi:10.1016/j.ejps.2017.04.013.

Motwani SK, Chopra S, Talegaonkar S, Kohli K, Ahmad FJ, Khar RK. 2008. Chitosan-sodium alginate nanoparticles as submicroscopic reservoirs for ocular delivery: Formulation, optimisation and in vitro characterisation. Eur J Pharm Biopharm. doi:10.1016/j.ejpb.2007.09.009.

Mourya VK, Inamdar NN, Tiwari A. 2010. Carboxymethyl chitosan and its applications. Adv Mater Lett. doi:10.5185/amlett.2010.3108.

Moustafa MA, El-Refaie WM, Elnaggar YSR, Abdallah OY. 2018. Gel in core carbosomes as novel ophthalmic vehicles with enhanced corneal permeation and residence. Int J Pharm. doi:10.1016/j.ijpharm.2018.05.040.

Moustafa MA, Elnaggar YSR, El-Refaie WM, Abdallah OY. 2017. Hyalugel-integrated liposomes as a novel ocular nanosized delivery system of fluconazole with promising prolonged effect. Int J Pharm. doi:10.1016/j.ijpharm.2017.10.007.

Mudgil M, Pawar PK. 2013. Preparation and in Vitro/Ex Vivo evaluation of moxifloxacin-loaded PLGA nanosuspensions for ophthalmic application. Sci Pharm. doi:10.3797/scipharm.1204-16.

Mui AM, Yang V, Aung MH, Fu J, Adekunle AN, Prall BC, Sidhu CS, Park H na, Boatright JH, Iuvone PM, et al. 2018. Daily visual stimulation in the critical period enhances multiple aspects of vision through BDNF-mediated pathways in the mouse retina. PLoS One. doi:10.1371/journal.pone.0192435.

Naarendorp F, Sato Y, Cajdric A, Hubbard NP. 2001. Absolute and relative sensitivity of the scotopic system of rat: Electroretinography and behavior. Vis Neurosci. doi:10.1017/S0952523801184142.

Nagarwal RC, Singh PN, Kant S, Maiti P, Pandit JK. 2011. Chitosan nanoparticles of 5-fluorouracil for ophthalmic delivery: Characterization, in-vitro and in-vivo study. Chem Pharm Bull. doi:10.1248/cpb.59.272.

Nakai T, Hirakura T, Sakurai Y, Shimoboji T, Ishigai M, Akiyoshi K. 2012. Injectable Hydrogel for Sustained Protein Release by Salt-Induced Association of Hyaluronic Acid Nanogel. Macromol Biosci. 12(4):475–483. doi:10.1002/mabi.201100352.

Nasr FH, Khoee S. 2015. Design, characterization and in vitro evaluation of novel shell crosslinked poly(butylene adipate)-co-N-succinyl chitosan nanogels containing loteprednol etabonate: A new system for therapeutic effect enhancement via controlled drug delivery. Eur J Med Chem. doi:10.1016/j.ejmech.2015.07.045.

Natesan S, Pandian S, Ponnusamy C, Palanichamy R, Muthusamy S, Kandasamy R. 2017. Co-encapsulated resveratrol and quercetin in chitosan and peg modified chitosan nanoparticles: For efficient intra ocular pressure reduction. Int J Biol Macromol. doi:10.1016/j.ijbiomac.2017.04.117.

Nayak K, Misra M. 2018. A review on recent drug delivery systems for posterior segment of eye. Biomed Pharmacother. doi:10.1016/j.biopha.2018.08.138.

Nepp J, Knoetzl W, Prinz A, Hoeller S, Prinz M. 2020. Management of moderate-to-severe dry eye disease using chitosan-N-acetylcysteine (Lacrimera®) eye drops: a retrospective case series. Int Ophthalmol. doi:10.1007/s10792-020-01324-5.

Noailles A, Fernández-Sánchez L, Lax P, Cuenca N. 2014. Microglia activation in a model of retinal degeneration and TUDCA neuroprotective effects. J Neuroinflammation. doi:10.1186/s12974-014-0186-3.

Nucci C, Bari M, Spanò A, Corasaniti MT, Bagetta G, Maccarrone M, Morrone LA. 2008. Potential roles of (endo)cannabinoids in the treatment of glaucoma: from intraocular pressure control to neuroprotection. Prog Brain Res. doi:10.1016/S0079-6123(08)01131-X.

Nucci C, Russo R, Martucci A, Giannini C, Garaci F, Floris R, Bagetta G, Morrone LA. 2016. New strategies for neuroprotection in glaucoma, a disease that affects the central nervous system. Eur J Pharmacol. doi:10.1016/j.ejphar.2016.04.030.

Nucci C, Tartaglione R, Cerulli A, Mancino R, Spanò A, Cavaliere F, Rombolà L, Bagetta G, Corasaniti MT, Morrone LA. 2007. Retinal Damage Caused by High Intraocular Pressure-Induced Transient Ischemia is Prevented by Coenzyme Q10 in Rat. Int Rev Neurobiol. doi:10.1016/S0074-7742(07)82022-8.

Nucci C, Tartaglione R, Rombolà L, Morrone LA, Fazzi E, Bagetta G. 2005. Neurochemical evidence to implicate elevated glutamate in the mechanisms of high intraocular pressure (IOP)-induced retinal ganglion cell death in rat. In: NeuroToxicology.

Ofri R, Narfström K. 2007. Light at the end of the tunnel? Advances in the understanding and treatment of glaucoma and inherited retinal degeneration. Vet J. doi:10.1016/j.tvjl.2006.08.014.

Omura T, Asari M, Yamamoto J, Oka K, Hoshina C, Maseda C, Awaya T, Tasaki Y, Shiono H, Yonezawa A, et al. 2013. Sodium tauroursodeoxycholate prevents paraquat-induced cell death by suppressing endoplasmic reticulum stress responses in human lung epithelial A549 cells. Biochem Biophys Res Commun. doi:10.1016/j.bbrc.2013.01.131.

Orasugh JT, Sarkar G, Saha NR, Das B, Bhattacharyya A, Das S, Mishra R, Roy I, Chattoapadhyay A, Ghosh SK, et al. 2019. Effect of cellulose nanocrystals on the performance of drug loaded in situ gelling thermo-responsive ophthalmic formulations. Int J Biol Macromol. doi:10.1016/j.ijbiomac.2018.11.217.

Othman N, Masarudin MJ, Kuen CY, Dasuan NA, Abdullah LC, Jamil SNAM. 2018. Synthesis and optimization of chitosan nanoparticles loaded with l-ascorbic acid and thymoquinone. Nanomaterials. doi:10.3390/nano8110920.

Ott C, Martens H, Hassouna I, Oliveira B, Erck C, Zafeiriou MP, Peteri UK, Hesse D, Gerhart S, Altas B, et al. 2015. Widespread expression of erythropoietin receptor in

brain and its induction by injury. Mol Med. doi:10.2119/molmed.2015.00192.

Ou K, Li Y, Liu L, Li H, Cox K, Wu J, Liu J, Dick AD. 2022. Recent developments of neuroprotective agents for degenerative retinal disorders. Neural Regen Res. doi:10.4103/1673-5374.335140.

Oveson BC, Iwase T, Hackett SF, Lee SY, Usui S, Sedlak TW, Snyder SH, Campochiaro PA, Sung JU. 2011. Constituents of bile, bilirubin and TUDCA, protect against oxidative stress-induced retinal degeneration. J Neurochem. doi:10.1111/j.1471-4159.2010.07092.x.

Pai R V., Vavia PR. 2020. Chitosan oligosaccharide enhances binding of nanostructured lipid carriers to ocular mucins: Effect on ocular disposition. Int J Pharm. doi:10.1016/j.ijpharm.2020.119095.

Pandit J, Sultana Y, Aqil M. 2021. Chitosan coated nanoparticles for efficient delivery of bevacizumab in the posterior ocular tissues via subconjunctival administration. Carbohydr Polym. doi:10.1016/j.carbpol.2021.118217.

Pang IH, Clark AF. 2007. Rodent models for glaucoma retinopathy and optic neuropathy. J Glaucoma. doi:10.1097/IJG.0b013e3181405d4f.

Paolicelli P, De La Fuente M, Sánchez A, Seijo B, Alonso MJ. 2009. Chitosan nanoparticles for drug delivery to the eye. Expert Opin Drug Deliv. doi:10.1517/17425240902762818.

Pardue MT, Allen RS. 2018. Neuroprotective strategies for retinal disease. Prog Retin Eye Res. 65:50–76. doi:10.1016/j.preteyeres.2018.02.002. https://linkinghub.elsevier.com/retrieve/pii/S1350946217300848.

Park IH, Kim MK, Kim SU. 2008. Ursodeoxycholic acid prevents apoptosis of mouse sensory neurons induced by cisplatin by reducing P53 accumulation. Biochem Biophys Res Commun. doi:10.1016/j.bbrc.2008.06.014.

Passani A, Posarelli C, Sframeli AT, Perciballi L, Pellegrini M, Guidi G, Figus M. 2020. Cannabinoids in glaucoma patients: The never-ending story. J Clin Med. doi:10.3390/jcm9123978.

Patel A. 2013. Ocular drug delivery systems: An overview. World J Pharmacol. doi:10.5497/wjp.v2.i2.47.

Pepić I, Hafner A, Lovrić J, Pirkić B, Filipović-Grčić J. 2010. A nonionic surfactant/chitosan micelle system in an innovative eye drop formulation. J Pharm Sci. doi:10.1002/jps.22137.

Pescina S, Govoni P, Antopolsky M, Murtomäki L, Padula C, Santi P, Nicoli S. 2015. Permeation of Proteins, Oligonucleotide and Dextrans Across Ocular Tissues: Experimental Studies and a Literature Update. J Pharm Sci. 104(7):2190–2202. doi:10.1002/jps.24465.

Pescosolido N, Parisi F, Russo P, Buomprisco G, Nebbioso M. 2013. Role of dopaminergic receptors in glaucomatous disease modulation. Biomed Res Int. doi:10.1155/2013/193048.

Peter MG. 1995. Pure and Applied Chemistry Applications and Environmental Aspects of Chitin and Chitosan APPLICATIONS AND ENVIRONMENTAL ASPECTS. J Macromol Sci Part A Pure Appl Chem. 32(4):629–640.

Peynshaert K, Devoldere J, De Smedt SC, Remaut K. 2018. In vitro and ex vivo models to study drug delivery barriers in the posterior segment of the eye. Adv Drug Deliv Rev. 126:44–57. doi:10.1016/j.addr.2017.09.007. https://doi.org/10.1016/j.addr.2017.09.007.

Phillips MJ, Walker TA, Choi HY, Faulkner AE, Kim MK, Sidney SS, Boyd AP, Nickerson JM, Boatright JH, Pardue MT. 2008. Tauroursodeoxycholic acid preservation of photoreceptor structure and function in the rd10 mouse through postnatal day 30. Investig Ophthalmol Vis Sci. doi:10.1167/iovs.07-1012.

Pignatello Rosario, Bucolo C, Ferrara P, Maltese A, Puleo A, Puglisi G. 2002.

Eudragit RS100® nanosuspensions for the ophthalmic controlled delivery of ibuprofen. Eur J Pharm Sci. doi:10.1016/S0928-0987(02)00057-X.

Pignatello R., Bucolo C, Puglisi G. 2002. Ocular tolerability of Eudragit RS100® and RL100® nanosuspensions as carriers for ophthalmic controlled drug delivery. In: Journal of Pharmaceutical Sciences.

Pignatello R., Bucolo C, Spedalieri G, Maltese A, Puglisi G. 2002. Flurbiprofen-loaded acrylate polymer nanosuspensions for ophthalmic application. Biomaterials. doi:10.1016/S0142-9612(02)00080-7.

Pignatello R, Ricupero N, Bucolo C, Maugeri F, Maltese A, Puglisi G. 2006. Preparation and characterization of Eudragit Retard nanosuspensions for the ocular delivery of cloricromene. AAPS PharmSciTech. doi:10.1208/pt070127.

Posthumus RG. 1952. The use and the possibilities of progesterone in the treatment of glaucoma. Ophthalmologica. doi:10.1159/000301245.

Prausnitz MR. 1998. Permeability of cornea, sciera, and conjunctiva: A literature analysis for drug delivery to the eye. J Pharm Sci. 87(12):1479–1488. doi:10.1021/js9802594.

Prosperi-Porta G, Kedzior S, Muirhead B, Sheardown H. 2016. Phenylboronic-Acid-Based Polymeric Micelles for Mucoadhesive Anterior Segment Ocular Drug Delivery. Biomacromolecules. doi:10.1021/acs.biomac.6b00054.

Puia G, Belelli D. 2001. Neurosteroids on our minds. In: Trends in Pharmacological Sciences.

Quigley HA. 2011. Glaucoma. In: The Lancet. 2011 March 30; 377 (9774):1367-1377. https://doi.org/10.1016/S0140-6736(10)61423-7

Quiñones JP, Peniche H, Peniche C. 2018. Chitosan based self-assembled nanoparticles in drug delivery. Polymers (Basel). doi:10.3390/polym10030235.

Quinteros D, Vicario-De-La-Torre M, Andrés-Guerrero V, Palma S, Allemandi D, Herrero-Vanrell R, Molina-Martínez IT. 2014. Hybrid formulations of liposomes and bioadhesive polymers improve the hypotensive effect of the melatonin analogue 5-MCA-NAT in rabbit eyes. PLoS One. doi:10.1371/journal.pone.0110344.

Quinteros DA, Ferreira LM, Schaffazick SR, Palma SD, Allemandi DA, Cruz L. 2016. Novel Polymeric Nanoparticles Intended for Ophthalmic Administration of Acetazolamide. J Pharm Sci. doi:10.1016/j.xphs.2016.06.023.

Radhakrishnan K, Sonali N, Moreno M, Nirmal J, Fernandez AA, Venkatraman S, Agrawal R. 2017. Protein delivery to the back of the eye: barriers, carriers and stability of anti-VEGF proteins. Drug Discov Today. 22(2):416–423. doi:10.1016/j.drudis.2016.10.015. http://dx.doi.org/10.1016/j.drudis.2016.10.015.

Rah MJ. 2011. A review of hyaluronan and its ophthalmic applications. Optometry. 82(1):38–43. doi:10.1016/j.optm.2010.08.003. http://dx.doi.org/10.1016/j.optm.2010.08.003.

Ranta VP, Urtti A. 2006. Transscleral drug delivery to the posterior eye: Prospects of pharmacokinetic modeling. Adv Drug Deliv Rev. doi:10.1016/j.addr.2006.07.025.

Rathore P, Mahor A, Jain S, Haque A, Kesharwani P. 2020. Formulation development,: In vitro and in vivo evaluation of chitosan engineered nanoparticles for ocular delivery of insulin. RSC Adv. doi:10.1039/d0ra07640f.

Rawas-Qalaji M, Williams C-A. 2012. Advances in ocular drug delivery. Curr Eye Res. 37(5):345–56. doi:10.3109/02713683.2011.652286.

Reimondez-Troitiño S, Csaba N, Alonso MJ, De La Fuente M. 2015. Nanotherapies for the treatment of ocular diseases. Eur J Pharm Biopharm. doi:10.1016/j.ejpb.2015.02.019.

Ren T, Lin X, Zhang Q, You D, Liu X, Tao X, Gou J, Zhang Y, Yin T, He H, et al. 2018. Encapsulation of Azithromycin Ion Pair in Liposome for Enhancing Ocular Delivery and Therapeutic Efficacy on Dry Eye. Mol Pharm.

doi:10.1021/acs.molpharmaceut.8b00516.

Resende AP, Rosolen SG, Nunes T, São Braz B, Delgado E. 2018. Functional and Structural Effects of Erythropoietin Subconjunctival Administration in Glaucomatous Animals. Biomed Hub. 3(2):1–11. doi:10.1159/000488970.

Resende AP, São-Braz B, Delgado E. 2013. Alternative route for erythropoietin ocular administration. Graefe's Arch Clin Exp Ophthalmol. 251(8):2051–2056. doi:10.1007/s00417-013-2367-7. http://link.springer.com/10.1007/s00417-013-2367-7.

Resende AP, São Braz B, Delgado E. 2016. Ocular Erythropoietin Penetration after Subconjunctival Administration in Glaucomatous Rats. Ophthalmic Res. 56(2):104–110. doi:10.1159/000444327. https://www.karger.com/Article/FullText/444327.

Resende AP, Silva B, Braz BS, Nunes T, Gonçalves L, Delgado E. 2017. Ex vivo permeation of erythropoietin through porcine conjunctiva, cornea, and sclera. Drug Deliv Transl Res. doi:10.1007/s13346-017-0399-y.

Rex TS, Allocca M, Domenici L, Surace EM, Maguire AM, Lyubarsky A, Cellerino A, Bennett J, Auricchio A. 2004. Systemic but not intraocular Epo gene transfer protects the retina from light-and genetic-induced degeneration. Mol Ther. doi:10.1016/j.ymthe.2004.07.027.

Reza Razeghinejad M, Hossein Nowroozzadeh M, Hossein Eghbal M. 2016. Levodopa and other pharmacologic interventions in ischemic and traumatic optic neuropathies and amblyopia. Clin Neuropharmacol. doi:10.1097/WNF.0000000000000115.

Rhee J, Shih KC. 2021. Use of gene therapy in retinal ganglion cell neuroprotection: Current concepts and future directions. Biomolecules. doi:10.3390/biom11040581.

Rodrigues CMP, Fan G, Wong PY, Kren BT, Steer CJ. 1998. Ursodeoxycholic acid may inhibit deoxycholic acid-induced apoptosis by modulating mitochondrial transmembrane potential and reactive oxygen species production. Mol Med. doi:10.1007/bf03401914.

Rodríguez I, Vázquez JA, Pastrana L, Khutoryanskiy V V. 2017. Enhancement and inhibition effects on the corneal permeability of timolol maleate: Polymers, cyclodextrins and chelating agents. Int J Pharm. doi:10.1016/j.ijpharm.2017.06.075.

Romero-Ramírez L, Nieto-Sampedro M, Yanguas-Casás N. 2017. Tauroursodeoxycholic acid: more than just a neuroprotective bile conjugate. Neural Regen Res. doi:10.4103/1673-5374.198979.

Romero GB, Keck CM, Müller RH, Bou-Chacra NA. 2016. Development of cationic nanocrystals for ocular delivery. Eur J Pharm Biopharm. doi:10.1016/j.ejpb.2016.07.005.

Rosolen SG, Rigaudière F, Le Gargasson JF, Brigell MG. 2005. Recommendations for a toxicological screening ERG procedure in laboratory animals. Doc Ophthalmol. doi:10.1007/s10633-005-7344-y.

Rusanen E, Florin M, Hässig M, Spiess BM. 2010. Evaluation of a rebound tonometer (Tonovet®) in clinically normal cat eyes. Vet Ophthalmol. doi:10.1111/j.1463-5224.2009.00752.x.

Russo R., Cavaliere F, Berliocchi L, Nucci C, Gliozzi M, Mazzei C, Tassorelli C, Corasaniti MT, Rotiroti D, Bagetta G, et al. 2008. Modulation of pro-survival and death-associated pathways under retinal ischemia/reperfusion: Effects of NMDA receptor blockade. J Neurochem. doi:10.1111/j.1471-4159.2008.05694.x.

Russo Rossella, Cavaliere F, Rombolà L, Gliozzi M, Cerulli A, Nucci C, Fazzi E, Bagetta G, Corasaniti MT, Morrone LA. 2008. Rational basis for the development of coenzyme Q10 as a neurotherapeutic agent for retinal protection. Prog Brain Res. doi:10.1016/S0079-6123(08)01139-4.

Russo R, Varano GP, Adornetto A, Nucci C, Corasaniti MT, Bagetta G, Morrone LA. 2016. Retinal ganglion cell death in glaucoma: Exploring the role of neuroinflammation.

Eur J Pharmacol. doi:10.1016/j.ejphar.2016.03.064.

Sabzevari A, Adibkia K, Hashemi H, De Geest BG, Mohsenzadeh N, Atyabi F, Ghahremani MH, Khoshayand MR, Dinarvand R. 2013. Improved anti-inflammatory effects in rabbit eye model using biodegradable poly beta-amino ester nanoparticles of triamcinolone acetonide. Investig Ophthalmol Vis Sci. doi:10.1167/iovs.13-12296.

Sadeghi R, Etemad SG, Keshavarzi E, Haghshenasfard M. 2015. Investigation of alumina nanofluid stability by UV–vis spectrum. Microfluid Nanofluidics. doi:10.1007/s10404-014-1491-y.

Sahoo SK, Dilnawaz F, Krishnakumar S. 2008. Nanotechnology in ocular drug delivery. Drug Discov Today. 13(3–4):144–151. doi:10.1016/j.drudis.2007.10.021.

Salama AH, Mahmoud AA, Kamel R. 2016. A Novel Method for Preparing Surface-Modified Fluocinolone Acetonide Loaded PLGA Nanoparticles for Ocular Use: In Vitro and In Vivo Evaluations. AAPS PharmSciTech. doi:10.1208/s12249-015-0448-0.

Salinas-Navarro M, Alarcón-Martínez L, Valiente-Soriano FJ, Ortín-Martínez A, Jiménez-López M, Avilés-Trigueros M, Villegas-Pérez MP, de la Villa P, Vidal-Sanz M. 2009. Functional and morphological effects of laser-induced ocular hypertension in retinas of adult albino Swiss mice. Mol Vis.

Salzillo R, Schiraldi C, Corsuto L, D'Agostino A, Filosa R, De Rosa M, La Gatta A. 2016. Optimization of hyaluronan-based eye drop formulations. Carbohydr Polym. 153:275–283. doi:10.1016/j.carbpol.2016.07.106. http://dx.doi.org/10.1016/j.carbpol.2016.07.106.

Sandri G, Motta S, Bonferoni MC, Brocca P, Rossi S, Ferrari F, Rondelli V, Cantù L, Caramella C, Del Favero E. 2017. Chitosan-coupled solid lipid nanoparticles: Tuning nanostructure and mucoadhesion. Eur J Pharm Biopharm. doi:10.1016/j.ejpb.2016.10.010.

Santalices I, Gonella A, Torres D, Alonso MJ. 2017. Advances on the formulation of proteins using nanotechnologies. J Drug Deliv Sci Technol. doi:10.1016/j.jddst.2017.06.018.

Saravanakumar G, Min KH, Min DS, Kim AY, Lee CM, Cho YW, Lee SC, Kim K, Jeong SY, Park K, et al. 2009. Hydrotropic oligomer-conjugated glycol chitosan as a carrier of paclitaxel: Synthesis, characterization, and in vivo biodistribution. J Control Release. doi:10.1016/j.jconrel.2009.06.015.

Sarmento B, Ribeiro A, Veiga F, Ferreira D. 2006. Development and characterization of new insulin containing polysaccharide nanoparticles. Colloids Surfaces B Biointerfaces. doi:10.1016/j.colsurfb.2006.09.012.

Sasaki H, Yamamura K, Nishida K, Nakamura J, Ichikawa M. 1996. Delivery of drugs to the eye by topical application. Prog Retin Eye Res. doi:10.1016/1350-9462(96)00014-6.

Saxena A, Sachin K, Bohidar HB, Verma AK. 2005. Effect of molecular weight heterogeneity on drug encapsulation efficiency of gelatin nano-particles. Colloids Surfaces B Biointerfaces. 45(1):42–48. doi:10.1016/j.colsurfb.2005.07.005.

Sayed S, Elsayed I, Ismail MM. 2018. Optimization of β-cyclodextrin consolidated micellar dispersion for promoting the transcorneal permeation of a practically insoluble drug. Int J Pharm. doi:10.1016/j.ijpharm.2018.08.001.

Schwartz M, London A. 2009. Erratum to: Immune maintenance in glaucoma: boosting the body's own neuroprotective potential. J Ocul Biol Dis Infor. doi:10.1007/s12177-009-9037-3.

Shareef SR, Garcia-Valenzuela E, Salierno A, Walsh J, Sharma SC. 1995. Chronic ocular hypertension following episcleral venous occlusion in rats. Exp Eye Res. doi:10.1016/S0014-4835(05)80131-9.

Sharma OP, Patel V, Mehta T. 2016. Nanocrystal for ocular drug delivery: hope or hype. Drug Deliv Transl Res. doi:10.1007/s13346-016-0292-0.

Shen J, Deng Y, Jin X, Ping Q, Su Z, Li L. 2010. Thiolated nanostructured lipid carriers as a potential ocular drug delivery system for cyclosporine A: Improving in vivo ocular distribution. Int J Pharm. doi:10.1016/j.ijpharm.2010.10.008.

Shen J, Wang Y, Ping Q, Xiao Y, Huang X. 2009. Mucoadhesive effect of thiolated PEG stearate and its modified NLC for ocular drug delivery. J Control Release. doi:10.1016/j.jconrel.2009.04.021.

Shibagaki K, Okamoto K, Katsuta O, Nakamura M. 2015. Beneficial protective effect of pramipexole on light-induced retinal damage in mice. Exp Eye Res. doi:10.1016/j.exer.2015.07.007.

Shinde U, Ahmed MH, Singh K. 2013. Development of Dorzolamide Loaded 6-O - Carboxymethyl Chitosan Nanoparticles for Open Angle Glaucoma . J Drug Deliv. doi:10.1155/2013/562727.

Shirley Ding SL, Leow SN, Munisvaradass R, Koh EH, Bastion MLC, Then KY, Kumar S, Mok PL. 2016. Revisiting the role of erythropoietin for treatment of ocular disorders. Eye. 30(10):1293–1309. doi:10.1038/eye.2016.94. http://dx.doi.org/10.1038/eye.2016.94.

Silva B, Gonçalves LM, Braz BS, Delgado E. 2022. Chitosan and Hyaluronic Acid Nanoparticles as Vehicles of Epoetin Beta for Subconjunctival Ocular Delivery. Mar Drugs. 20(2). doi:10.3390/md20020151.

Silva B, Marto J, Braz BS, Delgado E, Almeida AJ, Gonçalves L. 2020. New nanoparticles for topical ocular delivery of erythropoietin. Int J Pharm. doi:10.1016/j.ijpharm.2020.119020.

Silva B, São Braz B, Delgado E, Gonçalves L. 2021. Colloidal nanosystems with mucoadhesive properties designed for ocular topical delivery. Int J Pharm. doi:10.1016/j.ijpharm.2021.120873.

Silva MM, Calado R, Marto J, Bettencourt A, Almeida AJ, Gonçalves LMD. 2017. Chitosan nanoparticles as a mucoadhesive drug delivery system for ocular administration. Mar Drugs. 15(12):1–16. doi:10.3390/md15120370.

Silva NC, Silva S, Sarmento B, Pintado M. 2013. Chitosan nanoparticles for daptomycin delivery in ocular treatment of bacterial endophthalmitis. Drug Deliv. 7544(February):1–9. doi:10.3109/10717544.2013.858195.

da Silva SB, Ferreira D, Pintado M, Sarmento B. 2016. Chitosan-based nanoparticles for rosmarinic acid ocular delivery--In vitro tests. Int J Biol Macromol. 84:112–20. doi:10.1016/j.ijbiomac.2015.11.070.

Singh KH, Shinde UA. 2011. Chitosan nanoparticles for controlled delivery of brimonidine tartrate to the ocular membrane. Pharmazie. doi:10.1691/ph.2011.0349.

Skaat A, Solomon A, Moroz I, Hai OV, Rechtman E, Vishnevskia Dai V, Rotenstreich Y. 2011. Increased electroretinogram a-wave amplitude after intravitreal bevacizumab injection for neovascular age-related macular degeneration. Acta Ophthalmol. doi:10.1111/j.1755-3768.2010.02005.x.

Smart JD. 2005. The basics and underlying mechanisms of mucoadhesion. Adv Drug Deliv Rev. doi:10.1016/j.addr.2005.07.001.

Soltani S, Zakeri-Milani P, Barzegar-Jalali M, Jelvehgari M. 2016. Design of eudragit RL nanoparticles by nanoemulsion method as carriers for ophthalmic drug delivery of ketotifen fumarate. Iran J Basic Med Sci. doi:10.22038/ijbms.2016.6940.

Sosnik A, Das Neves J, Sarmento B. 2014. Mucoadhesive polymers in the design of nano-drug delivery systems for administration by non-parenteral routes: A review. Prog Polym Sci. doi:10.1016/j.progpolymsci.2014.07.010.

Strom AR, Hässig M, Iburg TM, Spiess BM. 2011. Epidemiology of canine glaucoma presented to University of Zurich from 1995 to 2009. Part 2: Secondary glaucoma (217 cases). Vet Ophthalmol. doi:10.1111/j.1463-5224.2010.00854.x.

Sucher NJ, Lipton SA, Dreyer EB. 1997. Molecular basis of glutamate toxicity in

retinal ganglion cells. Vision Res. doi:10.1016/S0042-6989(97)00047-3.

Sullivan TA, Geisert EE, Hines-Beard J, Rex TS. 2011. Systemic adeno-associated virus-mediated gene therapy preserves retinal ganglion cells and visual function in DBA/2J glaucomatous mice. Hum Gene Ther. doi:10.1089/hum.2011.052.

Sullivan TA, Geisert EE, Templeton JP, Rex TS. 2012. Dose-dependent treatment of optic nerve crush by exogenous systemic mutant erythropoietin. Exp Eye Res. doi:10.1016/j.exer.2012.01.006.

Tahara K, Karasawa K, Onodera R, Takeuchi H. 2017. Feasibility of drug delivery to the eye's posterior segment by topical instillation of PLGA nanoparticles. Asian J Pharm Sci. doi:10.1016/j.ajps.2017.03.002.

Tai L, Liu C, Jiang K, Chen X, Feng L, Pan W, Wei G, Lu W. 2017. A novel penetratin-modified complex for noninvasive intraocular delivery of antisense oligonucleotides. Int J Pharm. doi:10.1016/j.ijpharm.2017.06.090.

Tamba BI, Dondas A, Leon M, Neagu AN, Dodi G, Stefanescu C, Tijani A. 2015. Silica nanoparticles: Preparation, characterization and in vitro/in vivo biodistribution studies. Eur J Pharm Sci. 71(February):46–55. doi:10.1016/j.ejps.2015.02.002. http://dx.doi.org/10.1016/j.ejps.2015.02.002.

Tan G, Li J, Song Y, Yu Y, Liu D, Pan W. 2019. Phenylboronic acid-tethered chondroitin sulfate-based mucoadhesive nanostructured lipid carriers for the treatment of dry eye syndrome. Acta Biomater. doi:10.1016/j.actbio.2019.08.035.

Tan G, Yu S, Li J, Pan W. 2017. Development and characterization of nanostructured lipid carriers based chitosan thermosensitive hydrogel for delivery of dexamethasone. Int J Biol Macromol. doi:10.1016/j.ijbiomac.2017.05.132.

Tan G, Yu S, Pan H, Li J, Liu D, Yuan K, Yang X, Pan W. 2017. Bioadhesive chitosan-loaded liposomes: A more efficient and higher permeable ocular delivery platform for timolol maleate. Int J Biol Macromol. 94:355–363. doi:10.1016/j.ijbiomac.2016.10.035.

Tan J, Zhang X, Li D, Liu G, Wang Y, Zhang D, Wang X, Tian W, Dong X, Zhou L, et al. 2020. scAAV2-Mediated C3 Transferase Gene Therapy in a Rat Model with Retinal Ischemia/Reperfusion Injuries. Mol Ther - Methods Clin Dev. doi:10.1016/j.omtm.2020.04.014.

Tao W, Wen R, Goddard MB, Sherman SD, O'Rourke PJ, Stabila PF, Bell WJ, Dean BJ, Kauper KA, Budz VA, et al. 2002. Encapsulated cell-based delivery of CNTF reduces photoreceptor degeneration in animal models of retinitis pigmentosa. Investig Ophthalmol Vis Sci.

Tatke A, Dudhipala N, Janga KY, Balguri SP, Avula B, Jablonski MM, Majumdar S. 2019. In situ gel of triamcinolone acetonide-loaded solid lipid nanoparticles for improved topical ocular delivery: Tear kinetics and ocular disposition studies. Nanomaterials. doi:10.3390/nano9010033.

Tayel SA, El-Nabarawi MA, Tadros MI, Abd-Elsalam WH. 2013. Promising ion-sensitive in situ ocular nanoemulsion gels of terbinafine hydrochloride: Design, in vitro characterization and in vivo estimation of the ocular irritation and drug pharmacokinetics in the aqueous humor of rabbits. Int J Pharm. doi:10.1016/j.ijpharm.2012.12.049.

Terreni E, Chetoni P, Tampucci S, Burgalassi S, Al-Kinani AA, Alany RG, Monti D. 2020. Assembling surfactants-mucoadhesive polymer nanomicelles (ASMP-nano) for ocular delivery of cyclosporine-A. Pharmaceutics. doi:10.3390/pharmaceutics12030253.

Thanou M, Verhoef JC, Junginger HE. 2001. Oral drug absorption enhancement by chitosan and its derivatives. Adv Drug Deliv Rev. doi:10.1016/S0169-409X(01)00231-9.

Tian B, Luo Q, Song S, Liu D, Pan H, Zhang W, He L, Ma S, Yang X, Pan W. 2012. Novel surface-modified nanostructured lipid carriers with partially deacetylated water-soluble chitosan for efficient ocular delivery. J Pharm Sci. doi:10.1002/jps.22813.

Tonglairoum P, Brannigan RP, Opanasopit P, Khutoryanskiy V V. 2016. Maleimide-

bearing nanogels as novel mucoadhesive materials for drug delivery. J Mater Chem B. doi:10.1039/c6tb02124g.

Tratta E, Pescina S, Padula C, Santi P, Nicoli S. 2014. In vitro permeability of a model protein across ocular tissues and effect of iontophoresis on the transscleral delivery. Eur J Pharm Biopharm. doi:10.1016/j.ejpb.2014.04.018.

Tsai JC, Song BJ, Wu L, Forbes M. 2007. Erythropoietin: A candidate neuroprotective agent in the treatment of glaucoma. J Glaucoma. doi:10.1097/IJG.0b013e318156a556.

Tsai JC, Wu L, Worgul B, Forbes M, Cao J. 2005. Intravitreal administration of erythropoietin and preservation of retinal ganglion cells in an experimental rat model of glaucoma. Curr Eye Res. 30(11):1025–1031. doi:10.1080/02713680500320729.

Tuomela A, Liu P, Puranen J, Rönkkö S, Laaksonen T, Kalesnykas G, Oksala O, Ilkka J, Laru J, Järvinen K, et al. 2014. Brinzolamide nanocrystal formulations for ophthalmic delivery: Reduction of elevated intraocular pressure in vivo. Int J Pharm. doi:10.1016/j.ijpharm.2014.03.048.

Uccello-Barretta G, Nazzi S, Zambito Y, Di Colo G, Balzano F, Sansò M. 2010. Synergistic interaction between TS-polysaccharide and hyaluronic acid: Implications in the formulation of eye drops. Int J Pharm. 395(1–2):122–131. doi:10.1016/j.ijpharm.2010.05.031.

Uchegbu IF, Carlos M, Mckay C, Hou X, Schätzlein AG. 2014. Chitosan amphiphiles provide new drug delivery opportunities. Polym Int. doi:10.1002/pi.4721.

Ueno H, Mori T, Fujinaga T. 2001. Topical formulations and wound healing applications of chitosan. Adv Drug Deliv Rev. 52(2):105–115. doi:10.1016/S0169-409X(01)00189-2. www.elsevier.com/locate/drugdeliv.

Upadhayay P, Kumar M, Pathak K. 2016. Norfloxacin loaded pH triggered nanoparticulate in-situ gel for extraocular bacterial infections: Optimization, ocular irritancy and corneal toxicity. Iran J Pharm Res. doi:10.22037/ijpr.2016.1795.

Urtti A. 2006. Challenges and obstacles of ocular pharmacokinetics and drug delivery. Adv Drug Deliv Rev. 58(11):1131–1135. doi:10.1016/j.addr.2006.07.027.

Üstündağ-Okur N, Gökçe EH, Bozbiyik DI, Eğrilmez S, Özer Ö, Ertan G. 2014. Preparation and in vitro-in vivo evaluation of ofloxacin loaded ophthalmic nano structured lipid carriers modified with chitosan oligosaccharide lactate for the treatment of bacterial keratitis. Eur J Pharm Sci. doi:10.1016/j.ejps.2014.07.013.

Vandamme TF, Brobeck L. 2005. Poly(amidoamine) dendrimers as ophthalmic vehicles for ocular delivery of pilocarpine nitrate and tropicamide. J Control Release. doi:10.1016/j.jconrel.2004.09.015.

Varela-Fernández R, Díaz-Tomé V, Luaces-Rodríguez A, Conde-Penedo A, García-Otero X, Luzardo-álvarez A, Fernández-Ferreiro A, Otero-Espinar FJ. 2020. Drug delivery to the posterior segment of the eye: Biopharmaceutic and pharmacokinetic considerations. Pharmaceutics. doi:10.3390/pharmaceutics12030269.

Varela-Fernández R, García-Otero X, Díaz-Tomé V, Regueiro U, López-López M, González-Barcia M, Lema MI, Otero-Espinar FJ. 2021. Design, Optimization, and Characterization of Lactoferrin-Loaded Chitosan/TPP and Chitosan/Sulfobutylether-β-cyclodextrin Nanoparticles as a Pharmacological Alternative for Keratoconus Treatment. ACS Appl Mater Interfaces. doi:10.1021/acsami.0c18926.

Verheul RJ, Van Der Wal S, Hennink WE. 2010. Tailorable thiolated trimethyl chitosans for covalently stabilized nanoparticles. Biomacromolecules. 11(8):1965–1971. doi:10.1021/bm1002784.

Verma A, Sharma G, Jain A, Tiwari A, Saraf S, Panda PK, Katare OP, Jain SK. 2019. Systematic optimization of cationic surface engineered mucoadhesive vesicles employing Design of Experiment (DoE): A preclinical investigation. Int J Biol Macromol. doi:10.1016/j.ijbiomac.2019.04.118.

Verma P, Gupta RN, Jha AK, Pandey R. 2013. Development, in vitro and in vivo characterization of Eudragit RL 100 nanoparticles for improved ocular bioavailability of acetazolamide. Drug Deliv. doi:10.3109/10717544.2013.834417.

Vicario-de-la-Torre M, Caballo-González M, Vico E, Morales-Fernández L, Arriola-Villalobos P, Heras B de las, Benítez-del-Castillo JM, Guzmán M, Millar T, Herrero-Vanrell R, et al. 2018. Novel Nano-liposome formulation for dry eyes with components similar to the preocular tear film. Polymers (Basel). doi:10.3390/polym10040425.

Vidal-Sanz M, Salinas-Navarro M, Nadal-Nicolás FM, Alarcón-Martínez L, Valiente-Soriano FJ, Miralles de Imperial J, Avilés-Trigueros M, Agudo-Barriuso M, Villegas-Pérez MP. 2012. Understanding glaucomatous damage: Anatomical and functional data from ocular hypertensive rodent retinas. Prog Retin Eye Res. doi:10.1016/j.preteyeres.2011.08.001.

Vidal L, Díaz F, Villena A, Moreno M, Campos JG, Pérez de Vargas I. 2010. Reaction of Müller cells in an experimental rat model of increased intraocular pressure following timolol, latanoprost and brimonidine. Brain Res Bull. doi:10.1016/j.brainresbull.2010.02.011.

Vishwaraj CR, Kavitha S, Venkatesh R, Shukla AG, Chandran P, Tripathi S. 2022. Neuroprotection in glaucoma. Indian J Ophthalmol. doi:10.4103/ijo.IJO_1158_21.

Vivekanantham S, Shah S, Dewji R, Dewji A, Khatri C, Ologunde R. 2015. Neuroinflammation in Parkinson's disease: Role in neurodegeneration and tissue repair. Int J Neurosci. doi:10.3109/00207454.2014.982795.

Vohra R, Tsai JC, Kolko M. 2013. The Role of Inflammation in the Pathogenesis of Glaucoma. Surv Ophthalmol. doi:10.1016/j.survophthal.2012.08.010.

Vyas SP, Paliwal R, Paliwal SR. 2011. Ocular delivery of peptides and proteins. In: Peptide and Protein Delivery.

Wadhwa S, Paliwal R, Paliwal SR, Vyas SP. 2010. Hyaluronic acid modified chitosan nanoparticles for effective management of glaucoma: Development, characterization, and evaluation. J Drug Target. 18(4):292–302. doi:10.3109/10611860903450023.

Wang WH, Millar JC, Pang IH, Wax MB, Clark AF. 2005. Noninvasive measurement of rodent intraocular pressure with a rebound tonometer. Investig Ophthalmol Vis Sci. doi:10.1167/iovs.05-0781.

Wang WY, Yao C, Shao YF, Mu HJ, Sun KX. 2011. Determination of puerarin in rabbit aqueous humor by liquid chromatography tandem mass spectrometry using microdialysis sampling after topical administration of puerarin PAMAM dendrimer complex. J Pharm Biomed Anal. doi:10.1016/j.jpba.2011.07.017.

Wang Y, Rajala A, Rajala R. 2015. Lipid Nanoparticles for Ocular Gene Delivery. J Funct Biomater. doi:10.3390/jfb6020379.

Wang YS, Liu LR, Jiang Q, Zhang QQ. 2007. Self-aggregated nanoparticles of cholesterol-modified chitosan conjugate as a novel carrier of epirubicin. Eur Polym J. doi:10.1016/j.eurpolymj.2006.09.007.

Wang Z yang, Shen L jun, Tu LL, Hu D ning, Liu GY, Zhou Z lou, Lin Y, Chen LH, Qu J. 2009. Erythropoietin protects retinal pigment epithelial cells from oxidative damage. Free Radic Biol Med. doi:10.1016/j.freeradbiomed.2008.11.027.

Wang ZY, Zhao KK, Zhao PQ. 2010. Erythropoietin is increased in aqueous humor of glaucomatous eyes. Curr Eye Res. doi:10.3109/02713681003778780.

Warsito MF, Agustiani F. 2021. A review on factors affecting chitosan nanoparticles formation. In: IOP Conference Series: Materials Science and Engineering.

Weng Y, Liu J, Jin S, Guo W, Liang X, Hu Z. 2017. Nanotechnology-based strategies for treatment of ocular disease. Acta Pharm Sin B. 7(3):281–291. doi:10.1016/j.apsb.2016.09.001. http://dx.doi.org/10.1016/j.apsb.2016.09.001.

Weymouth AE, Vingrys AJ. 2008. Rodent electroretinography: Methods for

extraction and interpretation of rod and cone responses. Prog Retin Eye Res. doi:10.1016/j.preteyeres.2007.09.003.

Wheeler L, WoldeMussie E, Lai R. 2003. Role of alpha-2 agonists in neuroprotection. Surv Ophthalmol. doi:10.1016/S0039-6257(03)00004-3.

Widjaja LK, Bora M, Chan PNPH, Lipik V, Wong TTL, Venkatraman SS. 2014. Hyaluronic acid-based nanocomposite hydrogels for ocular drug delivery applications. J Biomed Mater Res - Part A. doi:10.1002/jbm.a.34976.

Willoughby CE, Ponzin D, Ferrari S, Lobo A, Landau K, Omidi Y. 2010. Anatomy and physiology of the human eye: Effects of mucopolysaccharidoses disease on structure and function - a review. Clin Exp Ophthalmol. doi:10.1111/j.1442-9071.2010.02363.x.

Wood RW, Li VHK, Kreuter J, Robinson JR. 1985. Ocular disposition of poly-hexyl-2-cyano[3-14C]acrylate nanoparticles in the albino rabbit. Int J Pharm. doi:10.1016/0378-5173(85)90007-9.

World Health Organization. 2014. Media centre Visual impairment and blindness. Http://WwwWhoInt/Mediacentre/Factsheets/Fs282/En/#.

Wu XG, Xin M, Yang LN, Shi WY. 2011. The biological characteristics and pharmacodynamics of a mycophenolate mofetil nanosuspension ophthalmic delivery system in rabbits. J Pharm Sci. doi:10.1002/jps.22356.

Xie Z, Chen F, Wu X, Zhuang C, Zhu J, Wang J, Ji H, Wang Y, Hua X. 2012. Safety and efficacy of intravitreal injection of recombinant erythropoietin for protection of photoreceptor cells in a rat model of retinal detachment. Eye. doi:10.1038/eye.2011.254.

Xing Y, Zhu L, Zhang K, Li T, Huang S. 2021. Nanodelivery of triamcinolone acetonide with PLGA-chitosan nanoparticles for the treatment of ocular inflammation. Artif Cells, Nanomedicine Biotechnol. doi:10.1080/21691401.2021.1895184.

Xu X, Sun L, Zhou L, Cheng Y, Cao F. 2020. Functional chitosan oligosaccharide nanomicelles for topical ocular drug delivery of dexamethasone. Carbohydr Polym. doi:10.1016/j.carbpol.2019.115356.

Yamasaki M, Mishima HK, Yamashita H, Kashiwagi K, Murata K, Minamoto A, Inaba T. 2005. Neuroprotective effects of erythropoietin on glutamate and nitric oxide toxicity in primary cultured retinal ganglion cells. Brain Res. doi:10.1016/j.brainres.2005.05.037.

Yandrapu SK, Kanujia P, Chalasani KB, Mangamoori L, Kolapalli R V., Chauhan A. 2013. Development and optimization of thiolated dendrimer as a viable mucoadhesive excipient for the controlled drug delivery: An acyclovir model formulation. Nanomedicine Nanotechnology, Biol Med. doi:10.1016/j.nano.2012.10.005.

Yang H, Leffler CT. 2013. Hybrid dendrimer hydrogel/poly(lactic-Co-glycolic acid) nanoparticle platform: An advanced vehicle for topical delivery of antiglaucoma drugs and a likely solution to improving compliance and adherence in glaucoma management. J Ocul Pharmacol Ther. doi:10.1089/jop.2012.0197.

Yang H, Tyagi P, Kadam RS, Holden CA, Kompella UB. 2012. Hybrid dendrimer hydrogel/PLGA nanoparticle platform sustains drug delivery for one week and antiglaucoma effects for four days following one-time topical administration. ACS Nano. doi:10.1021/nn301873v.

Yang X, Wang L, Li L, Han M, Tang S, Wang T, Han J, He Xiaoyan, He Xiuting, Wang A, et al. 2019. A novel dendrimer-based complex co-modified with cyclic RGD hexapeptide and penetratin for noninvasive targeting and penetration of the ocular posterior segment. Drug Deliv. doi:10.1080/10717544.2019.1667455.

Yao C, Wang W, Zhou X, Qu T, Mu H, Liang R, Wang A, Sun K. 2011. Effects of poly(amidoamine) dendrimers on ocular absorption of puerarin using microdialysis. J Ocul Pharmacol Ther. doi:10.1089/jop.2010.0196.

Yao W, Sun K, Mu H, Liang N, Liu Y, Yao C, Liang R, Wang A. 2010. Preparation and characterization of puerarindendrimer complexes as an ocular drug delivery system.

Drug Dev Ind Pharm. doi:10.3109/03639041003610799.

Yao XL, Liu J, Lee E, Ling GSF, McCabe JT. 2005. Progesterone differentially regulates pro- and anti-apoptotic gene expression in cerebral cortex following traumatic brain injury in rats. J Neurotrauma. doi:10.1089/neu.2005.22.656.

Yavuz B, Kompella UB. 2017. Ocular drug delivery. In: Handbook of Experimental Pharmacology.

Yavuz B, Pehlivan SB, Vural I, Ünlü N. 2015. In Vitro/In Vivo Evaluation of Dexamethasone - PAMAM Dendrimer Complexes for Retinal Drug Delivery. J Pharm Sci. doi:10.1002/jps.24588.

Ye T, Yuan K, Zhang W, Song S, Chen F, Yang X, Wang S, Bi J, Pan W. 2013. Prodrugs incorporated into nanotechnology-based drug delivery systems for possible improvement in bioavailability of ocular drugs delivery. Asian J Pharm Sci. doi:10.1016/j.ajps.2013.09.002.

Yenice I, Mocan MC, Palaska E, Bochot A, Bilensoy E, Vural I, Irkeç M, Atilla Hincal A. 2008. Hyaluronic acid coated poly-ε-caprolactone nanospheres deliver high concentrations of cyclosporine A into the cornea. Exp Eye Res. doi:10.1016/j.exer.2008.04.002.

Yi H, Wu LQ, Bentley WE, Ghodssi R, Rubloff GW, Culver JN, Payne GF. 2005. Biofabrication with chitosan. Biomacromolecules. 6(6):2881–2894. doi:10.1021/bm050410l.

Yi XJ, Wang Y, Yu FSX. 2000. Corneal epithelial tight junctions and their response to lipopolysaccharide challenge. Investig Ophthalmol Vis Sci.

Yingfang F, Zhuang B, Wang C, Xu X, Xu W, Lv Z. 2016. Pimecrolimus micelle exhibits excellent therapeutic effect for Keratoconjunctivitis Sicca. Colloids Surfaces B Biointerfaces. doi:10.1016/j.colsurfb.2015.11.059.

Yoncheva K, Vandervoort J, Ludwig A. 2011. Development of mucoadhesive poly(lactide-co-glycolide) nanoparticles for ocular application. Pharm Dev Technol. 16(1):29–35. doi:10.3109/10837450903479954.

Yu A, Shi H, Liu H, Bao Z, Dai M, Lin Dan, Lin Deqing, Xu X, Li X, Wang Y. 2020. Mucoadhesive dexamethasone-glycol chitosan nanoparticles for ophthalmic drug delivery. Int J Pharm. doi:10.1016/j.ijpharm.2019.118943.

Yu Y, Feng R, Li J, Wang Y, Song Y, Tan G, Liu D, Liu W, Yang X, Pan H, et al. 2019. A hybrid genipin-crosslinked dual-sensitive hydrogel/nanostructured lipid carrier ocular drug delivery platform. Asian J Pharm Sci. doi:10.1016/j.ajps.2018.08.002.

Zaki NM, Hafez MM. 2012. Enhanced antibacterial effect of ceftriaxone sodium-loaded chitosan nanoparticles against intracellular Salmonella typhimurium. AAPS PharmSciTech. doi:10.1208/s12249-012-9758-7.

Zambito Y, Di G. 2011. Polysaccharides as Excipients for Ocular Topical Formulations. In: Biomaterials Applications for Nanomedicine.

Zeng W, Li Q, Wan T, Liu C, Pan W, Wu Z, Zhang G, Pan J, Qin M, Lin Y, et al. 2016. Hyaluronic acid-coated niosomes facilitate tacrolimus ocular delivery: Mucoadhesion, precorneal retention, aqueous humor pharmacokinetics, and transcorneal permeability. Colloids Surfaces B Biointerfaces. 141:28–35. doi:10.1016/j.colsurfb.2016.01.014.

Zhang J, Hu LM, Xu G, Wu Y, Shen J, Luo Y, Zhong Y, Sinclair SH, Yanoff M, Li W, et al. 2010. Anti-VEGF effects of intravitreal erythropoietin in early diabetic retinopathy. Front Biosci - Elit. doi:10.2741/e151.

Zhang J, Wang S. 2009. Topical use of Coenzyme Q10-loaded liposomes coated with trimethyl chitosan: Tolerance, precorneal retention and anti-cataract effect. Int J Pharm. doi:10.1016/j.ijpharm.2009.01.001.

Zhang W, Zhang Lihai, Liu J, Zhang Licheng, Zhang J, Tang P. 2017. Repairing sciatic nerve injury with an EPO-loaded nerve conduit and sandwiched-in strategy of

transplanting mesenchymal stem cells. Biomaterials. doi:10.1016/j.biomaterials.2017.06.024.

Zhang X, Wu Y, Sun K, Tan J. 2014. Effect of erythropoietin loading chitosan-tripolyphosphate nanoparticles on an IgA nephropathy rat model. Exp Ther Med. 7(6):1659–1662. doi:10.3892/etm.2014.1643.

Zhong L, Bradley J, Schubert W, Ahmed E, Adamis AP, Shima DT, Robinson GS, Ng YS. 2007. Erythropoietin promotes survival of retinal ganglion cells in DBA/2J glaucoma mice. Investig Ophthalmol Vis Sci. 48(3):1212–1218. doi:10.1167/iovs.06-0757.

Zhong Y, Liu X, Cheng Y, Min Y. 2008. Erythropoietin with Retrobulbar Administration Protects Retinal Ganglion Cells from Acute Elevated Intraocular Pressure in Rats. J Ocul Pharmacol Ther. 24(5):453–460. doi:10.1089/jop.2008.0021.

Zhong Y, Yao H, Deng L, Cheng Y, Zhou X. 2007. Promotion of neurite outgrowth and protective effect of erythropoietin on the retinal neurons of rats. Graefe's Arch Clin Exp Ophthalmol. doi:10.1007/s00417-007-0671-9.

Zhou M, Chen S, Wang W, Huang W, Cheng B, Ding X, Zhang X. 2013. Levels of erythropoietin and vascular endothelial growth factor in surgery-required advanced neovascular glaucoma eyes before and after intravitreal injection of bevacizumab. Investig Ophthalmol Vis Sci. doi:10.1167/iovs.12-11507.

Zhou W, Wang Y, Jian J, Song S. 2013. Self-aggregated nanoparticles based on amphiphilic poly(lactic acid)-grafted-chitosan copolymer for ocular delivery of amphotericin B. Int J Nanomedicine. doi:10.2147/IJN.S51186.

Zhu J, Zhang E, Del Rio-Tsonis K. 2012. Eye Anatomy. In: eLS.

Zhu X, Su M, Tang S, Wang L, Liang X, Meng F, Hong Y, Xu Z. 2012. Synthesis of thiolated chitosan and preparation nanoparticles with sodium alginate for ocular drug delivery. Mol Vis.

Zubairu Y, Negi LM, Iqbal Z, Talegaonkar S. 2014. Design and development of novel bioadhesive niosomal formulation for the transcorneal delivery of anti-infective agent: In-vitro and ex-vivo investigations. Asian J Pharm Sci. doi:10.1016/j.ajps.2015.02.001.

Zylberberg C, Matosevic S. 2016. Pharmaceutical liposomal drug delivery: a review of new delivery systems and a look at the regulatory landscape. Drug Deliv. 23(9):3319–3329. doi:10.1080/10717544.2016.1177136.